Performance of Pressure Sensitive Adhesive Tapes In Wood Light-Frame Shear Walls

By:
William P. Jacobs, V

Thesis submitted to the faculty of the
Virginia Polytechnic Institute and State University
In partial fulfillment of the requirements for the degree of

MASTER OF SCIENCE
IN
CIVIL ENGINEERING

Approved by:

J. Daniel Dolan	Donatus C. Ohanehi
David A. Dillard	W. Samuel Easterling

April 28, 2003
Blacksburg, Virginia

Keywords: shear wall, pressure sensitive adhesive, cyclic loading, wood adhesive, acrylic foam

Performance of Pressure Sensitive Adhesive Tapes In Wood Light-Frame Shear Walls

By:
William P. Jacobs, V
Committee Chairman: Dr. James D. Dolan
Civil Engineering

(Abstract)

The performance of connections and full-scale shear walls constructed with acrylic foam pressure sensitive adhesive (PSA) tape is the focus of this thesis. The objectives of this study were first to investigate the bonding characteristics of adhesive tape to wood substrates and then to expand this investigation to cover adhesive-based shear walls subjected to high wind and seismic loadings. A total of 287 monotonic connection tests and 23 reversed cyclic wall tests were performed to achieve these objectives. Connection tests were performed in accordance with ASTM D 1761-88 (2000), and walls were tested using the CUREE (Consortium of Universities for Earthquake Engineering) general displacement-based protocol.

Variables investigated within the main study were the following: the use of OSB versus plywood sheathing, the effect of priming and surface sanding on adhesion, and the comparison of connections involving mechanical fasteners with those that utilized only adhesive tape or a combination of the two. It was found that an application pressure of 207 kPa (30 psi) or greater was needed to form a sound bond between the acrylic foam adhesive tape and a wood substrate. Properly bonded OSB and plywood connections provided fairly ductile failure modes. Full-scale walls constructed with adhesive tape performed similarly to traditional wall configurations, while walls constructed with a combination of adhesive tape and mechanical fasteners provided significant gains in strength and toughness. The results of this study serve to provide a foundation for expanding the engineering uses of acrylic foam adhesive tape for structural applications.

Dedication

To my parents, Bill and Theresa Jacobs, who have raised and guided me with a love and faith stronger than any I could hope to deserve. Thank you.

Acknowledgements

I would like to express my appreciation to my committee chair, Dr. Dan Dolan, for his insight and guidance through the completion of this project. I would also like to thank Dr. David Dillard, Dr. Samuel Easterling, and Dr. Donatus Ohanehi for willingly giving of their time, assistance, and valuable suggestions.

I extend my gratitude to everyone who contributed to the completion of the testing phase of this project. It could not have been completed without the countless hours of assistance that Rick Caudill, Kenny Albert, and Danny Bredel provided me. I also appreciate the practical insights provided by Dr. Alexander Salenikovich and Harrison Sizemore. I owe special thanks to Adam Toothman for his friendship and support throughout the monotony of connection testing.

I have been extremely fortunate to have so many caring people supporting me on my academic journey. I thank all my friends in Clemson and Blacksburg for providing me with so many pleasant memories and good times. The journey would also not have been possible without the wealth of knowledge passed down from my professors.

I respectfully acknowledge the financial support provided by the National Science Foundation Grant #0122124, for the Partnership for Advancing Technologies in Housing (PATH) program.

In addition to my parents (and thesis editors) Bill and Theresa, to whom this thesis is dedicated, I would like to thank my big sister Laura for her love and caring. Also to my Grandparents, Jake and Erna, thank you; Grandmother, Charles, and Nana, I love you and miss you dearly.

Last, but certainly not least, I would like to thank Ashley Dearhart. Her endless love, friendship, and devotion have sustained me through the peaks and valleys I have experienced during the past five years. Her ability to shine joy into my life and her steadfast patience and understanding have filled me with happiness. With her love, I have truly been blessed.

Table of Contents

Chapter 1: Introduction 1

1.1 Background 1

1.2 Objectives 4

1.3 Applications 5

1.4 Thesis Organization 6

1.5 Limitations of Study 7

Chapter 2: Literature Survey and Background 8

2.1 Introduction 8

2.2 Adhesives in the Timber Industry 8
2.2.1 Wood as a Substrate 9
2.2.2 Structural Adhesives for Engineered Wood Products 9
2.2.3 Construction Adhesives 10

2.3 Acrylic Foam Adhesive Tape 11
2.3.1 Breakdown of Acrylic Foam Tapes 11
2.3.2 Research on Acrylic Foam Adhesive Tape 12

2.4 Experimental Connection and Shear Wall Studies 14
2.4.1 Recent Experimental Shear Wall Studies 14
2.4.2 Adhesives in Shear Walls 15

2.5 Testing Procedures and Loading Effects 16
2.5.1 Monotonic Testing Protocols 17
2.5.2 Cyclic Load Testing Protocols 18
2.5.3 Performance Comparison of Cyclic Protocols 20

2.6 Numeric Modeling of Connections and Shear Walls 21
2.6.1 Adhesive Connections 21
2.6.2 Mechanical Connections 22
2.6.3 Shear Walls 23

2.7 Summary 25

Chapter 3: Materials and Test Procedures 26

3.1 General 26

3.2 Specimen Designations 26

3.3 Material Properties 29
3.3.1 Structural Member Material Properties 29

3.3.2 Pressure Sensitive Adhesive Properties 31
3.3.3 Mechanical Fasteners 31
3.4 Connection Specimens 33
3.4.1 Specimen Introduction 33
3.4.2 Comparison Test Construction 35
3.4.2.1 Adhesive Application 35
3.4.2.2 Sheathing Surface Energy 36
3.4.2.3 Methods of Increased Bonding Capability 37
3.4.2.4 Mechanical Fasteners for Comparison Tests 38
3.4.2.5 Other Comparison Test Considerations 39
3.4.3 Pressure Application Connection Specimens 39
3.4.4 Time of Application Connection Specimens 42
3.4.5 Statistical Connection Specimens 43
3.4.5.1 Sample Size 43
3.4.5.2 Connection Information 43
3.4.6 Additional Tests of Interest 44
3.5 Connection Testing 46
3.5.1 Testing Equipment 46
3.5.2 Testing Procedure 48
3.6 Full-Scale Shear Wall Specimens 49
3.6.1 Shear Wall Introduction 49
3.6.2 Adhesive Application Pressure 49
3.6.2.1 Pressure Application Alternatives 49
3.6.2.2 Tests of Pressure Application Hose System 51
3.6.2.3 Real World Application 53
3.6.3 Specimen Construction 54
3.6.3.1 Frame Construction 54
3.6.3.2 Application of Tape Adhesive to Full-Scale Walls 55
3.6.3.3 Nail Schedules 57
3.7 Wall Testing 58
3.7.1 Testing Equipment 58
3.7.2 Attachment of Specimens to Test Frame 58
3.7.3 Instrumentation of Wall Specimens 60
3.7.4 Testing Procedures 63
3.7.4.1 Monotonic Loading 63
3.7.4.2 CUREE Protocol Background 64
3.7.4.3 CUREE Displacement Based General Protocol 65
3.8 Summary 66
Chapter 4: Performance Parameters and Analysis Techniques 67
4.1 General 67
4.2 Basic Monotonic Definitions 67
4.2.1 Peak Load and Failure 67

4.2.2 Elastic Stiffness 68
4.3 Monotonic Equivalent Energy Elastic-Plastic (EEEP) Parameters 69
4.3.1 Yield Load and Displacement 70
4.3.2 Five-percent-offset Yield 70
4.3.3 Ductility 71
4.3.4 Energy (Work Performed) 72
4.3.5 Slack 72
4.4 Cyclic Definitions and Performance Parameters 72
4.4.1 Energy (Work Performed) 73
4.5 Earthquake Performance Parameters 74
4.5.1 Hysteretic and Strain Energy 74
4.5.2 Damping 75
4.5.3 Cyclic Stiffness 75
4.5.4 Inertia 76
4.6 Deflection Parameters 77
4.6.1 Rigid Body Rotation 77
4.6.2 Shear Deformation 78
4.6.3 Connection Slip and Bending 79
4.6.4 Deflection Summary 80
4.7 Data Analysis 80
4.8 Summary 81
Chapter 5: Connection Test Results and Discussion 82
5.1 General 82
5.2 Comparison Subset 83
5.2.1 General Construction Observations 84
5.2.1.1 Specimen Construction 84
5.2.1.2 Commentary on Validity of Results 85
5.2.2 Load-Displacement Curves 85
5.2.3 Oriented Strand Board Tests 86
5.2.3.1 Surface Treatments 86
5.2.3.2 Mechanical Fasteners and Application Pressure 87
5.2.3.3 Light-Gauge Steel Framing 87
5.2.4 Plywood Tests 88
5.2.4.1 Surface Treatments & Comparison to OSB 88
5.2.4.2 Mechanical Fasteners and Application Pressure 89
5.2.4.3 Light-Gauge Steel Framing 89
5.2.5 Additional Comparison Test Observations 89
5.2.6 Failure Modes 90
5.2.7 Comparison Test Summary 91
5.3 Pressure Application Subset 92
5.3.1 Load-Displacement Curves 94

5.3.2 Peak Load and Displacement Comparison 95
5.3.3 Work to Failure (Energy) Comparison 97
5.3.4 Commentary on Other Performance Parameters 98
5.3.5 Pressure Test Failure Modes 98
5.3.6 Pressure Test Conclusions 99
5.4 Time of Application Subset 100
5.4.1 Load-Displacement Curves 102
5.4.2 Peak Load and Displacement Comparisons 103
5.4.3 Work to Failure (Energy) Comparison 104
5.4.4 Commentary on Other Performance Parameters and Failure Modes 105
5.4.5 Time Duration of Application Pressure Conclusions 106
5.5 Statistically Significant: Subset Introduction 107
5.5.1 General Notes 108
5.6 Statistically Significant: Overall General Summary of Results 109
5.6.1 Load-Displacement Curves 109
5.6.2 Peak Capacity and Displacement 112
5.6.3 Elastic Stiffness 115
5.6.4 Work to Failure 117
5.6.5 Displacement at Failure 118
5.6.6 Five-Percent-Offset Yield 119
5.6.7 Other Performance Parameters 120
5.7 Statistically Significant: OSB Connection Discussion 121
5.7.1 Surface Treatments 121
5.7.2 Performance Vs. Mechanical Fasteners 122
5.7.3 Failure Modes of OSB Connections 123
5.8 Statistically Significant: Plywood Connection Discussion 125
5.8.1 Performance Vs. Mechanical Fasteners 125
5.8.2 Failure Modes of Plywood Connections 126
5.9 Statistically Significant: Alternate Manufacturer Study 127
5.9.1 Performance Parameter Comparison 127
5.9.2 Failure Mode Comparison 129
5.9.3 Alternate Product Conclusions 130
5.10 Connection Tests of Additional Interest 131
5.10.1 Performance Parameters 131
5.10.2 Failure Modes of Traditional Adhesives 133
5.10.3 Conclusions Based on Traditional Adhesives 134
5.11 Summary 134
Chapter 6: Shear Wall Test Results and Discussion 137
6.1 General 137
6.2 Monotonic Test Results 138
6.2.1 Load-Displacement Curves 138

6.2.2 Target Cyclic Deflections (Δ) 139
6.3 Cyclic Tests: Introduction 140
6.4 Cyclic Tests: Performance Parameter Results 141
6.5 Cyclic Tests: Shear Wall Strength 144
6.5.1 General Strength Comparison 144
6.5.2 Strength Design Tables 145
6.5.3 Shear Wall Strength Summary 146
6.6 Cyclic Tests: Shear Wall Toughness 147
6.6.1 Displacement (Interstory Drift) Capacity 147
6.6.2 Hysteretic Energy 148
6.6.3 Shear Wall Toughness Summary 151
6.7 Cyclic Tests: Earthquake Performance 152
6.7.1 Cyclic Stiffness 152
6.7.2 Equivalent Viscous Damping 155
6.7.3 Ductility 157
6.7.4 The System Response Modification Factor "R" 158
6.7.4.1 Current use of the R-factor 158
6.7.4.2 Research on Analytical Formulation of R 159
6.7.4.3 Conclusions and Recommendations for PSA Tape Walls 161
6.7.4.4 Ramifications of Proposed R-factor 163
6.7.5 Earthquake Performance Summary 164
6.8 Cyclic Tests: Overall Wall Response 165
6.8.1 Deformation Components 165
6.8.2 Failure Modes 167
6.8.3 Commentary on Moisture and Temperature Effects 171
6.8.4 Commentary on CUREE Testing Protocol 172
6.8.5 Loading Rate Effects 174
6.9 Feasibility of Acrylic Foam PSA Tape Wall Manufacturing 175
6.9.1 Manufacturing Methods 175
6.9.2 Economic Viability 176
6.9.3 Feasibility Summary 177
6.10 Wind Design Example 178
6.10.1 Wind Design Example Conclusions 186
6.11 Seismic Design Example 187
6.11.1 Seismic Design Example Conclusions 193
6.12 Summary 194

Chapter 7: Summary and Conclusions 197

7.1 Summary 197
7.2 Conclusions 198
7.2.1 Overall Conclusions and Recommendations 198

7.2.2 Connection Test Results and Observations 200
7.2.3 Wall Test Results and Observations 202
7.3 Future Research 204

Bibliography 207

Appendices

Appendix A A1

A1 Data Records A3
A2 Application Pressure Data A25
A3 Duration of Application Pressure Data A39
A4 Statistically Significant: Main Connection Study A52

Appendix B B1

B1 W-OAP Wall Data B1
B2 W-OAS Wall Data B25
B3 W-ON Wall Data B48
B4 W-OAN Wall Data B71
B5 W-PA Wall Data B94
B6 W-PN Wall Data B117
B7 W-PAN Wall Data B140

Table of Figures

Figure 1.1: Diaphragm and Shear Wall Action (After Diekmann 1995) 2
Figure 1.2: Typical Foam Tape Cross Section 3
Figure 3.1: Sawn Lumber Grade Stamp and Product Label 29
Figure 3.2: Grade Stamps for OSB (Left) and Plywood (Right) Sheathing 30
Figure 3.3: Basic Connection Specimen 33
Figure 3.4: Connection Tests in Environmental Chamber 34
Figure 3.5: Adhesive Application to Connection Member 35
Figure 3.6: Recording Moisture Content 36
Figure 3.7: Water Drop Test 37
Figure 3.8: Surface Sanding of OSB 38
Figure 3.9: Pressure Application Steps 40
Figure 3.10: Adhesive Application Pressure vs. Time of Application 41
Figure 3.11: Application Pressure vs. Time of Application 42
Figure 3.12: Application of Elastomeric Adhesive 45
Figure 3.13: Connection Test Setup 46
Figure 3.14: Connection Test Fixture Without Specimen 47
Figure 3.15: Connection Test Fixture With Specimen 47
Figure 3.16: Wall Pressure Application Setup (Hose Deflated) 50
Figure 3.17: Force Flow of Wall Pressure Application Setup (Hose Inflated) 50
Figure 3.18: Ends of Fire Hose 51
Figure 3.19: MTS Hose Test Setup 52
Figure 3.20: Pressure vs. Time Plot for Dynamic Hose Test 53
Figure 3.21: Frame Construction Jig 54
Figure 3.22: Construction Details for “Adhesive + Nails” Wall Specimen (After Heine 1997). 57
Figure 3.23: Elevation and Plan Views of Wall Testing Setup 59
Figure 3.24: Photograph of Test Setup (Multimedia Object – Shear.mov) 60
Figure 3.25: Instrumentation of Wall Specimens 61
Figure 3.26: Connection of String Potentiometers to Wall Specimen 62
Figure 3.27: Time History of Displacement Based General CUREE Protocol 63
Figure 4.1: Basic Monotonic Definitions 68
Figure 4.2: EEEP Parameters for Monotonic Tests 69
Figure 4.3: Typical Cyclic Hysteresis with Envelope and EEEP Curves 73
Figure 4.4: Typical Hysteretic Loop 74
Figure 4.5: Rigid Body Component of Deflection 78
Figure 4.6: Shear Deformation Component of Deflection 79
Figure 4.7: Bending Component of Deflection 80
Figure 5.1: Connection Strength Directions 84
Figure 5.2: Macro Curvature of Specimens 85
Figure 5.3: OSB Comparison Test Load-Displacement Graph 86
Figure 5.4: Plywood Comparison Test Load-Displacement Graph 88
Figure 5.5: Moisture Content Scatter-Graph 90
Figure 5.6: (a) Adhesive Bond Failure (b) “Rolling” Tape Failure 91
Figure 5.7: Application Pressure Average Load-Displacement Curves 94

Figure 5.8: Pressure Application Peak Load Comparison 95
Figure 5.9: Pressure Application Work to Failure (Energy) Comparison 97
Figure 5.10: High Pressure Bond Failure 99
Figure 5.11: Time Duration of Application Pressure Load-Displacement Curves 102
Figure 5.12: Time Duration – Peak Load Comparison 103
Figure 5.13: Time Duration Work to Failure (Energy) Comparison 104
Figure 5.14: Statistically Significant Average Load-Displacement Curves 109
Figure 5.15: Peak Capacity vs. Displacement 112
Figure 5.16: Elastic Stiffness Comparisons 115
Figure 5.17: Work to Failure Comparisons 117
Figure 5.18: Failure Load vs. Failure Displacement Comparison 118
Figure 5.19: Five-Percent-Offset Yield Load Vs. Displacement Comparison 119
Figure 5.20: Typical Nail-Only Load Displacement Curve 120
Figure 5.21: OSB Average Load-Displacement Curves 121
Figure 5.22: Surface Sanded Specimen Broken After Testing 123
Figure 5.23: Primed Specimen Broken After Testing 123
Figure 5.24: Mode IIIs Yielding of Mechanical Fastener 124
Figure 5.25: Highlighted Area of Localized Bonding Near Nail 124
Figure 5.26: Plywood Average Load-Displacement Curves 125
Figure 5.27: Main Member Adhesive Failure 126
Figure 5.28: Average Load-Displacement Curves for Alternate Adhesive Tapes 128
Figure 5.29: S-PMT1 Inspecting Adhesive Bond After Testing 129
Figure 5.30: S-PMT2 Investing Adhesive Bond After Testing 129
Figure 5.31: S-PMT3 Cohesive Tape Failure 130
Figure 5.32: Average Load-Displacement Curves for Traditional Adhesives 132
Figure 5.33: (a) Cohesive Failure in Plywood (b) Brittle Sheathing Failure 133
Figure 5.34: Liquid Nails® Cohesive Failure 133
Figure 6.1: Monotonic Wall Test Load-Displacement Curves 138
Figure 6.2: Average Load Capacities of Shear Wall Tests 144
Figure 6.3: Interstory Drift Capacities 147
Figure 6.4: Hysteretic Energy vs. Displacement of OSB Wall Specimens 149
Figure 6.5: Hysteretic Energy vs. Displacement of Plywood Wall Specimens 150
Figure 6.6: Cyclic Stiffness Degradation (OSB Walls) 153
Figure 6.7: Cyclic Stiffness Degradation (Plywood Walls) 153
Figure 6.8: Equivalent Viscous Damping Ratios (OSB Walls) 155
Figure 6.9: Equivalent Viscous Damping Ratios (Plywood Walls) 156
Figure 6.10: Example of Ductile Combination System Failure (W-OAN-3) 157
Figure 6.11: Summary of Deflection Components 165
Figure 6.12: Effectiveness of Hold-Down Devices on End Studs 166
Figure 6.13: Nail-Only Failures 167
Figure 6.14: Centerline Failure of Adhesive-Only Bond 168
Figure 6.15: Post-Failure Bridging of Adhesive Tape Between Framing and Sheathing 169
Figure 6.16: Typical Minimal Deformation of Nail 169
Figure 6.17: Observed and Recorded Diagonal Displacement Data 170
Figure 6.18: Average Backbone Curves of W-OAS Test Series 172
Figure 6.19: MiTek® RoofGlider Truss Roller System (Used With Permission) 175

Figure 6.20: Basic House Configuration (Red = Shear Wall to be Designed) 179
Figure 6.21: Proposed Shear Wall Geometry 179
Figure 6.22: Wind Tributary Areas..... 181
Figure 6.23: Reactions on Diaphragms..... 181
Figure 6.24: Roof Diaphragm Reactions 182
Figure 6.25: 2nd Floor Diaphragm Reactions..... 183
Figure 6.26: Shear Wall With Additional Window 185
Figure 6.27: Basic House Configuration (Red Wall = Shear Wall to be Designed) 188
Figure 6.28: Force Distribution on Shear Wall..... 188

Figure A2.1: Application Pressure Average Curves..... A35
Figure A2.2: Application Pressure Curves – 103kPa (15psi) for 30 seconds..... A35
Figure A2.3: Application Pressure Curves – 207kPa (30psi) for 30 seconds..... A36
Figure A2.4: Application Pressure Curves – 310kPa (45psi) for 30 seconds..... A36
Figure A2.5: Application Pressure Curves – 414kPa (60psi) for 30 seconds..... A37
Figure A2.6: Application Pressure Curves – 552kPa (80psi) for 30 seconds..... A37
Figure A2.7: Application Pressure Curves – 690kPa (100psi) for 30 sec. A38
Figure A2.8: Application Pressure Curves – 827kPa (120psi) for 30 sec. A38
Figure A3.1: Duration of Application Pressure Average Load-Displacement Curves..... A48
Figure A3.2: Pressure Duration Curves – 414kPa (60psi) for 15 seconds A48
Figure A3.3: Pressure Duration Curves – 414kPa (60psi) for 30 seconds A49
Figure A3.4: Pressure Duration Curves – 414kPa (60psi) for 45 seconds A49
Figure A3.5: Pressure Duration Curves – 414kPa (60psi) for 60 seconds A50
Figure A3.6: Pressure Duration Curves – 414kPa (60psi) for 90 seconds A50
Figure A3.7: Pressure Duration Curves – 414kPa (60psi) for 120 seconds A51
Figure A4.1: Average Load-Displacement Curves (Including Traditional Adhesives) A79
Figure A4.2: Average Load-Displacement Curves (Excluding Traditional Adhesives) A79
Figure A4.3: Alternate Tape Manufacturer Average Load-Displacement Curves A80
Figure A4.4: S-OA Load-Displacement Curves..... A80
Figure A4.5: S-OAS Load-Displacement Curves..... A81
Figure A4.6: S-OAP Load-Displacement Curves..... A81
Figure A4.7: S-OAN Load-Displacement Curves..... A82
Figure A4.8: S-ON Load-Displacement Curves..... A82
Figure A4.9: S-PA Load-Displacement Curves..... A83
Figure A4.10: S-PAN Load-Displacement Curves..... A83
Figure A4.11: S-PN Load-Displacement Curves..... A84
Figure A4.12: S-PMT1 Load-Displacement Curves A84
Figure A4.13: S-PMT2 Load-Displacement Curves A85
Figure A4.14: S-PMT3 Load-Displacement Curves A85
Figure A4.15: Wood Glue Load-Displacement Curves..... A86
Figure A4.16: Liquid Nails Load-Displacement Curves A86
Figure A4.17: S-OA-1 ..... A87
Figure A4.18: S-OA-2 ..... A87
Figure A4.19: S-OA-3 ..... A87
Figure A4.20: S-OA-4 ..... A87
Figure A4.21: S-OA-5 ..... A87

Figure A4.22: S-OA-6 ..... A87
Figure A4.23: S-OA-7 ..... A88
Figure A4.24: S-OA-9 ..... A88
Figure A4.25: S-OA-10 ..... A88
Figure A4.26: S-OA-11 ..... A88
Figure A4.27: S-OA-12 ..... A88
Figure A4.28: S-OA-13 ..... A88
Figure A4.29: S-OA-14 ..... A89
Figure A4.30: S-OA-15 ..... A89
Figure A4.31: S-OAS-1 ..... A89
Figure A4.32: S-OAS-2 ..... A89
Figure A4.33: S-OAS-3 ..... A89
Figure A4.34: S-OAS-4 ..... A89
Figure A4.35: S-OAS-5 ..... A90
Figure A4.36: S-OAS-6 ..... A90
Figure A4.37: S-OAS-7 ..... A90
Figure A4.38: S-OAS-8 ..... A90
Figure A4.39: S-OAS-9 ..... A90
Figure A4.40: S-OAS-10 ..... A90
Figure A4.41: S-OAS-11 ..... A91
Figure A4.42: S-OAS-12 ..... A91
Figure A4.43: S-OAS-13 ..... A91
Figure A4.44: S-OAS-14 ..... A91
Figure A4.45: S-OAS-15 ..... A91
Figure A4.46: S-OAP-1 ..... A91
Figure A4.47: S-OAP-2 ..... A92
Figure A4.48: S-OAP-3 ..... A92
Figure A4.49: S-OAP-4 ..... A92
Figure A4.50: S-OAP-5 ..... A92
Figure A4.51: S-OAP-6 ..... A92
Figure A4.52: S-OAP-7 ..... A92
Figure A4.53: S-OAP-8 ..... A93
Figure A4.54: S-OAP-9 ..... A93
Figure A4.55: S-OAP-10 ..... A93
Figure A4.56: S-OAP-11 ..... A93
Figure A4.57: S-OAP-12 ..... A93
Figure A4.58: S-OAP-13 ..... A93
Figure A4.59: S-OAP-14 ..... A94
Figure A4.60: S-OAP-15 ..... A94
Figure A4.61: S-OAN-1 ..... A94
Figure A4.62: S-OAN-2 ..... A94
Figure A4.63: S-OAN-3 ..... A94
Figure A4.64: S-OAN-4 ..... A94
Figure A4.65: S-OAN-5 ..... A95
Figure A4.66: S-OAN-6 ..... A95
Figure A4.67: S-OAN-7 ..... A95

Figure A4.68: S-OAN-8 ..... A95
Figure A4.69: S-OAN-9 ..... A95
Figure A4.70: S-OAN-10 ..... A95
Figure A4.71: S-OAN-11 ..... A96
Figure A4.72: S-OAN-12 ..... A96
Figure A4.73: S-OAN-13 ..... A96
Figure A4.74: S-OAN-14 ..... A96
Figure A4.75: S-OAN-15 ..... A96
Figure A4.76: S-ON-1 ..... A96
Figure A4.77: S-ON-2 ..... A97
Figure A4.78: S-ON-3 ..... A97
Figure A4.79: S-ON-4 ..... A97
Figure A4.80: S-ON-5 ..... A97
Figure A4.81: S-ON-6 ..... A97
Figure A4.82: S-ON-7 ..... A97
Figure A4.83: S-ON-8 ..... A98
Figure A4.84: S-ON-9 ..... A98
Figure A4.85: S-ON-10 ..... A98
Figure A4.86: S-ON-11 ..... A98
Figure A4.87: S-ON-12 ..... A98
Figure A4.88: S-ON-13 ..... A98
Figure A4.89: S-ON-15 ..... A99
Figure A4.90: S-PA-1 ..... A99
Figure A4.91: S-PA-2 ..... A99
Figure A4.92: S-PA-3 ..... A99
Figure A4.93: S-PA-4 ..... A99
Figure A4.94: S-PA-5 ..... A99
Figure A4.95: S-PA-6 ..... A100
Figure A4.96: S-PA-7 ..... A100
Figure A4.97: S-PA-8 ..... A100
Figure A4.98: S-PA-9 ..... A100
Figure A4.99: S-PA-10 ..... A100
Figure A4.100: S-PA-11 ..... A100
Figure A4.101: S-PA-12 ..... A101
Figure A4.102: S-PA-13 ..... A101
Figure A4.103: S-PA-14 ..... A101
Figure A4.104: S-PA-15 ..... A101
Figure A4.105: S-PAN-1 ..... A101
Figure A4.106: S-PAN-2 ..... A101
Figure A4.107: S-PAN-3 ..... A102
Figure A4.108: S-PAN-4 ..... A102
Figure A4.109: S-PAN-5 ..... A102
Figure A4.110: S-PAN-6 ..... A102
Figure A4.111: S-PAN-7 ..... A102
Figure A4.112: S-PAN-8 ..... A102
Figure A4.113: S-PAN-9 ..... A103

Figure A4.114: S-PAN-10 ..... A103
Figure A4.115: S-PAN-12 ..... A103
Figure A4.116: S-PAN-13 ..... A103
Figure A4.117: S-PAN-14 ..... A103
Figure A4.118: S-PAN-15 ..... A103
Figure A4.119: S-PN-1 ..... A104
Figure A4.120: S-PN-2 ..... A104
Figure A4.121: S-PN-3 ..... A104
Figure A4.122: S-PN-4 ..... A104
Figure A4.123: S-PN-5 ..... A104
Figure A4.124: S-PN-6 ..... A104
Figure A4.125: S-PN-7 ..... A105
Figure A4.126: S-PN-8 ..... A105
Figure A4.127: S-PN-9 ..... A105
Figure A4.128: S-PN-10 ..... A105
Figure A4.129: S-PN-11 ..... A105
Figure A4.130: S-PN-12 ..... A105
Figure A4.131: S-PN-13 ..... A106
Figure A4.132: S-PN-14 ..... A106
Figure A4.133: S-PN-15 ..... A106
Figure A4.134: S-PMT1-1 ..... A106
Figure A4.135: S-PMT1-2 ..... A106
Figure A4.136: S-PMT1-3 ..... A106
Figure A4.137: S-PMT1-4 ..... A107
Figure A4.138: S-PMT1-5 ..... A107
Figure A4.139: S-PMT1-6 ..... A107
Figure A4.140: S-PMT1-7 ..... A107
Figure A4.141: S-PMT1-8 ..... A107
Figure A4.142: S-PMT1-9 ..... A107
Figure A4.143: S-PMT1-10 ..... A108
Figure A4.144: S-PMT1-11 ..... A108
Figure A4.145: S-PMT1-12 ..... A108
Figure A4.146: S-PMT1-13 ..... A108
Figure A4.147: S-PMT1-14 ..... A108
Figure A4.148: S-PMT1-15 ..... A108
Figure A4.149: S-PMT2-1 ..... A109
Figure A4.150: S-PMT2-2 ..... A109
Figure A4.151: S-PMT2-3 ..... A109
Figure A4.152: S-PMT2-4 ..... A109
Figure A4.153: S-PMT2-5 ..... A109
Figure A4.154: S-PMT2-6 ..... A109
Figure A4.155: S-PMT2-7 ..... A110
Figure A4.156: S-PMT2-8 ..... A110
Figure A4.157: S-PMT2-9 ..... A110
Figure A4.158: S-PMT2-10 ..... A110
Figure A4.159: S-PMT2-11 ..... A110

Figure A4.160: S-PMT2-12 ..... A110
Figure A4.161: S-PMT2-13 ..... A111
Figure A4.162: S-PMT2-14 ..... A111
Figure A4.163: S-PMT2-15 ..... A111
Figure A4.164: S-PMT3-1 ..... A111
Figure A4.165: S-PMT3-2 ..... A111
Figure A4.166: S-PMT3-3 ..... A111
Figure A4.167: S-PMT3-4 ..... A112
Figure A4.168: S-PMT3-5 ..... A112
Figure A4.169: S-PMT3-6 ..... A112
Figure A4.170: S-PMT3-7 ..... A112
Figure A4.171: S-PMT3-8 ..... A112
Figure A4.172: S-PMT3-9 ..... A112
Figure A4.173: S-PMT3-10 ..... A113
Figure A4.174: S-PMT3-11 ..... A113
Figure A4.175: S-PMT3-12 ..... A113
Figure A4.176: S-PMT3-13 ..... A113
Figure A4.177: S-PMT3-14 ..... A113
Figure A4.178: S-PMT3-15 ..... A113
Figure A4.179: WG-O1 ..... A114
Figure A4.180: WG-O2 ..... A114
Figure A4.181: WG-P1 ..... A114
Figure A4.182: WG-P2 ..... A114
Figure A4.183: WG-P3 ..... A114
Figure A4.184: LN-O1 ..... A114
Figure A4.185: LN-O2 ..... A115
Figure A4.186: LN-P1 ..... A115
Figure A4.187: LN-P2 ..... A115
Figure A4.188: LN-P3 ..... A115

Figure B1.1: W-OAP Construction Schematic B2
Figure B1.2: W-OAP Average Envelope Curves B4
Figure B1.3: W-OAP Average Displacement Components B4
Figure B1.4: W-OAP Average Cyclic Stiffness Degradation vs. Interstory Drift B5
Figure B1.5: W-OAP Average Energy Values vs. Interstory Drift B5
Figure B1.6: W-OAP Average Equivalent Viscous Damping Ratios vs. Interstory Drift B6
Figure B1.7: View of Primed Specimen B7
Figure B1.8: Adhesive Failure B7
Figure B1.9: W-OAP-1 Hysteresis Envelope and EEEP Curve B9
Figure B1.10: W-OAP-1 Displacement Components B9
Figure B1.11: W-OAP-1 Cyclic Stiffness Degradation vs. Interstory Drift B10
Figure B1.12: W-OAP-1 Energy Values vs. Interstory Drift B10
Figure B1.13: W-OAP-1 Equivalent Viscous Damping Ratios vs. Interstory Drift B11
Figure B1.14: W-OAP-1 Forcing Function B11
Figure B1.15: W-OAP-1 Bottom Plate Displacement B12
Figure B1.16: W-OAP-1 Diagonal String Potentiometer Displacements B12

Figure B1.17: W-OAP-1 Bottom Plate Uplift B12
Figure B1.18: Adhesive De-bonding Along Top Plate B13
Figure B1.19: Adhesive Residue on OSB and Stud B13
Figure B1.20: W-OAP-2 Hysteresis Envelope and EEEP Curve B15
Figure B1.21: W-OAP-2 Displacement Components B15
Figure B1.22: W-OAP-2 Cyclic Stiffness Degradation vs. Interstory Drift B16
Figure B1.23: W-OAP-2 Energy Values vs. Interstory Drift B16
Figure B1.24: W-OAP-2 Equivalent Viscous Damping Ratios vs. Interstory Drift B17
Figure B1.25: W-OAP-2 Forcing Function B17
Figure B1.26: W-OAP-2 Bottom Plate Displacement B18
Figure B1.27: W-OAP-2 Diagonal String Potentiometer Displacements B18
Figure B1.28: W-OAP-2 Bottom Plate Uplift B18
Figure B1.29: Collapse of Sheathing B19
Figure B1.30: Adhesive Residue on OSB and Stud B19
Figure B1.31: W-OAP-3 Hysteresis Envelope and EEEP Curve B21
Figure B1.32: W-OAP-3 Displacement Components B21
Figure B1.33: W-OAP-3 Cyclic Stiffness Degradation vs. Interstory Drift B22
Figure B1.34: W-OAP-3 Energy Values vs. Interstory Drift B22
Figure B1.35: W-OAP-3 Equivalent Viscous Damping Ratios vs. Interstory Drift B23
Figure B1.36: W-OAP-3 Forcing Function B23
Figure B1.37: W-OAP-3 Bottom Plate Displacement B24
Figure B1.38: W-OAP-3 Diagonal String Potentiometer Displacements B24
Figure B1.39: W-OAP-3 Bottom Plate Uplift B24
Figure B2.1: W-OAS Construction Schematic B25
Figure B2.2: W-OAS Average Envelope Curves B27
Figure B2.3: W-OAS Average Displacement Components B27
Figure B2.4: W-OAS Average Cyclic Stiffness Degradation vs. Interstory Drift B28
Figure B2.5: W-OAS Average Energy Values vs. Interstory Drift B28
Figure B2.6: W-OAS Average Equivalent Viscous Damping Ratios vs. Interstory Drift B29
Figure B2.7: Complete Adhesive Failure at the OSB Bond B30
Figure B2.8: Minimal Stud Separation at Corners B30
Figure B2.9: W-OAS-1 Hysteresis Envelope and EEEP Curve B32
Figure B2.10: W-OAS-1 Displacement Components B32
Figure B2.11: W-OAS-1 Cyclic Stiffness Degradation vs. Interstory Drift B33
Figure B2.12: W-OAS-1 Energy Values vs. Interstory Drift B33
Figure B2.13: W-OAS-1 Equivalent Viscous Damping Ratios vs. Interstory Drift B34
Figure B2.14: W-OAS-1 Forcing Function B34
Figure B2.15: W-OAS-1 Bottom Plate Displacement B35
Figure B2.16: W-OAS-1 Diagonal String Potentiometer Displacements B35
Figure B2.17: W-OAS-1 Bottom Plate Uplift B35
Figure B2.18: Complete Adhesive Failure at OSB Bond B36
Figure B2.19: W-OAS-2 Hysteresis Envelope and EEEP Curve B38
Figure B2.20: W-OAS-2 Displacement Components B38
Figure B2.21: W-OAS-2 Cyclic Stiffness Degradation vs. Interstory Drift B39
Figure B2.22: W-OAS-2 Energy Values vs. Interstory Drift B39
Figure B2.23: W-OAS-2 Equivalent Viscous Damping Ratios vs. Interstory Drift B40

Figure B2.24: W-OAS-2 Forcing Function B40
Figure B2.25: W-OAS-2 Bottom Plate Displacement B41
Figure B2.26: W-OAS-2 Diagonal String Potentiometer Displacements B41
Figure B2.27: W-OAS-2 Bottom Plate Uplift B41
Figure B2.28: Adhesive Residue on Corner Sheathing B42
Figure B2.29: W-OAS-3 Hysteresis Envelope and EEEP Curve B44
Figure B2.30: W-OAS-3 Displacement Components B44
Figure B2.31: W-OAS-3 Cyclic Stiffness Degradation vs. Interstory Drift B45
Figure B2.32: W-OAS-3 Energy Values vs. Interstory Drift B45
Figure B2.33: W-OAS-3 Equivalent Viscous Damping Ratios vs. Interstory Drift B46
Figure B2.34: W-OAS-3 Forcing Function B46
Figure B2.35: W-OAS-3 Bottom Plate Displacement B47
Figure B2.36: W-OAS-3 Diagonal String Potentiometer Displacements B47
Figure B2.37: W-OAS-3 Bottom Plate Uplift B47
Figure B3.1: W-ON Construction Schematic B48
Figure B3.2: W-ON Average Envelope Curves B50
Figure B3.3: W-ON Average Displacement Components B50
Figure B3.4: W-ON Average Cyclic Stiffness Degradation vs. Interstory Drift B51
Figure B3.5: W-ON Average Energy Values vs. Interstory Drift B51
Figure B3.6: W-ON Average Equivalent Viscous Damping Ratios vs. Interstory Drift B52
Figure B3.7: Nail Pull-Out at Sheathing Perimeter B53
Figure B3.8: W-ON-1 Hysteresis Envelope and EEEP Curve B55
Figure B3.9: W-ON-1 Displacement Components B55
Figure B3.10: W-ON-1 Cyclic Stiffness Degradation vs. Interstory Drift B56
Figure B3.11: W-ON-1 Energy Values vs. Interstory Drift B56
Figure B3.12: W-ON-1 Equivalent Viscous Damping Ratios vs. Interstory Drift B57
Figure B3.13: W-ON-1 Forcing Function B57
Figure B3.14: W-ON-1 Bottom Plate Displacement B58
Figure B3.15: W-ON-1 Diagonal String Potentiometer Displacements B58
Figure B3.16: W-ON-1 Bottom Plate Uplift B58
Figure B3.17: Overall Wall Layout B59
Figure B3.18: W-ON-2 Hysteresis Envelope and EEEP Curve B61
Figure B3.19: W-ON-2 Displacement Components B61
Figure B3.20: W-ON-2 Cyclic Stiffness Degradation vs. Interstory Drift B62
Figure B3.21: W-ON-2 Energy Values vs. Interstory Drift B62
Figure B3.22: W-ON-2 Equivalent Viscous Damping Ratios vs. Interstory Drift B63
Figure B3.23: W-ON-2 Forcing Function B63
Figure B3.24: W-ON-2 Bottom Plate Displacement B64
Figure B3.25: W-ON-2 Diagonal String Potentiometer Displacements B64
Figure B3.26: W-ON-2 Bottom Plate Uplift B64
Figure B3.27: Edge Vs. Interior Stud Pull-Out B65
Figure B3.28: W-ON-3 Hysteresis Envelope and EEEP Curve B67
Figure B3.29: W-ON-3 Displacement Components B67
Figure B3.30: W-ON-3 Cyclic Stiffness Degradation vs. Interstory Drift B68
Figure B3.31: W-ON-3 Energy Values vs. Interstory Drift B68
Figure B3.32: W-ON-3 Equivalent Viscous Damping Ratios vs. Interstory Drift B69

Figure B3.33: W-ON-3 Forcing Function B69
Figure B3.34: W-ON-3 Bottom Plate Displacement B70
Figure B3.35: W-ON-3 Diagonal String Potentiometer Displacements B70
Figure B3.36: W-ON-3 Bottom Plate Uplift B70
Figure B4.1: W-OAN Construction Schematic B71
Figure B4.2: W-OAN Average Envelope Curves B73
Figure B4.3: W-OAN Average Displacement Components B73
Figure B4.4: W-OAN Average Cyclic Stiffness Degradation vs. Interstory Drift B74
Figure B4.5: W-OAN Average Energy Values vs. Interstory Drift B74
Figure B4.6: W-OAN Average Equivalent Viscous Damping Ratios vs. Interstory Drift B75
Figure B4.7: Top Plate Separation B76
Figure B4.8: Adhesive Failure B76
Figure B4.9: W-OAN-3 Hysteresis Envelope and EEEP Curve B78
Figure B4.10: W-OAN-3 Displacement Components B78
Figure B4.11: W-OAN-3 Cyclic Stiffness Degradation vs. Interstory Drift B79
Figure B4.12: W-OAN-3 Energy Values vs. Interstory Drift B79
Figure B4.13: W-OAN-3 Equivalent Viscous Damping Ratios vs. Interstory Drift B80
Figure B4.14: W-OAN-3 Forcing Function B80
Figure B4.15: W-OAN-3 Bottom Plate Displacement B81
Figure B4.16: W-OAN-3 Diagonal String Potentiometer Displacements B81
Figure B4.17: W-OAN-3 Bottom Plate Uplift B81
Figure B4.18: Separation of Sheathing and Framing Members B82
Figure B4.19: Adhesive Failure B82
Figure B4.20: W-OAN-4 Hysteresis Envelope and EEEP Curve B84
Figure B4.21: W-OAN-4 Displacement Components B84
Figure B4.22: W-OAN-4 Cyclic Stiffness Degradation vs. Interstory Drift B85
Figure B4.23: W-OAN-4 Energy Values vs. Interstory Drift B85
Figure B4.24: W-OAN-4 Equivalent Viscous Damping Ratios vs. Interstory Drift B86
Figure B4.25: W-OAN-4 Forcing Function B86
Figure B4.26: W-OAN-4 Bottom Plate Displacement B87
Figure B4.27: W-OAN-4 Diagonal String Potentiometer Displacements B87
Figure B4.28: W-OAN-4 Bottom Plate Uplift B87
Figure B4.29: Adhesive Failure at Anchor Point B88
Figure B4.30: W-OAN-5 Hysteresis Envelope and EEEP Curve B90
Figure B4.31: W-OAN-5 Displacement Components B90
Figure B4.32: W-OAN-5 Cyclic Stiffness Degradation vs. Interstory Drift B91
Figure B4.33: W-OAN-5 Energy Values vs. Interstory Drift B91
Figure B4.34: W-OAN-5 Equivalent Viscous Damping Ratios vs. Interstory Drift B92
Figure B4.35: W-OAN-5 Forcing Function B92
Figure B4.36: W-OAN-5 Bottom Plate Displacement B93
Figure B4.37: W-OAN-5 Diagonal String Potentiometer Displacements B93
Figure B4.38: W-OAN-5 Bottom Plate Uplift B93
Figure B5.1: W-PA Construction Schematic B94
Figure B5.2: W-PA Average Envelope Curves B96
Figure B5.3: W-PA Average Displacement Components B96
Figure B5.4: W-PA Average Cyclic Stiffness Degradation vs. Interstory Drift B97

Figure B5.5: W-PA Average Energy Values vs. Interstory Drift B97
Figure B5.6: W-PA Average Equivalent Viscous Damping Ratios vs. Interstory Drift B98
Figure B5.7: Plywood Adhesive Failure B99
Figure B5.8: Small Stud Separation B99
Figure B5.9: W-PA-1 Hysteresis Envelope and EEEP Curve B101
Figure B5.10: W-PA-1 Displacement Components B101
Figure B5.11: W-PA-1 Cyclic Stiffness Degradation vs. Interstory Drift B102
Figure B5.12: W-PA-1 Energy Values vs. Interstory Drift B102
Figure B5.13: W-PA-1 Equivalent Viscous Damping Ratios vs. Interstory Drift B103
Figure B5.14: W-PA-1 Forcing Function B103
Figure B5.15: W-PA-1 Bottom Plate Displacement B104
Figure B5.16: W-PA-1 Diagonal String Potentiometer Displacements B104
Figure B5.17: W-PA-1 Bottom Plate Uplift B104
Figure B5.18: Adhesive Bridging B105
Figure B5.19: Centerline Failure B105
Figure B5.20: W-PA-2 Hysteresis Envelope and EEEP Curve B107
Figure B5.21: W-PA-2 Displacement Components B107
Figure B5.22: W-PA-2 Cyclic Stiffness Degradation vs. Interstory Drift B108
Figure B5.23: W-PA-2 Energy Values vs. Interstory Drift B108
Figure B5.24: W-PA-2 Equivalent Viscous Damping Ratios vs. Interstory Drift B109
Figure B5.25: W-PA-2 Forcing Function B109
Figure B5.26: W-PA-2 Bottom Plate Displacement B110
Figure B5.27: W-PA-2 Diagonal String Potentiometer Displacements B110
Figure B5.28: W-PA-2 Bottom Plate Uplift B110
Figure B5.29: Adhesive Bridging at Anchor Point B111
Figure B5.30: Adhesive Residue at Centerline B111
Figure B5.31: W-PA-3 Hysteresis Envelope and EEEP Curve B113
Figure B5.32: W-PA-3 Displacement Components B113
Figure B5.33: W-PA-3 Cyclic Stiffness Degradation vs. Interstory Drift B114
Figure B5.34: W-PA-3 Energy Values vs. Interstory Drift B114
Figure B5.35: W-PA-3 Equivalent Viscous Damping Ratios vs. Interstory Drift B115
Figure B5.36: W-PA-3 Forcing Function B115
Figure B5.37: W-PA-3 Bottom Plate Displacement B116
Figure B5.38: W-PA-3 Diagonal String Potentiometer Displacements B116
Figure B5.39: W-PA-3 Bottom Plate Uplift B116
Figure B6.1: W-PN Construction Schematic B117
Figure B6.2: W-PN Average Envelope Curves B119
Figure B6.3: W-PN Average Displacement Components B119
Figure B6.4: W-PN Average Cyclic Stiffness Degradation vs. Interstory Drift B120
Figure B6.5: W-PN Average Energy Values vs. Interstory Drift B120
Figure B6.6: W-PN Average Equivalent Viscous Damping Ratios vs. Interstory Drift B121
Figure B6.7: Sheathing Nail Pull-Out B122
Figure B6.8: Small Top Plate Separation B122
Figure B6.9: W-PN-1 Hysteresis Envelope and EEEP Curve B124
Figure B6.10: W-PN-1 Displacement Components B124
Figure B6.11: W-PN-1 Cyclic Stiffness Degradation vs. Interstory Drift B125

Figure B6.12: W-PN-1 Energy Values vs. Interstory Drift B125
Figure B6.13: W-PN-1 Equivalent Viscous Damping Ratios vs. Interstory Drift..... B126
Figure B6.14: W-PN-1 Forcing Function B126
Figure B6.15: W-PN-1 Bottom Plate Displacement..... B127
Figure B6.16: W-PN-1 Diagonal String Potentiometer Displacements B127
Figure B6.17: W-PN-1 Bottom Plate Uplift B127
Figure B6.18: Complete Failure of Interior Wall Structure..... B128
Figure B6.19: W-PN-2 Hysteresis Envelope and EEEP Curve B130
Figure B6.20: W-PN-2 Displacement Components..... B130
Figure B6.21: W-PN-2 Cyclic Stiffness Degradation vs. Interstory Drift..... B131
Figure B6.22: W-PN-2 Energy Values vs. Interstory Drift B131
Figure B6.23: W-PN-2 Equivalent Viscous Damping Ratios vs. Interstory Drift..... B132
Figure B6.24: W-PN-2 Forcing Function B132
Figure B6.25: W-PN-2 Bottom Plate Displacement..... B133
Figure B6.26: W-PN-2 Diagonal String Potentiometer Displacements B133
Figure B6.27: W-PN-2 Bottom Plate Uplift B133
Figure B6.28: Interior Studs Separate from Sole Plate..... B134
Figure B6.29: W-PN-3 Hysteresis Envelope and EEEP Curve B136
Figure B6.30: W-PN-3 Displacement Components..... B136
Figure B6.31: W-PN-3 Cyclic Stiffness Degradation vs. Interstory Drift..... B137
Figure B6.32: W-PN-3 Energy Values vs. Interstory Drift B137
Figure B6.33: W-PN-3 Equivalent Viscous Damping Ratios vs. Interstory Drift..... B138
Figure B6.34: W-PN-3 Forcing Function B138
Figure B6.35: W-PN-3 Bottom Plate Displacement..... B139
Figure B6.36: W-PN-3 Diagonal String Potentiometer Displacements B139
Figure B6.37: W-PN-3 Bottom Plate Uplift B139
Figure B7.1: W-PAN Construction Schematic..... B140
Figure B7.2: W-PAN Average Envelope Curves B142
Figure B7.3: W-PAN Average Displacement Components B142
Figure B7.4: W-PAN Average Cyclic Stiffness Degradation vs. Interstory Drift..... B143
Figure B7.5: W-PAN Average Energy Values vs. Interstory Drift B143
Figure B7.6: W-PAN Average Equivalent Viscous Damping Ratios vs. Interstory Drift B144
Figure B7.7: Separation of Studs from Top Plate..... B145
Figure B7.8: Adhesive Failure and Stud Separation..... B145
Figure B7.9: W-PAN-1 Hysteresis Envelope and EEEP Curve B147
Figure B7.10: W-PAN-1 Displacement Components..... B147
Figure B7.11: W-PAN-1 Cyclic Stiffness Degradation vs. Interstory Drift..... B148
Figure B7.12: W-PAN-1 Energy Values vs. Interstory Drift B148
Figure B7.13: W-PAN-1 Equivalent Viscous Damping Ratios vs. Interstory Drift..... B149
Figure B7.14: W-PAN-1 Forcing Function B149
Figure B7.15: W-PAN-1 Bottom Plate Displacement..... B150
Figure B7.16: W-PAN-1 Diagonal String Potentiometer Displacements B150
Figure B7.17: W-PAN-1 Bottom Plate Uplift B150
Figure B7.18: Failure of Adhesive and Mechanical Fasteners..... B151
Figure B7.19: W-PAN-2 Hysteresis Envelope and EEEP Curve B153
Figure B7.20: W-PAN-2 Displacement Components..... B153

Figure B7.21: W-PAN-2 Cyclic Stiffness Degradation vs. Interstory Drift B154
Figure B7.22: W-PAN-2 Energy Values vs. Interstory Drift B154
Figure B7.23: W-PAN-2 Equivalent Viscous Damping Ratios vs. Interstory Drift B155
Figure B7.24: W-PAN-2 Forcing Function B155
Figure B7.25: W-PAN-2 Bottom Plate Displacement B156
Figure B7.26: W-PAN-2 Diagonal String Potentiometer Displacements B156
Figure B7.27: W-PAN-2 Bottom Plate Uplift B156
Figure B7.28: Adhesive Residue on Plywood B157
Figure B7.29: Top Plate Separation B157
Figure B7.30: W-PAN-3 Hysteresis Envelope and EEEP Curve B159
Figure B7.31: W-PAN-3 Displacement Components B159
Figure B7.32: W-PAN-3 Cyclic Stiffness Degradation vs. Interstory Drift B160
Figure B7.33: W-PAN-3 Energy Values vs. Interstory Drift B160
Figure B7.34: W-PAN-3 Equivalent Viscous Damping Ratios vs. Interstory Drift B161
Figure B7.35: W-PAN-3 Forcing Function B161
Figure B7.36: W-PAN-3 Bottom Plate Displacement B162
Figure B7.37: W-PAN-3 Diagonal String Potentiometer Displacements B162
Figure B7.38: W-PAN-3 Bottom Plate Uplift B162

Index of Tables

Table 3.1: Specimen Abbreviations 27
Table 3.2: Connection Specimen List 28
Table 3.3: Wall Specimen List 29
Table 3.4: Design Values for No. 2 Grade Spruce-Pine-Fir (AF&PA 2001) 30
Table 3.5: Sheathing Material Properties (APA 2002) 31
Table 3.6: Adhesive Tape General Properties 32
Table 3.7: Design Values for Nails in 38 mm (1.5 in.) Spruce-Pine-Fir (AF&PA 2001) 32
Table 3.8: Construction of Full-Scale Shear Walls 56
Table 3.9: Instrumentation Details 61
Table 3.10: CUREE Protocol (0.5 Hz) 66
Table 5.1: Comparison Specimens 83
Table 5.2: Pressure Application Specimens 92
Table 5.3: Summary of Pressure Application Performance Parameters 93
Table 5.4: Peak Load T-Test Results 96
Table 5.5: Peak Displacement T-Test Results 96
Table 5.6: Duration of Pressure Application (Time) Specimens 100
Table 5.7: Summary of Duration of Pressure Application Performance Parameters 101
Table 5.8: Peak Load T-Test Results 104
Table 5.9: Work to Failure (Energy) T-Test Results 105
Table 5.10: Statistically Significant Specimens 107
Table 5.11: Statistically Significant Performance Parameter Summary (Metric) 110
Table 5.12: Statistically Significant Performance Parameter Summary (US Customary) 111
Table 5.13: Peak Load T-Test Results 113
Table 5.14: Displacement at Peak Load T-Test Results 114
Table 5.15: Stiffness T-Test Results 116
Table 5.16: Surface Treatment Performance Gains 122
Table 5.17: Combination System Performance Gains 122
Table 5.18: Performance Comparison Between Systems 126
Table 5.19: Performance of Alternate Manufacturer Tapes vs. 3M VHB 4941 128
Table 5.20: Traditional Adhesive Specimens 131
Table 5.21: Performance of Traditional Construction Adhesive 132
Table 6.1: Wall Specimen List 137
Table 6.2: Connection Test Displacement Ratios 139
Table 6.3: Monotonic and Cyclic Failure Displacements 139
Table 6.4: Full-Scale Shear Wall Performance Parameters 142
Table 6.5: Full-Scale Shear Wall Performance Parameters Per Unit Length 143
Table 6.6: Strength Modifiers to IBC Table 2306.4.1 (ICC 2000) 146
Table 6.7: Displacement Capacity Comparison 148
Table 6.8: Allowable Drift to Height Ratios (ICC 2000) 149
Table 6.9: Elastic Stiffness Comparison of Adhesive to Traditional Shear Walls 152
Table 6.10: Ductility Comparison 157
Table 6.11: Viscous Damping Factors 161
Table 6.12: R-factor Calculations 162

Table 6.13: Displacement Component Percentage Comparison..... 166
Table 6.14: Comparison of Target and Actual Failure Displacements..... 174
Table 6.15: Rough Material Cost for 2.4 m x 2.4 m (8 ft x 8 ft) Shear Wall 176

Table A1.1: Description of Terms Used in Data Records A1
Table A1.2: Data Record Sheet (DRS) for Comparison Series Connection Specimens (1)..... A4
Table A1.3: DRS for Comparison Series Connection Specimens (2) A5
Table A1.4: DRS for Comparison Series Connection Specimens (3) A6
Table A1.5: DRS for Comparison Series Connection Specimens (4) A7
Table A1.6: DRS for Adhesive Application Pressure Connection Specimens (1) A8
Table A1.7: DRS for Adhesive Application Pressure Connection Specimens (2) A9
Table A1.8: DRS for Adhesive Application Pressure Connection Specimens (3) A10
Table A1.9: DRS for Duration of Pressure Application Connections (1) A11
Table A1.10: DRS for Duration of Pressure Application Connections (2) A12
Table A1.11: DRS for Statistically Significant Connection Series – S-OA A13
Table A1.12: DRS for Statistically Significant Connection Series – S-OAS..... A14
Table A1.13: DRS for Statistically Significant Connection Series – S-OAP..... A15
Table A1.14: DRS for Statistically Significant Connection Series – S-OAN A16
Table A1.15: DRS for Statistically Significant Connection Series – S-ON A17
Table A1.16: DRS for Statistically Significant Connection Series – S-PA..... A18
Table A1.17: DRS for Statistically Significant Connection Series – S-PAN..... A19
Table A1.18: DRS for Statistically Significant Connection Series – S-PN..... A20
Table A1.19: DRS for Statistically Significant Connection Series – S-PMT1..... A21
Table A1.20: DRS for Statistically Significant Connection Series – S-PMT2..... A22
Table A1.21: DRS for Statistically Significant Connection Series – S-PMT3..... A23
Table A1.22: DRS for Additional Tests of Interest (Wood Glue & Liquid Nails)..... A24
Table A2.1a: Pressure Application Performance Summary (US Customary Units) A26
Table A2.1b: Pressure Application Performance Summary (Metric)..... A27
Table A2.2a: P-15 Series Performance Parameter Summary (US Customary Units) A28
Table A2.2b: P-15 Series Performance Parameter Summary (Metric Units)..... A28
Table A2.3a: P-30 Series Performance Parameter Summary (US Customary Units) A29
Table A2.3b: P-30 Series Performance Parameter Summary (Metric Units)..... A29
Table A2.4a: P-45 Series Performance Parameter Summary (US Customary Units) A30
Table A2.4b: P-45 Series Performance Parameter Summary (Metric Units)..... A30
Table A2.5a: P-60 Series Performance Parameter Summary (US Customary Units) A31
Table A2.5b: P-60 Series Performance Parameter Summary (Metric Units)..... A31
Table A2.6a: P-80 Series Performance Parameter Summary (US Customary Units) A32
Table A2.6b: P-80 Series Performance Parameter Summary (Metric Units)..... A32
Table A2.7a: P-100 Series Performance Parameter Summary (US Customary Units) A33
Table A2.7b: P-100 Series Performance Parameter Summary (Metric Units)..... A33
Table A2.8a: P-120 Series Performance Parameter Summary (US Customary Units) A34
Table A2.8b: P-120 Series Performance Parameter Summary (Metric Units)..... A34
Table A3.1a: Duration of Pressure Performance Summary (US Customary Units)..... A40
Table A3.1b: Duration of Pressure Performance Summary (Metric) A41
Table A3.2a: T-15 Series Performance Parameter Summary (US Customary Units)..... A42

Table A3.2b: T-15 Series Performance Parameter Summary (Metric Units)..... A42
Table A3.3a: T-30 Series Performance Parameter Summary (US Customary Units)..... A43
Table A3.3b: T-30 Series Performance Parameter Summary (Metric Units)..... A43
Table A3.4a: T-45 Series Performance Parameter Summary (US Customary Units)..... A44
Table A3.4b: T-45 Series Performance Parameter Summary (Metric Units)..... A44
Table A3.5a: T-60 Series Performance Parameter Summary (US Customary Units)..... A45
Table A3.5b: T-60 Series Performance Parameter Summary (Metric Units)..... A45
Table A3.6a: T-90 Series Performance Parameter Summary (US Customary Units)..... A46
Table A3.6b: T-90 Series Performance Parameter Summary (Metric Units)..... A46
Table A3.7a: T-120 Series Performance Parameter Summary (US Customary Units)..... A47
Table A3.7b: T-120 Series Performance Parameter Summary (Metric Units)..... A47
Table A4.1a: Statistically Significant Performance Summary (US Customary Units) A53
Table A4.1b: Statistically Significant Performance Parameter Summary (Metric) A54
Table A4.2a: S-OA Series Performance Parameters (US Customary Units) A55
Table A4.2b: S-OA Series Performance Parameters (Metric Units) A56
Table A4.3a: S-OAS Series Performance Parameters (US Customary Units) A57
Table A4.3b: S-OAS Series Performance Parameters (Metric Units)..... A58
Table A4.4a: S-OAP Series Performance Parameters (US Customary Units) A59
Table A4.4b: S-OAP Series Performance Parameters (Metric Units)..... A60
Table A4.5a: S-OAN Series Performance Parameters (US Customary Units) A61
Table A4.5b: S-OAN Series Performance Parameters (Metric Units) A62
Table A4.6a: S-ON Series Performance Parameters (US Customary Units) A63
Table A4.6b: S-ON Series Performance Parameters (Metric Units) A64
Table A4.7a: S-PA Series Performance Parameters (US Customary Units)..... A65
Table A4.7b: S-PA Series Performance Parameters (Metric Units)..... A66
Table A4.8a: S-PAN Series Performance Parameters (US Customary Units) A67
Table A4.8b: S-PAN Series Performance Parameters (Metric Units)..... A68
Table A4.9a: S-PN Series Performance Parameters (US Customary Units)..... A69
Table A4.9b: S-PN Series Performance Parameters (Metric Units)..... A70
Table A4.10a: S-PMT1 Series Performance Parameters (US Customary Units)..... A71
Table A4.10b: S-PMT1 Series Performance Parameters (Metric Units)..... A72
Table A4.11a: S-PMT2 Series Performance Parameters (US Customary Units)..... A73
Table A4.11b: S-PMT2 Series Performance Parameters (Metric Units)..... A74
Table A4.12a: S-PMT3 Series Performance Parameters (US Customary Units)..... A75
Table A4.12b: S-PMT3 Series Performance Parameters (Metric Units)..... A76
Table A4.13a: Wood Glue Series Performance Parameters (US Customary Units)..... A77
Table A4.13b: Wood Glue Series Performance Parameters (Metric Units)..... A77
Table A4.14a: Liquid Nail Series Performance Parameters (US Customary Units)..... A78
Table A4.14b: Liquid Nail Series Performance Parameters (Metric Units)..... A78

Table B1.1: Average Performance Parameters for W-OAP Series B3
Table B1.2: W-OAP-1 Performance Parameters..... B8
Table B1.3: W-OAP-2 Performance Parameters..... B14
Table B1.4: W-OAP-3 Performance Parameters..... B20
Table B2.1: Average Performance Parameters for W-OAS Series B26
Table B2.2: W-OAS-1 Performance Parameters..... B31

Table B2.3: W-OAS-2 Performance Parameters B37
Table B2.4: W-OAS-3 Performance Parameters B43
Table B3.1: Average Performance Parameters for W-ON Series B49
Table B3.2: W-ON-1 Performance Parameters B54
Table B3.3: W-ON-2 Performance Parameters B60
Table B3.4: W-ON-3 Performance Parameters B66
Table B4.1: Average Performance Parameters for W-OAN Series B72
Table B4.2: W-OAN-3 Performance Parameters B77
Table B4.3: W-OAN-4 Performance Parameters B83
Table B4.4: W-OAN-5 Performance Parameters B89
Table B5.1: Average Performance Parameters for W-PA Series B95
Table B5.2: W-PA-1 Performance Parameters B100
Table B5.3: W-PA-2 Performance Parameters B106
Table B5.4: W-PA-3 Performance Parameters B112
Table B6.1: Average Performance Parameters for W-PN Series B118
Table B6.2: W-PN-1 Performance Parameters B123
Table B6.3: W-PN-2 Performance Parameters B129
Table B6.4: W-PN-3 Performance Parameters B135
Table B7.1: Average Performance Parameters for W-PAN Series B141
Table B7.2: W-PAN-1 Performance Parameters B146
Table B7.3: W-PAN-2 Performance Parameters B152
Table B7.4: W-PAN-3 Performance Parameters B158

Chapter 1

Introduction

1.1 Background

In the United States, approximately 90% of new residential housing is built using wood-framed construction. The market for wood products is immense, with over 20 billion square feet of structural panels consumed by residential construction in 2002, and increases in production forecasted through 2007. Over the next five years, over 150 mills will increase total production of plywood and oriented strand board panels to approximately 17 billion square feet each (APA 2002). The reasons behind the large market share and incredible growth of timber-based products are simple: wood-framed construction is economical, energy efficient, and renewable.

Use of engineered wood materials in residential housing provides a savings of up to 30% when compared to other traditional construction materials. Wood is an excellent natural insulator, and combined with new products such as structurally insulated panels (SIPs), even the strictest energy regulations can easily be exceeded. Also, contrary to popular belief, the wood industry has made great strides in forest regulation and is now growing 27% more timber each year than it is harvesting (Wood Promotion Network 2003). Therefore, it is obvious that a large portion of the infrastructure in the U.S. and many other countries, both currently and for the foreseeable future, depends on wood-framed construction. To protect this infrastructure from natural disasters and other hazards, a continuing effort towards developing and testing new products and engineering methods is being made. Through the results of such research, safety and integrity of commercial and residential structures may be maintained.

Wood-framed construction has historically performed well in natural disasters such as earthquakes due to the relatively light mass of the structure as well as the large number of redundancies present in typical framing (Dolan 1989). Recent events have, however, pointed out that the performance of wood-framed structures is still in need of improvement. Over half of the property damage and 24 of the 25 fatalities in the 1994 Northridge, California, earthquake were due to damages associated with wood-framed buildings (Krawinkler et al., 2001). In addition to earthquakes, hurricanes also pose a sizable risk. Hurricanes Andrew and Hugo claimed almost 150 lives, and the economic losses resulting from these storms totaled over 33 billion dollars.

Statistics such as these have led to a concerted effort by the research contingent and construction industries to develop safer buildings through improved design and stronger, more efficient, construction techniques. This thesis is another step towards the goal of developing such buildings.

Currently over 90% of the nation's population lives in seismically active areas (as cited by Salenikovich 2000), and a large portion of the infrastructure on the East Coast and Gulf of Mexico are directly affected by potential hurricanes. Lateral loads due to wind and seismic events place shear forces on buildings that must be effectively resisted by the structure to prevent catastrophic failure. In construction of larger commercial buildings, these shear forces are typically resisted by the concrete core surrounding elevator shafts and stairwells, along with other forms of bracing and moment-resisting connections. In residential construction, lateral forces are resisted through the use of diaphragm and shear-wall action. The use of shear walls, as illustrated in Figure 1.1, serves to collect the load distributed by an elevated floor or roof diaphragm and transfer it into the building's foundation. Experimental testing has proven that the strength of shear walls primarily results from the fasteners between the sheathing panels and the main framing system (Dolan 1989), and these connections are the focus of this study.

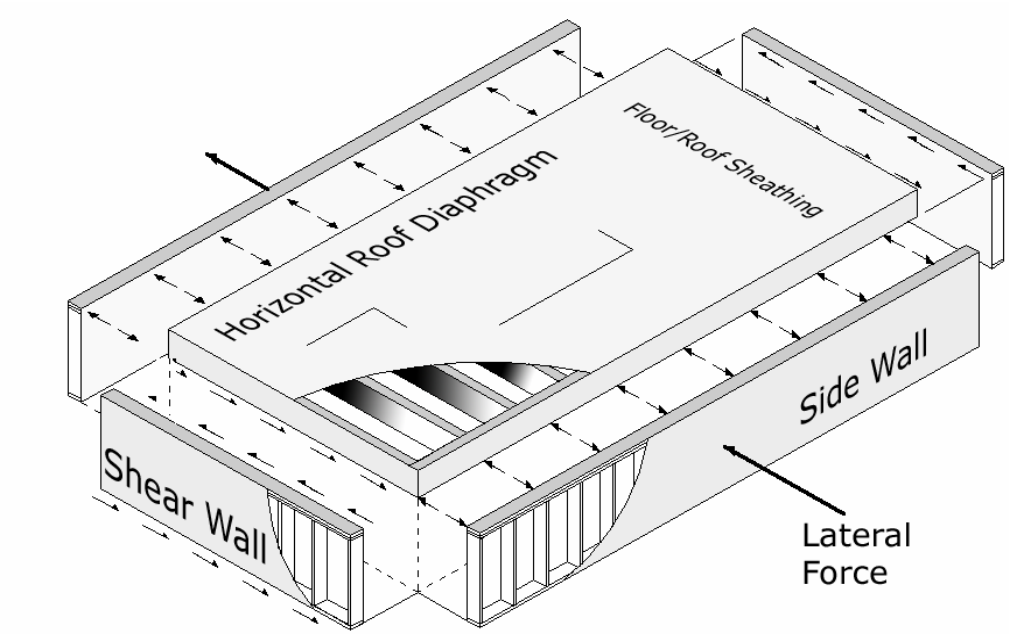

Figure 1.1: Diaphragm and Shear Wall Action (After Diekmann 1995)

Currently the connection between sheathing panels and main framing members is most commonly provided by dowel-type mechanical fasteners such as nails. Other mechanical connections, including spot welding and riveting, have also been used in the commercial construction and automotive industries for many years. In the past twenty years, however, the use of special purpose adhesives has become more common for such connections due to their continuous bonding capabilities, increased stiffness, and greater durability. Of particular interest to this study is the use of acrylic foam pressure sensitive adhesive (PSA) tapes.

Acrylic foam adhesive tapes were developed approximately twenty-five years ago and are composed of lightly crosslinked viscoelastic polymers (Heitman, 1990). Acrylic foam adhesives are commonly manufactured as two-sided tapes with a liner backing as illustrated in Figure 1.2. As the name implies, PSA tapes are activated through the use of an applied pressure as opposed to the chemical activation process required by many other high performance adhesives. The viscoelastic nature of the polymers means that formation of too many crosslinks or the presence of extremely low temperatures causes the adhesive tape to behave like a solid, while extremely high temperatures and low crosslinking tends to make the tape behave as a liquid.

Figure 1.2: Typical Foam Tape Cross Section

Current general uses of acrylic foam tapes include the bonding of small electronic components for shock absorption, the bonding of aluminum street signs to frames to prevent unsightly rivets and to provide increased wind resistance, and even the bonding of steel scuff strips to aluminum airplane wings (3M 1998). Use of acrylic foam PSA tapes in the construction industry has thus far been limited to the attachment of architectural cladding and glazing for curtain wall systems. This study further investigates the expansion of these construction uses to include residential housing applications in which the tape is used as a primary structural element of the load-resisting system of the house itself.

Two main structural uses of PSA tapes in housing construction are proposed. The first use is for the attachment of roof panels to houses in hurricane-prone areas. The adhesive tape could strengthen the roof panels against uplift winds while minimizing water intrusion into the structure. Water damage is the major cause of property damage in hurricanes, and this added benefit is worth significant research. The second main structural use, and the use that this study addresses, is to strengthen the previously-discussed connection between sheathing and framing elements in shear walls.

1.2 Objectives

There are two primary objectives for this study. The first objective is to develop a database of performance parameters for the bonding of wood substrates with acrylic foam pressure sensitive adhesive tape. Results of this objective will determine the feasibility of bonding wood with adhesives that have been previously used only on smoother materials such as aluminum and glass. The completed database can be used to describe adhesive connection characteristics in finite element models for further study.

The second main objective is to investigate the performance of full-scale walls constructed with PSA tape under reversed-cyclic (quasi-static) loading. Results of these tests will determine if such wall configurations can provide improvements over traditional construction methods under seismic and hurricane-level loads. Other objectives which complement the main purposes are as follows:

- Compare the effect of plywood versus oriented strand board sheathing on connection and wall performance.

- Explore possible ways to increase bonding of the adhesive tape through the use of sheathing surface treatments such as sanding and priming.

- Investigate and compare the difference in performance between wall configurations utilizing traditional mechanical fasteners, PSA tapes, and a combination of the two.

- Compare the performance of a minimum of three different manufacturers' tapes to determine the applicability of results to alternate products.

- Develop appropriate design tables and earthquake response parameters for the seismic and wind design of walls constructed with adhesive tape.

- Determine the effect of moisture content and temperature on wall performance.

- Observe and comment upon the use of the recently developed CUREE displacement protocol and its effect on test results.

- Investigate failure modes and determine the different deformation factors affecting the overall displacement of each wall configuration.

These objectives have been met through the experimental testing of a large number of connection and full-scale wall specimens. Each different connection configuration was tested 15 times to allow for a high confidence in and statistical analysis of the results. Only three different specimens for each shear wall configuration were tested due to the time and expense required for full-scale experiments. Data taken from each connection and wall specimen was analyzed to determine performance parameters such as peak load and displacement, failure load and displacement, yielding point, elastic stiffness, cyclic stiffness, ductility, and damping. These parameters and results are further defined within the body of this report.

1.3 Applications

The results presented in this thesis provide knowledge of the strength and seismic resistance of wood connections and shear walls constructed with acrylic foam pressure sensitive adhesive tape. These results can be directly applied to the design and construction of adhesive-based walls using recommended methods and examples provided in this thesis. Results are applicable to a number of different adhesive tape and sheathing panel products. Design values for other PSA tape products can be easily developed from the results of this report through the completion and comparison of a small number of connection tests. Loading curves and hysteretic properties of the adhesive tapes can also be applied to finite element based analytical models as previously mentioned. This research provides a basis upon which new structural uses for PSA tapes in housing construction can be developed.

1.4 Thesis Organization

Based on previously published research, Chapter 2 presents a brief background behind the use of adhesives involving timber connections as well as an overview of recent topics and developments in wood adhesion. Prior studies on the performance characteristics of acrylic foam pressure sensitive adhesive tapes are also discussed, though no previous research on their use with wood substrates is believed to exist. Due to the large number of excellent literature reviews on traditional shear wall performance and mechanics that have already been conducted, this topic is only briefly touched upon. Further attention is given to the topics of loading regimes and computer analysis techniques.

Chapter 3 provides an experimental plan for the testing of both connections and shear walls. The discussion includes descriptions of materials, instrumentation, construction details, methods of tape application, and testing procedures.

Chapter 4 defines the performance parameters used to compare monotonic connection and shear wall tests as well as cyclic tests. Typical equations and figures are provided to further clarify each term.

Chapter 5 presents results of the connection test study. Each part of the four-part study is discussed in detail, and observations and conclusions are displayed in comparison charts and figures. Statistical analysis results for each performance parameter are also provided. Failure modes are presented and commented upon through the use of both photographs and discussion.

Chapter 6 presents results of the full-scale shear wall testing. Monotonic and cyclic results are discussed and compared. Recommendations on the use of adhesive tape walls in both high wind and seismic zones are made, and design examples are provided for each case.

Chapter 7 focuses on the answers developed to achieve the objectives set forth in this study. Additional observations and recommendations are provided, and a list of pertinent future research is given.

The Appendix of this report represents a valuable resource for future research. Data for all connection and wall tests is presented, analyzed, and commented upon. Additional photographs of full-scale wall failures as well as further data on testing times, moisture contents, and tape designations are also located in the Appendix.

1.5 Limitations of Study

The time and expense required for the testing of full-scale shear wall specimens limited the number of variables that could be investigated by this study. Though connection testing was performed on three different manufacturer's adhesive tapes, only a single tape was used on the construction of all full-scale wall specimens. Also, the species of framing, geometry of wall, type of mechanical fasteners, and nail schedule all remained constant throughout testing. Finally, all walls were fitted with hold-downs on both ends and contained no openings in the sheathing panels.

Further limitations to this study involve the lack of two-sided testing with such materials as drywall or additional sheathing panels. The addition of drywall and other finishes can have a measurable effect on the strength and seismic performance of wall configurations, and the reader is directed to the work performed by previous researchers such as Toothman (2003) for further information on these effects.

As with all tests involving timber products, the structural and mechanical properties of the material varied. Though grade limits were imposed for sheathing and framing members, the locations of knots, initial moisture contents, and exact member strengths are beyond the control of the experimenter. Additionally, the properties of full-scale wall specimens rely partially on the skill of the carpenter who built them. All of these considerations are, however, taken into account in the acceptable range of values associated with wood-framed construction.

Connection testing was performed monotonically, and the majority of full-scale wall tests were performed using a reversed-cyclic (quasi-static) protocol. Dynamic shake-table tests were not performed due to the lack of proper equipment as well as to provide a reasonable limit on the scope of this study.

Finally, this project consisted solely of experimental testing and the resulting observations and design procedures. Use of mechanics or finite-element-based computer models of shear wall results was not explored.

Chapter 2

Literature Survey and Background

2.1 Introduction

This chapter provides an overview of previous research that has been performed on various topics relevant to this thesis. Multiple subjects are reviewed in the following sections including: current use of adhesives in the timber industry, properties and uses of acrylic foam adhesive tape, experimental testing of shear walls, development and characteristics of testing methods and loading protocols, and formulation of numeric modeling programs for connection and shear wall applications. Note that many of these areas of research, in particular development and use of wood adhesives and experimental testing of shear walls, cover a vast amount of data, and their scope is, therefore, limited in favor of more pertinent topics. Where necessary, the reader is directed to other sources and literary reviews containing more specific information. The author is unaware of any previous research pertaining to the use of pressure sensitive adhesives applied to wood substrates; thus, no information on this topic beyond that presented in this thesis is discussed.

2.2 Adhesives in the Timber Industry

Use of adhesives in the timber industry is a continuously growing area of research covering a broad range of products and applications. Different adhesive formulations are used in the manufacturing of plywood and oriented strand board (OSB), the repair of structural timbers, and the development of other engineered wood products such as GLULAM (Glue Laminated) beams. This topic covers widely varying fields of interest. Recent research ranges from the effect of gas cavities and glue outflows in furniture construction (Smardzewski 1999) to the chemical modification of natural resins to increase ductility in plywood panel construction (Barbosa et al., 2000). Though this section does not provide a complete overview of the subject, it does contain information pertinent to the use of wood as an adhesive substrate and a general guide to the path that adhesives have taken in the timber industry.

2.2.1 Wood as a Substrate

Davis (1997) provides an overview of the properties of timber as a substrate as well as the main classes of traditional timber adhesives. Seven main factors for determining the ability of wood to act as an adherend as outlined in Davis's research are: wettability, freedom from contamination, surface roughness, surface soundness, surface uniformity, adhesive compatibility, and stability in the operating environment. Wettability is the measure of the attractive force of the solid wood to the liquid adhesive. This property is affected by surface energy, chemistry, and the surface texture of the material. In general, wood adhesives require the ability to spread out easily in order to achieve maximum molecular contact with the timber substrate. Freedom of contamination is generally necessary for good adhesion on any material. The use of organic solvents or water can normally clean metallic surfaces from oil and other contaminants. This process, however, is ineffective for timber products whose contaminants can originate from the chemicals produced during growth and extracted to the surface. Special care must be taken to bond timber products shortly after their machining to reduce the effects of such chemicals. Rougher surfaces are more difficult to bond with most adhesives and should be avoided when possible. The soundness of a timber surface refers to the particles and inconsistencies left by sanding and cutting. Care should be given to making sure excess particles are removed, and it has been determined that the use of chiseled-type surfaces allows for optimum adhesion. Finally, surface variations such as knots and adhesive compatibility with the moisture and chemical content of the wood surface must be investigated.

2.2.2 Structural Adhesives for Engineered Wood Products

Structural adhesives are used to provide strength as well as stiffness to engineered wood products. These adhesives fall into either interior or exterior application categories depending on their resistance to moisture (APA 1998). Six main adhesives used in the creation of engineered wood products are: casein glues, urea-formaldehyde, phenol-formaldehyde, resorcinol-formaldehyde, phenol-resorcinol formaldehyde, and melamine-urea-formaldehyde (APA 1998). Casein glues have been used in the production of GLULAM timbers since before 1920 (Davis 1997), but they are vulnerable to fungal attacks. Urea-formaldehyde products are versatile but are susceptible to moisture. Phenol-formaldehyde is used in the modern production of plywood

and laminated veneer lumber. Both resorcinol-based products are currently used to produce GLULAM beams, and melamine-urea-formaldehyde products are suitable for some hot-press applications such as OSB fabrication.

2.2.3 Construction Adhesives

The previous section discussed chemical structural adhesives that are used in the production of timber products. Those adhesives typically require additional steps such as mixing and heat-treating to be activated. The focus of this thesis, however, is on the use of adhesives for the joining of wood substrates. For over 30 years, the dominant products in this market have been elastomeric construction adhesives. Elastomeric adhesives have a natural or rubber synthetic base and are generally classified as semi-structural adhesives. Semi-structural adhesives provide increased stiffness to a structural system but do not necessarily provide large strength increases (APA 1998b). Elastomeric adhesives have the advantage of being able to form relatively thick bond lines with a low shear modulus (Hoyle 1981). There are around 40 different APA-approved elastomeric adhesives for floor applications (APA 1994). In this context, the adhesives eliminate floor squeaks and provide an overall stiffer floor system. The composite action of elastomeric adhesives in beams has also been used to provide increased spans (APA 1994). In addition to semi-structural applications, some research on the use of certain elastomeric adhesives for load-bearing uses has been performed.

Research on elastomeric adhesives began in earnest in the 1960s and is currently on going. Countryman and Rose (1970) performed tests on field-glued plywood floor systems for the American Plywood Association. Vick (1971) performed tests on 20 different elastomeric adhesives to determine their ability to maintain strength under different environmental conditions. Hoyle (1976) developed a design procedure for built-up beams and for glued decks along with McGee (1974). Hoyle and Hsu (1978) investigated the shear strength and shear modulus of an elastomeric adhesive under fatigue conditions. Pellicane performed a series of experiments on elastomeric adhesives spanning the past 15 years. Pellicane (1988) performed 360 connection tests on three different bases of elastomeric adhesive to determine the effect of wood species, bond-line thickness, and plywood thickness on their load-slip characteristics. He found that due to the cohesive failure mode within the glue line, the wood species and plywood thickness had no effect on connection performance. Pellicane (1992a, 1992b) performed

research to determine if the combined effect of elastomeric adhesives and mechanical fasteners could be modeled using superposition theory for stiffnesses and loads. He found that superposition provided conservative and fair predictions for the strength and stiffness of the combined adhesive and nail systems at small deflections when the specimens were still elastic. Pellicane and Robinson (1997) numerically evaluated 16,000 light-frame, structural floor systems to analyze the effect of construction adhesives and joint variability on their deflection. Pellicane *et al.* (1999) tested the effect of wet and dry specimen fabrication and testing on three different construction adhesives. Additionally, the effect of chromate-copper-arsenic treatment was explored. They found that the construction conditions were of little consequence as long as testing conditions were fairly dry. They also concluded that the chemical treatment had no effect on performance. The use of elastomeric adhesives for certain applications is integral to the construction industry, and research into their behavior and performance will continue.

2.3 Acrylic Foam Adhesive Tape

Acrylic foam adhesive tapes have been available for over 20 years and are currently manufactured by numerous companies. These adhesive tapes, dubbed VHB or Very High Bond tapes by the 3M Company, serve multiple purposes over a wide range of applications. This section describes the formulation of these tapes as well as previous research into their engineering properties.

2.3.1 Breakdown of Acrylic Foam Tapes

Acrylic foam adhesive tapes are different from the traditional elastomeric adhesives described in the previous section in that instead of being compounded from rubber, they are formulated using acrylic-based, plastic-compound adhesives. Rubber-based adhesives generally exhibit a higher initial level of adhesion than acrylic products, but in the long run, offer significantly less ultimate shear strength (Pinder 1981). Acrylic-based adhesives are better used for permanent bonds and provide increased UV and thermal resistance when compare to rubber adhesives.

The pressure sensitive nature of the acrylic foam tapes means that bonding is produced through the momentary application of pressure rather than through chemical reactions involving

a catalyst or heat treatment. There are three different types of double-sided pressure-sensitive adhesive tapes: double-coated PSA tapes, double-coated foam tapes, and adhesive transfer tapes. Double-coated PSA tapes have a film carrier surrounded by adhesive tape to provide additional thickness and strength to the connection. Double-coated foam tapes have a thicker, softer core and provide the ability to fill and join irregular surfaces. Adhesive transfer tapes are the strongest tapes but are very thin and must be applied to extremely regular surfaces for proper adhesion (Pinder 1981). Double-coated foam tapes are most appropriate to bond wood substrates due to their gap filling abilities. The acrylic-polymer viscoelastic foam also provides high strength in shear, peel, and tension. In addition to the adhesive properties of the tape, the foam offers solvent resistance, vibration damping, and moisture and UV resistance (Smith 1987).

2.3.2 Research on Acrylic Foam Adhesive Tape

Surprisingly little research has been published on the properties and performance of acrylic foam adhesive tape bonding. Undoubtedly, much of this research has been performed within the manufacturing companies and has remained proprietary. One of the largest published studies on the possible engineering use of acrylic foam tapes was performed by Heitman (1990). This research studied the structural engineering properties of acrylic foam tapes used to attach glazing elements in curtain wall applications. Heitman performed tensile and shear strength tests, tension and shear creep tests, UV resistance tests, water resistance tests, and a fatigue study on five different adhesive tapes on both aluminum and clear glass substrates. The results of the testing indicated that short-term strength requirements in shear and tension were easily met or exceeded. The adhesive tape also performed well in environmental tests. Creep endurance was the limiting factor for the design properties in this application. Only two of the five tapes were able to meet 50-year design acceptance creep criteria.

Geiss and Brockmann (1997) performed single-lap-shear tests to determine the creep resistance of 3M 4945 adhesive tape on anodized and powder coated aluminum, as well as glass and mild steel. Ultimate shear strengths on these materials for strain rates of 1 mm/min (0.04 in/min) ranged from 228 to 345 kPa (33-50 psi). Test results revealed that humidity, temperature, strain rate, and, most importantly, type of substrate can greatly affect creep resistance. Geiss and Brockmann also investigated the use of glass filler beads to further increase shear resistance. Brockmann and Hüther (1996) studied the adhesion mechanisms of

pressure sensitive adhesives using 3M Scotch Isotac 9473. They found that the PSA tape had superior environmental stability over other common epoxide systems. Peel tests were performed on dry specimens and on specimens immersed in 80˚C water for four weeks. The 3M product was able to maintain 80% of its peel force after the water immersion while the comparison epoxy maintained less than 50% initial force. Brockmann and Grüner (2002) investigated the creep behavior of 3M VHB 4945 acrylic tapes under various load and temperature combinations. Testing was performed on stainless steel single-lap-shear specimens at temperatures up to 80˚C. Results indicated that loads of approximately 0.01 N/mm^2 (1.6 psi) could be sustained for 20 years or more.

In addition to the environmental and creep tests previously outlined, Brown (1999) studied the strain-rate sensitivity of 3M VHB tape and its significance for design. In this study, double-lap joints were formed using aluminum plates. These joints were then tested at strain rates of 5, 50, and 500 mm/min (0.2, 2, 19.7 in/min). Impact tests were also performed using a pendulum to provide impact speeds of approximately 2 m/s (6.6 ft/s). Results revealed that the viscoelastic nature of the tape lead to increased failure loads and stiffnesses as load rates were increased. Failure modes also shifted from interfacial adhesive failure (bond failure) to cohesive failure (internal failure) at high impact rates.

In many cases, acrylic foam tapes provide a better alternative than mechanical fasteners where resistance to dynamic shear effects is important. One of the largest examples of this use in practice is for traffic signs. The Louisiana Department of Transportation currently uses acrylic foam tape in all of its new panel-style traffic signs (Hart 1999). To qualify for this use, signs bonded with the tape had to meet certain criteria for crash testing. Testing was performed by a car striking one leg of the sign at 32 km/hr (20 mph) and 98 km/hr (60 mph). In both these tests, the sign performed more than adequately and failures occurred in the bolts and metal clips but not in the tape. Signs in service in Florida have withstood winds of 153 km/hr (95 mph) in Hurricanes Erin and Nicole (Hart 1999). Removal of holes in the signs and the resulting smooth surfaces has also decreased the opportunity for corrosion and increased sign visibility. Many other applications and uses for acrylic foam tapes exist that could provide similar benefits.

2.4 Experimental Connection and Shear Wall Studies

A tremendous amount of experimental research has been conducted on timber connections, full-scale shear walls, and even full-scale houses in the past 50 years. Recent experimental studies have investigated variables such as the effect of hold-downs, high aspect ratios, wall panel materials, openings, and dissimilar materials. Several excellent bibliographies exist regarding these and prior experiments. The reader is directed to Peterson (1983) for a review of early diaphragm and shear wall testing dating back to the late 1920s. Tissell (1990) published a summary of monotonic shear wall tests since 1965 for the American Plywood Association. Smart (2002) provided an excellent up-to-date review of experimental connection testing. Salenikovich (2000) provided a discussion of main observations and results garnered from the overall body of experimental test data. Toothman (2003) provided an even more up-to-date summary of both monotonic and cyclic wall tests and their results. Finally, Filiatrault (2001) recently edited a literature review for the CUREE-Caltech Woodframe project that includes several papers covering numerous timber-engineering topics of interest to this study.

2.4.1 Recent Experimental Shear Wall Studies

Several recent studies have been aimed at the effect of oversized oriented strand board (OSB) wall panels on shear wall performance. Lam *et al.* (1997) and Durham (1998) performed tests on long OSB panels and found that oversized panels provided increased strength and stiffness but with a loss in dissipated energy. Bredel (2003) investigated 2.7 m (9 ft) and 3 m (10 ft) tall OSB wall panels with both monotonic and reversed cyclic loading protocols. He *et al.* (1999) also performed studies on oversized OSB shear walls that included openings.

Many of the recent experimental studies have been performed to develop parameters for computer programs. Dinehart and Shenton (1998, 2000) tested numerous full-scale shear walls that were used to later validate a three degree of freedom (DOF) computer model that they proposed. Dinehart (1998) also performed experiments on the dynamic behavior of shear walls utilizing passive energy dissipation devices. Other investigators have shared data from recent studies in order to verify computer models. For instance, the results from Durham's (1998) study were used to calibrate the CASHEW program described in the following section (Folz and Filiatrault 2001b)

Also, quite a few recent projects have investigated the effect of loading protocol on wall performance. He *et al.* (1998) tested for the influence of three different loading protocols on the effect of shear wall performance. Ficcadenti *et al.* (1998) tested three variations of the Sequential Phased Displacement (SPD) protocol. Gatto and Uang (2002) also performed a large investigation and literature review on this subject, the results of which are presented in Section 2.5.2, which is devoted to this topic.

2.4.2 Adhesives in Shear Walls

The prior experimental testing of shear walls constructed with adhesives is of particular interest in the current study. Little work has been done in this area, and the most comprehensive study to date was performed by Filiatrault and Foschi (1991). Their project investigated the seismic behavior of thirteen 2.4 m x 2.4 m (8 ft x 8 ft) shear walls. Of these walls, six were constructed with nails only, and seven were constructed with a combination of nails and adhesive. The adhesive used for the study was Scotch Grip Wood Adhesive 5230 – an elastomeric construction adhesive from the 3M Company. Seven of the total walls were tested using a typical ASTM E 72 racking test as described in Section 2.5.1, and the remainder of the tests were performed dynamically using the San Fernando, El Centro, and Romania earthquake acceleration records.

Initial stiffness of the monotonically-racked walls was found to be 65% higher than the standard walls. Peak loads for the adhesive walls were 45% higher than standard, but these gains came at the sacrifice of twice the displacement capacity of the system. Note that Dolan (1989) had previously predicted that adhesive-based walls would have higher strength and less ductility. Filiatrault and Foschi (1991) found that the adhesive walls failed in an extremely brittle manner due to the breaking of the sole plate. Their study utilized specialized detailing and bracing schemes to increase the strength of the sole plate to aid in the prevention of such failures. It was obvious that the weakest link of the wall specimens lay not in the adhesive but in the wood framing. Note that the increased energy dissipation and ductile failure properties of the acrylic foam tape presented in Section 2.3 sets the tape used in this study apart from the Scotch Grip 5230.

Dynamic tests performed by Filiatrault and Foschi (1991) indicated that the walls would behave elastically during large earthquake excitations as long as the framing of the walls was

appropriately braced to prevent brittle failures. This behavior is contrary to the highly inelastic deformations observed in the traditional walls. Normally, traditional walls are designed to dissipate energy through yielding of their connectors during earthquake motions. Such walls can become badly damaged but still provide life-safety in natural disasters. The adhesive walls dissipated little to no energy during ground motion, but this was due to their ability to remain linearly elastic during loading. The prospect of designing adhesive walls to maintain elasticity during seismic motions was innovative. However, the required specialized wall detailing to prevent brittle framing failures led to the ban of all adhesives in the first edition of the International Building Code (ICC 2000) for high seismic zones.

Dolan and White (1992) performed an investigation of the design considerations that must be incorporated into building codes based on the results of Filiatrault and Foschi (1991). They noted that the increased shear loads required of anchorage connections when used in conjunction with adhesive walls were not sufficiently addressed in the building codes. To address this problem, they proposed that a response modification (R) factor of 4-4.5 be used for adhesive walls. The proposed factor was much lower than that factor of 8 used in the UBC (1991) code upon which their investigation was based. The resulting increase in required design strength served to improve the design of the anchorage connections and adjacent structural elements to provide for the elevated resistance requirements associated with adhesive shear walls. Dolan and White cautioned that the failure of the adhesives in such walls would be catastrophic if it occurred. They also noted that the anchorage connection was already one of the more common locations of shear wall failures and that the aggravation of this problem by the use of adhesive shear walls should be carefully considered.

2.5 Testing Procedures and Loading Effects

Test methods used for experimental investigations of shear walls can have a profound effect on their performance. Monotonic testing of shear walls has been standardized and updated by the American Society of Testing and Materials since 1977. Numerous cyclic testing procedures have also been developed and utilized within the past 20 years. Though ASTM has recently recognized a true reversed cyclic standard, its implementation has been sporadic, and multiple other protocols are commonly used. For this reason, there has recently been a concerted

effort to quantify the effects of the different testing procedures. This section outlines the various monotonic and cyclic testing methods and their effects upon wall performance.

2.5.1 Monotonic Testing Protocols

The ASTM E 72 test standard was first proposed in 1977 and is still an active standard as of ASTM E 72-02 (American Society of Testing and Materials 2002a). This method is used for various compressive, tensile, and racking testing of wall, floor, and roof elements for actual service conditions. As related to shear walls, ASTM E 72-02 is used primarily for the evaluation of different sheathing panels and is not used to determine overall performance. Racking load is applied at the top of a 2.4 m x 2.4 m (8 ft x 8 ft) test specimen that is restrained from rigid body rotation by a hold-down rod running from the top of the specimen into the base. The presence of this rod has been criticized (Griffiths 1984) as its restraint causes unrealistic failures. This criticism has been met with the response that the rod is not to simulate engineered hold-down devices but rather to model the effect of dead load on the wall (Skaggs and Rose 1996). Nevertheless, a procedure to investigate the overall response of a wall system was developed.

The ASTM E 564 procedure addressed the tie-down concerns of ASTM E 72 by allowing for the use of typical hold-downs in the corners of the wall assembly. This standard, last updated in ASTM E 564-00e1, has replaced ASTM E 72 for determining the overall strength of a statically racked shear wall specimen (American Society of Testing and Materials 2000b). There are two different loading procedures within ASTM E 564: a static racking procedure and an optional cyclic loading test. In the static procedure, a preload of 10% of the estimated ultimate load is to be applied for five minutes to "seat" all connections. Loads are applied at approximately one-third and two-thirds of the estimated ultimate load, with recovery allowed for five minutes between applications. The loading regime is then continued until failure of the wall occurs. The cyclic test procedure involves the initial preload followed by the application of loads in reversed directions, and the subsequent incremental recording of deflections until failure. This cyclic protocol is different from true quasi-static protocols in that it is simply a modified static test in which increasing load steps are provided at different intervals for deflection recording. The exact nature of the load and deflection steps is not discussed.

ASTM D 1761-88 (2000) allows for the testing of mechanical fasteners (connections) in wood. In this method, load is applied at a uniform rate of 2.54 mm/min (0.10 in/min) ±25% until

failure (American Society of Testing and Materials 2000a). It is noted within the procedure that special loading rates may be used to determine the resistance of connections to impact forces or repetitive loadings.

2.5.2 Cyclic Load Testing Protocols

The majority of cyclic protocols currently in use for shear wall testing are referred to as quasi-static protocols. These tests use reversed cyclic motions that often increase in amplitude over time until failure. The term static refers to the low frequency at which displacements or loads are applied (usually less than 1 Hz). These frequencies eliminate the contribution of inertial effects. Similar patterns with higher loading rates that include inertial effects are referred to as pseudo-dynamic tests. Random excitations such as earthquake records are labeled fully dynamic tests (Salenikovich 2000). An excellent in-depth overview including time-history graphs of many of the loading procedures described below was presented by Gatto and Uang (2002) as part of the CUREE-Caltech Woodframe project.

Many of the first cyclic tests were extensions of racking tests in which a small number of reverse cycles with increasing amplitudes were applied until failure. This procedure was used by Medearis and Young (1964) and Thurston and Flack (1980) in some of the pioneering cyclic testing experiments. Further cyclic tests on shear walls were performed by Stewart (1987) and Dean *et al.* (1986). In 1989, Dolan used a triangular sine wave pattern to experimentally verify his finite element model. These early tests used extremely slow loading rates and took anywhere from days for the earliest tests to 45 minutes for Dolan's later experiments.

Multiple time-history functions currently exist for quasi-static loading. One of the most common is the Sequential Phased Displacement (SPD) protocol developed by the Technical Coordinating Committee on Masonry Research (Porter 1987). The SPD protocol is based on the first main event (FME) of the wall specimen, which often corresponds to yielding. FMEs are determined through a monotonic test and calibration process. In 1994, the Structural Engineers Association of California (SEAOC) adopted a form of the SPD protocol for shear wall testing. The SPD procedure makes use of a series of initial reversed cycles leading up to the FME of the wall. After this point, displacements consist of three degradation cycles, a primary cycle, and three stabilization cycles. The degradation cycles were meant to produce damage typical of earthquake excitations. The stabilization cycles were meant to allow the wall to incur maximum

damage before the next increase in loading amplitude (Porter 1987). The SPD protocol was also recently adopted by ASTM E 2126-02a with a few minor changes (American Society of Testing and Materials 2002b). Most importantly, the ASTM procedure calculates displacements utilizing a ductility factor approach as opposed to the FME approach provided in the original SPD procedure. Also, discussion is under way to eliminate the stabilization SPD cycles and to calculate the shear strength from a single backbone curve (Salenikovich 2003).

The second major protocol currently in use is the CUREE-Caltech time-history, which was proposed as part of the CUREE-Caltech Woodframe project by Krawinkler *et al.* (2001). Three time histories were actually proposed: a general deformation-based protocol, a near-fault deformation-based protocol, and a force-controlled protocol. This thesis made extensive use of the general deformation-based load-history. The CUREE general protocol was developed to evaluate seismic performance of wood structures when subjected to ground motions (earthquakes) whose probability of exceedance in 50 years is 10%. The amplitude of the CUREE cyclic protocol is calibrated through prior monotonic testing. The loading-history consists of initiation cycles to simulate tremor movements, primary cycles to simulate large shocks, and trailing cycles to introduce damage into the system. The CUREE protocol is currently being evaluated for inclusion in the 2004 or 2005 ASTM standard as ASTM E 2126.

Several other cyclic loading procedures that are not currently as common as the SPD and CUREE protocols include the FCC-Forintek protocol, the CEN Short and Long protocols, the SAC protocol, and the ISP protocol. The FCC protocol was developed by the Forintek Canada Corporation (Karacabeyli 1996) and consists of sinusoidal groups of three equal magnitude cycles. The CEN Short and Long protocols are both included in European standards (CEN 1995). The CEN Short protocol is used to determine performance characteristics at a certain ductility level. The CEN Long procedure is a general protocol consisting of three cycle groups followed by a monotonic ramping of load until failure. The SAC protocol was developed by Krawinkler (SAC/BD 1997) and is one of the few loading regimes that requires no prior testing to calibrate loading conditions. The SAC protocol relies on interstory drift angles instead of FME or yielding values. Finally, the ISO standard (ISO 1998) was originally proposed for connection tests but has since been studied (Gatto and Uang 2002) for its use in full-scale testing.

2.5.3 Performance Comparison of Cyclic Protocols

Due to the large proliferation of testing protocols and the profound effect that these protocols have upon the behavior of shear walls, there have been many recent studies aimed at quantifying their differences. Skaggs and Rose (1996) studied the differences between the older ASTM E 72 and E 572 procedures and the SPD reversed cyclic protocol as investigated earlier by Rose (1995). They found that the cyclic procedure produced loads approximately 20% lower than the monotonic testing procedure. They also found that the SPD procedure appeared to produce nail fatigue failures inconsistent with the types of failures observed in actual earthquake conditions.

Karacabeyli and Ceccotti (1998) investigated the effect of numerous loading protocols on 4.8 m x 2.4 m (16 ft x 8 ft) shear walls. Testing covered all of the protocols described in the previous section with the exception of the CUREE protocol. Test results were consistent with those produced by Skaggs and Rose, in that the SPD protocol was one of the few (with FCC-Forintek) that produced nail fatigue failures. Specimens tested with other protocols exhibited nail pullout and tearing of the sheathing edges. All of the procedures predicted the same maximum load capacity to within 10%. Additional results indicated that the high energy demands of the SPD protocol resulting from the large number of cycles exceeding FME may be the cause of the nail fatigue and lower displacement capacity associated with the SPD protocol.

He *et al.* (1998) performed three shear wall tests using the FCC, CEN Short, and CEN Long loading protocols. Shear wall dimensions were 7.3 m x 2.5 m (25 ft x 8 ft). Test results indicated that the FCC protocol produced nail fatigue failures inconsistent with actual earthquake performance. Furthermore, the CEN Short protocol produced maximum loading on the first cycle and did not seem to provide useful data. The CEN Long protocol appeared to provide results and failure modes similar to those observed in true seismic conditions.

Ficcadenti *et al.* (1998) performed 24 tests on standard 2.4 m x 2.4 m (8 ft x 8 ft) plywood shear walls using three variations of the SPD protocol. These variations were put in place to determine the effect of removing the decay cycles as well as simulating near-fault conditions. Results of the study proved that the decay cycles significantly fatigued the nails, thus resulting in lower ultimate strengths. Displacement capacities, however, were unaffected by the loading protocols.

Gatto and Uang (2002) tested 36 standard 2.4 m x 2.4 m (8 ft x 8 ft) shear wall specimens with monotonic, CUREE, ISO, and SPD protocols. Many different variables were studied including the type of sheathing, near-fault effect, gypsum wallboard effect, dynamic effect, and stucco effect. Results of the study indicated that the ISO protocol might be a good choice for wood-frame testing due to its simplicity, but that the high energy demands imposed on the fasteners could be unrealistic. Gatto and Uang's study also supported the conclusion reached by previous researchers that the SPD protocol provides failures that are not representative of failures in actual earthquake events. Overall, this study concluded that the CUREE protocol produced similar load capacities to monotonic testing and provided failure modes consistent with seismic behavior. It was therefore "recommended that [the CUREE] protocol be established as the standard for future woodframe testing (Gatto and Uang 2002)."

2.6 Numeric Modeling of Connections and Shear Walls

Formation of accurate numerical models for connection and full-scale wall and building testing has been a primary goal of many researchers. The advantages are obvious; numerical models sharply reduce the costs associated with a full-scale experimental study and also increase the number of variable repetitions that can be examined in a given time-frame. Through the years, models have moved from close-formed solutions to complex finite-element approaches. As computer programs progressed, many of the numeric models moved from connection-test based origins to full-scale models that incorporated connection elements.

2.6.1 Adhesive Connections

Theoretical analysis of lap-joints connected with adhesives began with the work of Volkersen (1938). As reported by Zink *et al*. (1996), Volkersen determined that there were stress concentrations at either end of the joint overlap arising from the differential strain between the adherends. His work did not, however, take into account the possible bending deformations associated with single-lap joints. Goland and Reissner (1944) built on the previous experiments to develop a fairly complex and accurate mathematical model of adhesive joints that had fewer limitations than the earlier models. Cornell (1953) extended Goland and Reissner's research by developing a set of differential equations that described load transfer between adherends and the

adhesive bond-line. Many mathematical models of connection tests have since been created, but in general they have produced results similar to that of Goland and Reissner's work. Common results have indicated high stresses at the ends of the overlap gradually being reduced towards the center at rates dependant on overlap length.

Use of the finite element method has also been incorporated into the modeling of adhesive connections. Some early work was performed by Erdogan and Ratwani (1971) who investigated the problems associated with modeling the bond-line. As part of his finite element program for full-scale wall testing, Dolan (1989) developed a smeared line connection that could be used to model adhesives in shear walls. One of the most advanced timber-based adhesive models to date was proposed by Zink *et al.* (1996). The model used linear spring elements of zero dimension to represent the tension and shear stiffness of the bond-line between the adherends. This bond-line approach allowed the development of a mesh-independent model and did not rely on properties that are difficult to calculate. Zink *et al.* performed experimental tests and calculated strains using a white light, speckle technique. These strains were converted to stresses using Hooke's Law for comparison with the finite element model. The model worked well for normal and shear stresses, but obviously the experimental approach is limited to predicting elastic deformations of the wood.

2.6.2 Mechanical Connections

Many mathematical models have been created for the connection of wood specimens using dowel-type (nailed) fasteners in addition to the adhesive-based research previously discussed. An excellent survey of such material is presented in the literature review performed by Smart (2002).

Johansen (1949) was one of the first to derive mathematical models describing the various yield modes that could occur with dowel-type connections. These models added flexibility in calculations not available with the older, empirically-based systems. Connection test design is currently based on the initial assumption of a perfectly elastic-plastic, load-deflection relationship that has been proven by numerous researchers such as Aune and Patton-Mallory (1986) to provide accurate connection stresses.

Foschi (1974) extended the base load-deflection relationship to an exponential model that allowed for inelastic deflections. This model was again extended by Malhotra and Thomas

(1982) to allow for the effect of gaps and bearing between connection components. Loferski and Polensek (1982) also created a connection model that utilized straight-line approximations of nonlinear deflection curves.

All previously described connection test models were based on unidirectional loading. Research has also been directed at the hysteretic (cyclic) modeling of connections. Kivell, *et al* (1981) proposed such a model based on a modification of a previous derivation for concrete materials. Foliente (1995) derived a much more general hysteretic model that has been used for both connections and as a simplification for the dynamic investigation of full-scale structures. More recently Heine and Dolan (2001) developed an algorithm to incrementally calculate load-slip data through yield theory and plastic analysis of dowels. Ramskill (2002) proposed equations to predict lag screw connection capacity and 5% offset yield based on a series of connection test results and fracture mechanics.

2.6.3 Shear Walls

Many closed-form and computer models have been developed to determine the response of timber shear walls to static racking loads. Several models predicted load-deflection response based on stress analysis and energy derivations. Toumi and McCutcheon (1978) and Easley *et al.* (1982) both produced formulas that were capable of predicting wall deflections. Gupta and Kuo (1985) developed a model based on sinusoidal nail-force distribution for nonlinear analysis. Gupta and Kuo (1987) later expanded this model to allow for uplifting of the studs in shear walls. Other models have been proposed by Källsner (1984), Gutkowski and Castillo (1988), Kamiya (1988), and SaRibeiro and SaRibeiro (1991).

One of the first finite element diaphragm and shear wall models was proposed by Foschi in 1977. Foschi's program assumed nonlinear nail connections and was used to model frame, sheathing, and connection interaction. Itani and Cheung (1984) also proposed a finite element model that allowed for varied sheathing arrangements and geometry. Falk and Itani (1988) further developed a program that modeled all of the sheathing connectors as a single element to reduce degrees of freedom and, therefore, computational requirements.

To predict the response of timber shear walls to cyclic loads, researchers began to develop more comprehensive finite element models. Falk (1986) extended his model to allow for the dynamic response of shear walls in the elastic range. Dolan (1989) developed three

different finite element models that allowed for the investigation of monotonic, steady-state, and dynamic response of timber shear walls. These programs were verified through the experimental testing of 42 full-scale shear walls and were shown to provide good predictions. Dolan's initial model incorporated a wide degree of flexibility in modeling sheathing elements and included out-of-plane buckling effects of the sheathing. White and Dolan (1995) updated the program to remove unnecessary complexity and to allow for the calculation of forces and stresses within the walls.

Further recent work into the modeling of shear wall elements includes the development of a single-degree-of-freedom (SDOF) model by Foliente (1995) to determine the dynamic response of shear walls using the nonlinear hysteretic model he developed. A SDOF model created by van de Lindt and Walz (2003) was also used to perform reliability studies on wooden shear walls. This model used a four-part, linear hysteresis approximation to investigate the effects of hysteretic variability on predicted earthquake response.

Moving on from SDOF models, Tarabia and Itani (1997) developed a sophisticated finite element model for the dynamic testing of wood-frame buildings. In an effort to produce a simpler model suitable for design work and "bridge the gap" between SDOF and advanced finite element models, Dinehart and Shenton (2000) developed a discrete 3-DOF model for dynamic shear wall analysis. This model used a linear viscoelastic connection between sheathing and framing and, according to the developers, has the flexibility to account for variations in wall geometry, sheathing and framing materials, fastener type, and spacing. The Dinehart and Shenton model is only accurate for moderate to low displacements due to its inability to account for pinched hysteresis curves.

To complement the current trend towards quasi-static reversed cyclic testing of shear walls to predict seismic response, Folz and Filiatrault (2001a) developed a numerical model dubbed CASHEW for the Cyclic Analysis of Shear Walls. This program was developed for analytical modeling associated with the CUREE-Caltech Woodframe Project. CASHEW was verified through full-scale cyclic testing and showed good agreement. Folz and Filiatrault also proposed a method for studying the dynamic behavior of shear walls using the CASHEW program to calibrate a single DOF hysteretic model as opposed to using full-scale wall tests for such calibration. This procedure would eliminate the need for full-scale testing in order to provide dynamic wall performance estimates. Folz and Filiatrault (2002) incorporated the

CASHEW hysteretic model into the Seismic Analysis of Woodframe Structures (SAWS) program to predict the dynamic characteristic of simple wood-frame buildings. The SAWS program combines rigid, horizontal diaphragms with zero-height spring elements that predict the pinched, strength, and stiffness-degrading hysteretic behavior of shear walls.

2.7 Summary

This chapter has presented an overview of the many different research topics that are relevant to the work presented in this thesis. First, a summary of the use of adhesives in the timber industry has been presented. Adhesive use is currently divided into construction of building materials such as OSB with various adhesive chemical agents and stiffening of structural elements with elastomeric adhesives. Next, a discussion on experimental testing and current uses for acrylic foam adhesive tapes has been offered. Further information was given regarding the structure of these adhesives and their ability to dissipate energy through viscoelastic behavior. Readers were then provided with information regarding several valuable literary reviews on connection and shear wall testing. Recent experiments have been discussed as were the limited results from prior shear wall studies utilizing elastomeric-based construction adhesives. An overview of the many different loading protocols and the effects of different time-history functions on wall performance has been given. Finally, a summary of numeric modeling techniques for both adhesive and mechanical connections as well as more advanced finite element models for full-scale shear walls and structures has been presented. This thesis represents an extension of these topics and hopefully will contribute to the understanding of timber adhesion and its use in structural shear wall elements.

Chapter 3

Materials and Test Procedures

3.1 General

Over 275 shear connections and 23 full-scale shear walls were constructed and tested over the course of this study. These tests were composed of multiple specimen subsets that explored the bonding of various structural members using acrylic foam tape in replacement of, or in addition to, mechanical fasteners.

One of the main testing objectives was to classify the performance of these connections and walls for future design and analysis purposes. To advance this objective and ensure the repeatability of the results, this chapter will discuss all aspects of specimen construction and testing. This discussion includes material properties, construction details of both connections and walls, testing apparatus and procedures, and data acquisition systems. Due to the lack of previous research in bonding wood specimens with pressure sensitive adhesives, particular detail will be given to the methods developed for adhesive tape application.

3.2 Specimen Designations

Due to the large number of specimen permutations, a classification system for each subset was created and maintained throughout the project. This system consists of a prefix identifying the type of test, an initial letter identifying the sheathing material used, one or two following letters identifying the adhesive and/or mechanical fasteners, and finally a suffix for surface treatments. The designation of each specimen per subset is given by the number following the classification. All subsequent data and graphs are labeled with these abbreviations which are detailed fully in Table 3.1. Through use of this table, the characteristics of each specimen can be identified quickly without further reference. A complete list of all specimens tested, along with brief descriptions, is presented in Table 3.2 for connections and Table 3.3 for full-scale wall tests.

Table 3.1: Specimen Abbreviations

Test Type Prefix			
C	Comparison Single Lap Shear (SLS) (Connection Test)		
T	Time of Adhesive Application (SLS) (Connection Test)		
P	Adhesive Application Pressure (SLS) (Connection Test)		
S	Statistically Significant[1] Single Lap Shear (SLS) (Connection Test)		
W	Full-Scale Wall Test		
Structural Sheathing Designation			
P	9 mm (3/8 in.) Plywood		
O	11 mm (7/16 in.) Oriented Strand Board		
	Note: Unless otherwise designated a 38 mm x 89 mm (2 in. x4 in. Nominal) Spruce-Pine-Fir structural member was used in all tests.		
Fastener / Bonding Designations			
A	3M VHB 4941 Adhesive 38 mm (1.5 in.) wide		
MT1	Manufacturer 1: 3M VHB 4941 Adhesive 38 mm (1.5 in.) wide		
MT2	Manufacturer 2: Adco AT-2 Adhesive 38 mm (1.5 in.) wide		
MT3	Manufacturer 3: Avery 2333 Adhesive 38 mm (1.5 in.) wide		
N	Connection Tests: 2.9 mm x 60 mm (0.113 in. x 2 3/8 in.) Nail		
N	Wall Tests: 2.9 mm x 63.5 mm (0.113 in. x 2 1/2 in.) Nail		
Surface Treatment Suffix and other Descriptors			
S	Sanded	LN	Liquid Nails ®
P	Primed	WG	Tightbond 2 ® Wood Glue
Examples			
S-PAN-3	Specimen 3 of the Statistically Significant[1] Connection Test Subset bonding Plywood to a 38 mm x 89 mm (2 in. x 4 in. nom.) Spruce-Pine-Fir member with 3M VHB 4941 Adhesive in addition to a nail.		
S-OAS-4	Specimen 4 of the Statistically Significant[1] Connection Test Subset bonding Surface Sanded OSB to a 38 mm x 89 mm (2 in. x 4 in. nom.) Spruce-Pine-Fir member with 3M VHB 4941 Adhesive.		
W-PN-1	Wall Specimen 1 using Plywood Sheathing connected to primary structural members with nails only.		
Note 1: "Statistically Significant" denotes specimens that were part of the main body of connection tests whose repetitions were sufficient to provide a 90% confidence interval that the calculated performance paramaters were within 10% of the true average (See Section 3.4.5.1).			

Specific properties for all structural members, adhesives, and mechanical connections whose abbreviations are provided in Table 3.1 are discussed in the following materials section. Specific methods of construction and dimensions for connections and walls are also provided later in this chapter. Additional information regarding each specimen such as moisture content and failure modes is provided in the data sheets found in the Appendix.

Table 3.2: Connection Specimen List

Comparison Single Lap Shear Connection Tests							
I.D.	Member	Sheathing	Fastener	Treatment	Pressure[1]	Time[2]	No. Tests
C-OA	SPF	OSB	3M VHB	None	15 psi	20 sec	5
C-OAS	SPF	OSB	3M VHB	Sanded	15 psi	20 sec	5
C-OAP	SPF	OSB	3M VHB	Primed	15 psi	20 sec	5
C-OAN	SPF	OSB	3M VHB +8d Nail	None	15 psi	20 sec	5
C-OACL	SPF	OSB	3M VHB	Clamped[3]	Note 3	24 hours	2
C-OAMS	Metal Stud	OSB	3M VHB	None	15 psi	20 sec	5
C-PA	SPF	Plywood	3M VHB	None	15 psi	20 sec	5
C-PAP	SPF	Plywood	3M VHB	Primed	15 psi	20 sec	5
C-PAN	SPF	Plywood	3M VHB +8d Nail	None	15 psi	20 sec	5
C-PAMS	Metal Stud	Plywood	3M VHB	None	15 psi	20 sec	5
C-PACL	SPF	Plywood	3M VHB	Clamped[3]	Note 3	24 hours	2
						TOTAL	49
Adhesive Application Pressure Single Lap Shear Connection Tests							
I.D.	Member	Sheathing	Fastener	Treatment	Pressure[1]	Time[2]	No. Tests
P15	SPF	Plywood	3M VHB	None	15 psi	30 sec	5
P30	SPF	Plywood	3M VHB	None	30 psi	30 sec	5
P45	SPF	Plywood	3M VHB	None	45 psi	30 sec	5
P60	SPF	Plywood	3M VHB	None	60 psi	30 sec	5
P80	SPF	Plywood	3M VHB	None	80 psi	30 sec	5
P100	SPF	Plywood	3M VHB	None	100 psi	30 sec	5
P120	SPF	Plywood	3M VHB	None	120 psi	30 sec	5
						TOTAL	35
Adhesive Time of Application Single Lap Shear Connection Tests							
I.D.	Member	Sheathing	Fastener	Treatment	Pressure[1]	Time[2]	No. Tests
T15	SPF	Plywood	3M VHB	None	60 psi	15 sec	5
T30	SPF	Plywood	3M VHB	None	60 psi	30 sec	5
T45	SPF	Plywood	3M VHB	None	60 psi	45 sec	5
T60	SPF	Plywood	3M VHB	None	60 psi	60 sec	5
T90	SPF	Plywood	3M VHB	None	60 psi	90 sec	5
T120	SPF	Plywood	3M VHB	None	60 psi	120 sec	5
						TOTAL	30
Statistically Significant Single Lap Shear Connection Tests							
I.D.	Member	Sheathing	Fastener	Treatment	Pressure[1]	Time[2]	No. Tests
S-PA	SPF	Plywood	3M VHB	None	60 psi	60 sec	15
S-PN	SPF	Plywood	8d Nail	None	60 psi	60 sec	15
S-PAN	SPF	Plywood	3M VHB +8d Nail	None	60 psi	60 sec	15
S-OA	SPF	OSB	3M VHB	None	60 psi	60 sec	15
S-OAS	SPF	OSB	3M VHB	Sanded	60 psi	60 sec	15
S-OAP	SPF	OSB	3M VHB	Primed	60 psi	60 sec	15
S-ON	SPF	OSB	8d Nail	None	60 psi	60 sec	15
S-OAN	SPF	OSB	3M VHB +8d Nail	None	60 psi	60 sec	15
S-PMT1	SPF	Plywood	3M VHB 4941	Primed	60 psi	60 sec	15
S-PMT2	SPF	Plywood	Adco AT-2	Primed	60 psi	60 sec	15
S-PMT3	SPF	Plywood	Avery 2333	Primed	60 psi	60 sec	15
						TOTAL	165
Additional Tests of Interest							
I.D.	Member	Sheathing	Fastener	Treatment	Pressure[1]	Time[2]	No. Tests
WG	SPF	OSB / Ply.	Tightbond 2 Glue	None	N / A	N / A	5
LN	SPF	OSB / Ply.	Original Liquid Nails	None	N / A	N / A	5
						TOTAL	10

NOTES

1) Pressure applied to each specimen for alloted time to activate pressure sensitive adhesive.

2) Amount of time for which adhesive activation pressure was applied.

3) Clamped indicates activation pressure was applied with hand-tightened clamps for the alloted time.

Table 3.3: Wall Specimen List

Full Scale 2.4 m x 2.4 m (8 ft x 8 ft) Shear Wall Tests[1]						
I.D.	Member	Sheathing	Fastener	Treatment	Test Method	No. Tests
W-OAN-M	SPF	Plywood	3M VHB + 8d Nails	None	Monotonic	2
W-PA	SPF	Plywood	3M VHB	None	Cyclic CUREE	3
W-PN	SPF	Plywood	8d Nails	None	Cyclic CUREE	3
W-PAN	SPF	Plywood	3M VHB + 8d Nails	None	Cyclic CUREE	3
W-OAS	SPF	OSB	3M VHB	Sanded	Cyclic CUREE	3
W-OAP	SPF	OSB	3M VHB	Primed	Cyclic CUREE	3
W-ON	SPF	OSB	8d Nails	None	Cyclic CUREE	3
W-OAN	SPF	OSB	3M VHB + 8d Nails	None	Cyclic CUREE	3
					TOTAL	23

Notes:
1) Pressure applied for adhesive application was a minimum of 414 kPa (60 psi) for 60 seconds

3.3 Material Properties

3.3.1 Structural Member Material Properties

All sawn lumber members of connection tests and walls were composed of 38 mm x 89 mm (2 in. x 4 in. nom.) No. 2 Grade, Surface-Dry, Spruce-Pine-Fir. This lumber was purchased from a local Lowe's retail store in 2.4 m (96 in) lengths and cut as necessary. The grading stamp produced by the West Coast Lumber Inspection Bureau is provided in Figure 3.1 along with the product label.

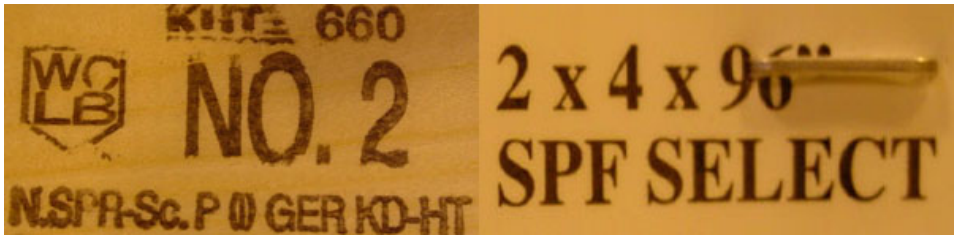

Figure 3.1: Sawn Lumber Grade Stamp and Product Label

All lumber was stored in a controlled environment with a temperature of 21˚C (±12˚C), 70˚F (±10˚F), and a relative humidity of 35-70% until time of specimen construction. Moisture content (MC) measurements were taken using an electric moisture meter upon receipt of the wood shipment. The MC of the wood ranged between approximately 10% and 15%. The MC was again checked at the time of specimen construction and testing as recorded in the Appendix.

Typical allowable design values for sawn lumber provided from the 2001 NDS Supplement are listed in Table 3.4 (AF&PA 2001).

Table 3.4: Design Values for No. 2 Grade Spruce-Pine-Fir
(Values extracted from NDS Table 4A (AF&PA 2001))

Bending		Tension Parallel to Grain		Shear Parallel to Grain		Compression Parallel to Grain		Modulus of Elasticiy	
psi	MPa	psi	MPa	psi	MPa	psi	MPa	ksi	MPa
1300	8.96	675	4.65	135	0.93	635	4.38	1,400	9,650
Note: Table Values include size factor adjustment for 2x4in nominal lumber									

Sheathing material used was either 11 mm (7/16 in.) oriented strand board (OSB) or 9 mm (3/8 in.) plywood. These materials were purchased from a local Lowe's retail store in 1.2 m x 2.4 m (4 ft x 8 ft) panels and cut as necessary. The OSB panels were manufactured by Louisiana Pacific and rated 24/16 Exposure I Sheathing. The plywood panels were manufactured by Georgia Pacific and rated 24/0 Exposure I Sheathing. Grading stamps for both panels are provided in Figure 3.2.

Figure 3.2: Grade Stamps for OSB (Left) and Plywood (Right) Sheathing

Sheathing materials were stored in a controlled environment with a temperature of 21˚C (±12˚C), 70˚F (±10˚F), and a relative humidity of 35-70% until time of specimen construction. Design capacities of these "performance rated structural-use panels" are provided from APA Technical Note N375B supplementary update (APA 2002) in Table 3.5.

Table 3.5: Sheathing Material Properties
(Values extracted from Technical Note N375B, Tables 2.1-2.2 (APA 2002))

Sheathing	Description	Units	Stress applied parallel to Strength Axis	Stress applied perpendicular to Strength Axis
OSB	Panel bending stiffness, EI	KN-mm^2/m width	734,000	152,000
		lb-in^2/ft. width	78,000	16,120
	Panel axial stiffness, EA	kN/m	55,400	42,300
		lb/ft	3,800,000	2,900,000
	Panel rigidity through thickness, G_vt_v	N/mm of depth	14,700	14,700
		lb/ft	83,700	83,700
Plywood	Panel bending stiffness, EI	KN-mm^2/m width	621,000	33,900
		lb-in^2/ft. width	66,000	3,600
	Panel axial stiffness, FA	kN/m	48,800	42,300
		lb/ft	3,350,000	2,900,000
	Panel rigidity through thickness, G_vt_v	N/mm of depth	4,400	4,400
		lb/ft	25,000	25,000

3.3.2 Pressure Sensitive Adhesive Properties

Acrylic-foam, pressure sensitive adhesive (PSA) tapes were provided by three different manufacturers for testing. Manufacturers were asked to select tapes that would be well suited for application to a wood substrate. These very-high-bond tapes are readily available and currently being used in other industries. Thirty-eight millimeter (1.5 in.) wide tape was requested to match the nominal width of the sawn framing lumber. If this width was not available, larger rolls were cut to size.

Basic properties for each adhesive tape are summarized from the respective manufacturer's technical data in Table 3.6. All tapes were stored in an enclosed room-temperature environment until their use. All tapes were applied before the end of their acceptable shelf life as listed in their respective manufacturer's data sheet (3M 1998, ADCO 2000, Avery Dennison 2001).

3.3.3 Mechanical Fasteners

Four different types of mechanical fasteners were used throughout the project. For the sheathing to framing connection tests, an 8d, 2.9 mm x 60 mm (0.113 in. x 2 3/8 in.), ½ head, Interchange Framing Nail was used. For full-scale wall tests, a Senco 8d, 2.9 mm x 65 mm (0.113 in. x 2 1/2 in.), full head, bright box nail was used for sheathing connections. For full-

scale wall framing connections, a Senco, 16d, 3.4 mm x 89 mm (0.135 in. x 3 1/2 in.), full head, box nail was used. Finally, 16d, 3.8 mm x 83 mm (0.148 in. x 3 1/8 in.), sinker nails were used to secure hold-down devices to framing members. More information regarding connection and wall construction details are provided later in this chapter. Allowable nail properties taken from the 2001 National Design Specification are provided in Table 3.7 (AF&PA 2001).

Table 3.6: Adhesive Tape General Properties

Manufacturer		ADCO[2]	AVERY[2]	3M[2]
Tape Designation		AT-2	2333	4941 VHB
Property	Units			
Color	N / A	Gray	White	Gray
Thickness	mm	1.143	2.4	1.1
	in	0.045	0.0945	0.045
Tensile Strength	kPa	931	Not	586
	psi	135	Provided	85
Peel Adhesion[1]	N/mm	1.751	3.5	3.5
	pli	10	20	20
Dynamic Shear Strength	kPa	414	Not	480
	psi	60	Provided	70
Installation Temperature	°C	10-38	10-?	16-38
	°F	50-100	50-?	60 - 100
Operation Temperature Limits	°C	-34 - 93	Max 49	Max 93
	°F	-30 - 200	Max 120	Max 200
Shelf Life	Years	1	1	2

1) Note: Peel Adhesion was 90° for ADCO, 3M, and 180° for Avery
2) Note: Values compiled from Company Product Information Bulletins - Information given is dependent on manufacturer's testing methods.

Table 3.7: Design Values for Nails in 38 mm (1.5 in.) Spruce-Pine-Fir (Values extracted from NDS Table 11N (AF&PA 2001))

Nail	Diameter		Length		Design Value for Single Shear	
	inches	mm	inches	mm	lbs	N
8d Sinker	0.113	2.9	2 3/8	60	61	271
8d Box	0.113	2.9	2 1/2	65	61	271
16d Box	0.135	3.4	3 1/2	89	88	391
16d Sinker	0.148	3.8	3 1/4	83	100	445

3.4 Connection Specimens

3.4.1 Specimen Introduction

Connection specimens were all constructed by fastening a 160 mm (6.25 in.) long framing member to a 457 mm x 90 mm (18 in. x 3.5 in.) sheathing panel to create a single-lap-shear joint. The majority of framing members were constructed of a 38 mm x 89 mm (2 in. x 4 in. nom.) piece of Spruce-Pine-Fir member as described in the preceding section. A small sample of connections was also initially tested using 32.5 mm x 89 mm (1.25 in. x 3.5 in.) metal studs. A general overview of the specimen geometry is illustrated in Figure 3.3. Note that the framing member extends a small distance of 6.35 mm (0.25 in.) past the end of the sheathing to ensure proper positioning in the connection test fixture. The length of the sheathing panel was also chosen to ensure that the test fixture could provide a sturdy grip on the connection. The odd framing member length of 160 mm (6.25 in.) was chosen so that when subtracting the 6.35 mm (0.25 in.) extension of the framing member past the sheathing, exactly 152.4 mm (6 in.) would be available for adhesive tape application.

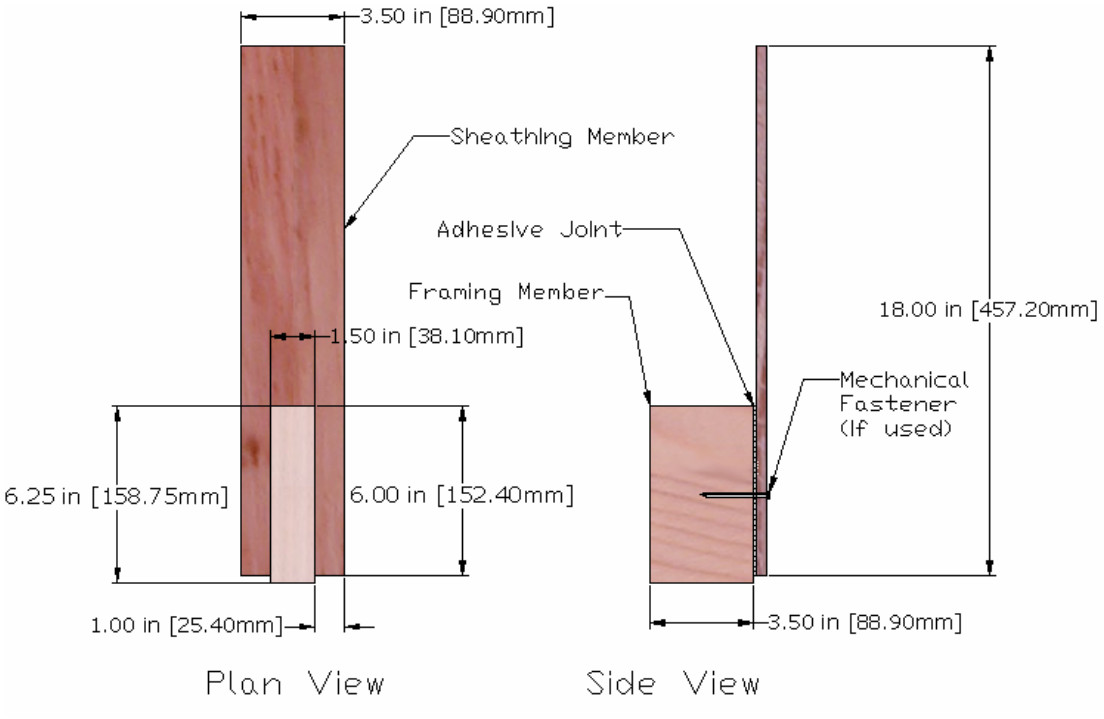

Figure 3.3: Basic Connection Specimen

All connection tests were constructed within two days of the receipt of the materials to simulate the worst expected moisture conditions (MC = 19%) for surface-dry lumber. Following their completion, each specimen was placed in a temperature and humidity controlled chamber for at least two weeks to allow relaxation of the wood around mechanical fasteners and to stabilize moisture content at approximately 12%. This waiting period also allowed curing time for the adhesive to reach maximum performance. Product data from 3M estimates that at room temperature, 100% of the ultimate strength gain for VHB tape will occur within three days. Figure 3.4 displays racks of connection test specimens placed in the environmental chamber. Data records that include moisture content of each connection framing member at the time of both construction and testing are provided in the Appendix.

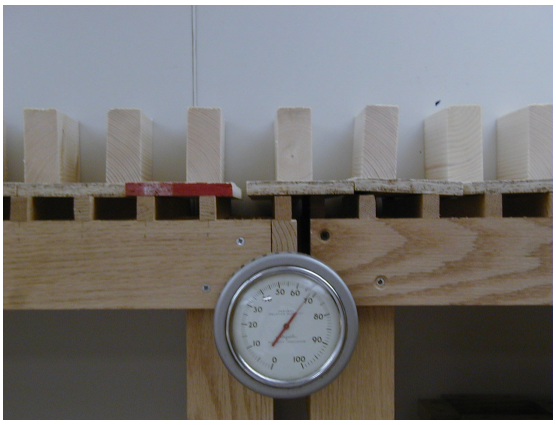

Figure 3.4: Connection Tests in Environmental Chamber

Due to the exploratory nature of the research and the wide variety of connection tests performed as shown in Table 3.2, construction methods differed depending on the connection type and the stage of the project. The following sections will outline these construction methods in the order that tests were conducted: comparison, pressure of application, time of application, statistical sets, and additional tests of interest.

3.4.2 Comparison Test Construction

The comparison series connections were constructed and tested to provide a general idea of the project validity and performance trends of many different types of connections. These tests were not meant to provide data for future design and were constructed based on existing research on adhesive tape performance with other materials such as aluminum. All comparison tests were constructed using 3M VHB 4941 acrylic foam tape.

3.4.2.1 Adhesive Application

Product literature from the 3M Company gave 100-140 kPa (15-20 psi) as a reasonable pressure for adequate bonding (3M 1998). Before application of the adhesive, the surfaces of both sheathing and framing members were cleaned of all dirt and loose particles. A 38 mm x 152 mm (1.5 in.. x 6 in.) strip of adhesive tape was cut from the supplied roll, placed on the surface of the framing member, and gently pressed down as illustrated in Figure 3.5. The adhesive backing was then peeled off at 180 degrees, and the sheathing panel was placed onto the framing member. Pressure was applied through the application of a 710 N (160 lb) live load to the framing member for an arbitrary time of 20 seconds. This load provided an indirect pressure of 123 kPa (18 psi) to the adhesive tape.

Figure 3.5: Adhesive Application to Connection Member

As each specimen was completed, its moisture content (MC) was recorded using a hand-held electric moisture-meter as shown in Figure 3.6. Moisture contents for newly completed specimens ranged from 11 to 15.6%.

In addition to the MC of each specimen, all comparison shear connections were labeled with the 2.4 m (96 in.) long piece of framing lumber from which they originated. Each subset was constructed with pieces from at least three different original members. The extra step of recording and tracking this information was eliminated in the remainder of the connection tests, as results showed no substantial correlation between performance and original material.

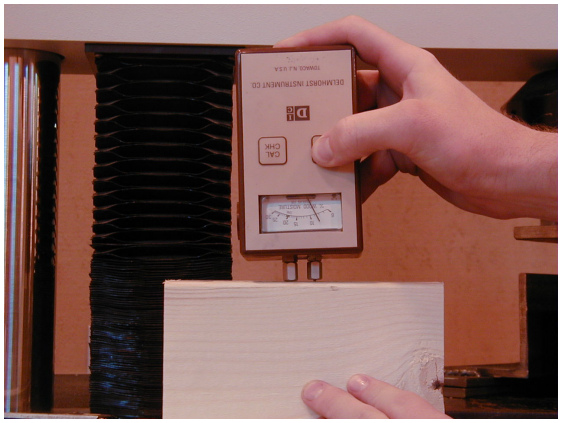

Figure 3.6: Recording Moisture Content

3.4.2.2 Sheathing Surface Energy

The strength of an adhesive bond between two materials is a function of the attraction of molecular forces between them, which in turn is a function of their surface energies. In general, the higher the surface energy of the substrate, the better an adhesive can flow ("wet out") to achieve a stronger bond. A quick way to test the surface energy of a material is to place a single drop of water on the substrate as shown in Figure 3.7. If the drop of water flattens out or flows, then the adhesive has a better chance of bonding which is indicative of a high surface energy material. If the drop of water remains semi-spherical, then the substrate exhibits low surface energy and bonding will be more difficult.

Oriented strand board (OSB) is fabricated by bonding wood flakes with exterior-grade adhesives such as phenol-formaldehyde or isocyanate, under intense heat and pressure (Forest Industries 1998). It is believed that this intense heat deactivates the surface of the final product and decreases its ability to form an adhesive bond. OSB also typically has one smooth side and one side stamped with a rough texture. This texture is provided so that construction workers using the material as roof sheathing can gain a better foot-hold while placing roof covering.

Both sides of the OSB material were tested for bonding characteristics using the water drop test. It was found that the textured side had a slightly higher initial surface energy; therefore this side was chosen and used as the bonding side for the remainder of the project.

Figure 3.7: Water Drop Test

Plywood is manufactured by the fabrication of dried veneer sheets from cut timber which are then glued together and finish sanded (Simpson Plywood 2003). This final sanding re-activates the surface of the plywood, making it more suitable for bonding than OSB. Again a simple water-drop test revealed that plywood had a moderately higher surface energy than OSB. Both sides of plywood sheets are similar and orientation was not an issue.

3.4.2.3 Methods of Increased Bonding Capability

Two different methods of surface preparation were used in an attempt to increase the bonding capability of both OSB and plywood. These methods were surface sanding and priming. The first method was used only on OSB because plywood is finish-sanded by the manufacturer. Sanding was performed using a hand-held belt sander to produce a smooth surface as illustrated in Figure 3.8. The sanded surface was then wiped free of excess material. A water-drop test showed that surface energy had indeed increased significantly over the un-sanded material. It was decided to sand only the sheathing materials because cut framing lumber is planed after going through the drying kiln thus removing all surface activation considerations (Loferski 2002).

Use of a primer on sheathing and framing members was explored for both plywood and OSB. Many of the tape manufacturers produce primers designed specifically to enhance the bonding capacity of their adhesive tapes. The normal adhesive primers are, however, very low viscosity materials that perform well on dense materials but that require too many coats to be practical on porous materials such as wood (Steiner 2002). As one of the objectives of this project was to use readily obtainable materials to enhance construction practices, a common household primer was used. In the comparison tests, Kilz® Original indoor/outdoor, white, wood sealer/primer produced by Masterchem Industries, Inc. of Imperial, Missouri, was applied in two coats, three hours apart. The primer was then allowed to dry for a minimum of 24 hours before adhesive tape application. Priming also served to enhance bonding capability by filling the porous surfaces of the sheathing materials to provide a more even substrate.

Figure 3.8: Surface Sanding of OSB

3.4.2.4 Mechanical Fasteners for Comparison Tests

Performance of mechanical fasteners in combination with adhesive tape was tested using 8d, 2.9 mm x 60 mm (0.113 in. x 2 3/8 in.) sinker nails. For connection tests that utilized mechanical fasteners, the nail was applied immediately after the adhesive tape had been applied. A single nail was shot into the center of the connection using a pneumatic gun in order to model an interior nailing point. Care was taken to ensure that the head of the nail did not penetrate into the sheathing itself.

3.4.2.5 Other Comparison Test Considerations

In addition to the connection tests covered in the previous sections, a small number of tests were performed using light-gauge steel studs as the primary framing member. The construction and adhesive application of these specimens were completed in the same manner as for wood-framed connections. These tests were performed strictly for initial comparison and were not repeated in later connection subsets as this study focused primarily on wood construction.

A number of exploratory tests were performed using clamps to monitor the effect of increased application pressure on performance. In this case, adhesive tape was applied and then multiple clamps were hand-tightened to hold the sheathing and framing together for 24 hours. Results from these tests led to the full-scale pressure application study discussed in the following section.

3.4.3 Pressure Application Connection Specimens

Pressure application tests were performed to provide information on an optimum adhesive application pressure to a wood substrate. These tests were only conducted on 3M VHB 4491 as it was hypothesized that all tapes would perform within a similar range. In addition, all connection tests were performed by attaching a piece of 9 mm (3/8 in.) plywood with no surface treatments to a wooden framing member. Additional material properties are provided in Section 3.3. The ratio of performance improvement associated with the pressure of tape application was believed to be similar, and thus transferable, between plywood and OSB sheathing materials. Furthermore, the time of application of each test was set at a constant 30 seconds to ensure a complete bond. Time of application was believed to be insignificant after a short initial range. This assumption was later tested and proven correct.

To produce consistent pressures ranging from 103 to 830 kPa (15-120 psi), a better pressure application system than the live load used for the initial comparison tests was designed. This system involved a custom metal fixture and an MTS model 10/gl screw driven Universal Testing Machine with a 45 kN (10 kip) capacity. A step-by-step application procedure is listed on the following page.

Steps for applying pressure to connection specimens during construction:

1) Sheathing material was cut to size and slid into the bottom of the connection fabrication fixture as illustrated in Figure 3.9 (a).
2) Adhesive tape was then cut to length and applied to the main framing member.
3) The adhesive tape backing was peeled back as illustrated in Figure 3.9 (b).
4) The main member was oriented so that the adhesive tape faced down towards the sheathing substrate and then slid into the connection fixture as illustrated in Figure 3.9 (c). The connection fixture was designed so that it held the main framing member straight above the center of the sheathing connection.
5) Once the framing member was slid in position, it was allowed to contact the sheathing member.
6) The MTS was then activated, and the horizontal plate attached to the load cell (Figure 3.9 (a)) pressed down on the framing member until the load had reached a high enough value so that with relaxation, the average load applied to the connection during the application time would equal the load required to reach the target pressure. The computer control system of the MTS was used to automatically retract the machine after a given time period.

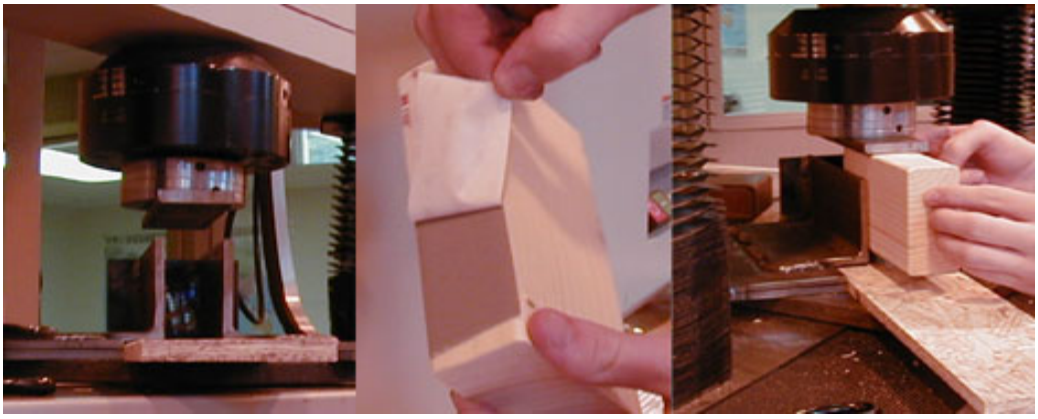

(a) (b) (c)

Figure 3.9: Pressure Application Steps

To accurately estimate the required initial load so that relaxation losses over the application time period yielded an average load corresponding to the target pressure as described

in Step 6, up to three practice specimens were first tested at each different pressure level. Once the appropriate initial load had been found, the actual specimens were constructed. For example, if the target pressure was 415 kPa (60 psi), the target average load was 60 psi (area tape = 9 in^2) = 2.4 kN (540 lb) over the 30 second application period. A typical pressure vs. time plot for three of the 60 psi specimens is presented in Figure 3.10.

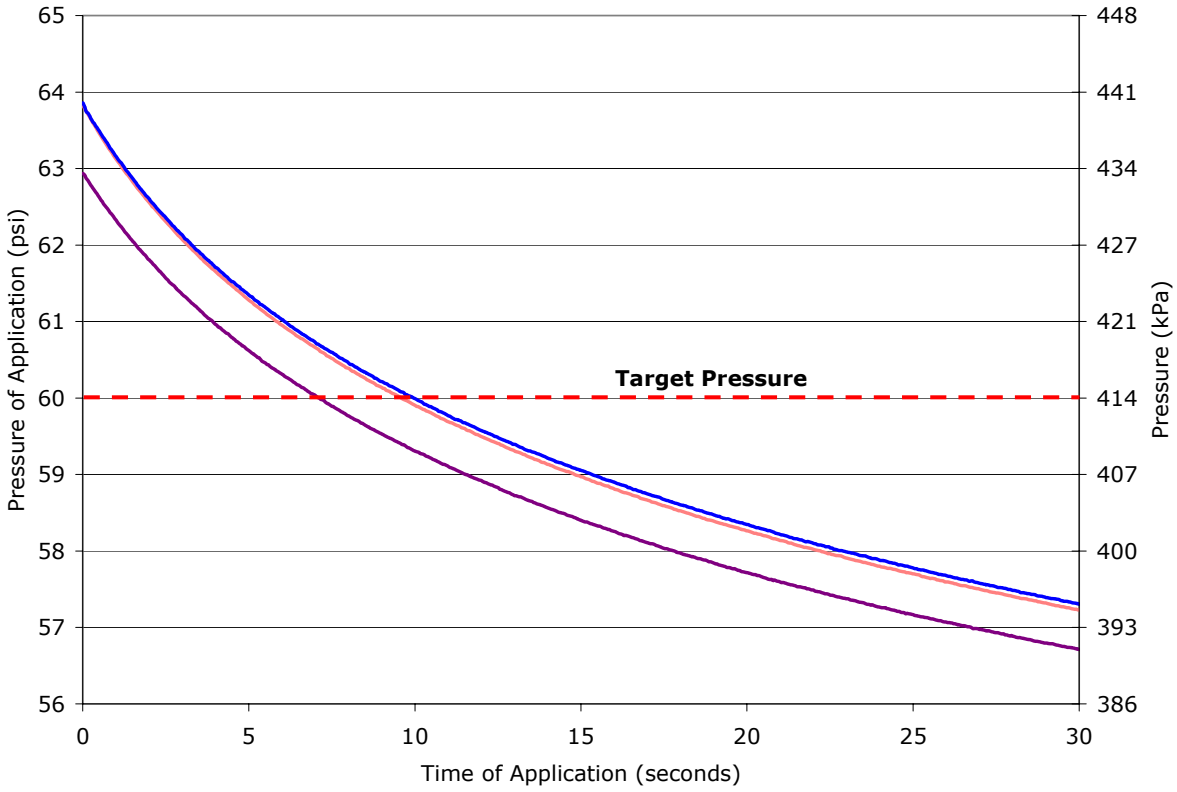

Figure 3.10: Adhesive Application Pressure vs. Time of Application

Note that the average pressure during the time of application is equal to the target value ±7 kPa (1 psi). This value represents typical results and is well within acceptable limits for this study. Application curves for all specimens were recorded and examined but are not presented within this document as they were all within acceptable limits and do not provide any additional useful information. Peak and final application pressures for all connection subsets, with the exception of the comparison sets, are listed in the data recording sheets presented in the Appendix. Once each shear connection was constructed, the moisture content was recorded, and it was placed in the environmental control chamber until testing began.

3.4.4 Time of Application Connection Specimens

Time of application tests were performed to provide information on the optimum time required to form an adhesive bond with a wood substrate. As with the application pressure tests, these connections were only conducted on 3M VHB 4491 as it was hypothesized that all tapes would perform within a similar range. Time of application connection tests were constructed of the same materials and in the same manner as the application pressure tests. The optimum pressure calculated in the previous test series was held constant, and the application time was varied. A plot of a pressure vs. application time curve for a representative sample from each time series is displayed in Figure 3.11.

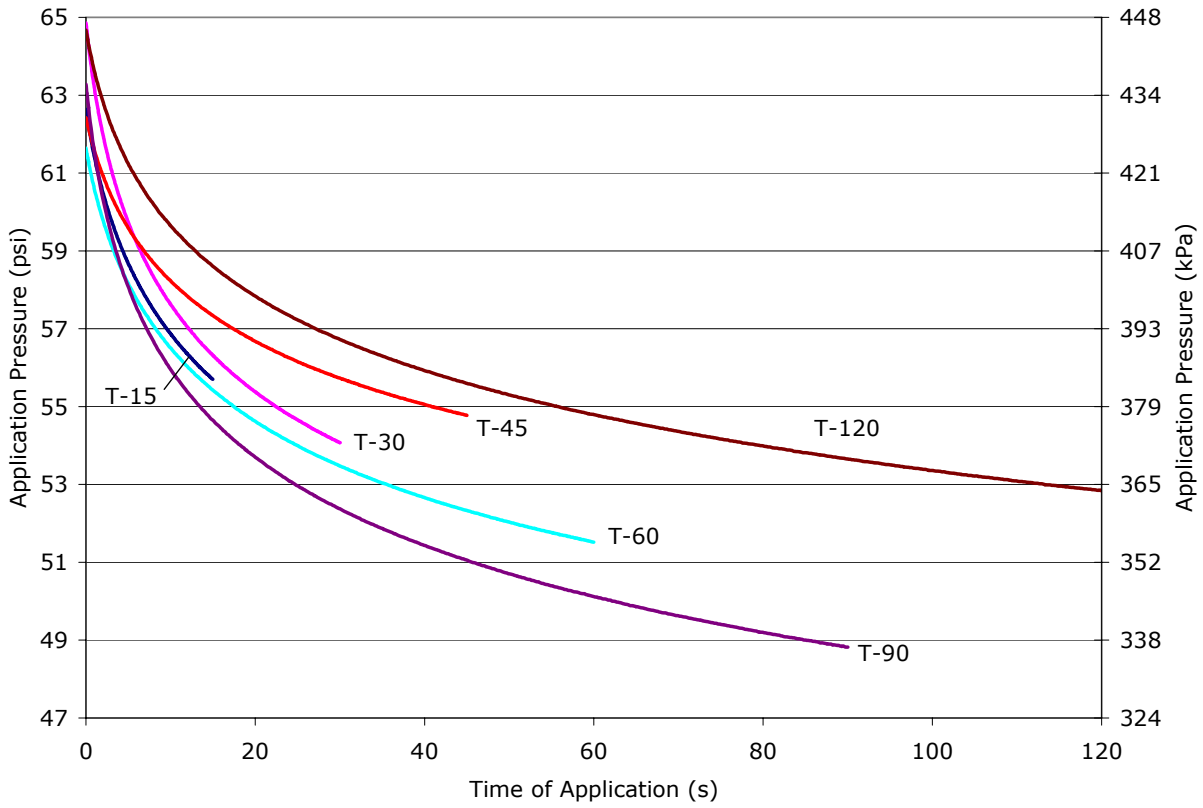

Figure 3.11: Adhesive Application Pressure vs. Time of Application

Due to the varying rate of relaxation, the average pressure values for each of these connections were in the range of 400 kPa (57 psi). This level of precision was deemed acceptable for this study as human error and material variability rendered further minimization of inaccuracies difficult.

3.4.5 Statistical Connection Specimens

Eleven different shear connection subsets, consisting of fifteen specimens each, were constructed and tested in order to provide a significant body of information that can be used in future analysis and design programs. Types of connections tested are explicitly detailed in Table 3.2, and were chosen to represent a wide variety of surface and bonding conditions that were deemed promising from the initial comparison connection data.

3.4.5.1 Sample Size

Sample sizes were chosen based on estimates performed by Anderson (2001) and Heine (2001) which indicated that for bolted single shear connections a sample size of ten would yield with 90% confidence an estimated mean peak load within 12% of the true mean peak load. Due to the perceived increased variability of the adhesive bond compared to a bolted connection, this sample size was increased to 15 to achieve the same level of accuracy.

This estimate was later verified when the average value of the Coefficient of Variation (COV) of the connection test peak loads was calculated to be 16%. A 90% confidence interval gives the area under the normal curve to be z=1.65. Given the number of specimens (n), the actual error percentage (e) was calculated according to the following:

$$e = \sqrt{\frac{2z^2 COV^2}{n}} = \sqrt{\frac{2(1.65)^2(16)^2}{15}} \approx 10\% \tag{3.1}$$

The sample size of 15 yielded maximum average peak loads within 10% of the actual average peak load.

3.4.5.2 Connection Information

All connections in this set were constructed with geometries and methods identical to the time and pressure variation test connections. Where applicable, the optimum time and pressure of tape application derived from the previous experiments were used in construction. Sanding and priming were performed when required using the same methods and materials as presented in the comparison test discussion of Section 3.4.2.

In addition to many of the connection alternatives explored to a lesser scale in the initial comparison tests, two sets were tested using only a single 8d, 2.9 mm x 60 mm (0.113 x 2 3/8

in.) sinker nail in plywood and OSB, respectively. These sets were tested to provide a basis of comparison for any performance benefits provided by the adhesive.

Until this portion of the project, all specimens constructed with pressure sensitive adhesive had made use of 3M VHB 4941. To explore other tape and manufacturer alternatives, two connection test subsets of 15 specimens each were constructed using ADCO AT-2 and Avery 2333 acrylic foam tapes. Each of these manufacturers indicated that the use of a primer would be extremely beneficial to the ultimate strength of the wood-adhesive bond. Personal correspondence with Ted Steiner (2002), Senior Technical Service Specialist of 3M Corporation, suggested that commonly available Sherwin Williams ProBlock solvent-based paint/sealer had proven to provide a good bonding surface for wood applications. To investigate the maximum possible benefit of each adhesive tape, all three manufacturers' connections were primed on both framing and sheathing surfaces with Problock. These three test subsets were initially labeled S-PMT-1 (3M VHB), S-PMT-2 (ADCO AT-2), and S-PMT-3 (Avery 2333) for objectivity and performance tracking. MT stands for alternate manufacturer's tape. All connection tests were constructed using 9 mm (3/8 in.) plywood. It was believed that the relative performance of each tape would be similar on both plywood and OSB sheathing.

As with the previous test sets, initial and relaxed application pressures, as well as the moisture content of the main framing member, were recorded at the time of construction. The connection was then placed into the environmental control chamber for a minimum of 14 days.

3.4.6 Additional Tests of Interest

The use of adhesive bonding in the construction industry is not a new development. Traditional wood glue is used in many applications, and solvent-based elastomeric adhesives such as Liquid Nails® have been utilized for over 40 years (Macco 2001). Though both materials provide greatly increased strength, they do so with severely reduced displacement capacity as compared to traditional mechanical fasteners. This reduction of displacement capacity causes brittle failures when subjected to earthquake or oscillating wind-load movements.

To provide some basis of comparison to these traditional adhesives, a small group of connection tests were performed for informational purposes. These connection tests were performed using Tightbond II® wood glue produced by the Tightbond Company in Columbus, Ohio, and Liquid Nails® Projects & Construction LN 601 Formula produced by Macco Adhesives in Cleveland, Ohio. Connections were constructed with OSB and plywood using the manufacturer instructions. Tightbond II® connections were hand-clamped and allowed to dry for two hours. Liquid Nails® was applied using the quick-bond method in which a zigzag 6 mm (1/4 in.) bead of product was first applied to the framing member as shown in Figure 3.12. The sheathing was then pressed firmly into place, pulled away for three minutes, and pressed back into place.

Figure 3.12: Application of Elastomeric Adhesive

Results from this set of connection tests do not represent a full study of these alternative adhesives and are meant for informational purposes only. Only 24 hours of drying time was allowed before the connections were tested, and construction conditions were not as strictly controlled as those of the adhesive tape tests.

3.5 Connection Testing

3.5.1 Testing Equipment

All connections were tested in the Wood Engineering Lab of the Brooks Forest Products Research Center at Virginia Polytechnic Institute and State University. Tests were conducted using an MTS model 810 servo-hydraulic Ultimate Testing Machine with an 89 kN (20 kip) capacity. Displacement and load data were recorded at a rate of 5 Hz using a personal-computer-based data acquisition system. Figure 3.13 provides an overview of the testing and data acquisition system.

Figure 3.13: Connection Test Setup

Load readings were recorded using a 4.45 kN (1 kip) capacity load-cell for all connections with the exception of the wood glue and Liquid Nails® connections which made use of an 89 kN (20 kip) load-cell. Displacement values were measured using the internal displacement transducer of the MTS which had a range of ±63.5 mm (±2.5 in.).

Connections were held in place with a test fixture designed to impose shear loading directly on the adhesive bond with minimal to no moment induced from the eccentricity of the single-lap-shear specimen. This fixture is illustrated in Figures 3.14 and 3.15 both with and without a connection test in place. Greased "frictionless" steel rollers on both sides of the sheathing constrained peel to model actual wall construction.

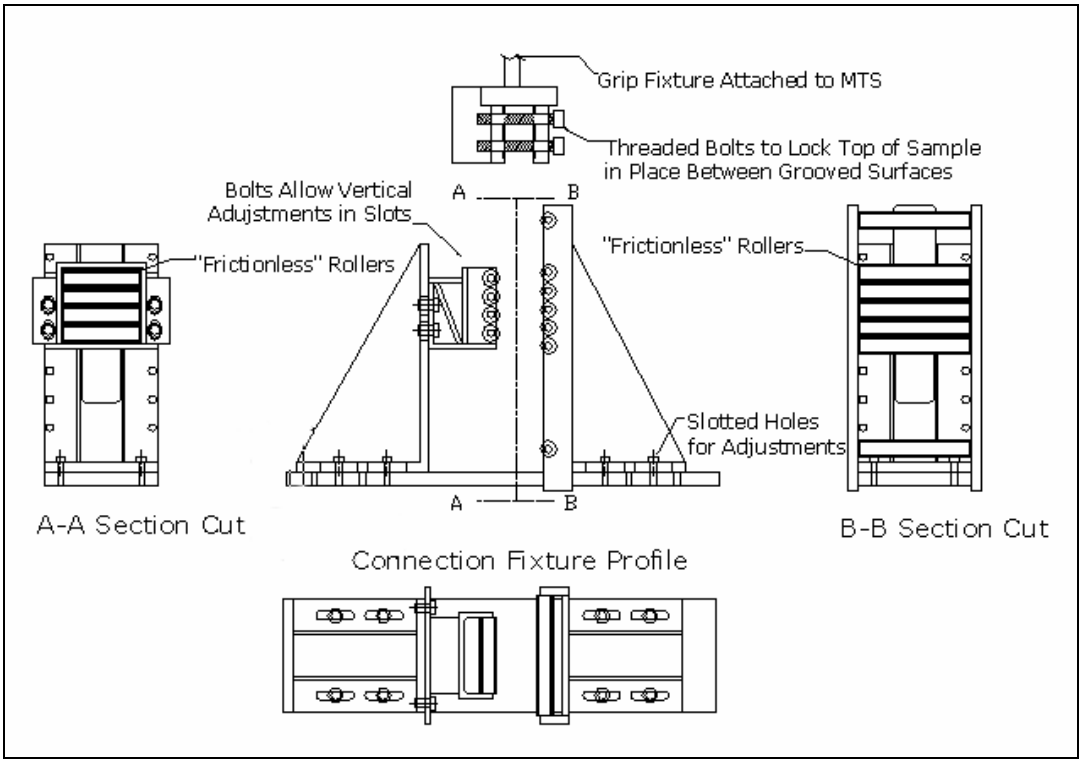

Figure 3.14: Connection Test Fixture Without Specimen

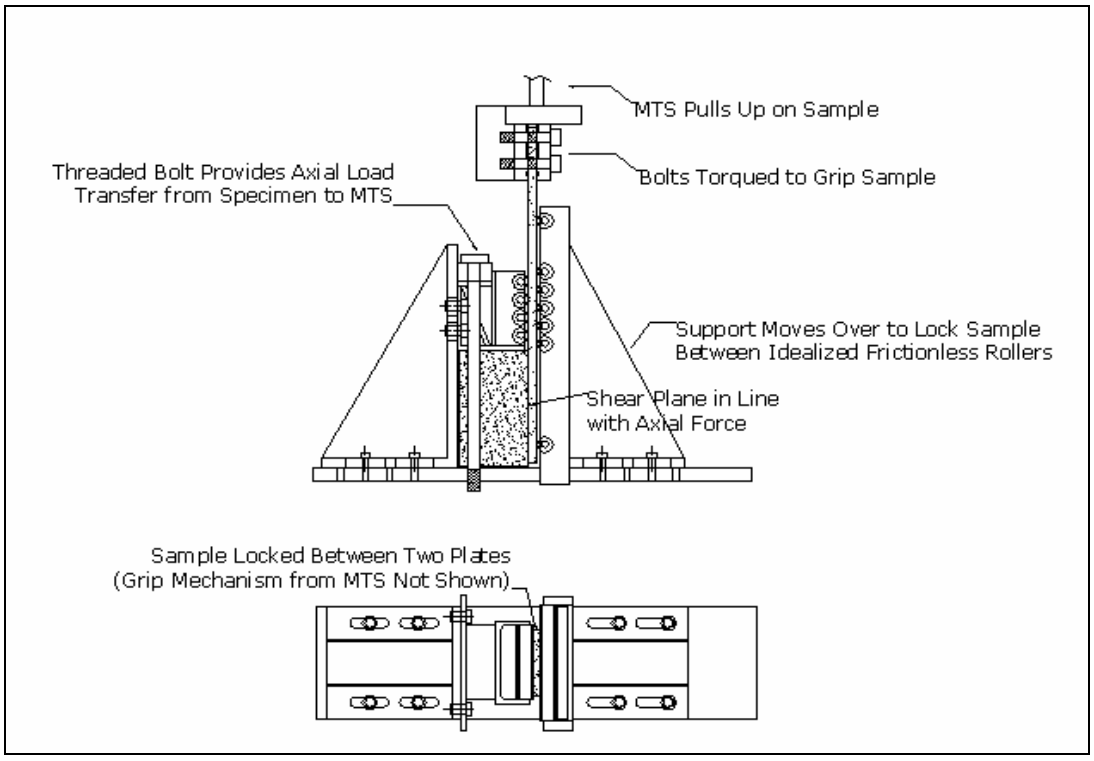

Figure 3.15: Connection Test Fixture With Specimen

3.5.2 Testing Procedure

Connection testing was performed in accordance with ASTM D 1761-88 (2000) protocol (American Society for Testing and Materials 2000a). Loading was applied at a constant rate of 1.3 mm/min (0.05 in/min) until failure occurred or the maximum time limit of ten minutes was reached. It was found through sample testing that this loading rate produced peak loads in approximately five minutes and failure loads in approximately eight minutes. Peak loads were recorded directly from the MTS readout to verify the results of the data acquisition system. The step-by-step procedure followed was:

1) Each connection was first removed from the environmental chamber and placed in the testing fixture.
2) The grips attached to the MTS machine were tightened about the sheathing material using a torque wrench.
3) The MTS load readout was double-checked to ensure no eccentricity of the connection had produced excess initial load during the tightening process.
4) The data acquisition system was started, and the MTS displacement cycle was initiated.
5) After failure had been reached, failure modes, peak loads, and main member moisture contents were recorded as shown on the data record sheets in the Appendix.

After all connection tests had been completed, the data was analyzed for performance parameters which are described fully in Chapter 4.

3.6 Full-Scale Shear Wall Specimens

3.6.1 Shear Wall Introduction

Twenty-three full-scale 2.4 m x 2.4 m (8 ft x 8 ft) walls were constructed and tested as a part of this study. Two of these walls were tested monotonically, and 21 were tested using a quasi-static cyclic protocol. All walls were constructed by attaching two 1.2 m x 2.4 m (4 ft x 8 ft) plywood or OSB sheathing panels to a framework of 38 mm x 89 mm (2 in. x 4 in. nom.) Spruce-Pine-Fir framing members. Additional materials information is provided in Section 3.3.

Full-scale tests were conducted for the purpose of collecting construction and performance information for cyclically-loaded shear walls bonded with acrylic foam tape. This information will then be analyzed and used to form design procedures for real-world applications. In this section, information on specimen construction including adhesive application, test setup, and testing procedures is provided.

3.6.2 Adhesive Application Pressure

Results from the application pressure connection tests which are discussed in Chapter 5 revealed that approximately 415 kPa (60 psi) is needed to assure consistent bonding of the adhesive tape to the wood substrate. When applying only 152 mm (6 in.) of adhesive tape to connection tests, this pressure was easily provided using a universal testing machine. When applying the same amount of pressure to a full-scale wall, however, the amount of tape and cumbersome size of the specimen posed a problem. Each wall required approximately 12.2 m (40 ft) of length around the perimeter of the two sheathing panels to be bonded to the framing. Applying 415 kPa (60 psi) to a 38 mm (1.5 in.) strip of adhesive tape running along this length would require almost 200 kN (43,200 lb) of force. The application of this amount of pressure using any system of weights was impractical for a lab setting; therefore several alternatives were evaluated.

3.6.2.1 Pressure Application Alternatives

Creating a vacuum over the entire wall and thus providing a consistent pressure over the surface of the sheathing was considered but was rejected due to size limitations and concerns over the amount of force that would be directed to the bond lines as opposed to the interior studs.

Air bags were also rejected due to expense and size limitations. The final solution involved concentrating the force applied to a single bond-line using an inflated hose, constrained within a steel channel, to provide even pressure as illustrated in Figure 3.16 and Figure 3.17.

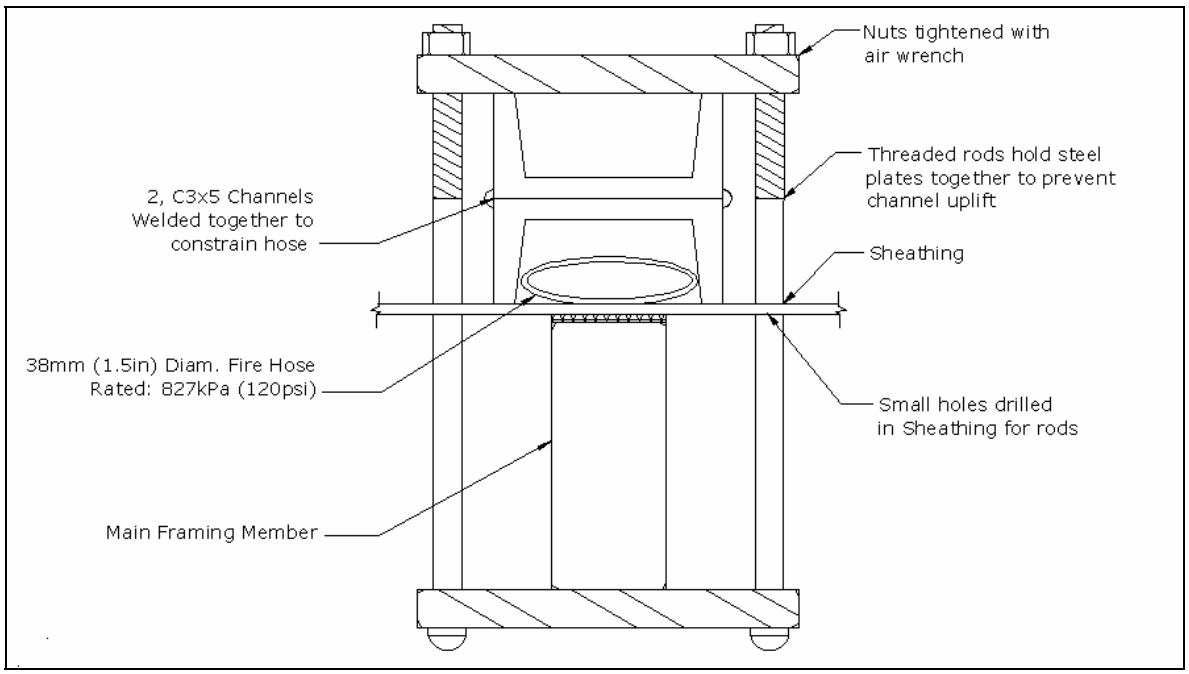

Figure 3.16: Wall Pressure Application Setup (Hose Deflated)

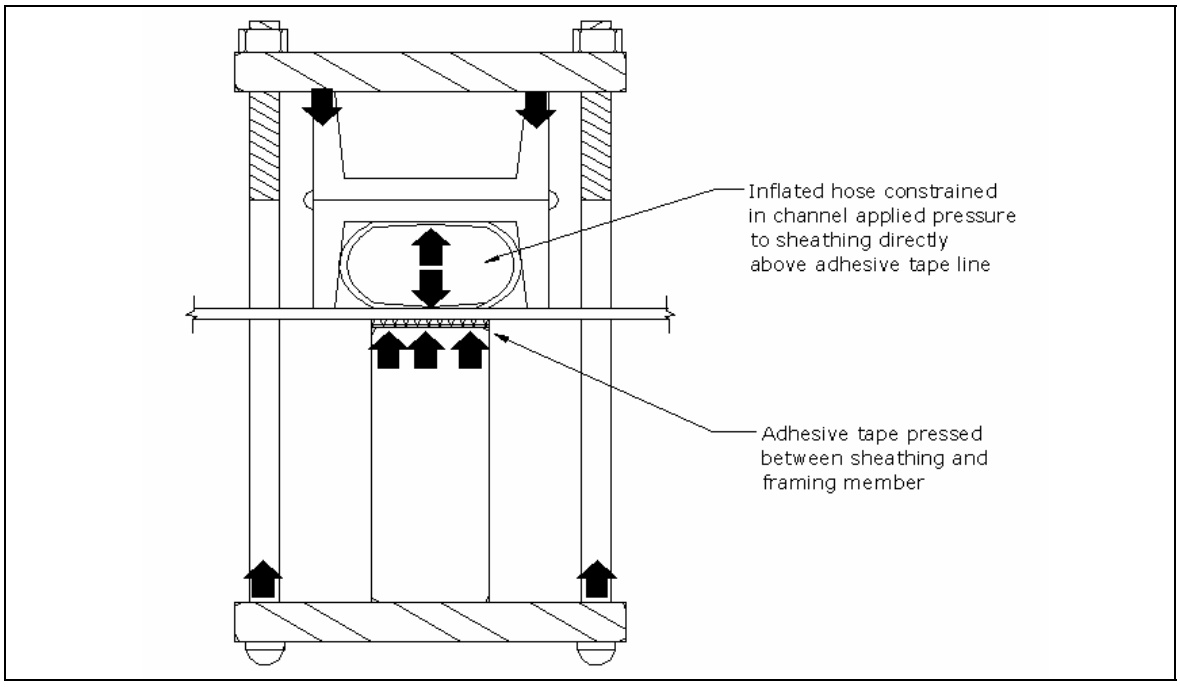

Figure 3.17: Force Flow of Wall Pressure Application Setup (Hose Inflated)

The pressure application setup made use of a 38 mm (1.5 in.) diameter fire hose that was purchased from a local fire department supplier and was rated to a capacity of 827 kPa (120 psi). The hose was cut to a length of approximately 3 m (10 ft) and fitted with a typical Schrader valve on one end and a quick release ball valve at the other as illustrated in Figure 3.18. An 827 kPa (120 psi) rated compressor was used to pressurize the hose and a gauge fitted next to the Schrader valve verified actual hose pressure.

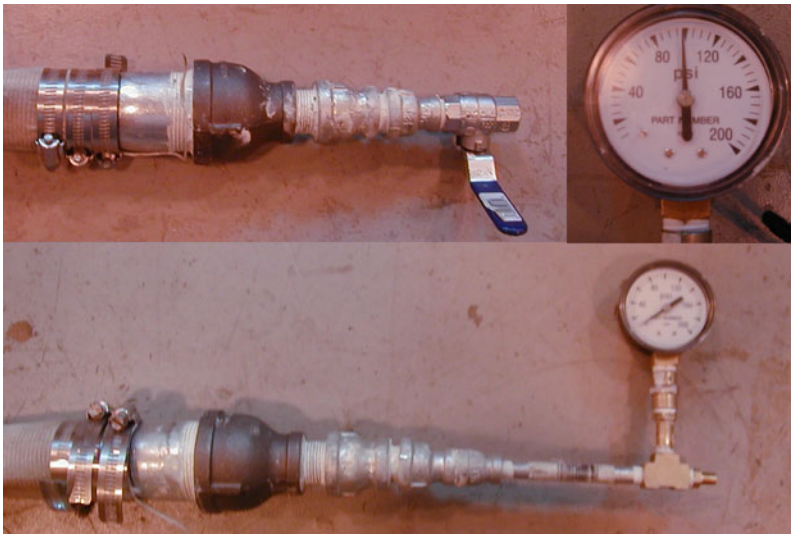

Figure 3.18: Ends of Fire Hose

Inflation tests of the hose revealed that small holes and imperfect seals resulted in a loss of approximately 35-70 kPa (5-10 psi) over a span of one minute. Instead of having the compressor constantly cycle on and off to waver about the correct value, it was decided to inflate the hose to a high enough pressure so that despite losses over the time period of application, the required 415 kPa (60 psi) would be met or exceeded.

3.6.2.2 Tests of Pressure Application Hose System

To investigate the actual performance of the hose-based pressure application system, further tests were undertaken. These tests involved the creation of a fixture for the universal testing machine that consisted of a 305 mm (1 ft) long section of the same metal channel used to constrain the fire hose. This fixture was then leveled and fitted to the load-cell of the MTS. A piece of sheathing material was also fixed to the MTS table to simulate any “give” that the

sheathing might have under the intense pressure. The hose was placed on the MTS table and the cross-head was lowered until the channel was barely touching the plywood. As the hose was inflated, the load-cell experienced the force required to hold the channel in place. In a real testing situation, the plywood would be pressing down directly onto the adhesive tape, and therefore the load cell reading could be converted to pressure applied to the bond-line by dividing the load by the area of tape under 305 mm (12 in.) of channel. In this case, the load corresponding to 415 kPa (60 psi) is 4.8 kN (1080 lb). Figure 3.19 provides an overview of the test setup.

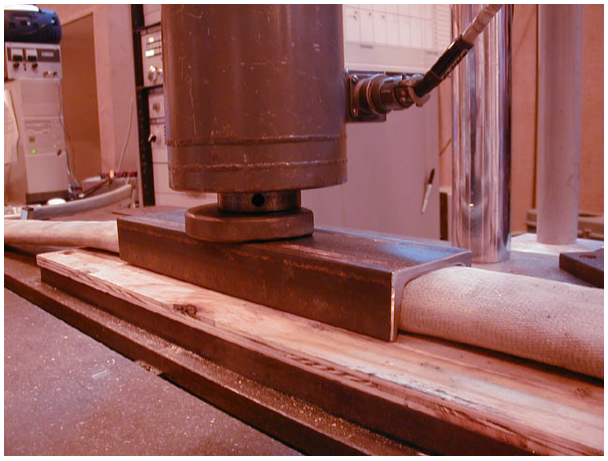

Figure 3.19: MTS Hose Test Setup

Multiple tests were performed to determine the performance of the hose system. Initial tests were conducted with the channel flush with the plywood to simulate a perfectly rigid system. It took approximately 15-20 seconds to fill the fire hose to its maximum pressure, and an initial maximum pressure gauge reading of 690 kPa (100 psi) was required to achieve true bond-line pressures exceeding 415 kPa (60 psi) for a period of 60 seconds.

As no system is perfectly rigid, additional tests were performed with the channel slightly above the plywood surface to model a deflected shape. Deflections were estimated for the steel channel between bracing points 1.22 m (4 ft) apart. These bracing points represented the steel u-braces used to constrain the channel against the sheathing as illustrated in Figure 3.16. These bracing points were later actually spaced at 0.61 m (2 ft) apart. Also, in an effort to decrease deflections, an additional channel was welded to the original channel to form a built-up section with a significantly larger moment of inertia. An initial pressure gauge reading of 760 kPa (110

psi) was found adequate to maintain the required pressure for the required time with a fixture deflection of approximately 4 mm (0.16 in.).

A final set of hose tests was performed using dynamic deflections. In these tests the MTS machine was set to raise its crosshead to 4 mm (0.16 in.) over the estimated period of 20 seconds required to fully inflate the hose. This movement simulated the maximum deflection of the channel between bracing points as the hose was inflated. Again it was found that a reading of 760 kPa (110 psi) on the hose pressure gauge was adequate to maintain actual bond-line pressures in excess of 415 kPa (60 psi). A typical graph of the pressure vs. time plots acquired during this series of experimental tests is presented in Figure 3.20.

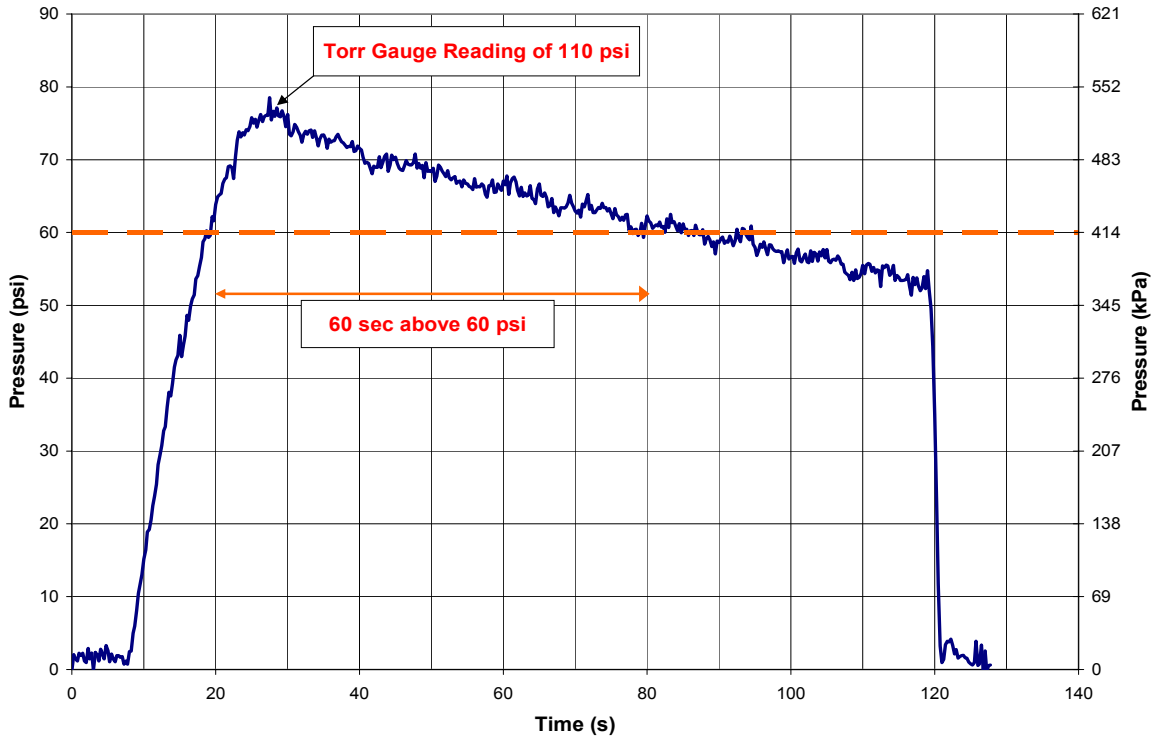

Figure 3.20: Pressure vs. Time Plot for Dynamic Hose Test

3.6.2.3 Real World Application

It should be noted that this method of applying pressure to activate the adhesive tape is not practical for real world use. There are, however, several methods of construction which were not feasible in a lab environment that are available to potential wall manufacturers. This problem is addressed in greater detail in Chapter 6.

3.6.3 Specimen Construction

3.6.3.1 Frame Construction

All wall frames were constructed with double top plates and single bottom plates 2.4 m (8 ft) in length. These plates were connected with five 2.32 m (91.5 in.) long intermediate studs at 406 mm (16 in.) on center between two double end-studs. All framing connections were made using Senco, 16d, 3.4 mm x 89 mm (0.135 in. x 3 ½ in.), full head, box nails. Pneumatically-driven box nails were used to simulate construction conditions in a pre-fabrication plant. Two nails were used per foot along both the top plate and the end studs.

Tie-down devices were placed 38 mm (1.5 in.) above the bottom plate on each end of the wall. USP HTT22 63.5 mm x 546 mm (2.5 in. x 21.5 in.) Heavy Tension tie-downs were secured with 32 hand-driven 16d, 3.8 mm x 83 mm (0.148 in. x 3 1/8 in.), sinker nails.

To reduce variability and produce consistent specimen frames, a jig was built that aligned all framing members correctly for construction. Double end and bottom plates were first connected and then placed along with the intermediate and top studs into the jig, where all members were nailed together. This jig also served as a stable platform for the adhesive tape application. A completed wall frame prior to the application of the sheathing is displayed in Figure 3.21.

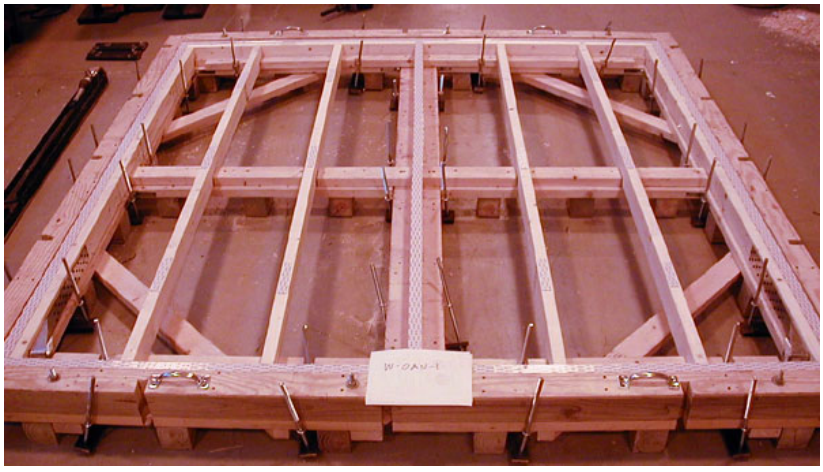

Figure 3.21: Frame Construction Jig

3.6.3.2 Application of Tape Adhesive to Full-Scale Walls

Application of the tape adhesive to the walls was the most critical and time-consuming portion of wall construction. Before the actual application of the adhesive tape, moisture content readings were taken from three different locations on the frame. These three locations were also marked so that readings could be taken in a similar location at the time of testing. Moisture contents for each specimen are recorded in the Appendix and ranged from 10 to 11%.

Any surface treatments to the sheathing were also completed before tape application could take place. As previously discussed in Section 3.4.2.3, both surface sanding and priming of the sheathing were used to increase the strength of the bond. Due to the time and expense involved with testing full-scale walls, sanding and priming were only performed on the specimens with OSB sheathing. Kilz original, indoor/outdoor, white, spray sealer/primer used in the comparison connection tests was used for the full-scale walls due to its ease of application over the Problock primer used in the connection tests. Performance gains were found to be similar when comparing the two primer types.

To reduce the deflection of the channel meant to constrain the fire hose and provide application pressure to the adhesive tape, 13 mm (1/2 in.) diameter carriage bolts were used in conjunction with custom fabricated steel plates to create u-clamps around the perimeter and center of the framing jig. This necessitated the pre-drilling of holes in all sheathing panels to match the placement of the interior carriage bolts. Nineteen millimeter (3/4 in.) holes were drilled using a template to allow some margin of error. Previous researchers such as Dolan (1989) have found that the failure mechanism of engineered shear walls is predominately in the fastening of the sheathing to the framing. The small amount of material removed during drilling was therefore assumed negligible to the overall shear strength of the wall specimen.

After the frame was in place and the pre-drilled sheathing pieces were properly treated, the process of tape application and pressurization began. This step-by-step process is shown pictorially in Table 3.8.

Table 3.8: Construction of Full-Scale Shear Walls

Step 1: Tape Application 33 m (108 ft) long rolls of 38 mm (1.5 in. wide) 3M VHB 4941 were placed down the perimeter and middle interior framing members and cut to length. The tape was then pressed down to the framing members using a roller.	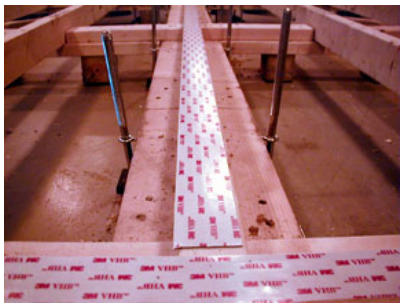
Step 2: Sheathing Placement Three additional 305 mm (1 ft) strips of adhesive tape were placed on each interior stud to prevent out-of-plane buckling. The liner was then peeled off of the tape and the sheathing panels were lowered into place over the carriage bolts.	
Step 3: Placement of Air Hose The fire hose was placed directly above a bond-line before being fixed in place by a series of u-bolts tightened with an air-wrench to prevent deflection. The compressor was then brought up to pressure and connected to the hose.	
Step 4: Pressurization The air-hose was inflated to (760 kPa) 110 psi to provide the downward adhesive activation pressure. Deflections were monitored using dial-gauges to make sure they were within acceptable limits. After exactly 60 seconds, the ball valve was turned to release the pressure.	
Step 5: Finishing Touches The inflation process was repeated five times to apply pressure to all of the bond-lines. The channel was then removed, and any mechanical fasteners required were shot into place before the removal of the completed wall.	

3.6.3.3 Nail Schedules

For walls designated as "adhesive-only," a single Senco 8d, 2.9 mm x 65 mm (0.113 in. x 2 1/2 in.), full head, bright box nail was hand driven into each corner before the wall was removed from the construction jig. These few nails were to make sure that any unforeseen impacts during handling would not loosen the adhesive bond during the manufacturer's recommended 72 hour curing time.

For walls designated as "nail-only," a construction industry standard nail schedule of 152 mm (6 in.) around the perimeter and 305 mm (12 in.) along the interior studs was utilized. A consistent edge spacing of 19 mm (3/4 in.) along the perimeter and 9.5 mm (3/8 in.) along the interior edge of the sheathing panels was achieved using a marking template.

Walls designated as "adhesive + nails" were constructed using a non-code conforming nail schedule of 305 mm (12 in.) along both the interior and perimeter of the sheathing panels. This schedule was used To explore the strength benefit that such a hybrid attachment system could produce with reduced labor and material costs for mechanical fasteners. A perspective diagram of the "adhesive + nails" wall construction is provided in Figure 3.22. Similar figures for each wall specimen are provided in the Appendix.

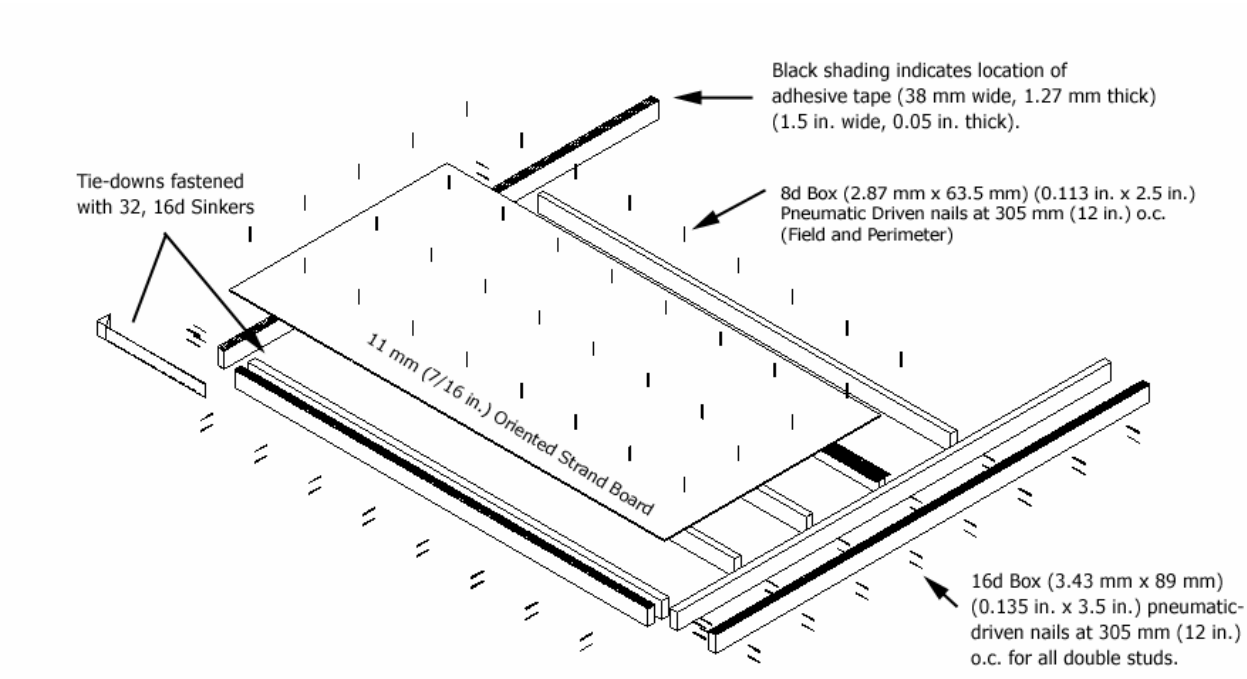

Figure 3.22: Construction Details for "Adhesive + Nails" Wall Specimen (After Heine 1997)

After construction each wall was placed in a storage rack located in a controlled environment until time of testing. Both temperature and relative humidity were monitored daily to ensure quality control.

3.7 Wall Testing

3.7.1 Testing Equipment

All walls were tested on a concrete reaction slab located outside of the Brooks Forest Products Research Center at Virginia Polytechnic Institute and State University. Walls were tested in a horizontal configuration to represent the worst-case scenario of non-load bearing conditions as shown in Figure 3.23. A hydraulic ram with a range of ±153 mm (±6 in.) and a load capacity of 245 kN (55 kip) was used to displace the top right corner of the shear wall. The hydraulic ram had two hinge-points between the reaction wall and the shear specimens to ensure that deflection induced moments were not transferred to the load-cell.

Displacement was transferred through a load-distribution bar which rolled on a greased caster. A fixture at the end of the bar restricted warping uplift of the wall from the horizontal position to simulate the intermediate tie-in and end-walls of a real-world system.

3.7.2 Attachment of Specimens to Test Frame

Shear walls were attached to the test frame through both the bottom and top plates. The bottom plate was attached using 16 mm (5/8 in.) diameter course threaded bolts to a 76 mm x 127 mm (3 in. x 5 in.) steel tube fixed to anchor bolts in the concrete reaction wall. The walls were attached in such a manner that the sheathing could move independently of the framing without interference from the thinner steel tube. Bolts were placed both in the tie-downs as well as 305 mm (1 ft) from each end of the wall and 610 mm (2 ft) on center thereafter. 12.7 mm (1/2 in.) thick, 76 mm (3 in.) square washers were used at each bolt location to reduce damage to the framing members and minimize cross-grain bending stress that could cause plate failure. All bolt holes were drilled 1.6 mm (1/16 in.) large to allow some margin of error while still minimizing slip.

The top plate was attached to another steel tube which served as the load-distribution mechanism from the hydraulic ram. The same bolting schedule was used, with the exception of tie-downs. All bolts were tightened using a pneumatic wrench.

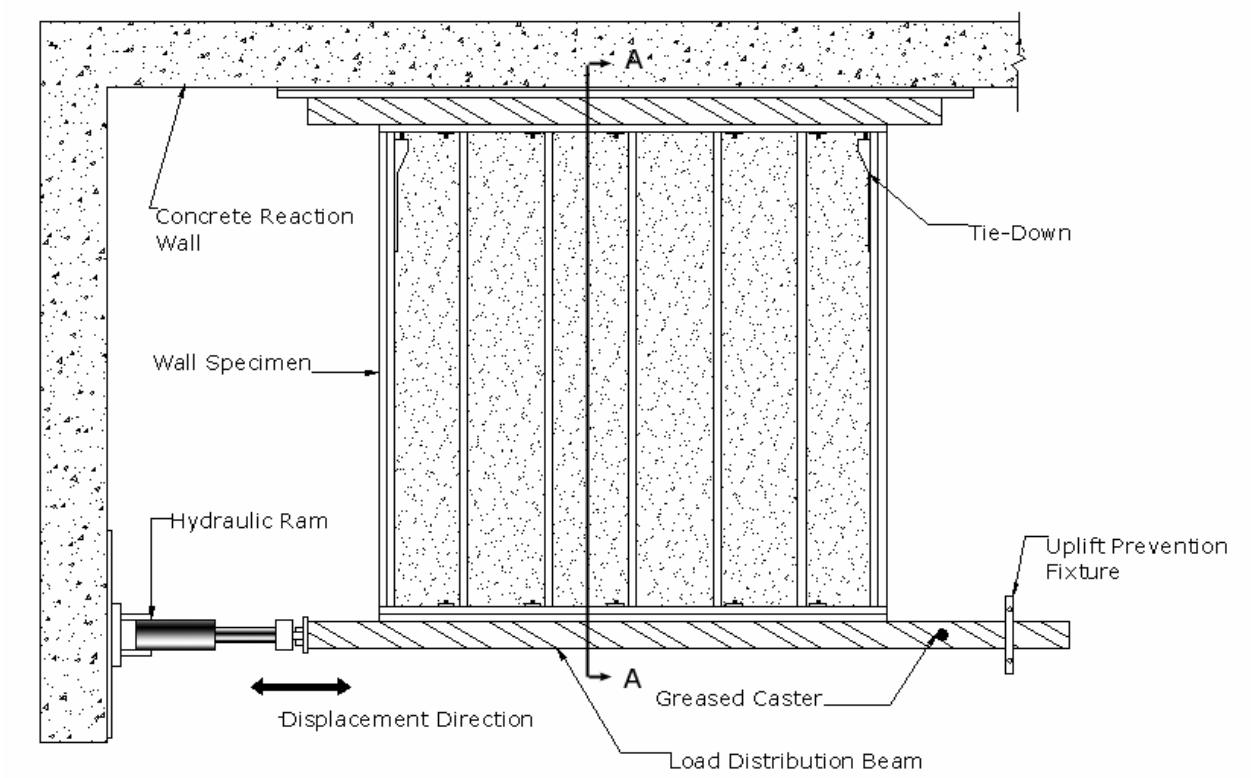

(a) Elevation

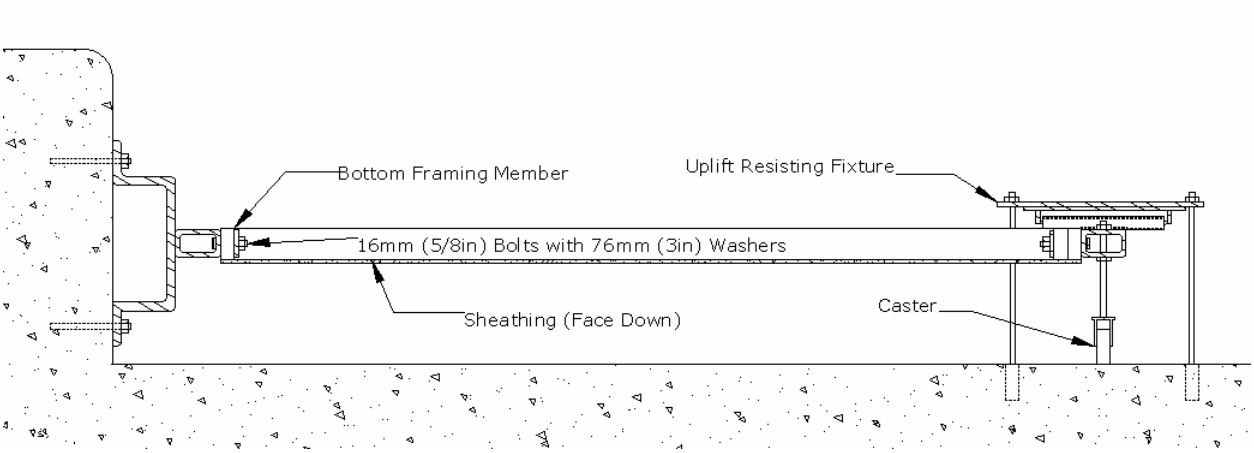

(b) Plan View (Section A-A)

Figure 3.23: Elevation and Plan Views of Wall Testing Setup

Walls were tested so that the sheathing was face-down. This orientation was used so that when failure occurred the sheathing could release from the framing as is typical of actual construction in a vertical wall. A photograph of a wall prior to testing is provided in Figure 3.24.

Figure 3.24: Photograph of Test Setup (Click for Shear.mov, 1200K)

3.7.3 Instrumentation of Wall Specimens

Seven main instruments were used to record wall behavior during each test. The instrumentation set was composed of five string potentiometers, a linear variance displacement transducer (LVDT), and a load cell. The layout of these instruments in relation to the testing assembly and wall specimens is illustrated in Figure 3.25 and described in Table 3.9. All data were recorded using an EnduraTech acquisition system in conjunction with a personal computer. Measurements were taken at a rate of 50 Hz for all channels. This sampling rate ensured that a smooth hysteresis curve containing all actual relative maximum and minimum values could be produced.

The load cell (Channel 2) had a capacity of 245 kN (55 kip) with a resolution of 0.22 kN (50 lb). Load measurements taken without wall specimens to calculate the maximum frictional force inherent in the rolling system yielded loads below 2.5% of the average peak wall load and were neglected in calculations. The LVDT (Channel 1) used was internal to the hydraulic actuator and measured the applied displacement values of the forcing function. This internal LVDT had a resolution of 0.061 mm (0.0024 in.) using a 16bit analog/digital converter card.

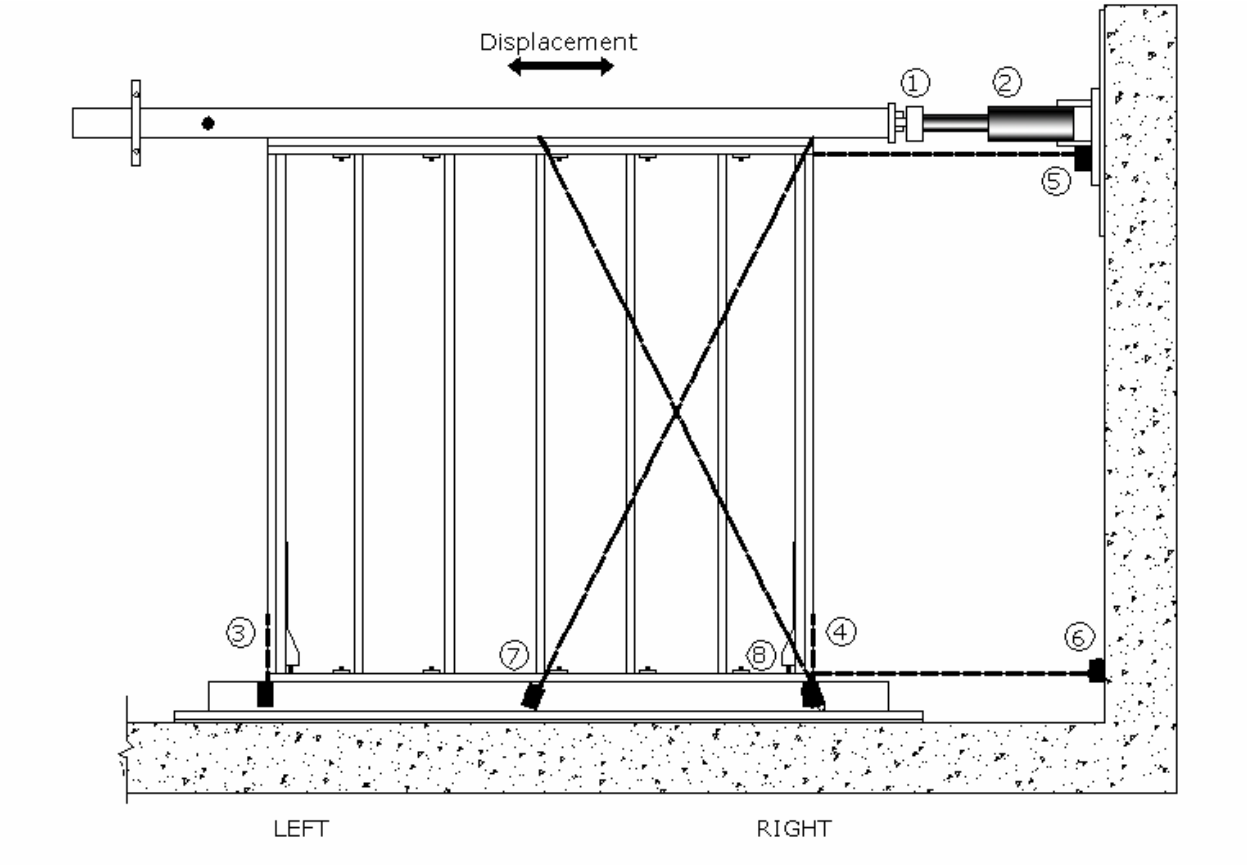

Figure 3.25: Instrumentation of Wall Specimens

Table 3.9: Instrumentation Details

Channel	Instrument	Measurement	Range		Resolution	
			SI	US Custom	SI	US Custom
1	Load Cell	Wall Force (Load)	245 kN	55,000 lb	0.22 kN	50 lb
2	Internal LVDT	Forcing Displacement	153 mm	6 in	0.061 mm	0.0024 in
3	UniMeasure PA-5 Potentiometer	Left Uplift	127 mm	5 in	0.18 mm	0.007 in
4	UniMeasure PA-5 Potentiometer	Right Uplift	127 mm	5 in	0.18 mm	0.007 in
5	UniMeasure PA-20 Potentiometer	Wall Displacement	508 mm	20 in	0.3 mm	0.012 in
6	UniMeasure PA-5 Potentiometer	Base Horizontal Slip	127 mm	5 in	0.18 mm	0.007 in
7	UniMeasure PA-20 Potentiometer	Left-Right Diagonal	508 mm	20 in	0.3 mm	0.012 in
8	UniMeasure PA-20 Potentiometer	Right-Left Diagonal	508 mm	20 in	0.3 mm	0.012 in

Channels 3-7 were UniMeasure Model PA 127 mm (5 in.) or 508 mm (20 in.) travel string potentiometers. These "string-pots" utilized a standard tension, ∅ 0.4 mm (0.016 in.), steel wire to measure certain displacement values. The 127 mm (5 in.) models had a resolution of 0.18 mm (0.007 in.), and the 508 mm (20 in.) models had a resolution of 0.3 mm (0.012 in.). Channels 3 and 4 measured the uplift on the bottom left and right of the wall per ASTM E564-00

(American Society for Testing and Materials 2000b). Each of these string pots was connected to a metal plate directly in-line with the ends of the walls so that eccentricities induced by mounting locations were negligible as illustrated in Figure 3.26. Channel 5 measured the displacement of the top plate of the wall and allowed the potential slip between the top plate and the load-distribution beam to be monitored as well as providing a check for the forcing function measurements provided by the internal LVDT. Channel 6 measured the slip of the bottom plate in relation to the fixed steel tube to assure that the wall had been properly secured. Channels 7 and 8 allowed the pure shear displacement of the wall to be calculated which was used in conjunction with the rigid body rotations and total deflection to compute the connection slip and bending component of the displacement as described in Chapter 4. A graph of the data produced from each channel is included for all wall specimens in the Appendix.

Figure 3.26: Connection of String Potentiometers to Wall Specimen

Temperature values were recorded in addition to force and displacement components. Ambient temperature was recorded in the sun and shade for each specimen. Walls that utilized adhesive tape as part of the construction were fitted with a thermocouple at the bond line between the framing member and the sheathing. This thermocouple was used to continuously monitor adhesive temperatures throughout the test, and both initial and final values were recorded. Temperature readings are presented for each wall specimen in the Appendix.

3.7.4 Testing Procedures

Wall specimens were tested using either a monotonic or a CUREE (Consortium of Universities for Research in Earthquake Engineering) based quasi-static protocol. The methods and loading patterns involved in each protocol are provided in this section.

3.7.4.1 Monotonic Loading

Monotonic loading was carried out on two walls using a modified ASTM E564-00 procedure (American Society for Testing and Materials 2000b). Unlike the incremental loading procedure outlined in ASTM E564-00, displacement was applied continuously until failure. A displacement rate of 101.6 mm (4 in.) over a period of six minutes was used to approximate the average increase in magnitude of the CUREE general cyclic protocol as illustrated in Figure 3.27.

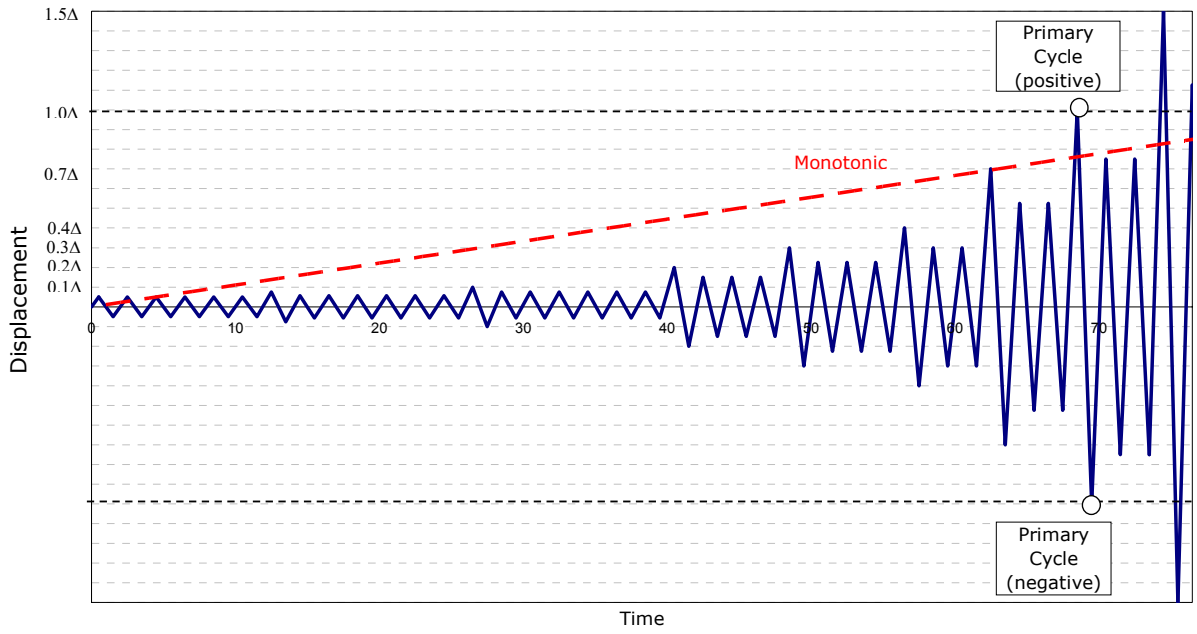

Figure 3.27: Time History of Displacement Based General CUREE Protocol

The emphasis of this study was the performance of the tape adhesive product in shear-walls subjected to high wind and seismic events. Monotonic tests were therefore used strictly to predict the displacement capacity for use in quasi-static cyclic loading. Furthermore, Dolan

(1989) and others have proven that the sheathing to framing connection governs the displacement capacity of typical shear walls. To conserve materials and labor for cyclic tests, ratios of the connection test displacement at peak loading were used to estimate the displacement capacity of wall specimens constructed with adhesives. The two walls tested monotonically were of type W-OAN (OSB sheathing with Adhesive tape and Nails) as they exhibited the smallest displacement capacity during connection tests and would therefore reduce the potential of over-predicting displacement capacity and prematurely failing other wall types.

3.7.4.2 CUREE Protocol Background

The CUREE project was initiated in direct response to the 1994 Northridge, California Earthquake. Wooden structures were responsible for an overwhelming number of the total casualties and amount of property loss (Gatto and Uang 2002). To better test the response of wood structures subjected to earthquake loadings and to provide a consistent basis for the comparison of cyclic test results, the CUREE loading protocol was developed. Many derivations of the basic protocol exist including deformation and force-controlled loading patterns for both general and near-fault ground motions (Krawinkler et al. 2001). The general displacement-controlled protocol was chosen due to the broad nature of this project and the available testing equipment.

The CUREE protocol was chosen over the Sequential Phase Displacement (SPD) protocol used in many previous shear wall studies, including Heine (1997), Salenikovich (2000), and Toothman (2003) for a variety of reasons. The first of these reasons is that the CUREE protocol was developed specifically for wood-framed structures while the SPD protocol was initially adopted from the Technical Coordinating Committee on Masonry Research (Porter 1987). The SPD protocol has also been found to under-predict deformation capacity and peak strength. The large number of cycles in the SPD protocol following the expected yield load has been found to produce fastener fatigue failures that are not indicative of actual earthquake failure modes (Gatto and Uang 2002). Fatigue of the adhesive tape is a critical consideration, and the false failure modes produced from the SPD protocol could severely affect performance conclusions.

3.7.4.3 CUREE Displacement Based General Protocol

The CUREE protocol is based on ordinary ground motions whose probability of exceedance in 50 years is 10%. The time-history consists of initiation cycles that simulate small tremors followed by a series of primary cycles and trailing cycles. The primary cycles are greater in magnitude than those directly preceding them and represent increasingly severe tremors. Trailing cycles have amplitudes equal to 75% of the preceding primary cycle and serve to more accurately model earthquake response while providing a realistic amount of damage to the system (Krawinkler et al. 2001). A general graph of the time-history of the CUREE protocol is provided in Figure 3.27.

The CUREE protocol is based on a target failure displacement (Δ). This target displacement is derived from a percentage of the monotonic failure displacement (Δ_m). The percentage used in this study was 60%, which is also the percentage recommended by the CUREE protocol. This reduction reflects the increased damage associated with reverse cyclic loading over monotonic loading. As previously described, monotonic displacement values were calculated through the testing of a limited number of shear walls combined with data gathered from connection tests. In addition, a Δ of 91.5 mm (3.6 in.) was used for plywood and OSB walls with only nail fasteners based on research by Toothman (2003) performed using the same testing apparatus.

A time step of two seconds (0.5 Hz) was used for the forcing frequency in all tests. The actual frequency of an earthquake is generally around 5 Hz. Realistic dynamic shake-table testing would therefore occur at higher frequencies. Shake table testing is, however, hard to interpret and requires back-calculating forces from accelerations. Additionally, inertial affects are present in cyclic tests oscillating at about 1 Hz or above. A value of 0.5Hz is reasonable for quasi-static cyclic loading to eliminate inertial affects and provide useful data which can be compared with similar studies.

A cycle-by-cycle summary of the CUREE time-history at 0.5 Hz is provided in Table 3.10. Note that the protocol is completely symmetric which is realistic for non-near-fault ground motion, and only positive strokes are provided. For further detail regarding the formulation of the protocol, as well as its comparison with common loading protocols other than Sequential Phase Displacement, the reader is referred to CUREE Publications No. W-02 and W-13 (Krawinkler et al, 2001, Gatto and Uang 2002).

Table 3.10: CUREE Protocol (0.5 Hz)

Cycle	Time (sec)	Magnitude	Type		Cycle	Time (sec)	Magnitude	Type
1	0.5	0.05Δ	Initiation		21	40.5	0.2Δ	Primary 3
2	2.5	0.05Δ	Initiation		22	42.5	75% (0.2Δ)	Trailing
3	4.5	0.05Δ	Initiation		23	44.5	75% (0.2Δ)	Trailing
4	6.5	0.05Δ	Initiation		24	46.5	75% (0.2Δ)	Trailing
5	8.5	0.05Δ	Initiation		25	48.5	0.3Δ	Primary 4
6	10.5	0.05Δ	Initiation		26	50.5	75% (0.3Δ)	Trailing
7	12.5	0.075Δ	Primary 1		27	52.5	75% (0.3Δ)	Trailing
8	14.5	75% (0.075Δ)	Trailing		28	54.5	75% (0.3Δ)	Trailing
9	16.5	75% (0.075Δ)	Trailing		29	56.5	0.4Δ	Primary 5
10	18.5	75% (0.075Δ)	Trailing		30	58.5	75% (0.4Δ)	Trailing
11	20.5	75% (0.075Δ)	Trailing		31	60.5	75% (0.4Δ)	Trailing
12	22.5	75% (0.075Δ)	Trailing		32	62.5	0.7Δ	Primary 6
13	24.5	75% (0.075Δ)	Trailing		33	64.5	75% (0.7Δ)	Trailing
14	26.5	0.1Δ	Primary 2		34	66.5	75% (0.7Δ)	Trailing
15	28.5	75% (0.1Δ)	Trailing		35	68.5	1.0Δ	Primary 7
16	30.5	75% (0.1Δ)	Trailing		36	70.5	75% (0.7Δ)	Trailing
17	32.5	75% (0.1Δ)	Trailing		37	72.5	75% (0.7Δ)	Trailing
18	34.5	75% (0.1Δ)	Trailing		38	74.5	1.5Δ	Primary 8
19	36.5	75% (0.1Δ)	Trailing		39	76.5	75% (1.5Δ)	Trailing
20	38.5	75% (0.1Δ)	Trailing		40	78.5	75% (1.5Δ)	Trailing

3.8 Summary

The experimental program for both connection tests and full-scale shear walls has been presented. The rational behind specimen naming and materials used in construction were detailed. Construction practices including the development and testing of tape adhesive application methods for connections and shear walls were also provided. In addition, testing setups and procedures including instrumentation and limitations were given. Overall, 275 monotonic connection tests and 23 monotonic and reverse-cyclic wall tests were employed to assess the performance characteristics of the adhesive tape connection system. The performance characteristics analyzed and the results obtained from this analysis are presented in the following three chapters.

Chapter 4

Performance Parameters and Analysis Techniques

4.1 General

To provide a point of comparison between specimens within this study and with other similar studies, certain performance parameters were computed for all connection and shear wall tests. These performance parameters are based upon properties that have been given various definitions in previous studies. Consistent property definitions have been elusive in the context of wood structures primarily due to the lack of a definite yield point that is present in other materials such as steel. Due to the high possible variance in values, and therefore perceived performance resulting from these inconsistencies, all parameters and the methods with which they were calculated are presented in this chapter so that the reader may have a clear indication of how conclusions were drawn.

4.2 Basic Monotonic Definitions

This section will focus on the basic property definitions as they apply to both monotonic connection and shear wall tests. These definitions are based on the load versus deflection data recorded during testing. Many of these properties are intuitive; however, figures are provided where possible to provide greater clarity to the written discussion.

4.2.1 Peak Load and Failure

Peak load (F_{peak}) of a monotonic test is the ultimate capacity reached during the forced displacement applied to the specimen. The displacement of the specimen that corresponds to this load is known as the peak displacement (Δ_{peak}). The general displacement term was alternately called "slip" for connection tests and "interstory drift" for shear wall tests in keeping with previous studies.

Failure of wood specimens is less clearly defined. Unlike iron and other brittle materials, wood assemblies often fail through a gradual loss of load capacity occurring over a displacement range beyond (Δ_{peak}). It was, therefore, necessary to select a point at which the loss

of capacity was significant enough to be considered a failure. This point and the load associated with it ($F_{failure}$) have been defined in previous studies and later adopted by the Consortium of Universities for Research in Earthquake Engineering to equal 80% of F_{peak}. The displacement at failure ($\Delta_{failure}$) is defined as the drift that corresponds to a 20% loss of capacity beyond F_{peak}. These properties are illustrated on a typical load-displacement plot for a connection test in Figure 4.1.

4.2.2 Elastic Stiffness

Elastic stiffness (k_e) is a measure of the ability of a system to resist moderate loads without incurring significant damage that needs to be repaired. The elastic stiffness is defined as the slope of the linear secant which passes through the origin and $0.4F_{peak}$. This point of intersection is known as the proportional limit, and the displacement corresponding with the proportional limit was also recorded. This definition was employed in previous shear wall studies as well as in European standards (Heine 1997).

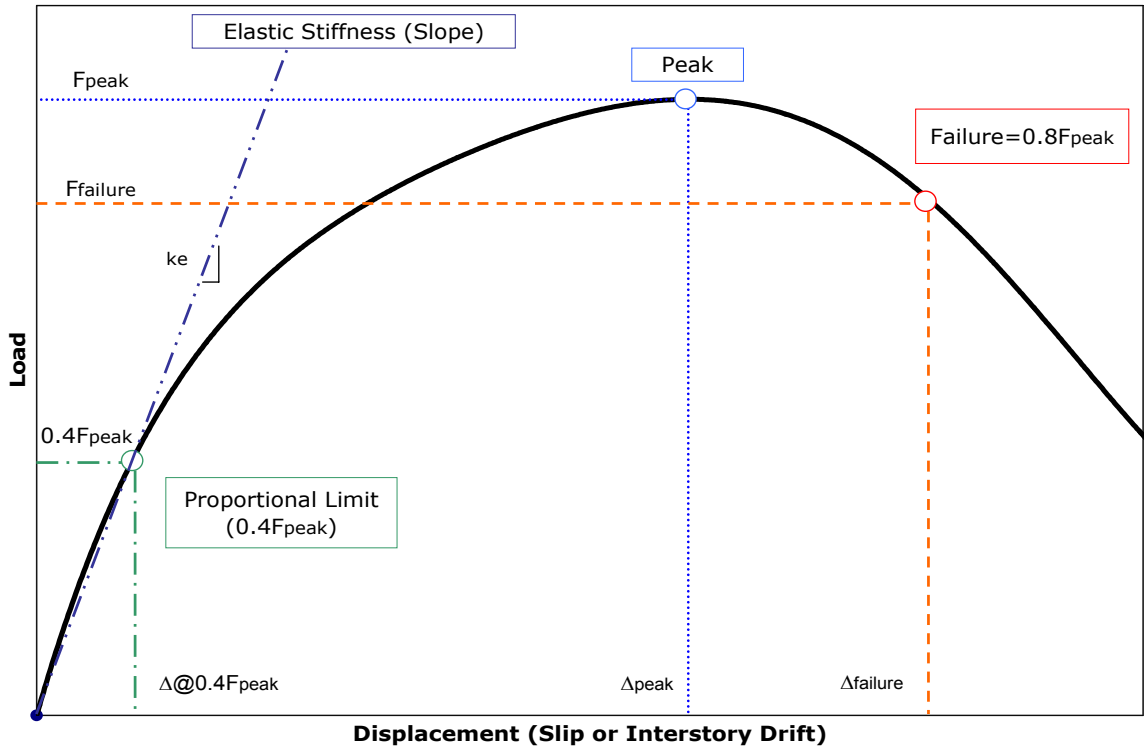

Figure 4.1: Basic Monotonic Definitions

4.3 Monotonic Equivalent Energy Elastic-Plastic (EEEP) Parameters

As wood structures do not exhibit a definite elastic-plastic behavior, it is difficult to define a yielding point for the system. To provide for the calculation of such a point, Porter proposed an idealized or equivalent energy elastic-plastic (EEEP) system (1987). With this system, a perfectly elastic line passing through the proportional limit and having slope k_e intersects a perfectly plastic (horizontal) line that is positioned to intercept a loading value greater than or equal to $F_{failure}$. This plastic limit is located such that the area (energy) under the actual load-deflection curve is equal to the area under the newly created EEEP lines up to $\Delta_{failure}$. Performance parameters associated with the EEEP curve are displayed in Figure 4.2 and described in the following sections.

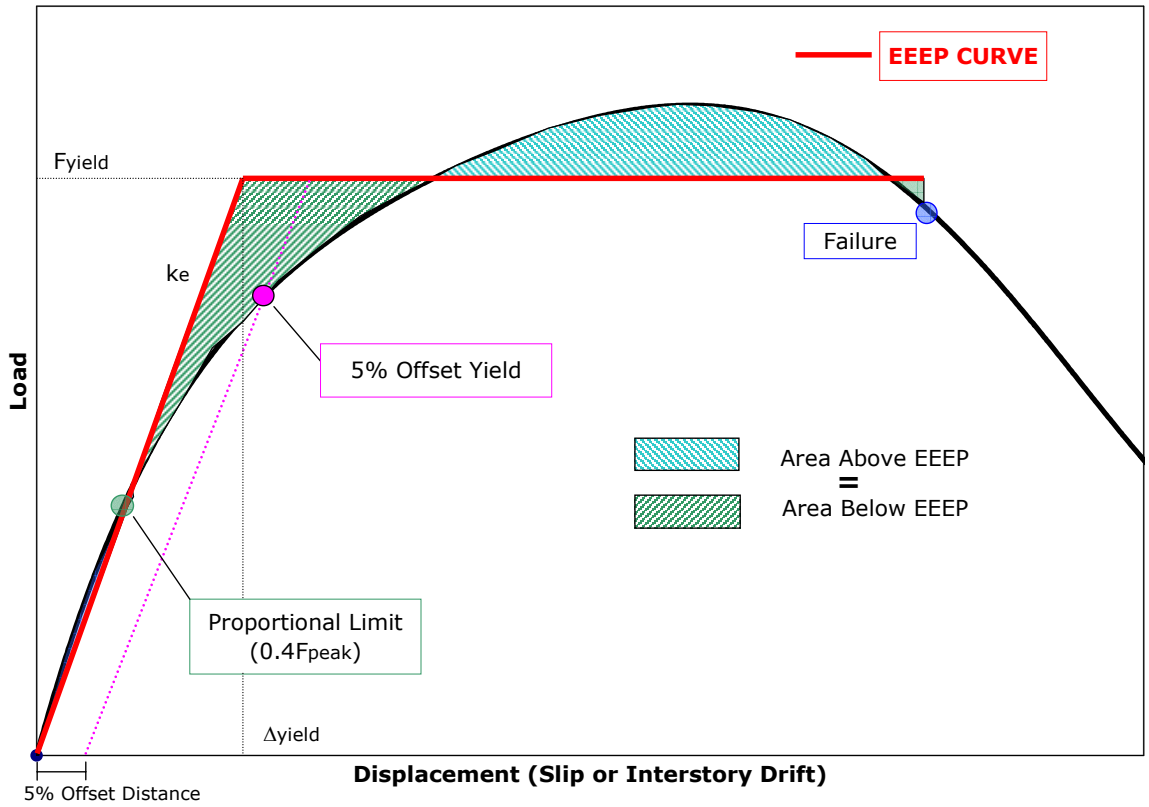

Figure 4.2: EEEP Parameters for Monotonic Tests

4.3.1 Yield Load and Displacement

Yield load is the loading value of the plastic portion of the EEEP curve. In other words, the yield load is the load at which the plastic portion of the EEEP curve intersects the elastic portion of the curve to circumscribe an area equal to that of the actual load-displacement history. By definition, this value must be greater than or equal to the failure load as previously described. Following this explanation, the yield loading can be calculated through the following formula (Heine 1997):

$$F_{yield} = \frac{-\Delta_{failure} \pm \sqrt{\Delta_{failure}^2 - \frac{2A}{k_e}}}{-\frac{1}{k_e}} \tag{4.1}$$

In this equation, A is the area under the actual load-displacement curve, k_e is the elastic stiffness as previously defined, and $\Delta_{failure}$ is the displacement associated with the failure load. Yield displacement, Δ_{yield}, is the displacement associated with the yield load.

4.3.2 Five-percent-offset Yield

The 5% offset yield value was first proposed for bolted connections by Harding and Fowkes (1984) and Patton-Mallory (1989). They proposed that a line parallel to the elastic stiffness line be offset from the origin by a displacement that equaled some percentage of the diameter of the fastener. This procedure was another way to produce a set yield point for comparison between tests. The offset percentage was to be determined so that the new line intersected the load-displacement plot in the curved region between the initial elastic segment and the plastic region before capacity. They determined that approximately 5% of the diameter of the fastener (e.g. nail or bolt diameter) provided a good estimate for the displacement offset. The intersection of this offset line with the load-displacement curve was called the 5% offset yield and is illustrated in Figure 4.2.

Offset yield values were calculated for connection tests only. Because the fastener consisted of a strip of adhesive tape, the use of a set diameter was not possible. The use of the thickness of the tape in place of the fastener diameter was evaluated and found to produce yield

values too close to the proportional limit and elastic range. The use of the width of the tape was also evaluated and found to produce yield values too close to the peak load. It was therefore decided to use an arbitrary limit of one-third of the tape width (12.7 mm or 1/2 in.) in place of the fastener diameter. This value was chosen as it provided a yielding point in the portion of the typical load-displacement curve that appeared to coincide with the transition from elastic to plastic behavior.

4.3.3 Ductility

Traditionally, a ductile material is one that can be deformed without breaking such as in the process of drawing a copper wire. Higher ductility results in the ability to draw longer and thinner wires. Ductility, as applied to shear walls, is a deformation in the form of wall distortion. The amount of ductility (D) for a wood system is defined as the ratio of the displacement at failure to the displacement at yield as calculated from the EEEP curve.

$$D = \frac{\Delta_{failure}}{\Delta_{yield}} \tag{4.2}$$

Ductility was not used as a main parameter for comparing shear walls because of its relative nature. Ductility represents the ratio of two displacements to one another and is therefore easily misinterpreted. For instance, a wall can have a displacement capacity of 2 units with a yield capacity of 0.5 units thus yielding D=4. Another wall can have a displacement capacity of 30 units and a yield capacity of 6 units thus yielding D=5. When comparing the two ductility ratios, the walls appear similar in deformation capacity, while in reality the second wall can withstand 15 times the displacement of the first wall. Ductility was, therefore, used in this study only in combination with other parameters to provide an indication of the amount of distortion occurring within each specimen. The actual displacement capacity of the specimens at failure is viewed to be a more meaningful quantity and was weighted more heavily in specimen comparisons.

4.3.4 Energy (Work Performed)

The classic definition of work is the force applied to a body through a displacement of the body in the direction of that force. This value is equal to the integral of, and thus the area under, the load-displacement curve. Recalling that the EEEP curve circumscribes the same amount of area to failure as the actual load-displacement curve, the work done by the system can be quickly calculated.

The amount of work done by the system is also referred to as the energy of the system. This performance parameter is useful in comparing specimens under constant wind loading, as it identifies the amount of energy that can be absorbed by each specimen at specific displacements.

4.3.5 Slack

Most connection specimens that make use of mechanical fasteners experience a certain amount of "slack" during testing. This slack is the relatively large displacement with little corresponding load at the beginning of a test that takes place as the mechanical fasteners seat themselves into the wood. This initial displacement is normally taken into account during the analysis of the load-displacement curve. The adhesive tape connections investigated in this project did not exhibit this behavior, and it was treated as negligible for all calculations.

4.4 Cyclic Definitions and Performance Parameters

The load-displacement curve for a reverse-cyclic test produces a continuous looping pattern known as the hysteresis of the system. To analyze the hysteresis loops, a series of points corresponding to the peaks of the primary cycles are plotted and connected to form an envelope curve as illustrated in Figure 4.3. The envelope curve is similar in shape to the load-displacement curve produced in a monotonic test, and is analyzed in much the same way. The basic definitions of peak load and displacement, failure load and displacement, and elastic stiffness given for monotonic tests hold true when applied to the envelope curve of a cyclic test. The only difference is that these parameters are calculated for both the positive displacement region and the negative displacement region and then averaged.

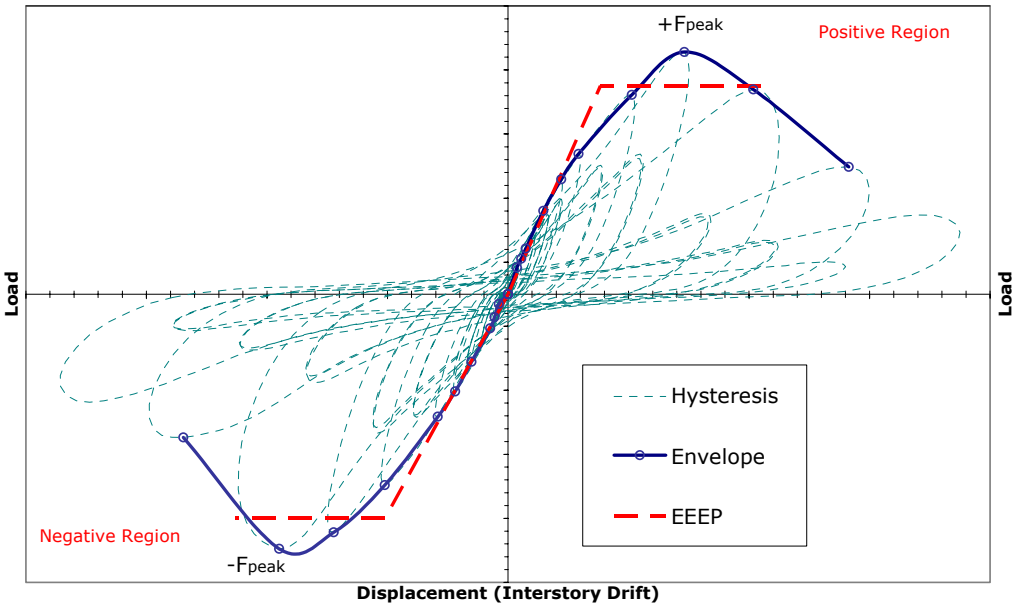

Figure 4.3: Typical Cyclic Hysteresis with Envelope and EEEP Curves

Continuing in this manner, the EEEP lines previously described can be applied to both the positive and negative regions of the envelope curve as displayed in Figure 4.3. The yield values and displacements for both regions can then be calculated and averaged. Unlike the connection tests, 5% offset yields are not used in the calculation of cyclic parameters.

4.4.1 Energy (Work Performed)

The energy or work performed by a specimen was previously defined as the area under the load-deflection curve. This definition must be altered somewhat for cyclically loaded walls. The work done by the system is the total area enclosed by the hysteresis loops to failure. The area is to include all initiation and trailing cycles. This definition takes into account the overlapping of the hysteresis loops.

Work done to failure is not an extremely useful performance parameter as it is dependent on the forcing function used to perform the test. For instance, the work performed up to 51 mm (2 in.) of displacement will be completely different if the CUREE protocol is used as opposed to the SPD protocol due to the variations in amplitude and numbers of cycles up to the target displacement. The work done to failure is, therefore, only used as a means of comparison between the different walls tested within this study.

For more general results, the work performed at a particular cycle can be plotted against the displacement at that cycle. This parameter is described as the hysteretic energy and is presented along with other earthquake performance parameters in the next section.

4.5 Earthquake Performance Parameters

The performance of a system subjected to reverse-cyclic loading can be analyzed by quantifying certain indicators for each complete hysteresis loop. In this study, only the primary cycles were analyzed, and a typical loop is displayed in Figure 4.4.

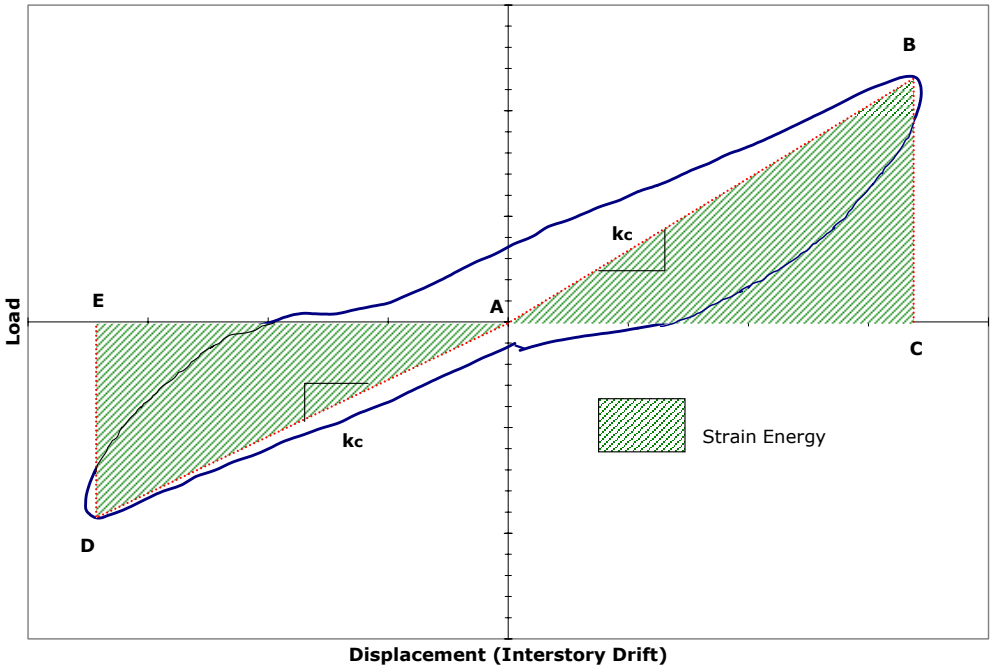

Figure 4.4: Typical Hysteretic Loop

4.5.1 Hysteretic and Strain Energy

The hysteretic energy (W_d) of a cycle can be calculated by taking the area enclosed within the load-displacement loop of that cycle. The strain or potential energy (U_1) of the same loop can be calculated by the area of triangles ABC and ADE as illustrated in Figure 4.4. These triangles represent the linear peak potential energy of both the positive and negative regions of the cycle. Note that this value is actually not the true strain energy of the system because it is based on a perfectly viscous assumption which shear walls do not always exhibit (Heine 1997).

When plotting these energies versus the corresponding interstory drift, the average maximum displacement of points C and E was used. Plots of hysteretic energy versus corresponding interstory drift, along with the displacement at failure, are good indicators of the toughness of a system.

4.5.2 Damping

The damping of a system indicates how much energy per cycle is lost from a vibrating body to heat through friction or radiation. Damping occurs in any non-conservative system and is necessary to help diffuse the large amounts of energy that an earthquake transfers to a structure. Damping can be quantified using the damping loss coefficient which is referred to as the equivalent viscous damping ratio (EVDR).

The EVDR is calculated by comparing the amount of hysteretic energy per radian (W_d) to the strain energy (U_l).

$$EVDR = \frac{W_d}{2\pi U_l} \tag{4.3}$$

As discussed by Heine (1997), the EVDR only provides accurate damping approximations within the elastic range of the system. EVDRs were, however, calculated for displacement values that were well beyond the elastic range of the walls for use in comparison with other tests.

4.5.3 Cyclic Stiffness

The cyclic stiffness (k_c) is defined as the average slope of lines AB and AD as illustrated in Figure 4.4. This stiffness value was calculated for all primary cycles of the hysteresis curve. By plotting the cyclic stiffness versus the corresponding interstory drift, the stiffness degradation of the wall over time can be analyzed. The stiffness degradation of a wall is a good indicator of the amount of damage that a wall can sustain up to a certain displacement.

4.5.4 Inertia

The dynamic forces due to inertia have been presumed to be negligible due to the low forcing frequency of 0.5 Hz as described in Chapter 3. This assumption will be validated using a small example in this section. It should be noted that in an actual earthquake the inertial forces would be quite large; therefore, analytical or shake table modeling of these systems is of particular use.

The mass of a single 2.4m x 2.4 m (8 ft x 8ft) wall with negligible fastener weight can be determined as shown below. Newton's Second Law of motion can then be applied to an acceleration derived from the frequency of oscillation. An average displacement value of 12.7 mm (1.5 in.) corresponding to the peak load is used based on preliminary results. U.S. Customary units are used for this example as they correspond with values listed in the 2001 National Design Specification (AF&PA 2001).

1. Density of SPF lumber (MC=12% G=0.42):

$$\text{Density} = 62.4\left[\frac{G}{1+G(0.009)(m.c.)}\right]\left[1+\frac{m.c.}{100}\right] = 28 \text{ lb/ft}^3$$

2. Weight of frame of one wall with 96 feet of lumber:

$$\text{Weight} = \left[\frac{(1.5\text{ in.})(3.5\text{ in.})}{144}\right]\left[\frac{28\text{ lb}}{ft^3}\right][96\text{ ft}] = 98 \text{ lb}$$

3. Weight of two 7/16 in. OSB sheathing panels (APA Technical Note N375B):

$$\text{Weight} = [1.3\,psf(1.10)][64\,ft^2] = 91.5 \text{ lb}$$

4. Total mass of system (Including approximately 250 lb Load Cell + Beam Weight):

$$\text{Mass} = \frac{98\text{ lb} + 91.5\text{ lb} + 250\text{ lb}}{g = 32.2\text{ ft}/s^2} = 13.65 \text{ slugs (lb·s}^2\text{/ft)}$$

5. Acceleration of 0.5 Hz system at 1.5 in. displacement:

$$p = 2\pi f = 3.14$$
$$a = \Delta p^2 = (1.5\text{ in.}/12)(3.14)^2 = 1.23\,ft/s^2$$

6. Force due to acceleration

$$F = ma = (13.65\ slugs)(1.23\ ft/s^2) = 16.8\ lbs$$

The force calculated of 75 N (16.8 lb) is negligible when compared with the peak expected capacities between 22 and 44 kN (5,000 to 10,000 lb). If a frequency of 5Hz had been used for the forcing function within the same series of calculations, the result would have been an inertial force of almost 7.6 kN (1,700 lb) which would have controlled the behavior of the test.

4.6 Deflection Parameters

The overall deformation in shear walls is the result of three distinct components: rigid body rotation, shear deformation, and connection slip plus bending. In supporting literature such as FEMA-273 (FEMA 1997) for seismic rehabilitation design, nail slipping is calculated as a separate component from bending. For this study, the amount of bending associated with shear walls that can be analytically modeled as short, deep beams was small and could be grouped with connection slip. The drift components were calculated for the displacement corresponding with the peak load. This peak displacement was chosen instead of the yield displacement called for by the CUREE protocol (Gatto and Uang 2002) because the calculation of the yield point is not as well-defined and varies depending on the EEEP calculations.

4.6.1 Rigid Body Rotation

Rigid body rotation (RBR) is the movement of the entire wall as a whole through an angle of displacement without deformation. Rigid body rotation was measured directly through the use of string potentiometers on each side of the base of the walls as described in Chapter 3 using the following equation:

$$RBR = |\Delta_1| + |\Delta_2| \tag{4.4}$$

Where: Δ_1 = Measured uplift on one end of wall

Δ_2 = Measured compaction on opposite end of wall

Note that Equation 4.4 is only suitable for walls having a height to width ratio of 1:1, as was the case with this study. Figure 4.5 illustrates the principal of rigid body rotation.

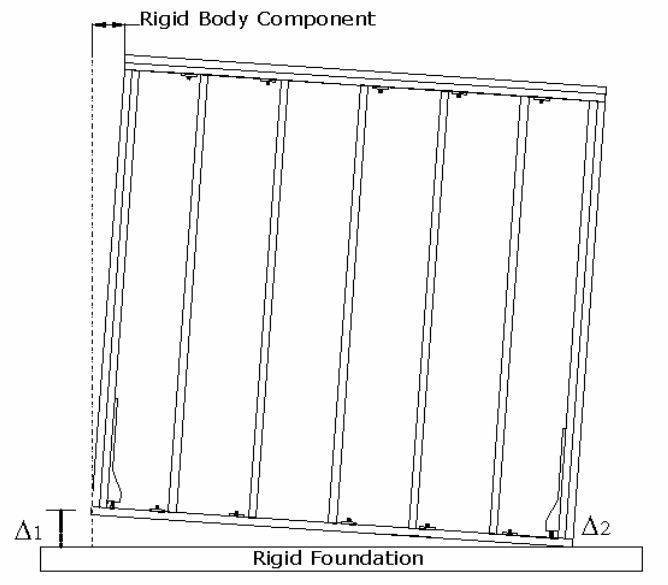

Figure 4.5: Rigid Body Component of Deflection

4.6.2 Shear Deformation

The shear deformation (SD) component of deflection is caused by the warping of the combined frame and panel system as shown in Figure 4.6. In this study only the global shear deformation was measured, as opposed to the sheathing shear deformation which can be calculated using strain measurements. Gatto and Uang (2002) proposed that global shear deformation be calculated using the readings of two diagonal string potentiometers in a crossing pattern as described by the following equation.

$$SD = \frac{H[\Delta_1 - \Delta_2]}{2ab\sqrt{a^2 + b^2}} \tag{4.5}$$

Where: SD = shear deformation component

H = Height of Wall

a = width of X-pattern

b = height of X-pattern

$\Delta_{1,2}$ = measured deformations of diagonals

Note that Equation 4.5 cannot be correct as the units of the numerator are distance squared and the units of the denominator are distance cubed thus leaving an incorrect 1/distance unit as the solution. The following formulation was derived from geometry using the same variables and was used in place of Equation 4.5

$$SD = \left[SIN(\,ATAN(a/b))\right]\left[|\Delta_1| + |\Delta_2|\right] \tag{4.6}$$

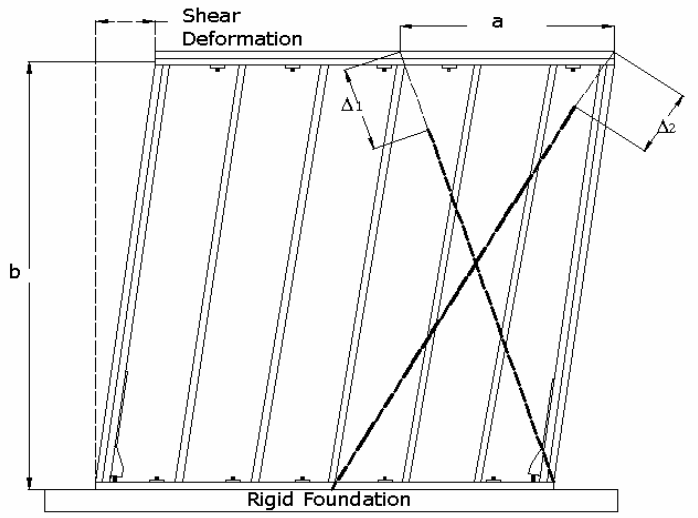

Figure 4.6: Shear Deformation Component of Deflection

4.6.3 Connection Slip and Bending

Pure chord bending occurs when the studs assume a curved shape due to the rigidity of their anchorage as illustrated in Figure 4.7. This phenomenon normally occurs when engineered tie-downs are used, as was the case with all walls in this study. Chord bending can be measured directly with a series of strain gauges, as was done by Gatto and Uang (2002), or indirectly, as was done in this study. For this study, the chord bending component was combined with the slip present in the nail or adhesive connection between sheathing and framing members. Using the indirect approach and considering the assumption that only rigid body rotation, shear deflection, and connection slip plus bending contribute to the overall drift of the wall, the connection slip and bending component can be calculated by subtracting the combined drift of the other two components from the total deflection of the wall. This method is not exact but will provide results which are sufficiently accurate to make comparisons.

4.6.4 Deflection Summary

Breaking the total wall drift into its three main components provides the ability to observe where possible improvements could be made to reduce total drift and where forces are likely concentrating on the shear wall mechanism. For additional discussion on deflection components including comparisons between walls with and without tie-down devices, see Salenikovich (2000) and Bredel (2003).

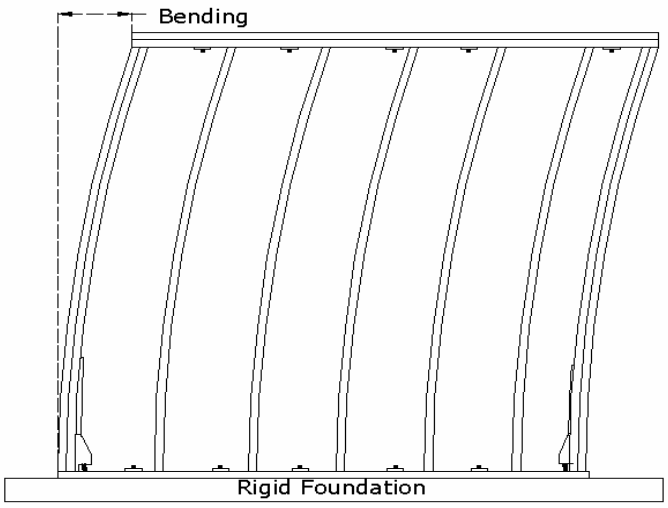

Figure 4.7: Pure Bending Component of Deflection

4.7 Data Analysis

The analysis of the data recorded during each test to produce the parameters described herein was performed using programs written in Visual Basic for Applications in Microsoft Excel. A large portion of the coding used to analyze shear walls was originally written and since updated by Dr. Alexander J. Salenikovich for his dissertation "The Racking Performance of Light-Frame Shear Walls" (2000). Additional coding was performed by the author of this thesis and Ramskill (2002).

Sample calculations for all performance parameters were completed for five connection tests and two shear wall tests to verify the accuracy of the program. As with all experimental tests, the accuracy of the results is dependent upon the accuracy of the instrumentation used to record data and the consistency with which specimens were constructed and tests were performed.

4.8 Summary

Performance parameters for both monotonic and cyclic testing regimes have been defined and explained. Indicators used to gauge the effect of an earthquake on a system were presented, and an example calculation was performed to verify that inertial effects were insignificant to this study. The three main components of deflection were also presented, and their significance given. Finally, the tools used to compute performance parameters were noted. In the following pages, the results obtained using the information presented in this chapter will be discussed for connections (Chapter 5) and shear walls (Chapter 6).

Chapter 5

Connection Test Results and Discussion

5.1 General

The connection test portion of this study was composed of 289 single-lap shear specimens. Each specimen was monotonically tested to provide information on the significance of surface treatments, member materials, application pressure and time, and tape manufacturer. These tests were broken down into comparison, application pressure, application time, statistically significant, and additional interest subsets. This chapter provides information on the performance of each specimen subset including general trends and direct comparisons of performance parameters.

The results presented in this chapter represent a summary of the entire body of test data. Detailed information on the performance characteristics of each specimen is presented in the Appendix which contains the following information:

1. Comparison Subsets
    - *a.* Sheathing and main member materials.
    - *b.* Connection type and comments on surface treatments.
    - *c.* Moisture content of main member at time of testing.
    - *d.* Peak load recorded from the testing and data acquisition systems.
    - *e.* Observed failure modes and general commentary.
    - *f.* Original main member from which specimen was constructed.
2. Application Pressure / Time and Statistically Significant Subsets.
    - *a.* (a-e) from Comparison Subsets.
    - *b.* Application pressure and time.
    - *c.* Moisture content at construction and testing.
    - *d.* Expanded summary tables of all performance parameters.
    - *e.* Additional subset average and variance load-displacement graphs.
    - *f.* Load-displacement plots for individual specimens.

Many of the summary graphs and tables that appear in this chapter are also provided in the Appendix in an expanded form. The Appendix provides complete documentation which gives additional information that might be of interest but which was not included in the main body for space considerations.

It is recommended that the information in the Appendix on failure modes, load-displacement plots of the individual elements, and comments on individual tests be read thoroughly as it provides a complete view of the variability between connections.

5.2 Comparison Subset

The comparison specimen subset consisted of 52 connection tests chosen to provide a general idea of the viability of bonding wood substrates with pressure sensitive adhesive (PSA) tapes. Different sheathing surface treatments, as well as the bonding capability of the tape to light-gauge steel framing studs, were also explored. A summary of the different comparison tests is provided in Table 5.1

Table 5.1: Comparison Specimens

Comparison Single Lap Shear Connection Tests							
I.D.	Member	Sheathing	Fastener	Treatment	Pressure[1]	Time[2]	No. Tests
C-OA	SPF	OSB	3M VHB	None	15 psi	20 sec	5
C-OAS	SPF	OSB	3M VHB	Sanded	15 psi	20 sec	5
C-OAP	SPF	OSB	3M VHB	Primed	15 psi	20 sec	5
C-OAN	SPF	OSB	3M VHB +8d Nail	None	15 psi	20 sec	5
C-OACL	SPF	OSB	3M VHB	Clamped[3]	Note 3	24 hours	2
C-OAMS	Metal Stud	OSB	3M VHB	None	15 psi	20 sec	5
C-PA	SPF	Plywood	3M VHB	None	15 psi	20 sec	5
C-PAP	SPF	Plywood	3M VHB	Primed	15 psi	20 sec	5
C-PAN	SPF	Plywood	3M VHB +8d Nail	None	15 psi	20 sec	5
C-PAMS	Metal Stud	Plywood	3M VHB	None	15 psi	20 sec	5
C-PACL	SPF	Plywood	3M VHB	Clamped[3]	Note 3	24 hours	2
						TOTAL	49

NOTES

1) Pressure applied to each specimen for alloted time to activate pressure sensitive adhesive.
2) Amount of time for which adhesive activation pressure was applied.
3) "Clamped" indicates activation pressure was applied with hand-tightened clamps for the alloted time.

5.2.1 General Construction Observations

The comparison test subset was not analyzed for performance parameters as rigorously as later subsets due to the general nature of the required information. Qualitative observations based on load-displacement curves regarding specimen construction and performance were the primary tools employed to draw conclusions based on this subset.

5.2.1.1 Specimen Construction

During the construction of each specimen it was observed that the adhesive tape often did not appear to be bonding or "wetting out" during the application of pressure. These specimens were handled with care with the assumption that the manufacturer-recommended curing time might resolve the issue. After approximately one week had passed, a general inspection of the specimens including slight pulling of the members in shear was performed by hand. At this time many of the members were deemed to have an excessively weak bond. Pressure was reapplied to all specimens for an additional 15 seconds to prevent premature failure during loading.

Additionally, it was observed that most of the specimens provided greater resistance to parallel shear loading than to perpendicular axial loading as illustrated in Figure 5.1. This discrepancy is, however, negligible in full-scale walls because the bending moment applied to an entire wall section does not locally warp framing members away from the sheathing. Full-scale wall moments warp the system as a whole.

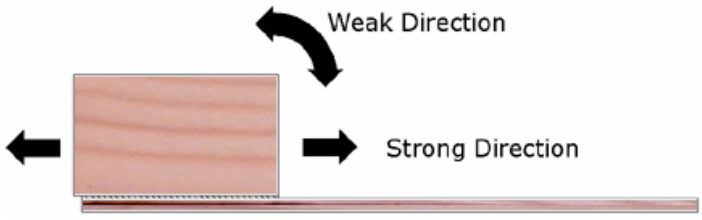

Figure 5.1: Connection Strength Directions

The cause of the weak bonds produced was attributed to the rigidity and macroscopic curvature of the wood members and sheathing panels. Wood is a material that easily becomes warped during shipment or exposure to adverse weather conditions, and rarely is a full-length framing member perfectly straight. The curvature of the larger pieces was present to a smaller

extent in each specimen. When pressure was applied to the rigid system, a small portion of the adhesive tape actually experienced the required pressure for activation as illustrated in Figure 5.2. The data sheet from 3M states that "rigid surfaces may require [two] or [three] times that much [15 psi] surface pressure to make the tape experience 15 psi" (3M 1998). Also, the roughness of the sheathing panels, in particular OSB, prevented full contact pressure from developing at the bond line. In light of this information, four test specimens were constructed using clamps to ensure a strong bond and to measure the effect of higher application pressures.

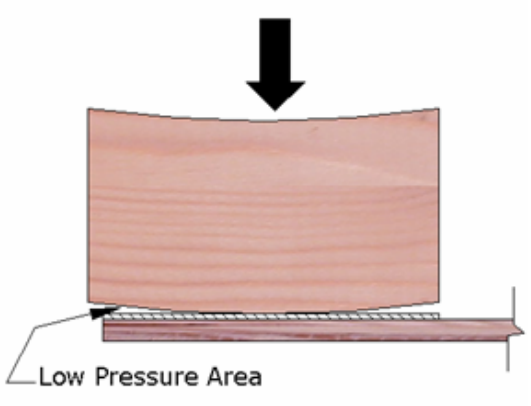

Figure 5.2: Macro Curvature of Specimens

5.2.1.2 Commentary on Validity of Results

Due to the issues with tape bonding and application pressure found after the construction of the comparison specimens, these tests did not represent the actual peak performance of the acrylic foam tape. However, they were still useful for comparisons between different surface treatments and materials within the subset.

5.2.2 Load-Displacement Curves

The load-displacement curves produced during the testing of these specimens exhibited a large amount of noise due to the low peak loads in comparison with the range of the testing equipment. Sixth-order polynomial trend-lines were fit to the actual data set to provide a clearer illustration of results. Neither the individual load-displacement curves nor the performance parameters for each specimen are provided in the Appendix due to the unrealistic actual performance of the connections that arose from low bonding pressures.

5.2.3 Oriented Strand Board Tests

Average load-displacement curves for each OSB connection specimen grouping are provided in Figure 5.3. These curves were calculated by averaging each connection specimen's load at a given displacement. Note that load-displacement curves are only illustrated up to the point where the first connection specimen in that group failed.

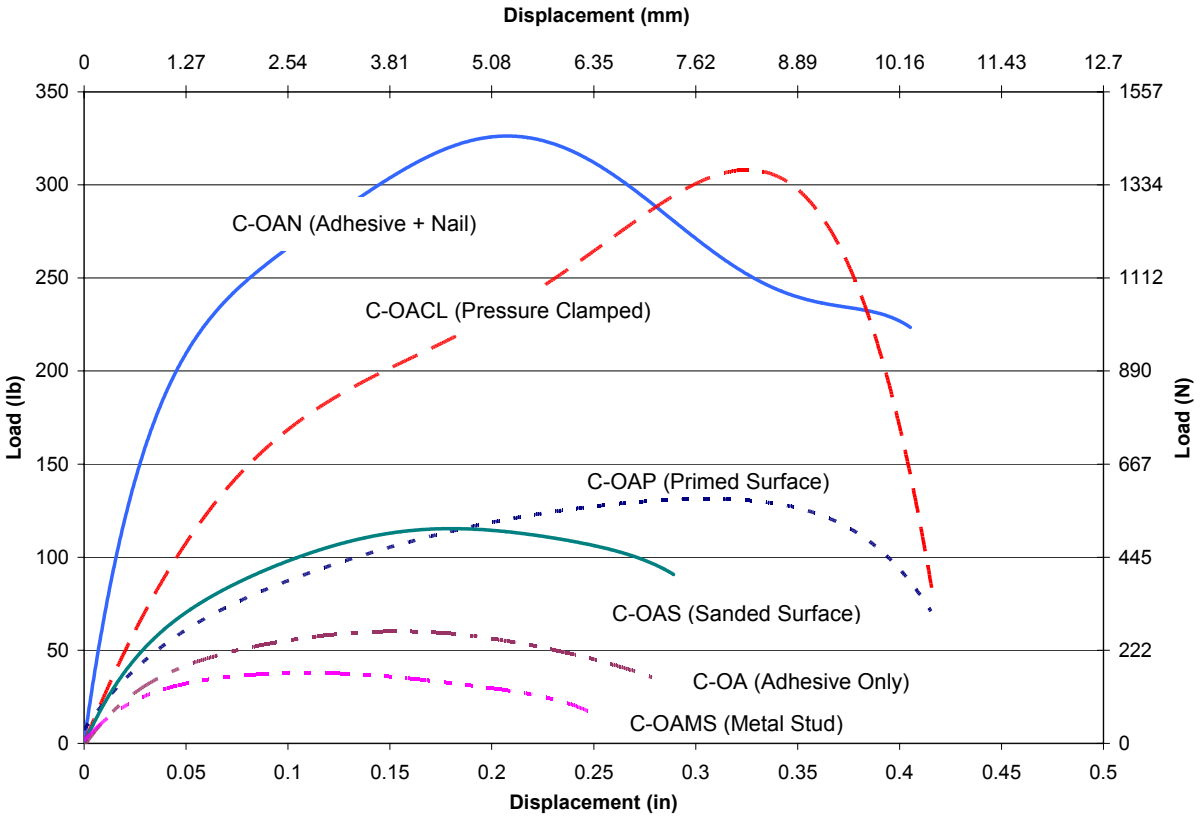

Figure 5.3: OSB Comparison Test Load-Displacement Graph

5.2.3.1 Surface Treatments

Both priming and sanding proved extremely beneficial to the performance of the connections. Priming provided twice the load capacity and a 25% increase in displacement capacity over the specimens that were constructed with no surface treatments. Sanding the OSB provided approximately twice the loading capacity over not sanding, but displacement capacity remained the same. It was concluded that both treatments should be included as variables in the larger set of statistically significant connections for further investigation.

5.2.3.2 Mechanical Fasteners and Application Pressure

The performance improvements gained by the use of increased application pressure were immediately apparent upon observation of the load-displacement curves in Figure 5.3. Note that the exact pressure generated by clamping the connection specimens during construction was not measured, and that the purpose of these tests was to discern if increased application pressure positively affected performance. The increased pressure used to bond the C-OACL series of connection tests resulted in a peak load capacity six times larger than the C-OA set that had been constructed using only 100 kPa (15 psi). The amount of energy or work performed to failure also experienced a similar gain.

Results of the C-OACL series were especially promising when compared to the C-OAN connections that were fastened with adhesive tape and a single nail. The clamped series showed a comparable peak load with a greater displacement capacity. Also, the elastic stiffness of the clamped adhesive-only set was lower than that for the adhesive and nail set. The ramifications of these results were that a properly bonded specimen could hold a significant amount of load at higher displacement capacities with lower susceptibility to damage than specimens with only mechanical fasteners. In response to these results, a series of tests to determine the optimum application pressure for the PSA tape was initiated.

5.2.3.3 Light-Gauge Steel Framing

Use of light-gauge steel framing studs in residential construction has been on the rise for many years due to their unique benefits and the fluctuating costs of wood products (NASFA 2003). Steel studs were initially included in this study and found to perform poorly as illustrated in Figure 5.3. This poor performance was attributed to a number of factors. The most critical factor was that, as with the wood tests, the application pressure required for the tape to "wet out" was not achieved. Also, the steel sections had a tendency to twist or warp during the pressure application of the tape.

Though the performance of steel studs could be attributed to the factors described above, they still compared poorly with wood specimens that were constructed under the same conditions. In light of this comparison, and to keep the scope of this study to a manageable level, steel studs were eliminated from further testing.

5.2.4 Plywood Tests

Average load-displacement curves for each plywood specimen grouping are provided in Figure 5.4.

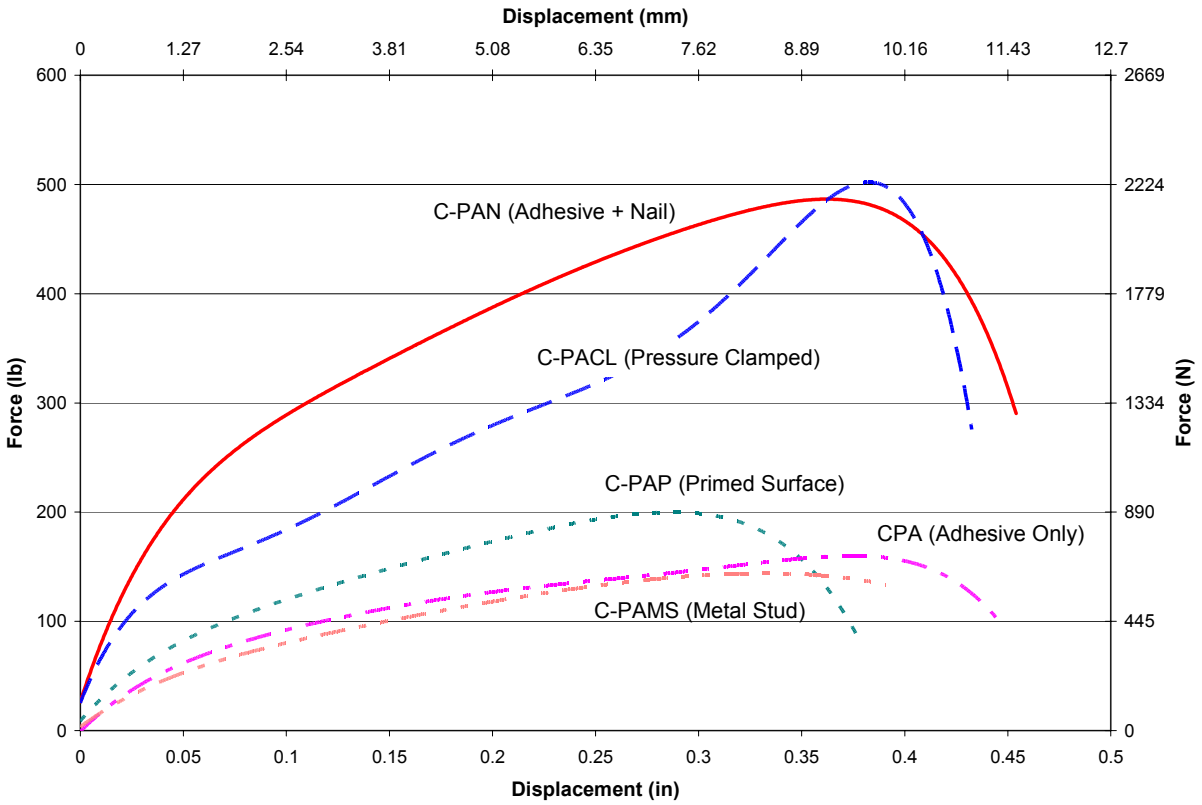

Figure 5.4: Plywood Comparison Test Load-Displacement Graph

5.2.4.1 Surface Treatments & Comparison to OSB

Priming was the only surface treatment tested on connections constructed with plywood sheathing. This surface treatment increased the peak capacity marginally over untreated specimens, but the increase was not statistically significant. Surface treatments did not provide as much of an impact on plywood specimens as on OSB specimens because of the surface sanding present in the manufacturing process of plywood and the reduced porosity of plywood compared to that of OSB.

In general, displacement capacities of similarly configured plywood and OSB connections were approximately the same, while the peak loads of the plywood specimens were up to twice of those for OSB. This increased strength was attributed to the surface energy and

roughness factors described above. Elastic stiffness of the OSB specimens was also larger than that of the plywood specimens in connections that were constructed using mechanical fasteners. This result was expected due to the greater thickness and density of the OSB.

5.2.4.2 Mechanical Fasteners and Application Pressure

As with OSB tests, the use of increased application pressure via hand-tightened clamps resulted in a significant strength increase over under-pressurized specimens. The work performed to failure by the C-PACL series represented an increase of 250% over the C-PA series.

The use of a mechanical fastener along with the adhesive tape in comparison to the pressure clamped series showed no significant strength gain with only a minor gain in work performed to failure. These results highlighted the fact that application pressure was key to providing a strong and durable adhesive connection.

5.2.4.3 Light-Gauge Steel Framing

Connections constructed using steel studs (C-PAMS) performed similarly to the comparable low pressure application, wood-stud set (C-PA). As previously outlined, however, steel studs were dropped from the study and wood was exclusively used for the main framing members for the rest of the project.

5.2.5 Additional Comparison Test Observations

Comparison specimens were also monitored for the effect of moisture content on the performance of the connection. Moisture contents ranged from 10% to 15% upon testing, and no observable relationship between performance and moisture content was found. All lumber was surface dried and conditioned, thus this finding is not necessarily valid for green lumber. A plot of moisture content versus peak load is provided in Figure 5.5 as an illustration of the data scatter. Moisture content is, however, a key parameter in the response of wood structures and was recorded for all subsequent connections for reference.

The original framing member from which each specimen was cut was an additional consideration. It was discovered that this variable had no effect on the performance of the connections. This result could be attributed to the fact that all framing members were ordered as

one bundle and that the variation in original framing members was minimal. Because future tests were also to be constructed with members ordered from the same bundle, this variable was eliminated from the study for the remainder of the tests.

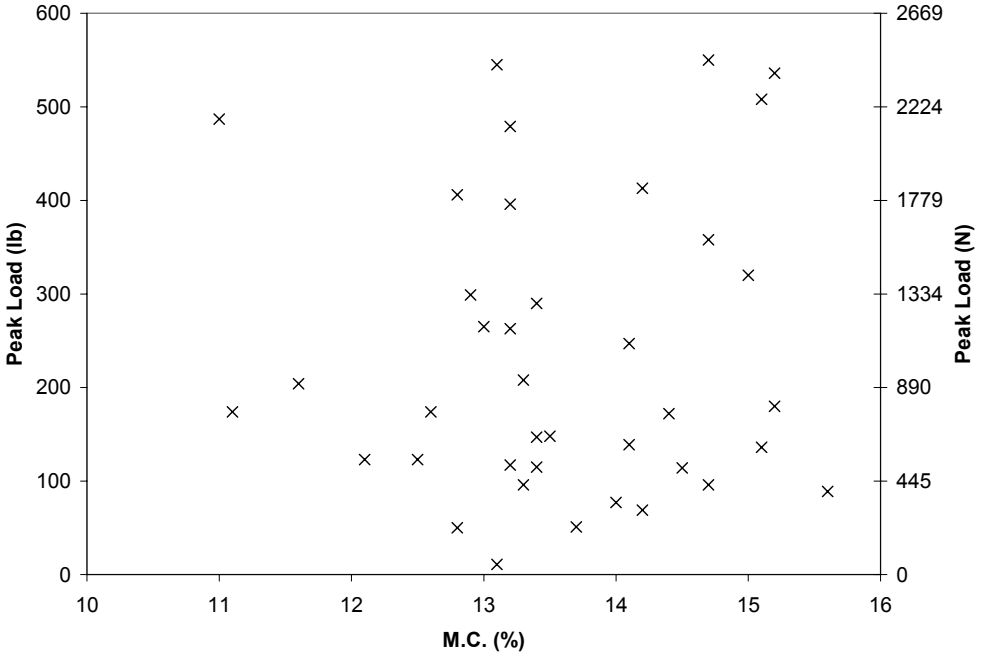

Figure 5.5: Moisture Content Scatter-Graph

5.2.6 Failure Modes

Failure modes for the comparison tests were separated into three different categories: adhesive bond failures, "rolling" tape failures, and tape "stretching." Connections that exhibited poor performance predominately experienced adhesive bond failures. This type of failure mode occurred most often in the OSB connections without surface treatments. Adhesive bond failures for comparison tests occurred most often between the sheathing material and the tape as shown in Figure 5.6 (a). This type of failure mode was observed to occur only when the tape bond had not properly "wet out."

Plywood connections and stronger OSB connections that had been surface treated exhibited either a "rolling" tape failure or tape "stretching." Both of these failure modes were similar and took place when the main framing member slipped in relation to the sheathing without actually de-bonding completely. "Rolling" failures occurred when this differential

movement was achieved through the rolling of the tape into s-shape curves as illustrated in Figure 5.6 (b). "Stretching" failures occurred when the tape appeared to elongate to follow the movement of the main member without localized de-bonding and rolling.

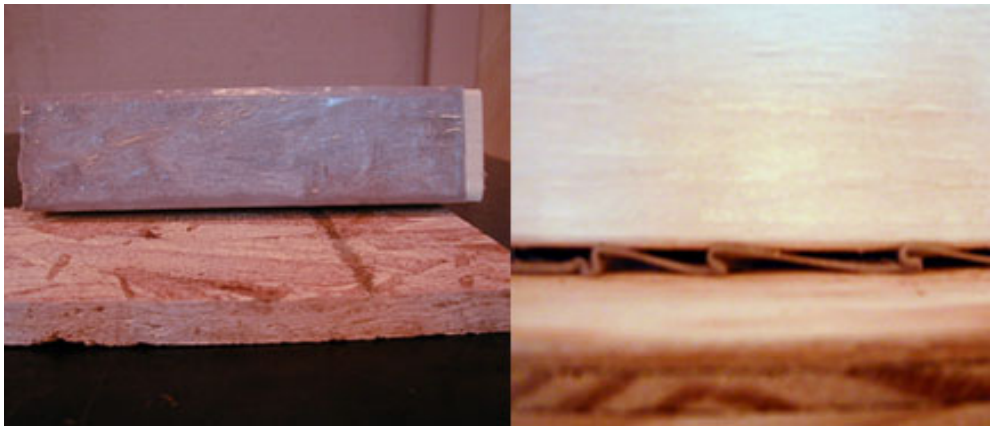

Figure 5.6: (a) Adhesive Bond Failure (b) "Rolling" Tape Failure

5.2.7 Comparison Test Summary

In summary, the performance of the comparison-connection-test subset provided the following information:

1. The application pressure used to "wet out" the tape bond is critical to the performance of the connection. The optimum pressure is higher for wood substrates than for metallic or plastic substrates due to the rigidity and roughness of the wood surface
2. Sanding and priming surface treatments were both extremely effective in increasing the performance of connection tests utilizing OSB sheathing. Priming was only moderately effective for plywood based connections.
3. Adhesive connections formed using high bond pressures performed equal to or better than those using lower bond pressures with a mechanical fastener. Peak loading, displacement capacity, and energy to failure remained constant or were improved. Elastic stiffness was also less than that for nailed connections in some cases.
4. Both moisture content and the original framing member from which the specimens were cut were found to have no effect on connection performance.
5. Plywood outperformed OSB in all categories due to better bonding characteristics resulting from reduced roughness and increased surface energy.

5.3 Pressure Application Subset

The pressure-application-specimen subset consisted of 35 connection tests chosen to determine the optimum pressure needed to form a strong bond between wood substrates with pressure sensitive adhesive (PSA) tapes. This testing was added into the scope of the project due to the results of the initial comparison tests. Unlike previous tests, this subset concentrated on only a single variable while holding all other factors constant. A summary of the different comparison tests is provided in Table 5.2.

Table 5.2: Pressure Application Specimens

Adhesive Application Pressure Single Lap Shear Connection Tests							
I.D.	Member	Sheathing	Fastener	Treatment	Pressure[1]	Time[2]	No. Tests
P15	SPF	Plywood	3M VHB	None	15 psi	30 sec	5
P30	SPF	Plywood	3M VHB	None	30 psi	30 sec	5
P45	SPF	Plywood	3M VHB	None	45 psi	30 sec	5
P60	SPF	Plywood	3M VHB	None	60 psi	30 sec	5
P80	SPF	Plywood	3M VHB	None	80 psi	30 sec	5
P100	SPF	Plywood	3M VHB	None	100 psi	30 sec	5
P120	SPF	Plywood	3M VHB	None	120 psi	30 sec	5
						TOTAL	35

NOTES

1) Pressure applied to each specimen for alloted time to activate pressure sensitive adhesive.
2) Amount of time for which adhesive activation pressure was applied.

Five specimens were constructed per application pressure level so that performance variations at each step could be monitored. Performance parameters for each specimen and specific Coefficient of Variation (COV) factors are provided in the Appendix. Table 5.3 lists average performance parameter information for each specimen category.

For this subset, peak load, peak displacement, and work performed to failure were used as the primary means of comparison. Ductility and 5% offset yield loads were used as secondary comparison factors. Stiffness values proved to be similar for all tests as shown in Table 5.3. The average COVs for all parameters were in the range of 15%.

Table 5.3: Summary of Pressure Application Performance Parameters

OVERALL AVERAGE RESULTS (Metric)							
Data Set	P-15	P-30	P-45	P-60	P-80	P-100	P-120
Max Load (N)=	452.6	917.3	1124.4	1387.2	1136.4	1608.9	1306.1
Displacement (mm)=	4.34	7.34	8.21	8.91	7.09	8.89	7.07
Failure Load (N)=	360.5	722.2	889.8	1097.2	893.7	1272.7	1027.2
Disp. @ Failure (mm)=	6.86	9.61	9.82	10.15	8.82	9.98	8.49
40% Max (N)=	177.3	361.2	441.4	552.0	450.1	637.4	515.0
Displacement (mm)=	0.521	1.172	1.527	1.941	1.422	2.144	1.453
Yield (N)=	407.4	800.8	938.7	1159.0	965.7	1331.3	1113.3
Displacement (mm)=	1.198	2.598	3.240	4.072	3.051	4.479	3.140
5% Offset Yield (N)=	340.1	556.4	630.0	765.4	667.6	867.8	785.0
Displacement (mm)=	1.689	2.483	2.841	3.362	2.818	3.607	2.931
Elastic Stiffness (N/mm)=	344.6	311.3	295.0	290.3	316.9	301.6	365.0
Energy (N*m)=	2.52	6.66	7.77	9.41	7.19	10.28	7.82
Ductility Ratio=	6.06	3.83	3.10	2.59	2.97	2.28	2.90

OVERALL AVERAGE RESULTS (US Customary Units)							
Data Set	P-15	P-30	P-45	P-60	P-80	P-100	P-120
Max Load (lbs)=	101.7	206.2	252.8	311.8	255.5	361.7	293.6
Displacement (in)=	0.171	0.289	0.323	0.351	0.279	0.350	0.278
Failure Load (lbs)=	81.0	162.4	200.0	246.7	200.9	286.1	230.9
Disp. @ Failure (in)=	0.270	0.378	0.387	0.400	0.347	0.393	0.334
40% Max (lbs)=	39.9	81.21	99.2	124.1	101.2	143.3	115.8
Displacement (in)=	0.021	0.046	0.060	0.076	0.056	0.084	0.057
Yield (lbs)=	91.6	180.0	211.0	260.6	217.1	299.3	250.3
Displacement (in)=	0.047	0.102	0.128	0.160	0.120	0.176	0.124
5% Offset Yield=	76.5	125.1	141.6	172.1	150.1	195.1	176.5
Displacement (in)=	0.067	0.098	0.112	0.132	0.111	0.142	0.115
Elastic Stiffness (lb/in)=	1967.8	1777.3	1684.8	1657.9	1809.8	1722.4	2084.0
Energy (lb*in)=	22.3	59.0	68.8	83.3	63.7	91.0	69.2
Ductility Ratio=	6.06	3.83	3.10	2.59	2.97	2.28	2.90

5.3.1 Load-Displacement Curves

Average load-displacement curves for each pressure specimen grouping are provided in Figure 5.7.

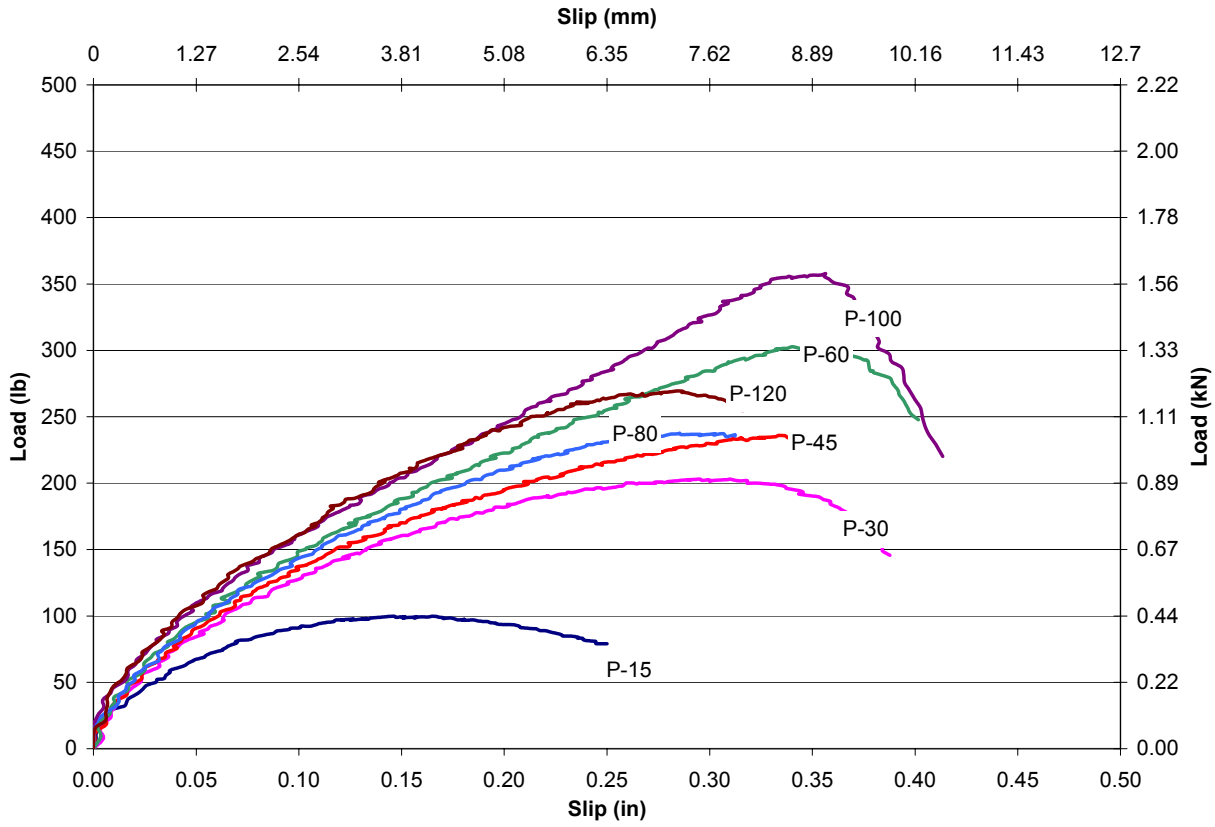

Figure 5.7: Application Pressure Average Load-Displacement Curves

The average load-displacement curves illustrated in Figure 5.7 revealed that the peak loads and displacements of all of the specimens constructed with pressures above 103 kPa (15 psi) were grouped together. These curves reinforce the conclusion drawn from the comparison tests that an apparent application pressure of 103 kPa (15 psi) was insufficient to activate the tape.

To differentiate between the higher-pressure tests, average peak-load and work-to-failure parameters were plotted along with their standard deviations as shown in the following two sections. Unequal variance t-tests were then performed to determine if the differences in average results were statistically significant.

5.3.2 Peak Load and Displacement Comparison

A bar graph of the peak load values for each subset variation is provided in Figure 5.8.

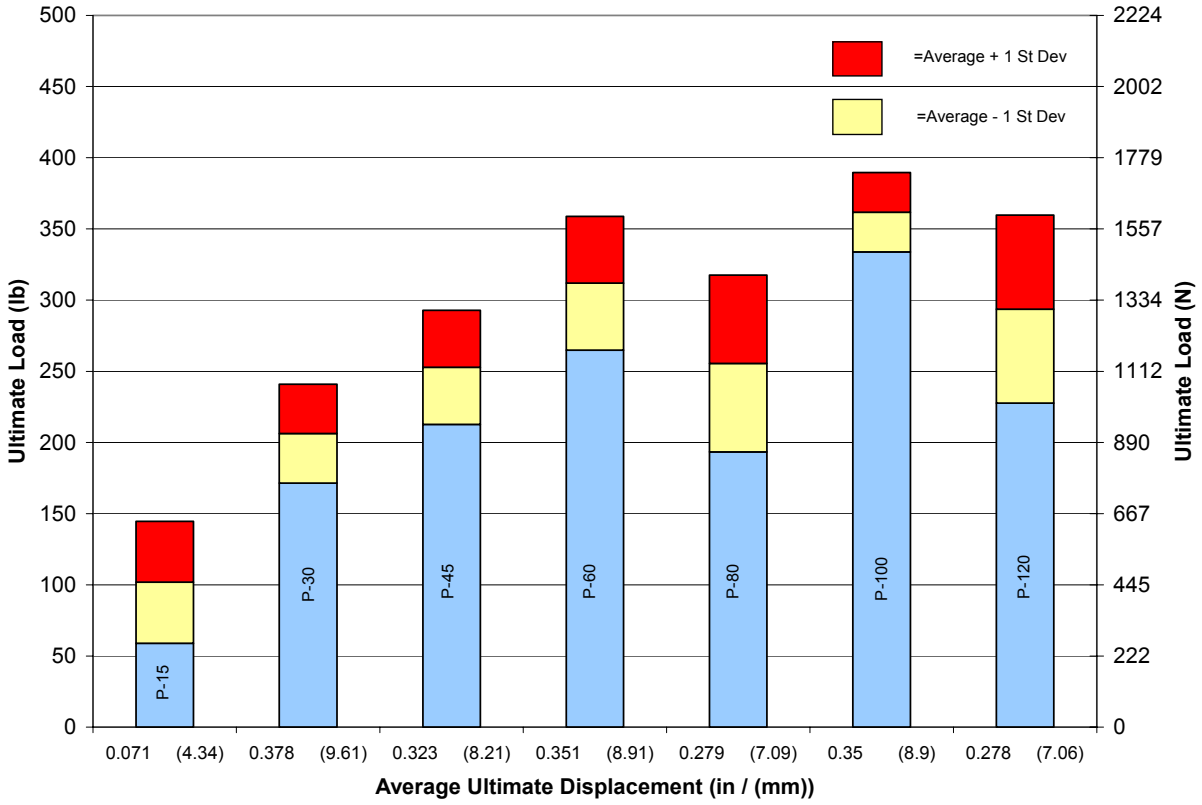

Figure 5.8: Pressure Application Peak Load Comparison

The data represented in Figure 5.8 revealed that the peak load values steadily increased along with application pressures from 103 kPa (15 psi) to 414 kPa (60 psi) while variation within the pressure steps remained approximately constant. Above 414 kPa (60 psi), application pressure increases did not affect the specimen strength, and capacities appear to be random depending upon the individual performances of the specimens.

Results from t-tests used to evaluate the significant differences between peak load averages providing for unequal variances and a 5% confidence level are provided in Table 5.4. These results indicated that the difference between the 207 kPa (30 psi) and 310 kPa (45 psi) specimens and the difference between the 310 kPa (45 psi) and 414 kPa (60 psi) sets were

insignificant. The tests did, however, find that the increase in performance between the 207 kPa (30 psi) and the 414 kPa (60 psi) sets was significant.

Table 5.4: Peak Load T-Test Results

Two Tailed T-Test	Primary	Vs.	T-STAT	T-CRIT	Sig. Diff?
5% Confidence Interval					
1	P-15	P-30	5.397	2.447	YES
2	P-30	P-45	1.758	2.306	NO
3	P-30	P-60	3.614	2.365	YES
4	P-45	P-60	1.913	2.306	NO
5	P-60	P-80	1.446	2.365	NO
6	P-80	P-100	3.120	2.447	YES

Average peak displacements are also listed for each subset in Figure 5.8. The same trend of significant differences between peak loads was found for peak displacements. There was a significant gain in peak displacement capacity between 207 kPa (30 psi) and 414 kPa (60 psi) but not for the intermediate pressure step. For higher pressures, there were significant differences, but they did not follow any observable trend and were attributed to the natural variability of the connections. Table 5.5 summarizes these results.

Table 5.5: Peak Displacement T-Test Results

Two Tailed T-Test	Primary	Vs.	T-STAT	T-CRIT	Sig. Diff?
5% Confidence Interval					
1	P-15	P-30	4.565	2.447	YES
2	P-30	P-45	1.052	2.365	NO
3	P-30	P-60	3.136	2.365	YES
4	P-45	P-60	0.930	2.571	NO
5	P-60	P-80	2.578	2.571	Possible
6	P-80	P-100	2.658	2.571	YES
7	P-100	P-120	2.685	2.571	YES

These results indicated that an application pressure of 414 kPa (60 psi) provided the best performance in the middle of the application pressure range. Also, pressures down to 207 kPa (30 psi) still activated the acrylic tape and achieved adequate performance.

5.3.3 Work to Failure (Energy) Comparison

To substantiate the previous findings, the work performed by the tape to failure was investigated. This investigation also considered the displacement capacity of the system. A bar graph of the energy for each subset variation is provided in Figure 5.9.

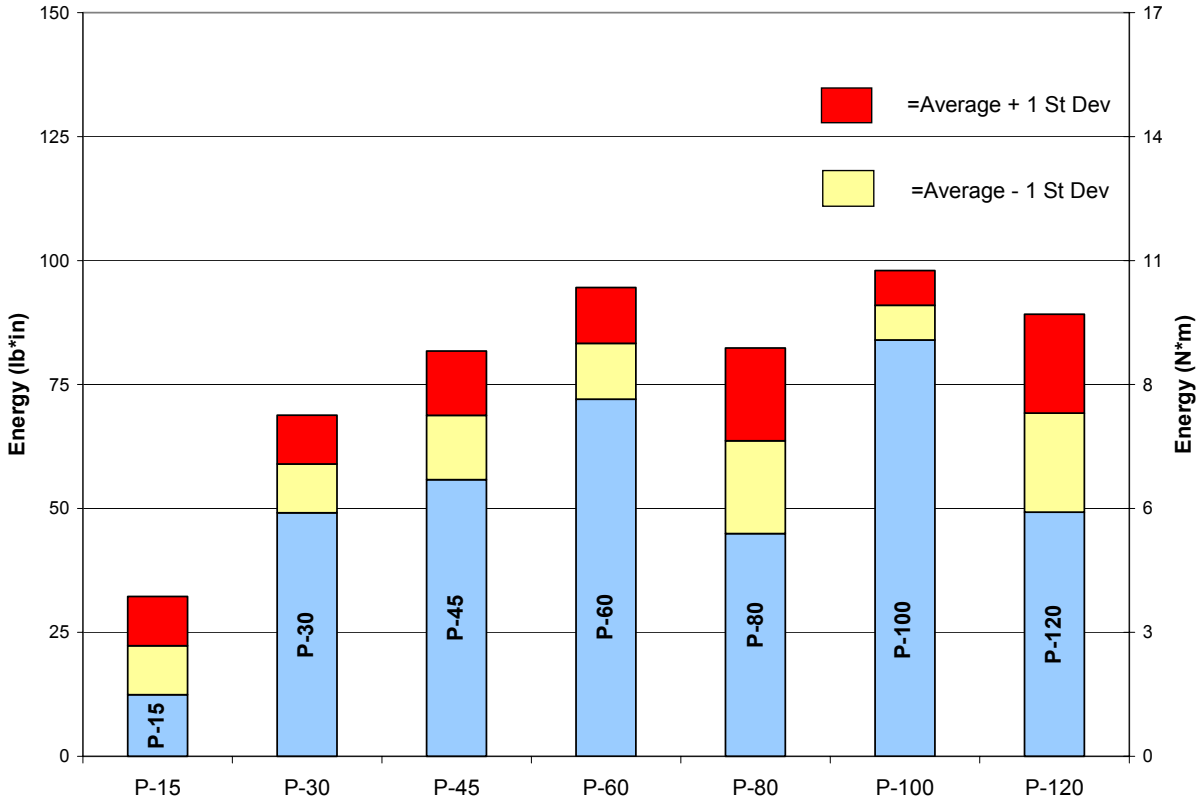

Figure 5.9: Pressure Application Work to Failure (Energy) Comparison

Figure 5.9 follows the same basic trend for the energy of the systems as was found for the peak load capacity. There was a significant difference in energy between the 207 kPa (30 psi) and 414 kPa (60 psi) systems, but not for the intermediate pressure step. After 414 kPa (60 psi) the trend between higher application pressures and greater energy values ceased. These findings verified the result that 414 kPa (60 psi) of application pressure provided the greatest performance while values down to 207 kPa (30 psi) provided acceptable results.

5.3.4 Commentary on Other Performance Parameters

Ductility values of all specimen categories, with the exception of one, were in the range of two to four. The single outlier was the 103 kPa (15 psi) set with a ductility factor in the range of six. This high ductility ratio was due to the flat yield plateau of the specimens that placed the proportional limit early in the deflection of the system. The resulting low yield values in the denominator of the ductility equation drove the ductility value higher.

Five-percent-offset yields for each specimen subset followed the same trends as Figures 5.8 and 5.9. As mentioned previously, elastic stiffness values were also fairly consistent throughout the entire range of tests indicating that the elastic portion of the load-displacement curve did not affect the final peak load capacity.

5.3.5 Pressure Test Failure Modes

Failure modes for the 103 kPa (15 psi) set were a combination of bond failures between the sheathing material and the adhesive tape and "rolling" tape failures. Bond failures at this pressure level left no residue on the main wood member. As the application pressure increased to 207 kPa (30 psi) and 310 kPa (45 psi), the failure modes shifted to "rolling" tape failures or tape "stretching" as explained in Section 5.2.6.

The failure mode at 414 kPa (60 psi) or above was consistently a "rolling" tape failure or a bond failure. In this case, bond failures occurred alternately between the tape and either the sheathing or the main framing member, and failure was characterized by the weakening of the bond, not the total release of the bond as in the lower pressure cases. Figure 5.10 shows a broken specimen after testing produced a bond failure. Note that this illustration is not the actual failure mechanism but was taken after physically rotating the main member away from the adhesive tape. The behavior of these connections indicated that the maximum capacity of the bond between both the sheathing and the main structural members had been reached. The adhesive capacity of the main members and sheathing was less than the internal strength of the tape itself, as no cohesive tape failures were observed.

Figure 5.10: High Pressure Bond Failure

5.3.6 Pressure Test Conclusions

In summary, the performance of the pressure application subset provided the following information:

1. The performance of the connections followed a positive trend as application pressures were increased from 103 kPa (15 psi) to 414 kPa (60 psi). Higher pressures than 414 kPa (60 psi) did not produce significant increases in performance.
2. An application pressure of 414 kPa (60 psi) provided the optimal performance.
3. An application pressure of 207 kPa (30 psi) or above was sufficient to "wet out" the tape and provided acceptable performance.
4. Failure modes indicated that the adhesive bond between main framing members, sheathing, and tape is the limiting factor for connection strength. No connection sustained a cohesive tape failure, and there was no indication that either the sheathing or the main framing member bonded significantly better than the other.

To investigate the best performance of the adhesive tape system, an application pressure of 414 kPa (60 psi) was used for the remainder of the connection tests.

5.4 Time of Application Subset

The time-of application specimen subset consisted of 30 connection tests performed to determine the duration of the optimum activation pressure required to provide the best results. This testing was added into the scope of the project due to the results of the initial comparison tests. Like the application pressure investigation, this subset concentrated on a single variable while holding all other factors constant. A summary of the different time of pressure application tests is provided in Table 5.6.

Table 5.6: Duration of Pressure Application (Time) Specimens

Adhesive Time of Application Single Lap Shear Connection Tests							
I.D.	Member	Sheathing	Fastener	Treatment	Pressure[1]	Time[2]	No. Tests
T15	SPF	Plywood	3M VHB	None	60 psi	15 sec	5
T30	SPF	Plywood	3M VHB	None	60 psi	30 sec	5
T45	SPF	Plywood	3M VHB	None	60 psi	45 sec	5
T60	SPF	Plywood	3M VHB	None	60 psi	60 sec	5
T90	SPF	Plywood	3M VHB	None	60 psi	90 sec	5
T120	SPF	Plywood	3M VHB	None	60 psi	120 sec	5
						TOTAL	30
NOTES							
1) Pressure applied to each specimen for alloted time to activate pressure sensitive adhesive.							
2) Amount of time for which adhesive activation pressure was applied.							

As with the application pressure tests, five specimens were tested for all time duration values to monitor performance variations at each step. Performance parameters for each specimen and specific coefficient of variation (COV) factors are listed in the Appendix. Table 5.7 provides a complete summary of performance parameters for each specimen subset.

The same set of primary performance parameters used to investigate pressure application was used for tape duration: peak load, displacement capacity, and energy to failure. The average COV for all parameters was approximately 17%. Note that the set of time-duration specimens constructed using a value of 30 seconds was essentially a repetition of the previous 414 kPa (60 psi) pressure set. The results, however, show that the performance parameters of the 30 second time duration set are less than that for the corresponding pressure set. This discrepancy was attributed mainly to the fact that one of the 30 second time tests performed abnormally poorly (attributing to the high COV of 25.5%) and pulled the total average performance values down significantly. There was no apparent reason found for the abnormal performance, thus the specimen was not censored.

Table 5.7: Summary of Duration of Pressure Application Performance Parameters

OVERALL AVERAGE RESULTS (Metric)						
Data Set	T-15	T-30	T-45	T-60	T-90	T-120
Max Load (N)=	946.6	925.9	1180.7	1277.6	1267.5	1204.7
Displacement (mm)=	8.23	7.44	8.48	8.16	8.73	8.51
Failure Load (N)=	745.8	734.1	937.1	1005.9	1000.9	953.9
Disp. @ Failure (mm)=	9.68	8.93	9.82	9.70	9.81	9.72
40% Max (N)=	358.7	364.2	466.8	503.8	501.0	474.2
Displacement (mm)=	1.310	1.191	1.438	1.389	1.628	1.765
Yield (N)=	792.8	786.0	974.6	1061.2	1026.4	993.6
Displacement (mm)=	2.790	2.560	3.003	2.926	3.333	3.690
5% Offset Yield (N)=	524.6	537.9	631.3	695.1	655.5	664.2
Displacement (mm)=	2.505	2.417	2.619	2.585	2.837	3.161
Elastic Stiffness (N/mm)=	443.6	350.7	325.6	378.3	316.2	277.7
Energy (N*m)=	6.53	6.11	8.14	8.75	8.36	7.83
Ductility Ratio=	6.27	4.14	3.33	3.45	3.05	2.76

OVERALL AVERAGE RESULTS (US Customary Units)						
Data Set	T-15	T-30	T-45	T-60	T-90	T-120
Max Load (lbs)=	212.8	208.1	265.4	287.2	284.9	270.8
Displacement (in)=	0.324	0.293	0.334	0.321	0.344	0.335
Failure Load (lbs)=	167.7	165.0	210.7	226.1	225.0	214.4
Disp. @ Failure (in)=	0.381	0.352	0.386	0.382	0.386	0.383
40% Max (lbs)=	80.6	81.9	104.9	113.3	112.6	106.6
Displacement (in)=	0.052	0.047	0.057	0.055	0.064	0.070
Yield (lbs)=	178.2	176.7	219.1	238.6	230.7	223.4
Displacement (in)=	0.110	0.101	0.118	0.115	0.131	0.145
5% Offset Yield=	117.9	120.9	141.9	156.3	147.4	149.3
Displacement (in)=	0.099	0.095	0.103	0.102	0.112	0.124
Elastic Stiffness (lb/in)=	2533.2	2002.8	1859.4	2160.2	1805.8	1585.9
Energy (lb*in)=	57.8	54.1	72.0	77.5	74.0	69.3
Ductility Ratio=	6.27	4.14	3.33	3.45	3.05	2.76

5.4.1 Load-Displacement Curves

Average load-displacement curves for each time duration specimen grouping are provided in Figure 5.11

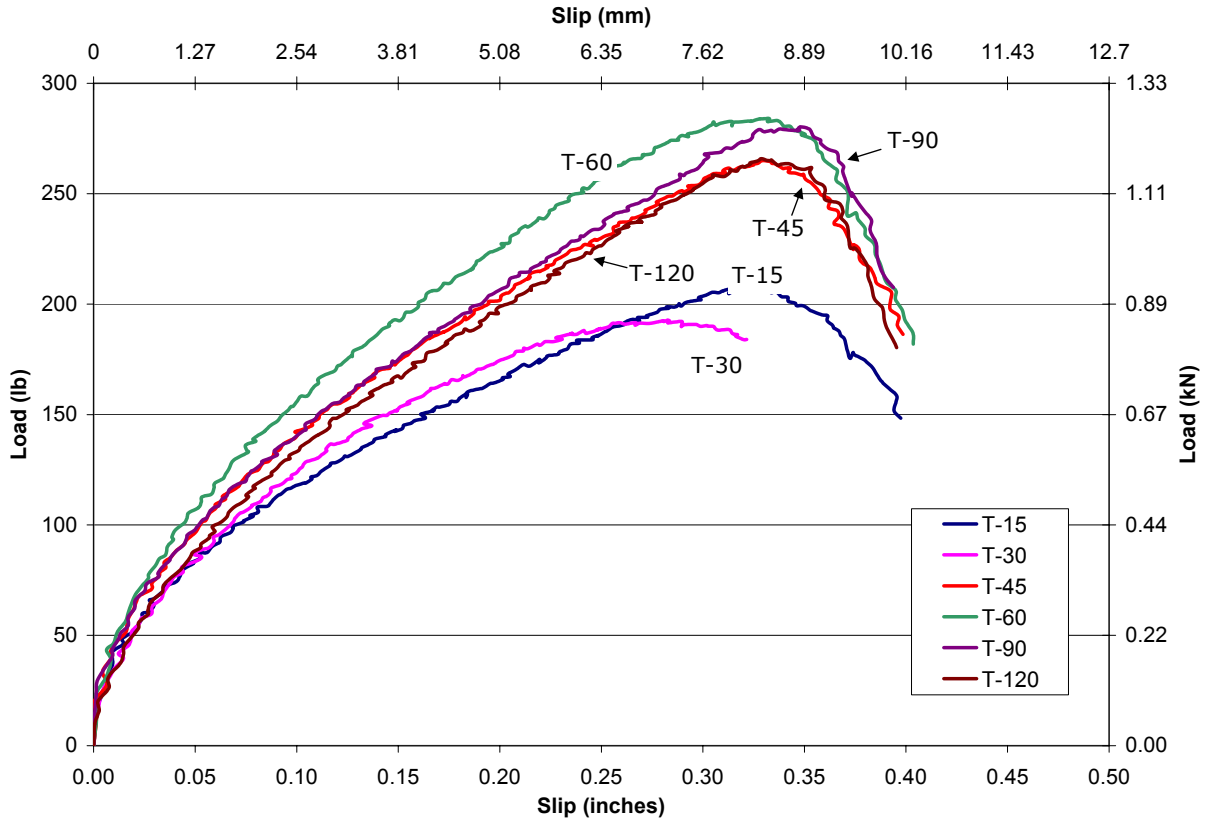

Figure 5.11: Time Duration of Application Pressure Load-Displacement Curves

Examination of load-displacement curves revealed that higher time durations for pressure application did not necessarily have a positive impact on performance. There did, however, appear to be a significant jump in performance values between the 15 and 30 second duration sets and all others.

To substantiate this observation, the peak-load and work-to-failure parameters were plotted along with their standard deviations as shown in the following two sections. As with the pressure application results, unequal variance t-tests were then performed to determine whether the differences in average results were statistically significant.

5.4.2 Peak Load and Displacement Comparisons

A bar graph of the peak-load values for each subset variation is provided in Figure 5.12. The axes are plotted on the same scale as those of the corresponding application pressure graph in Figure 5.8.

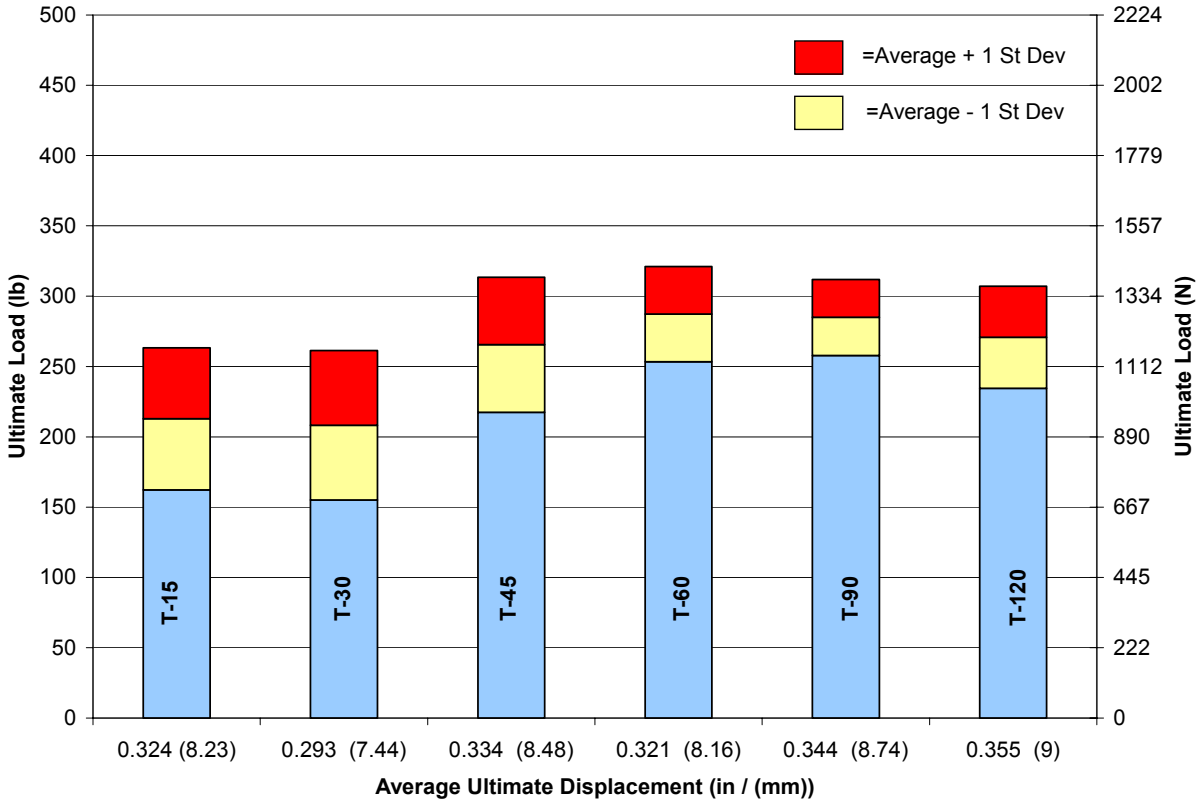

Figure 5.12: Time Duration – Peak Load Comparison

The data displayed in Figure 5.12 indicated that the connection tests with time duration values above 30 seconds performed slightly better, and with less variation, than those with time duration values less than 30 seconds. Table 5.8 provides the results of the t-tests that were performed to determine whether there were significant differences between the various specimen sets. Results from the t-tests indicated that, though there is a significant difference in performance between the 15 and 60 second or higher duration specimens, the difference is not pronounced; and, in general, time of application does not greatly affect the peak capacity performance. Displacements at these peak loads were consistently within approximately 10% of the average peak displacements.

Table 5.8: Peak Load T-Test Results

Two Tailed T-Test	Primary	Vs.	T-STAT	T-CRIT	Sig. Diff?
5% Confidence Interval					
1	T-15	T-30	0.127	2.306	NO
2	T-30	T-45	1.601	2.306	NO
3	T-15	T-45	1.510	2.306	NO
4	T-15	T-60	2.445	2.365	YES
5	T-60	T-90	0.105	2.306	NO
6	T-60	T-120	0.661	2.306	NO
7	T-15	T-90	2.517	2.447	YES
8	T-30	T-90	2.579	2.447	YES

5.4.3 Work to Failure (Energy) Comparison

To provide a better indication that the time duration of pressure application might not have a significant effect upon the connection test performance, the work to failure of the connections was examined. A bar graph of the energy for each subset variation is provided in Figure 5.13.

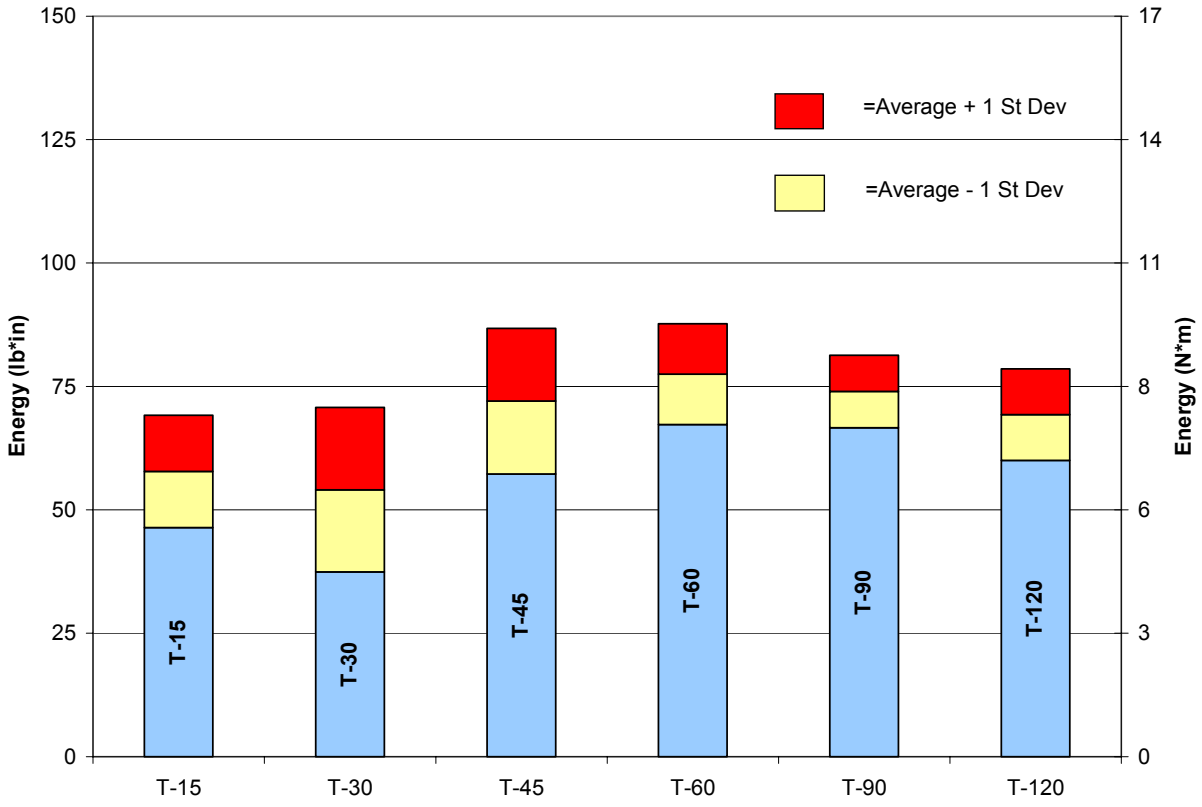

Figure 5.13: Time Duration Work to Failure (Energy) Comparison

The results of the energy bar graph in Figure 5.13 followed the same trend as that for the peak loads indicating that the displacements to failure were approximately equal. The results from a series of t-tests performed on the data are provided in Table 5.9. Significant differences, when found, were only moderately so (the t-statistic was extremely close to the t-critical value). It was concluded that, though a time duration of 60 seconds appeared to provide optimal results, the actual effect of time duration of pressure application was minimal.

Table 5.9: Work to Failure (Energy) T-Test Results

Two Tailed T-Test	Primary	Vs.	T-STAT	T-CRIT	Sig. Diff?
5% Confidence Interval					
1	T-15	T-30	0.367	2.365	NO
2	T-30	T-45	1.612	2.306	NO
3	T-15	T-45	1.527	2.306	NO
4	T-15	T-60	2.577	2.306	YES
5	T-60	T-90	0.558	2.365	NO
6	T-60	T-120	1.191	2.306	NO
7	T-15	T-90	2.392	2.365	YES
8	T-30	T-90	2.187	2.571	NO
9	T-30	T-60	2.396	2.365	YES

5.4.4 Commentary on Other Performance Parameters and Failure Modes

Ductility values were again within a range of two to four units with the exception of the 15 second set. This set would have been within the same range had it not been for an abnormal test (T-15-1) that had a ductility value of approximately 19 and severely skewed the average. This abnormal value was due to the steep elastic region and flat plastic region of the load-displacement curve as shown in the Appendix.

Five-percent-offset yield values followed the same trend as the peak-loading values and provided no additional insights into the behavior of the system. Elastic stiffness values were slightly higher than those calculated for the pressure application sets.

Failure modes for all time duration specimens were “rolling” tape or partial adhesive failures such as those described previously for the pressure application specimens. No obvious trends could be found between the duration of pressure application and the failure modes of the specimens.

5.4.5 Time Duration of Application Pressure Conclusions

In summary, performance of the time duration of application pressure subset provided the following information:

1. A time of application duration of 60 seconds provided the optimum performance characteristics for connection specimens constructed with an applied pressure of 414 kPa (60 psi).
2. Though 60 seconds was found to be the optimum time duration, the difference in performance between connections constructed at all time steps was minimal. It was concluded that any time of duration greater than 15 seconds would create an adequate bond.
3. Time durations below 15 seconds were not tested.

To investigate the best performance of the adhesive tape system, an application pressure of 414 kPa (60 psi) sustained over a period of 60 seconds was chosen to be used for the remainder of the connection tests.

5.5 Statistically Significant: Subset Introduction

The statistically significant subset consisted of 165 specimens and was the core of the connection test portion of this project. Specimens were chosen based on trends observed from the comparison test subsets and were constructed with the optimum application pressure and time duration. This testing is meant to provide a significant body of knowledge from which data on PSA tape adhesives can be taken for use in future design and computer modeling. A summary of the different configurations tested is provided in Table 5.10.

Table 5.10: Statistically Significant Specimens

Statistically Significant Single Lap Shear Connection Tests							
I.D.	Member	Sheathing	Fastener	Treatment	Pressure[1]	Time[2]	No. Tests
S-PA	SPF	Plywood	3M VHB	None	60 psi	60 sec	15
S-PN	SPF	Plywood	8d Nail	None	60 psi	60 sec	15
S-PAN	SPF	Plywood	3M VHB +8d Nail	None	60 psi	60 sec	15
S-OA	SPF	OSB	3M VHB	None	60 psi	60 sec	15
S-OAS	SPF	OSB	3M VHB	Sanded	60 psi	60 sec	15
S-OAP	SPF	OSB	3M VHB	Primed	60 psi	60 sec	15
S-ON	SPF	OSB	8d Nail	None	60 psi	60 sec	15
S-OAN	SPF	OSB	3M VHB +8d Nail	None	60 psi	60 sec	15
S-PMT1	SPF	Plywood	3M VHB 4941	Primed	60 psi	60 sec	15
S-PMT2	SPF	Plywood	Adco AT-2	Primed	60 psi	60 sec	15
S-PMT3	SPF	Plywood	Avery 2333	Primed	60 psi	60 sec	15
						TOTAL	165

1) Pressure applied to each specimen for alloted time to activate pressure sensitive adhesive.
2) Amount of time for which adhesive activation pressure was applied.

This portion of the testing investigated the following variables in greater detail: surface treatments, different sheathing materials, mechanical fasteners, and alternate tape products. A large amount of data was generated for each connection test, and the reader is directed to the Appendix for specific specimen information.

To provide a more focused and organized discussion, the data from the statistically significant tests was spread out over multiple main sections and broken down further into the groups shown on the following page. Within each of these sections, performance parameters, summary graphs, and trends are discussed. All main sections covering this specimen subset are titled beginning with "Statistically Significant." The chapter sections are:

Breakdown of Connection Test Groupings

1. Overall results and comparison graphs of all specimens ……. (Section 5.6)
2. Connections with OSB sheathing ……. (Section 5.7)
    a. Surface treatments and general results
    b. Effect of mechanical fasteners
    c. Failure modes
3. Connections with plywood sheathing…… (Section 5.8)
    a. Effect of mechanical fasteners
    b. Failure modes
4. Alternate manufacturers' tapes (3M, ADCO, Avery)……..(Section 5.9)

5.5.1 General Notes

Throughout the following sections, the terms "nail-only" or "adhesive-only" are used to describe specimens that were constructed using either a single mechanical fastener or a strip of adhesive tape. The term "combination" is used to describe specimens that were constructed using both a nail and a strip of adhesive tape. The term "system" is also frequently used to describe the overall connection test specimen.

Many of the graphs shown on the following pages have PMT1, PMT2, and PMT3 values that stand for other types of adhesive tapes. The performance of these tapes is described in Section 5.9 and is not commented upon in the initial discussion. They were placed in the graphs strictly for comparison purposes in the later section.

5.6 Statistically Significant: Overall General Summary of Results

Performance parameters for all 11 specimen configurations are displayed in Tables 5.11 and 5.12. Coefficients of variation among performance factors for each configuration are displayed with the data in the Appendix. All summary bar graphs have also been plotted to show the effect of one standard deviation on the data average.

5.6.1 Load-Displacement Curves

Average load-displacement curves for each specimen are illustrated in Figure 5.14.

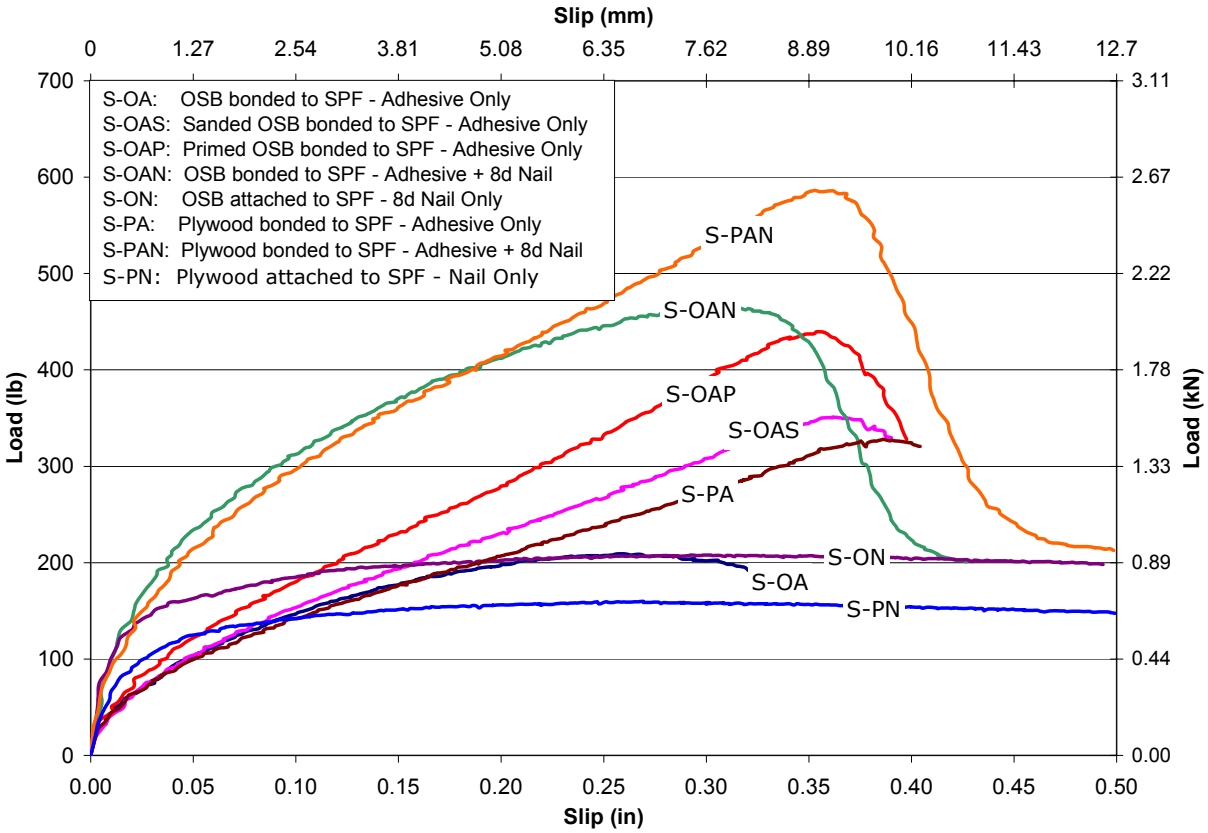

Figure 5.14: Statistically Significant Average Load-Displacement Curves

Examination of the average load-displacement curves revealed several main trends. First, the two sets constructed with only mechanical fasteners (S-ON, S-PN) performed poorly when comparing peak capacities to other connections constructed with adhesive. It is important to note, however, that these tests exhibited a large deflection capacity and that most of the nailed-

Table 5.11: Statistically Significant Performance Parameter Summary (Metric)

OVERALL AVERAGE RESULTS (Metric)										
Data Set	S-OA	S-OAS	S-OAP	S-OAN	S-ON	S-PA	S-PAN	S-PN	S-PMT1	S-PMT2	S-PMT3
Max Load (N)=	990.0	1603.7	1983.4	2107.4	949.5	1509.2	2637.3	724.9	1304.4	1118.0	1054.6
Displacement (mm)=	6.88	9.35	9.10	7.78	7.40	9.88	9.13	6.31	8.45	7.40	2.68
Failure Load (N)=	782.9	1264.2	1556.4	1662.8	N / A	1193.4	2079.2	N / A	1023.5	868.2	806.0
Disp. @ Failure (mm)=	8.81	10.41	9.99	9.22	N / A	10.84	10.13	N / A	9.36	8.08	3.23
40% Max (N)=	389.0	142.703	787.8	828.2	325.4	600.0	1045.0	269.2	514.8	441.9	405.1
Displacement (mm)=	0.875	2.245	2.486	0.799	0.195	2.296	1.576	0.268	1.645	2.550	0.887
Yield (N)=	840.0	1303.0	1638.0	1775.6	871.9	1217.4	2119.1	664.6	1069.5	1004.8	998.5
Displacement (mm)=	1.895	4.607	5.174	1.707	0.495	4.655	3.195	0.647	3.418	5.677	2.183
5% Offset Yield (N)=	565.0	827.4	1041.0	1186.5	708.8	745.3	1356.0	539.1	683.7	795.3	1004.6
Displacement (mm)=	2.001	3.618	3.992	1.850	1.107	3.555	2.742	1.233	2.863	5.417	2.911
Elastic Stiffness (N/mm)=	495.9	287.7	323.1	1088.3	3621.7	263.5	675.6	1639.8	316.7	177.0	473.0
Energy (N*m)=	6.68	10.53	12.07	14.85	10.90	10.25	17.86	8.21	8.17	5.18	2.15
Ductility Ratio=	5.42	2.33	1.98	5.70	49.24	2.42	3.25	31.92	2.89	1.54	1.54

NOTE: Nail-Only Sets did not fail within the time limit of the experiment

Table 5.12: Statistically Significant Performance Parameter Summary (US Customary)

OVERALL AVERAGE RESULTS (US Customary Units)

Data Set	S-OA	S-OAS	S-OAP	S-OAN	S-ON	S-PA	S-PAN	S-PN	S-PMT1	S-PMT2	S-PMT3
Max Load (lbs)=	222.5	360.5	445.9	473.8	213.4	339.3	592.9	163.0	293.2	251.3	237.1
Displacement (in)=	0.271	0.368	0.358	0.306	0.291	0.389	0.359	0.248	0.333	0.291	0.106
Failure Load (lbs)=	176.0	284.2	349.9	373.8	N / A	268.3	467.4	N / A	230.1	195.2	181.2
Disp. @ Failure (in)=	0.347	0.410	0.393	0.363	N / A	0.427	0.399	N / A	0.369	0.318	0.127
40% Max (lbs)=	87.5	142.703	177.1	186.2	73.1	134.9	234.9	60.5	115.7	99.3	91.1
Displacement (in)=	0.034	0.088	0.098	0.031	0.008	0.090	0.062	0.011	0.065	0.100	0.035
Yield (lbs)=	188.8	292.9	368.2	399.2	196.0	273.7	476.4	149.4	240.4	225.9	224.5
Displacement (in)=	0.075	0.181	0.204	0.067	0.019	0.183	0.126	0.025	0.135	0.224	0.086
5% Offset Yield=	127.0	186.0	234.0	266.7	159.3	167.5	304.8	121.2	153.7	178.8	225.9
Displacement (in)=	0.079	0.142	0.157	0.073	0.044	0.140	0.108	0.049	0.113	0.213	0.115
Elastic Stiffness (lb/in)=	2831.4	1642.6	1845.2	6214.6	20680.2	1504.4	3857.7	9363.5	1808.2	1010.6	2701.2
Energy (lb*in)=	59.1	93.2	106.9	131.5	96.5	90.7	158.1	72.7	72.3	45.8	19.0
Ductility Ratio=	5.42	2.33	1.98	5.70	49.24	2.42	3.25	31.92	2.89	1.54	1.54

NOTE: Nail-Only Sets did not fail within the time limit of the experiment

only specimens did not fail within the time-period set for the test (10 minutes). This detail was considered when comparing the energies of the systems in that the energy calculated is not the total work performed to failure, but rather the total work performed during the test period. As a reference, previous studies using similar nails with OSB have shown failure displacements for 8d mechanical fasteners to be in the range of 22mm (0.85 in.) (Salenikovich 2000).

Other basic trends follow those observed in the previous comparison tests. Plywood specimens in general exhibited a higher peak load and deflection capacity than comparable OSB specimens. Also, priming and sanding had a significant effect on the performance of the OSB-sheathed specimens. Performance parameters are broken down further in the following sections.

5.6.2 Peak Capacity and Displacement

The peak capacities of each specimen sub-grouping are plotted in Figure 5.15 from least average peak displacement to maximum average peak displacement.

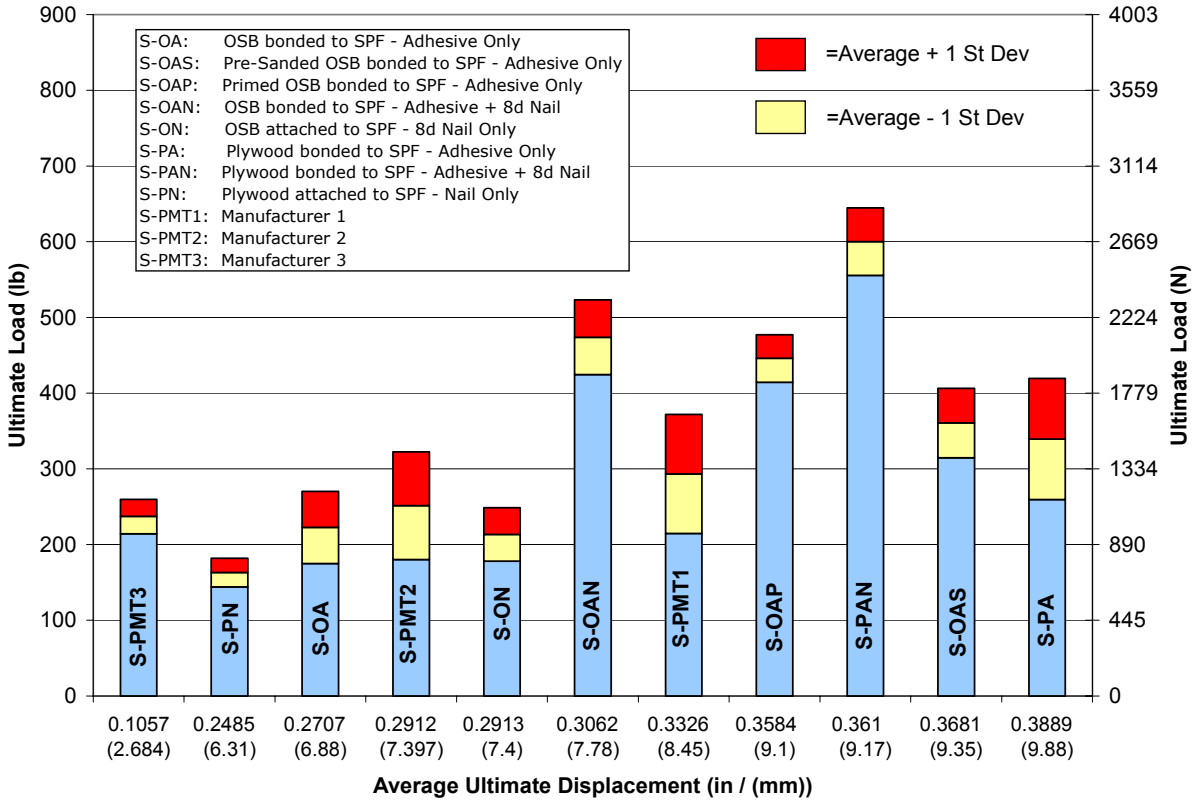

Figure 5.15: Peak Capacity vs. Displacement

Significant differences in peak loadings were determined through the unequal-variance t-test results displayed in Table 5.13.

Table 5.13: Peak Load T-Test Results

Two Tailed T-Test	Primary	Vs.	T-STAT	T-CRIT	Sig. Diff?
5% Confidence Interval					
1	S-PMT3	S-PMT2	0.713	2.110	NO
2	S-PN	S-ON	4.579	2.086	YES
3	S-PN	S-OA	4.215	2.110	YES
4	S-OA	S-ON	0.554	2.064	NO
5	S-PMT1	S-PMT2	1.477	2.048	NO
6	S-PMT1	S-PMT3	2.564	2.120	YES
7	S-PAN	S-OAN	6.992	2.052	YES
8	S-OAS	S-PA	0.863	2.074	NO
9	S-OAP	S-OAS	5.744	2.060	YES
10	S-OAP	S-PA	4.645	2.101	YES

The examination of Figure 5.15 and Table 5.13 lead to the following conclusions:

1. Priming is the most effective surface treatment for peak capacity with OSB sheathing. Both priming and sanding produce significantly greater peak capacities than those associating with untreated specimens.
2. Nail-only OSB specimens were significantly stronger than their plywood counterparts.
3. Combining adhesive tape with nails produced significantly stronger connections than any type of adhesive or nail-only connections with or without surface treatments for both plywood and OSB connections.
4. The combination of mechanical and adhesive tape bonding produced stronger plywood than OSB connections. Note that for nail-only systems, OSB was stronger than plywood. This reversal occurred due to the better adhesive bonding properties associated with plywood previously discussed in Section 5.2.4.1.

Average displacement at peak capacity was also checked for significant differences using a combination of Figure 5.15 and Table 5.14.

Table 5.14: Displacement at Peak Load T-Test Results

Two Tailed T-Test	Primary	Vs.	T-STAT	T-CRIT	Sig. Diff?
5% Confidence Interval					
1	S-PN	S-PMT3	7.585	2.131	YES
2	S-OA	S-PN	0.933	2.056	NO
3	S-PMT2	S-OA	1.296	2.131	NO
4	S-PMT2	S-PN	2.251	2.120	YES
5	S-ON	S-PMT2	0.003	2.160	NO
6	S-OAN	S-ON	0.393	2.145	NO
7	S-PMT1	S-OAN	2.784	2.052	YES
8	S-OAP	S-PMT1	3.824	2.074	YES
9	S-PAN	S-OAP	0.559	2.052	NO
10	S-OAS	S-PAN	1.055	2.074	NO
11	S-OAS	S-OAP	1.431	2.074	NO
12	S-PA	S-OAS	2.472	2.048	YES
13	S-ON	S-PN	1.034	2.093	NO

Conclusions drawn from this combination of data were as follows:

1. Sanding and priming did not produce significantly different peak load displacement capacities, but both surface treatments did perform better than untreated connections.
2. The difference in peak displacement capacities between nail-only plywood and OSB sheathing was insignificant
3. Peak displacement capacities of OSB based connections were not significantly different between adhesive-only, nail-only, and combination connections.
4. Peak displacement capacities of plywood-based connections were highest for adhesive-only systems followed by combination connections and, finally, nail-only connections.
5. Combination of adhesive tape and mechanical fasteners produced higher peak displacement capacities in plywood than in OSB.

In general, sanding and priming produced higher peak capacities and displacements than connections without surface treatments. Plywood performed considerably better than OSB for all connections involving adhesive tape. For nail-only connections, the denser OSB performed

better than the plywood specimens. Combination systems had much higher peak capacities than other systems.

5.6.3 Elastic Stiffness

Elastic stiffness of each specimen sub-grouping is plotted in descending order from greatest to least stiffness capacity in Figure 5.16. Standard deviations are not shown for S-ON and S-PN series due to the large graphical scale that their high variability would have required.

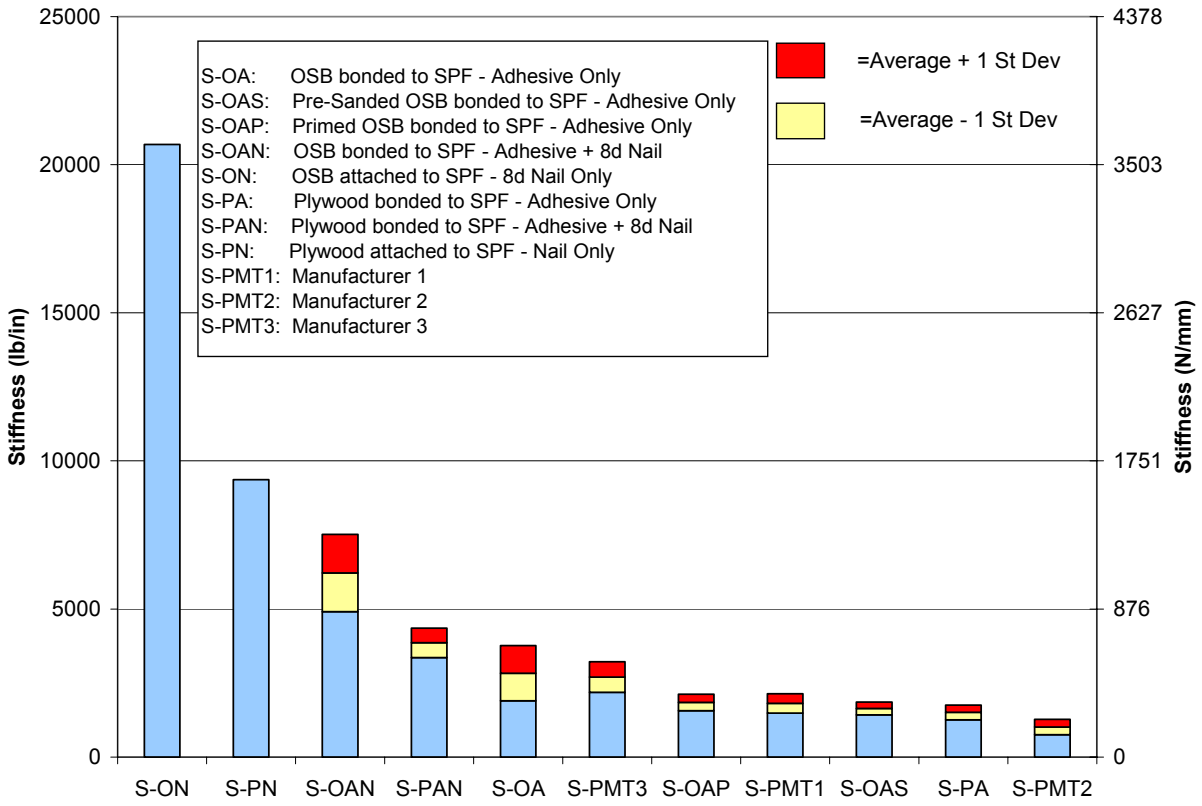

Figure 5.16: Elastic Stiffness Comparisons

Comparing the elastic stiffness of each system revealed the amount of damage they could effectively absorb through small displacements. This value is important in earthquake engineering as it allows the design of structures that can withstand small tremors without significant repair required. Data illustrated in Figure 5.16 leads to the conclusion that nail-only systems are less susceptible to damage (stiffer) than combination systems, which are in turn less

susceptible to damage (stiffer) than systems involving only adhesive tape. The data also matches numerous previous studies showing that OSB is, in general, stiffer than plywood.

Note that the true stiffness difference between nail-only and combination specimens for small deflections was not as large as might appear from Figure 5.16. First, the variation within each nailed set was considerable (COV≈80%). This shows that the adhesive tape results in a significantly more consistent connection. Also, the load-displacement curves followed approximately the same path through small displacements, but the much greater peak loading of the combination systems led to a proportional limit beyond the true elastic region of the curve. This proportional limit slightly skewed the elastic stiffness value down. T-test results were calculated to verify the above conclusions as shown in Table 5.15. These tests were performed in order from greatest to least stiffness so that, though some direct comparisons are not shown, they may easily be ascertained from the data.

Table 5.15: Stiffness T-Test Results

Two Tailed T-Test	Primary	Vs.	T-STAT	T-CRIT	Sig. Diff?
5% Confidence Interval					
1	S-ON	S-PN	2.172	2.120	YES
2	S-PN	S-OAN	1.743	2.131	NO
3	S-OAN	S-PAN	6.282	2.093	YES
4	S-PAN	S-OA	3.430	2.086	YES
5	S-OA	S-PMT3	0.445	2.086	NO
6	S-PMT3	S-OAP	5.518	2.074	YES
7	S-OAP	S-PMT1	0.325	2.052	NO
8	S-PMT1	S-OAS	1.585	2.064	NO
9	S-OAS	S-PA	1.573	2.052	NO
10	S-PA	S-PMT2	5.160	2.048	YES

In summary, the use of adhesive tape provided the connection tests with greater capacity to absorb small displacements than mechanical fasteners. Also, the differences between the elastic stiffness of the OSB connections involving different surface treatments were largely negligible.

5.6.4 Work to Failure

The work to failure of each specimen sub-grouping is plotted from the most to the least work in Figure 5.17. Note that as previously mentioned, the work of nail-only connections is not representative of the true work to failure.

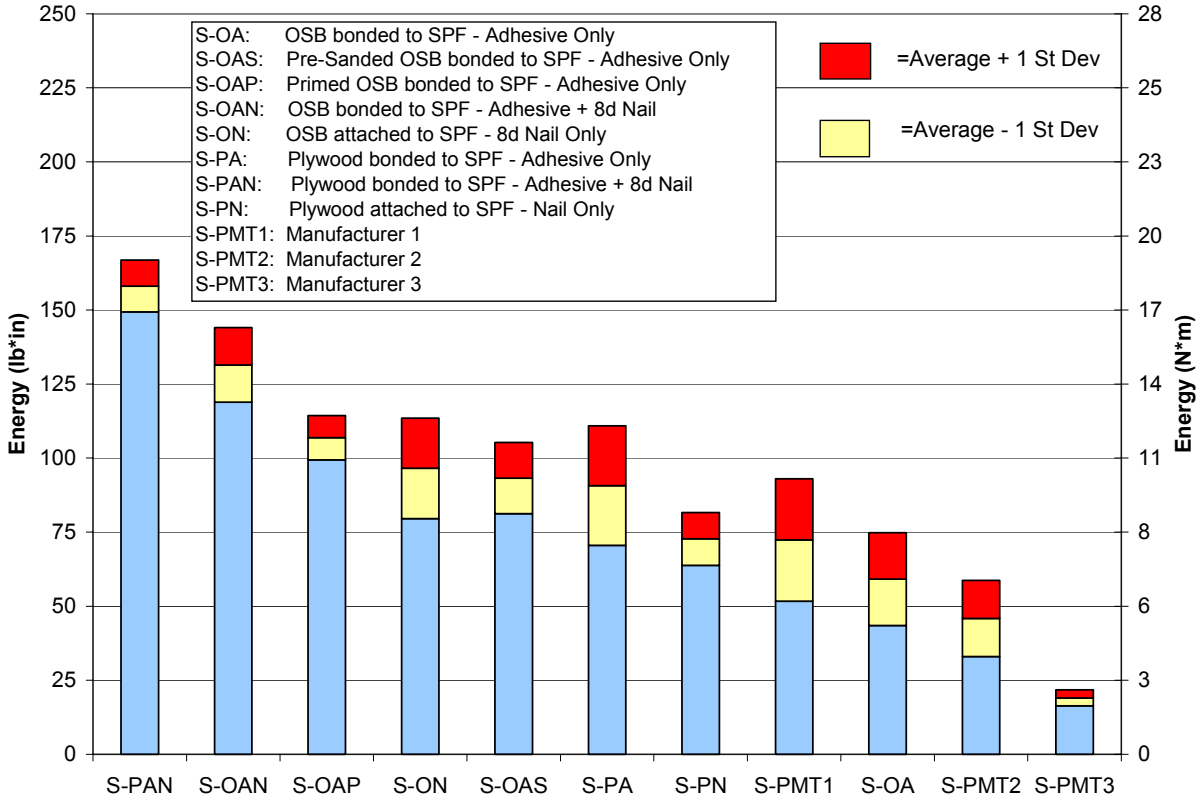

Figure 5.17: Work to Failure Comparisons

The work to failure followed essentially the same trends as determined for the peak capacity. This result indicated that the deflections to failure either followed the same trend or were similar enough not to affect the work results drastically. Connections constructed with the combined system required more work than all other specimen categories. Priming was slightly better than sanding, and both were significantly better than no surface treatment. Plywood systems again performed better than OSB systems when tape was involved, with the converse true for nail-only connections. T-tests used to verify the above conclusions were essentially the same as those for peak load and are, therefore, not shown.

5.6.5 Displacement at Failure

Displacement reached by each sub-grouping at failure is plotted in Figure 5.18 from the largest to the smallest displacement. It should be noted that since the failure load was previously defined as 80% of the peak loading, the trends were identical. The displacement at failure is a useful parameter to examine because it is a measure of the connection's toughness. As mentioned previously, nail-only tests did not fail and are, therefore, not shown below.

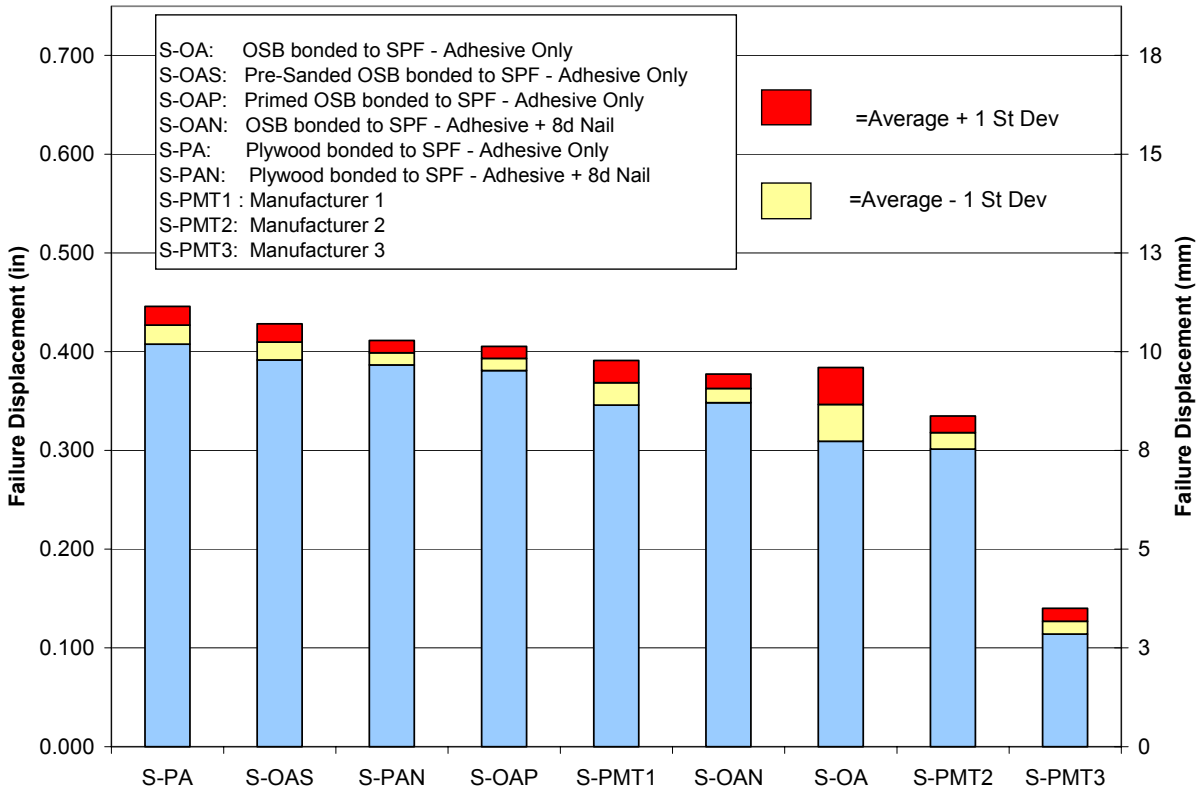

Figure 5.18: Failure Load vs. Failure Displacement Comparison

Failure displacements were fairly consistent with no clear trends through all connection sets involving the tape adhesive. This result was attributed to the maximum deformation capacity of the tape itself. Once the tape had stretched to a certain maximum amount for each connection, it lost its bonding capability and failed regardless of what surface it was attached to. Product literature indicated that this failure would take place at approximately three times the thickness of the tape (3.3 mm or 0.13 in.). In reality the tape was much more resilient, and failure did not occur until approximately eight times the thickness of the tape (8.8 mm or 0.36

in). Notice the small values of standard deviation within the sets indicated consistent performance.

5.6.6 Five-Percent-Offset Yield

Five-percent-offset yield values calculated for each specimen category are plotted in order of smallest to largest offset yield displacements in Figure 5.19.

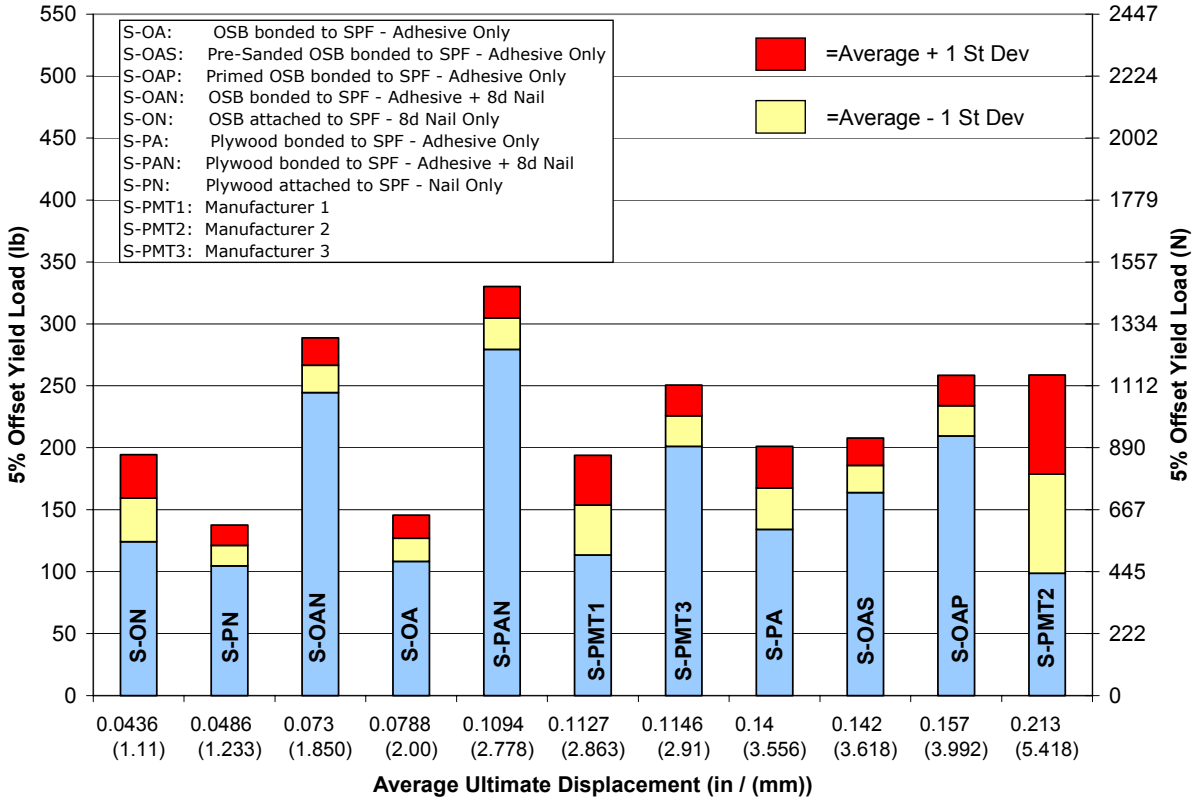

Figure 5.19: Five-Percent-Offset Yield Load vs. Displacement Comparison

In general, the connections that utilized mechanical fasteners had the lowest yield displacements due to their increased stiffness factors. Sanding and priming of the OSB specimens lead to increased yield loads and displacements. Plywood connections exhibited slightly higher yield displacements than their OSB counterparts, but these differences were found to be statistically insignificant. The trend of combined system connections outperforming all other specimens was again present.

5.6.7 Other Performance Parameters

Ductility ratios ranged from approximately two to five throughout the specimen sets. The exceptions were the two nail-only specimen groups (plywood and OSB) whose ductility ratios were much higher. Even these high ratios are actually underestimates, as the true failure displacement of the nail-only specimens was never reached. The high ductility values are a function of the extremely long and flat load-displacement curves and low yield loads associated with mechanical fasteners. A typical curve for a nail-only connection is provided in Figure 5.20. This type of curve displays, in essence, the loading required to "drag" a yielded nail through the wood specimen.

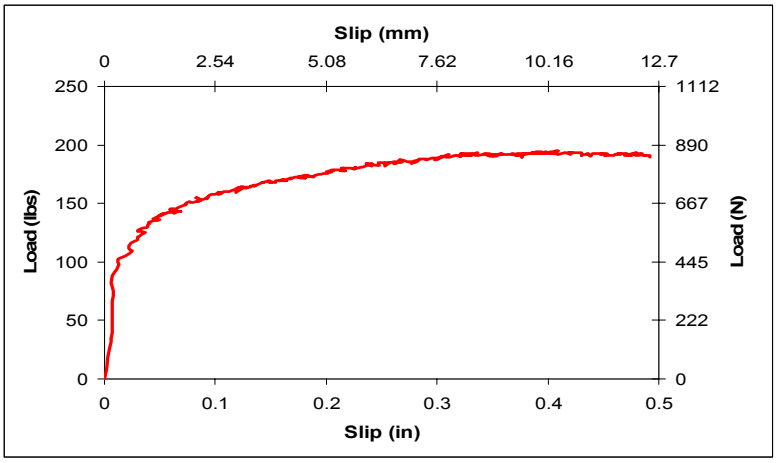

Figure 5.20: Typical Nail-Only Load Displacement Curve

Proportional limit values ($0.4F_{max}$) are provided in Tables 5.11 and 5.12 for informational purposes. These values were only used to calculate the elastic stiffness and EEEP curves for energy and yielding calculations.

5.7 Statistically Significant: OSB Connection Discussion

This section provides additional details and expanded discussion of the general trends and results presented in Section 5.6. Three main topics covered are the quantitative effect of surface treatments on connection strength, the effect of adhesive tape compared to that of mechanical fasteners, and the failure modes of the specimens. Though all specimen groups' load-displacement curves were previously illustrated in Figure 5.14, the average curves for only those connections constructed with OSB are provided again in Figure 5.21 for clarity.

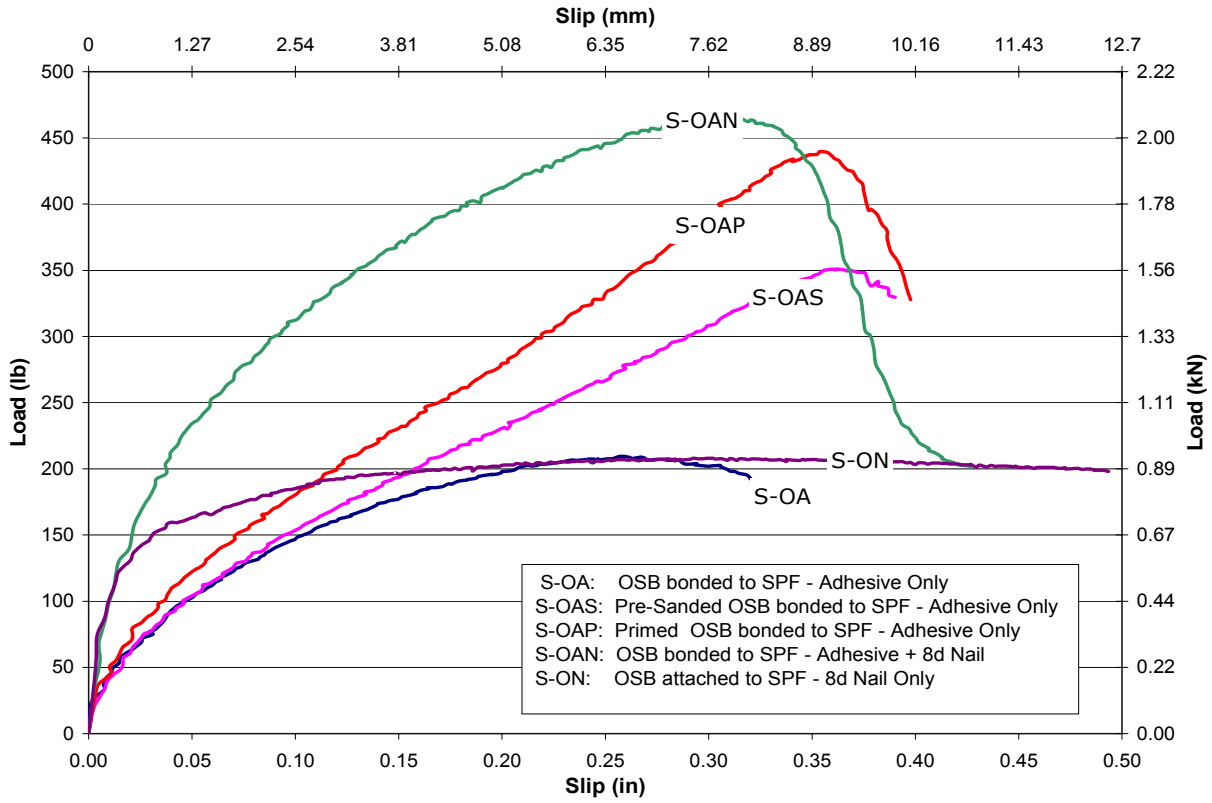

Figure 5.21: OSB Average Load-Displacement Curves

5.7.1 Surface Treatments

As described in Section 5.6, surface sanding and priming of the OSB sheathing improved the peak capacity, displacement at peak capacity, displacement at failure load, and work performed to failure when compare to specimens constructed without surface treatments. These performance improvements are quantified as percent gains over untreated specimens in Table 5.16.

Table 5.16: Surface Treatment Performance Gains

	Fpeak				Δfailure				Work to Failure			
Connection	lb	N	COV	% Gain	in	mm	COV	% Gain	lb*in	N*m	COV	% Gain
Untreated	222.5	990.0	21.4	-	0.347	8.81	10.8	-	59.14	6.68	26.5	-
Sanded	360.5	1603.7	12.7	62%	0.368	9.35	4.5	6%	93.2	10.53	12.9	58%
Priming	445.9	1983.4	7.0	100%	0.393	9.99	3.1	13%	106.87	12.07	7.0	81%

Surface sanding combined a modest gain in displacement capacity with a 60% gain in loading capacity and work to failure. Priming the sheathing surface offered even greater performance with double the peak capacity of untreated specimens. Also, it should be noticed that the COV values decreased as the performance increased. This trend was attributed to the fact that better performance is an indicator of a solid adhesive bond which can be predicted more precisely than a weaker and less consistent bond.

5.7.2 Performance Vs. Mechanical Fasteners

Data represented by the load-displacement curves in Figure 5.21 illustrated that a 152.4 mm (6 in.) long strip of adhesive tape provided approximately the same loading capacity as a single 8d box nail. Displacement capacity of the adhesive connection was much smaller than that of the more ductile nailed connection. When combining the two, it was found that the adhesive tape provided a large increase in peak capacity and strain energy up to the maximum displacement of the adhesive tape. As the adhesive failed, the energy was transferred to the mechanical fastener, and the load-displacement curve continued along the same path as the nail-only connection. Though the connection was technically "failed" by the definition of $0.8F_{peak}$, the displacement and load capacity after failure were significant. This important result indicated that tape adhesive can be used in addition to nails to provide greatly increased performance while maintaining the capacity of the mechanical fasteners after adhesive bond failure. Table 5.17 provides a summary of the key performance parameters.

Table 5.17: Combination System Performance Gains

	Fpeak				Work to Failure[1]			
Connection	lb	N	COV	% Gain	lb*in	N*m	COV	% Gain
Nailed-Only	213.4	949.5	16.6	-	69.9	7.89	17.6	-
Combined	473.8	2107.4	10.4	122%	131.5	14.85	9.6	88%

Note 1: Work values taken to failure displacement of combined system for comparison purposes as the nailed-only systems did not meet failure criteria within the time limit of the test.

5.7.3 Failure Modes of OSB Connections

Sanded, primed, and regular OSB connection tests constructed using only adhesive tape failed in similar modes. OSB connections without surface treatment tended to be fairly weak and often exhibited complete bond failure between the tape and the sheathing. The primed and sanded connections also experienced bond failures, but these failures were typically due to the weakening of the adhesive tape joint and not a complete release of the bond. Even after testing, many of these connections were quite difficult to break by manual force. Pictures of connections that were broken away from the sheathing after testing are provided in Figures 5.22 and 5.23.

Figure 5.22: Surface Sanded Specimen Broken After Testing

In all cases there was no tape residue left on the surface from which the tape adhesive de-bonded. As each connection test was broken after failure, fibrillation between the adhesive tape and the sheathing surface was observed.

Figure 5.23: Primed Specimen Broken After Testing

Nail-only specimens yielded primarily in Mode IIIs as defined by the American Forest & Paper Association and displayed in Figure 5.24 (AF&PA 2002). The head of the nail was observed to turn into the wood and begin to pull or "tunnel" through the sheathing at large displacements.

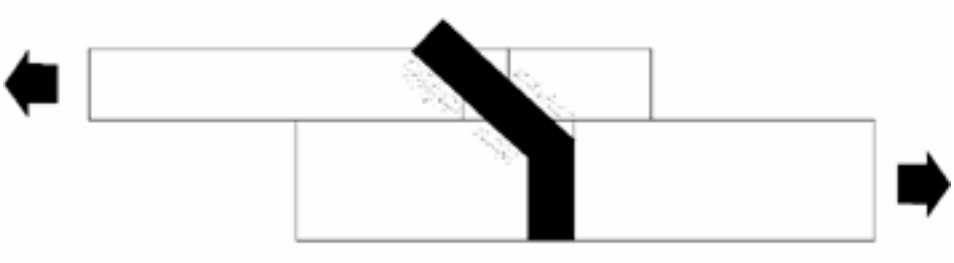

Figure 5.24: Mode IIIs Yielding of Mechanical Fastener

Specimens using a combination of mechanical and adhesive fasteners failed due to the weakening of the adhesive bond and subsequent transfer of force to the nail. When failed specimens were examined, each showed signs of increased localized bonding in the region of the nail. This observation indicated that a local area of high contact pressure between the sheathing and the main member formed where the nail had been shot into the specimen. This phenomenon is recorded in Figure 5.25.

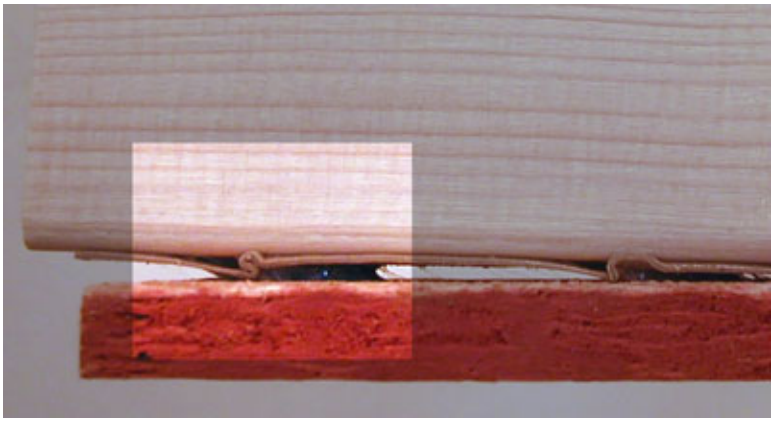

Figure 5.25: Highlighted Area of Localized Bonding Near Nail

5.8 Statistically Significant: Plywood Connection Discussion

This section provides additional details and discussion on plywood connections to supplement the general trends and results presented in Section 5.6. Two main topics covered are the effect of the adhesive tape compared to that of mechanical fasteners and the failure modes of plywood connections. Figure 5.26 displays all load-displacement curves associated with plywood connections.

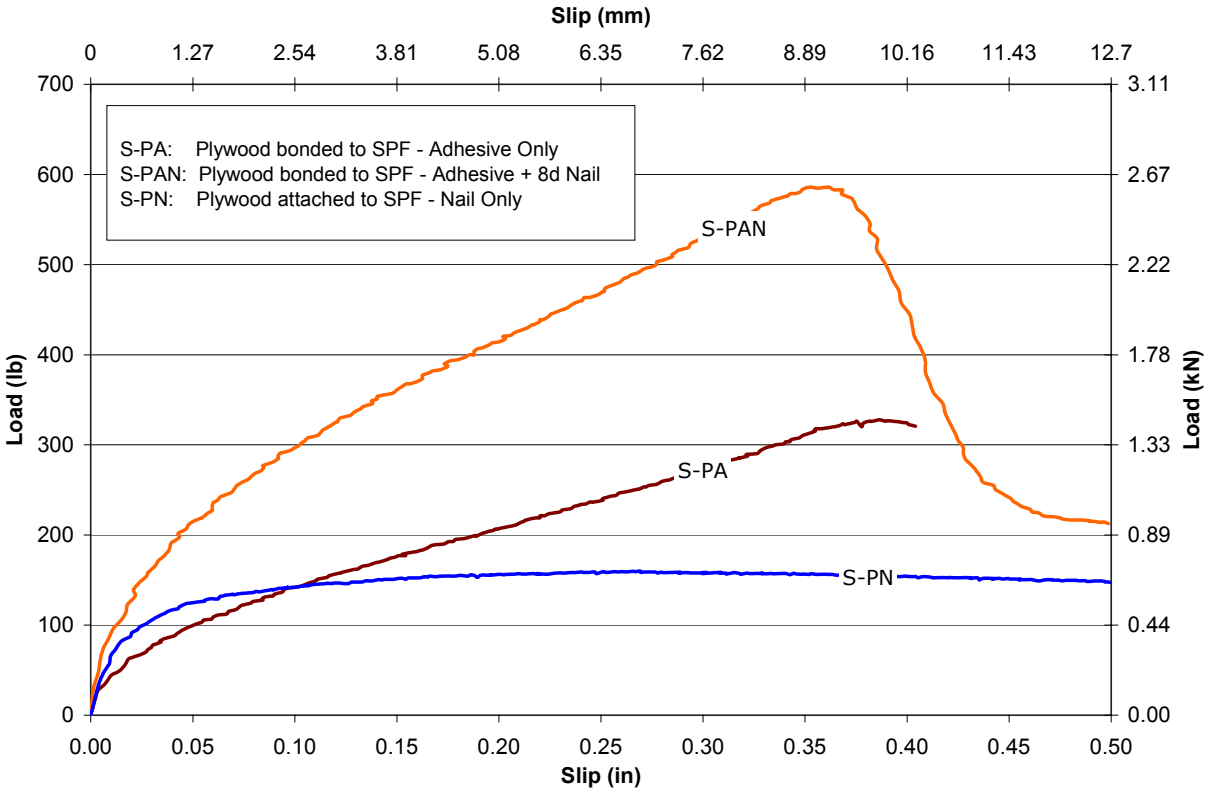

Figure 5.26: Plywood Average Load-Displacement Curves

5.8.1 Performance Vs. Mechanical Fasteners

The trend of plywood connection performance was similar to that of OSB connections. In this case, however, the better bonding characteristics of plywood were evident in the higher strength gains over mechanical fasteners as quantified in Table 5.18. A 152.4 mm (6 in.) long strip of adhesive tape provided approximately two times the loading capacity of a single 8d box nail. This strength gain came at the cost of displacement capacity. The combined system provided peak load capacities that almost quadrupled the capacities of the nail-only connections.

Table 5.18: Performance Comparison Between Systems

	F_{peak}				Work to Failure[1]				Elastic Stiffness			
Connection	lb	N	COV	% Gain	lb*in	N*m	COV	% Gain	lb*in	N*m	COV	x Less
Nailed-Only	163.0	724.9	11.6	-	58.2	8.21	12.2	-	9363	1640	70.8	-
Adhesive-Only	339.3	1509.2	23.6	108%	90.7	12.79	22.0	56%	1504	263	16.5	6.2
Combination	592.9	2637.3	7.0	264%	158.1	22.40	5.2	172%	3858	676	13.0	2.4
Note 1: Work values taken to failure displacement of combined system for comparison purposes as the nailed-only systems did not meet failure criteria within the time limit of the test.												

Table 5.18 also details the increased elastic stiffness associated with mechanical fasteners as opposed to adhesive tape. The use of nails provided stiffness values approximately six times larger than that of adhesive tape alone. This decreased adhesive stiffness was opposite that of the increase in stiffness values normally associated with elastomeric adhesives and indicated better capability to withstand small displacements with minimal damage.

5.8.2 Failure Modes of Plywood Connections

Failure modes for plywood connections constructed with only adhesive tape were typically "rolling" tape failures. This type of failure was described in Section 5.2.6 and illustrated in Figure 5.6 (b). When members were physically broken and inspected after testing had occurred, the adhesive bond failed alternately from the main member and from the sheathing as illustrated in Figure 5.27.

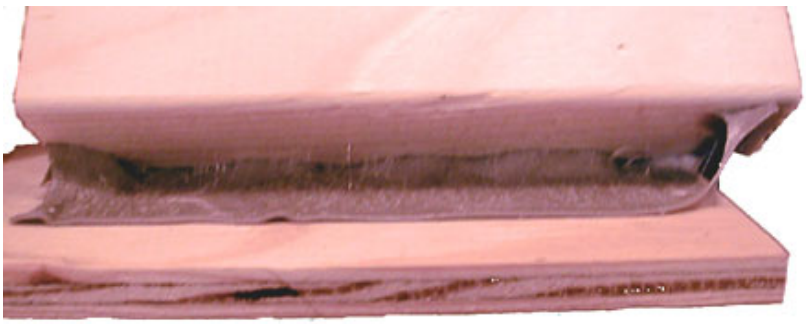

Figure 5.27: Main Member Adhesive Failure

Failure modes for nail-only and combination connections were identical to those that occurred in the corresponding OSB connections detailed in the previous section.

5.9 Statistically Significant: Alternate Manufacturer Study

This portion of the project was conducted to ascertain the viability of applying the results gained from testing 3M VHB 4941 tape to other similar acrylic foam tapes. To allow for the use of PSA tapes in housing construction to become wide-spread and economically viable, it is essential that multiple sources of materials with similar performance be available. To ensure that performance parameters were only affected by the type of adhesive tape used, an additional 3M VHB 4941 set was tested along with tapes from ADCO (AT-2), and Avery (2333).

5.9.1 Performance Parameter Comparison

Quantitative results of the comparison between the three adhesive tapes, though not commented upon, were presented within Section 5.6. All tables of results, t-tests, and performance parameter graphs included the results from these tapes that were labeled S-PMT1 (3M), S-PMT2 (ADCO), and S-PMT3 (Avery). This information was provided along with the results of the other tests for completeness so that comparisons could be made. It should be noted that each test was performed on primed framing and sheathing, allowing set S-PMT1 to be directly compared with the unprimed S-PA testing series which also used 3M VHB. Average load-displacement curves for each test series are provided in Figure 5.28.

The data showed that the S-PMT1 series matched well with the S-PA series with slightly less displacement capacity thus indicating that priming of plywood members was not beneficial to their performance. This result corroborates conclusions from the comparison test set that showed insignificant improvement from plywood priming.

The ADCO AT-2 product was physically similar to the 3M VHB 4941 tape and also proved to be similar in performance. The ADCO tape did not provide load or displacement capacities as high as the 3M product, but the load-displacement curves were similar in shape and provided similar values for work performed through approximately 6.4 mm (0.25 in.) of displacement. It was concluded that results from full-scale wall tests performed with 3M VHB would provide a fair approximation for walls constructed with the ADCO product.

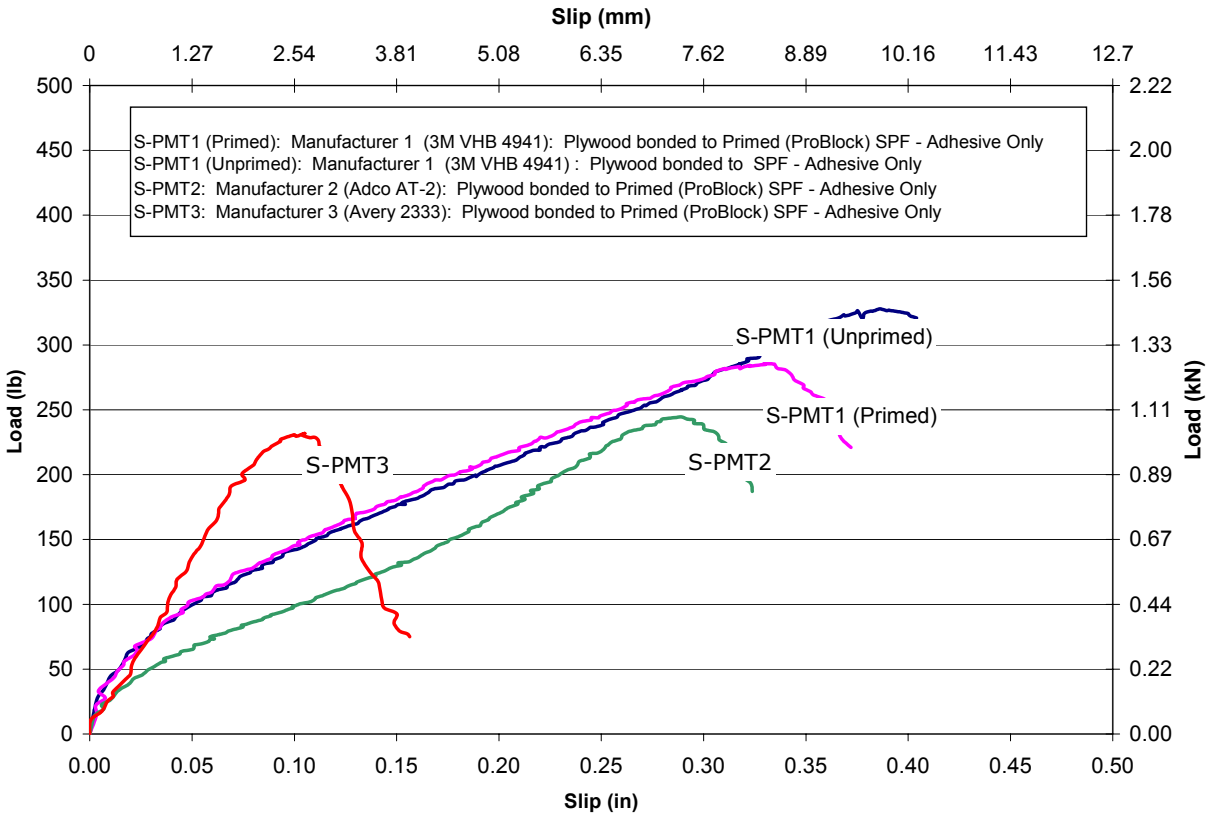

Figure 5.28: Average Load-Displacement Curves for Alternate Adhesive Tapes

The Avery 2333 tape produced peak capacities almost identical to that of the ADCO product. The displacement capacities of the Avery product were, however, between two and three times smaller than the capacities of the ADCO or 3M products. This lack of displacement capacity would result in poorer earthquake performance, and wall test results would not be comparable to those provided in this report. Table 5.19 lists comparison results for key performance parameters.

Table 5.19: Performance of Alternate Manufacturer Tapes vs. 3M VHB 4941

	Fpeak				Δfailure				Work to Failure			
Connection	lb	N	COV	% Diff	in	mm	COV	% Diff	lb*in	N*m	COV	% Gain
S-PMT1	293	1304	26.9	-	0.369	9.36	6.2	-	72.3	8.17	28.6	-
S-PA (Unprimed)	339	1509	23.6	16%	0.389	9.88	6.2	5%	90.7	10.25	28.6	25%
S-PMT2	251	1118	28.4	-14%	0.318	8.08	5.3	-14%	45.8	5.18	28.0	-37%
S-PMT3	237	1055	9.6	-19%	0.106	2.68	10.3	-71%	19.0	2.15	14.3	-74%

5.9.2 Failure Mode Comparison

Failure modes for the 3M VHB 4941 adhesive tape matched those found and described for the statistically significant plywood sheathing test series. Bond weakening failures and "rolling" tape failures both occurred. An illustration of a specimen being physically broken after bond weakening between the main member and the adhesive tape is provided in Figure 5.29.

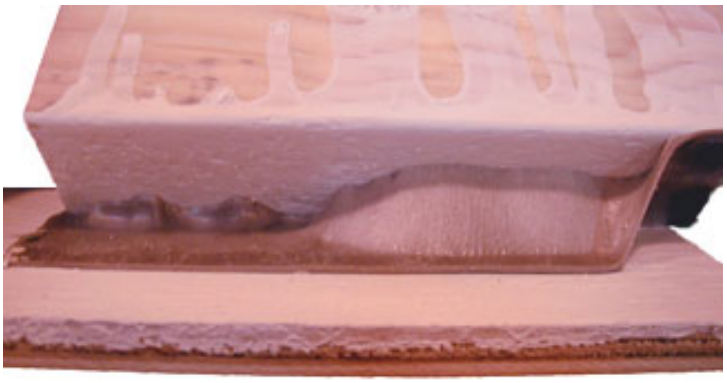

Figure 5.29: S-PMT1 Inspecting Adhesive Bond After Testing

Failure modes for the ADCO AT-2 adhesive tape were similar to those of the 3M VHB 4941. The adhesive tape was observed to roll slightly between the sheathing and the main member before the bond reached displacement capacity. Members physically broken after testing showed evidence of strong bonding, and adhesive failures were observed between both main members and plywood as illustrated in Figure 5.30.

Figure 5.30: S-PMT2 Investing Adhesive Bond After Testing

Failure modes for the Avery 2333 tape were different from those exhibited by the other two products. The adhesive bond often failed cohesively within the tape layer leaving fibers on both surfaces as illustrated in Figure 5.31. The Avery 2333 tape exhibited greater tackiness than the other two tapes, and failures occurred due to its lack of displacement capacity.

Figure 5.31: S-PMT3 Cohesive Tape Failure

5.9.3 Alternate Product Conclusions

Many commercially available acrylic foam adhesive tapes could possibly provide similar or better performance than that of the 3M VHB 4941. A limited study found that ADCO AT-2 provided performance that closely compared to that of the 3M product. This study also found that another acrylic foam tape, Avery 2333, did not provide similar performance. It is recommended that the use of the results and conclusions provided in the following chapter for full-scale walls constructed with 3M VHB 4941 be applied to other products only if a set of single-lap-shear connection tests indicate similar performance parameters to those presented in this chapter. Engineering judgment should then be used to determine whether appropriate scaling factors can be used or the range of performance warrants a more in-depth study.

5.10 Connection Tests of Additional Interest

As discussed in the introduction, the International Building Code (IBC) currently bans the use of adhesives in replacement for, or in addition to, mechanical fasteners (International Code Council 2000). This general ban on adhesives was enacted in response to previous studies such as Pellicane (1988), Filiatrault and Foschi (1991), and Dolan and White (1992). These studies, performed on connections and full-scale walls, focused on the bonding characteristics of traditional elastomeric adhesives such as 3M Scotch Grip 5230. Results from these tests indicated that the greatly increased strength provided by such connections was accompanied by an equally large increase in stiffness and loss of ductility. In effect, the connections became so stiff that during earthquake excitations the increased load capacity was exceeded and brittle failures occurred. One of the tasks of this project was to evaluate whether the use of acrylic foam PSA tapes should be governed by the general ban. Though test results of traditional adhesives are well documented, it was decided to perform a small study using the same testing equipment and materials to provide a general indication of the performance of traditional adhesives for comparison with acrylic foam tape products. A summary of the different connections tested is presented in Table 5.20.

Table 5.20: Traditional Adhesive Specimens

I.D.	Member	Sheathing	Fastener	Treatment	Pressure	Time	No. Tests
WG	SPF	OSB	Tightbond 2 Glue	None	N / A	N / A	2
WG	SPF	Plywood	Tightbond 2 Glue	None	N / A	N / A	3
LN	SPF	OSB	Original Liquid Nails	None	N / A	N / A	2
LN	SPF	Plywood	Original Liquid Nails	None	N / A	N / A	3
						TOTAL	10

5.10.1 Performance Parameters

The performance parameters presented are based on an extremely limited study and are provided for general comparison only. Full results for each connection test are recorded in the Appendix. Average load-displacement curves for each specimen set are displayed in Figure 5.32. Note that the traditional adhesive curves for OSB and plywood sheathing were combined due to the limited number of specimens. Results agree with those determined in the previously mentioned studies and give a clear indication as to why the ban in the IBC currently exists.

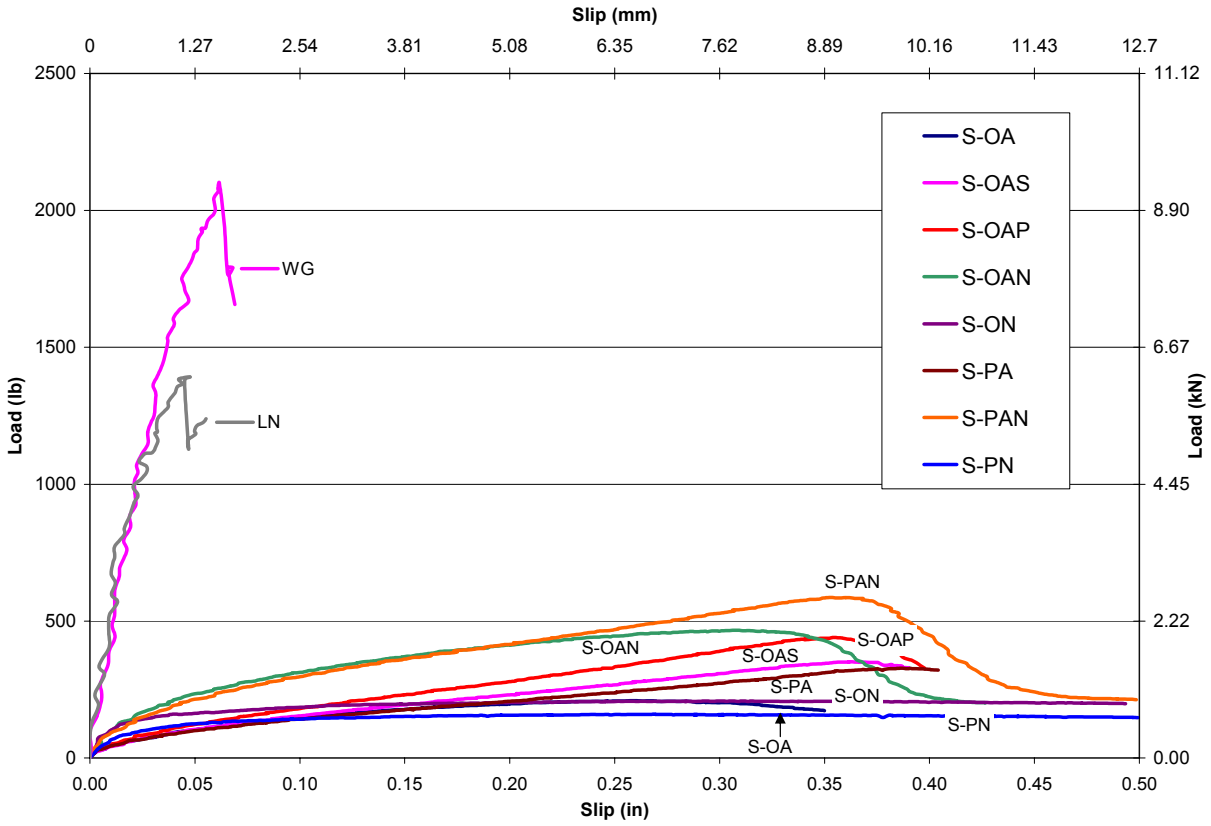

Figure 5.32: Average Load-Displacement Curves for Traditional Adhesives

As listed in Table 5.21, the peak capacities of wood glue and Liquid Nails® were approximately two to four times that of the best performing adhesive tape and nail connection previously tested. However, the displacement capacities were between four and five times lower than those of the adhesive tape system, and elastic stiffness values were over ten times those of the adhesive tape system.

Table 5.21: Performance of Traditional Construction Adhesive

	Fpeak				Δfailure				Elastic Stiffness			
Connection	lb	N	COV	x More	in	mm	COV	x Less	lb*in	N*m	COV	x Less
S-PAN	593	2637	7.0	-	0.4	10.13	3.1	-	3858	676	13.0	-
Wood Glue	2614	11626	20.8	4.4	0.10	2.637	29.8	3.8	50299	8809	27.0	13.0
Liquid Nails	1855	8249	16.4	2.1	0.08	2.07	25.3	4.9	42141	7380	27.0	10.9

5.10.2 Failure Modes of Traditional Adhesives

The main reason for the IBC ban on adhesives is the lack of ductility and brittle failure modes typical of traditional adhesives. This brittle behavior was also observed in this set of tests. Wood glue specimens failed by breaking the cohesive bond between plywood layers or breaking the sheathing panel above the main member as illustrated in Figure 5.33. These failure types were violent with loud cracks and an immediate loss of capacity.

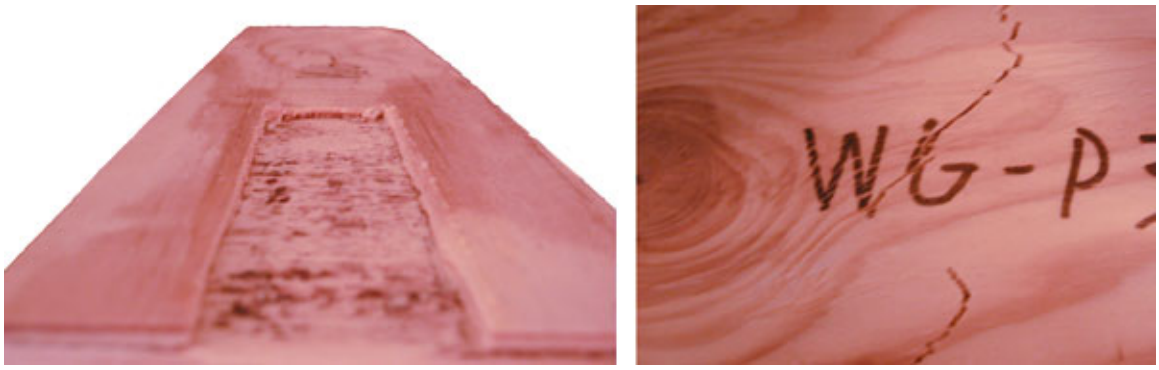

(a) (b)

Figure 5.33: (a) Cohesive Failure in Plywood (Viewed from End) (b) Brittle Sheathing Failure

The failure mode of Liquid Nails® was consistently a cohesive failure within the bond line that left adhesive residue on both sheathing and main framing members as illustrated in Figure 5.34. These failures were not as dramatic as those of wood glue, but they were still brittle failures that resulted in the immediate loss of load capacity at small displacements.

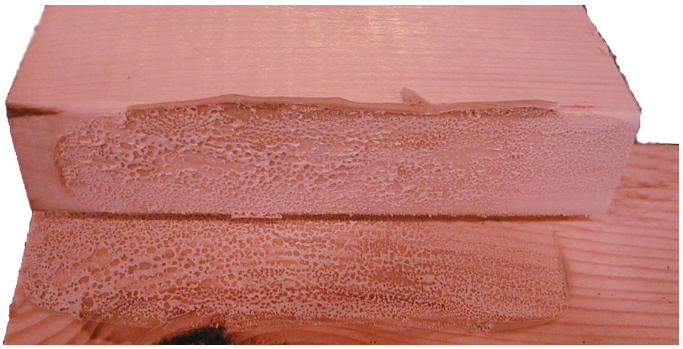

Figure 5.34: Liquid Nails® Cohesive Failure

5.10.3 Conclusions Based on Traditional Adhesives

Based on the connection test results performed on high-bond adhesive tapes, and noting the large increase in displacement capacity and reduction in elastic stiffness when compared to traditional wood adhesives, it is recommended that Section 2305.3.9 of the International Building Code be amended to allow for the use of acrylic foam PSA tapes in Seismic Design Categories D, E, and F. At this time, only adhesive tapes whose performance characteristics are proven similar to those found in this study through experimental means should be admissible. This recommendation is corroborated with full-scale wall testing results provided in the next chapter.

5.11 Summary

Performance results were presented and trends examined for comparison, pressure application, time duration, statistically significant, and traditional adhesive connection groups. Specific parameters were discussed and examined using statistical methods to quantitatively determine performance gains or losses. Based on the results that have been presented, the following conclusions can be drawn.

1. Acrylic foam adhesive tape requires an apparent application pressure of 207 kPa (30 psi) or greater to form a sound bond with a wood substrate of roughness similar to that used in this study. Application pressures of 414 kPa (60 psi) are needed for peak performance.
2. The duration for which bonding pressure is applied does not significantly affect the ultimate performance of the connection. The limits of this study require that 15 seconds be used as the minimum time duration. Though the differences were statistically insignificant, a time duration of 60 seconds was determined to provide maximum performance.
3. Neither moisture content of the framing member nor the piece of lumber from which the specimen originates has a significant effect on connection performance.
4. The displacement limit between wood members joined with acrylic foam tape is approximately eight times the thickness of the tape (8.8 mm or 0.36 in.). This displacement exceeded the value of three times the thickness of tape provided in the manufacturer's literature.

5. OSB specimens bonded with adhesive tape benefit greatly from the use of surface treatments to negate the roughness and low surface energy of the sheathing material. Priming the surface provides twice the load capacity and a 13% gain in displacement capacity over untreated sheathing. Surface sanding provides a 62% increase in load capacity and a 6% gain in displacement capacity.
6. Plywood specimens bonded with adhesive tape do not benefit greatly from surface treatments.
7. In general, OSB specimens perform better than plywood specimens when only mechanical fasteners are used due to the increased thickness and density of the OSB sheathing material tested. Plywood specimens, however, perform better for adhesive based applications, including those combined with mechanical fasteners, due to the favorable bonding properties exhibited by plywood.
8. The combination of acrylic foam adhesive with a mechanical fastener provides a large gain in both peak capacity and energy to failure in comparison with both adhesive-only and nail-only systems. Displacement capacities for adhesive systems are, however, less than those for nail-only connections.
9. Systems that make use of acrylic foam adhesive connections exhibit lower elastic stiffness values and are more susceptible to deflections resulting from applied loads than systems using mechanical fasteners.
10. Weak connections exhibit complete bond failures between the sheathing and tape. Connections where stronger bonds are formed fail by the "rolling" or stretching effect of the induced displacement on the adhesive tape. At no time was the internal strength of the tape reached.
11. Systems that used a combination of mechanical and adhesive fasteners showed areas of increased localized bonding around the point of nailing. This phenomenon is possibly due to the high pressure concentrations associated with this location.
12. ADCO AT-2 adhesive tape exhibited similar performance to 3M VHB 4941. Avery 2333 adhesive tape had only a third of the displacement capacity of the other two tapes. Other similar products should be tested using a series of single-lap-shear tests to determine if values and trends presented in this report are applicable to the products being investigated.

13. Connections constructed with acrylic foam adhesive tape were found to provide between 4 and 5 times the displacement capacity of traditional construction adhesives. Stiffness values of acrylic foam connections were also between 10 and 15 times lower than those of traditional adhesives. Based on these results and the history of the IBC ban on construction adhesives for shear walls in high seismic zones, it is recommended that an allowance be made for high-bond PSA tapes.

Chapter 6

Shear Wall Test Results and Discussion

6.1 General

The shear wall testing portion of this study was composed of 23 full-scale 8 ft x 8 ft (2.4 m x 2.4 m) specimens. Two specimens were tested monotonically, and the remaining specimens were testing using the CUREE reversed-cyclic protocol. Information provided by the monotonic tests was used in combination with results from the connection tests to calibrate the loading protocol for each cyclic configuration. Cyclic test results were broken down into strength, toughness, and seismic performance categories. Within each of these subsets, the performance of walls built using adhesive tape versus that of traditional wall construction was evaluated. Additionally, differences between OSB and plywood-sheathed specimens were investigated. The OSB subset also explored the effect of sanding and priming the sheathing surface. This chapter provides summary information on the results of each test series including general trends and direct comparisons of performance parameters. In addition, design examples for shear walls utilizing adhesive tape for wind and seismic loading conditions are provided. A listing of the different specimens tested is given in Table 6.1.

Table 6.1: Wall Specimen List

Full-Scale 2.4 m x 2.4 m (8 ft x 8 ft) Shear Wall Tests[1]						
I.D.	Member	Sheathing	Fastener	Treatment	Test Method	No. Tests
W-OAN-M	SPF	Plywood	3M VHB + 8d Nails	None	Monotonic	2
W-PA	SPF	Plywood	3M VHB	None	Cyclic CUREE	3
W-PN	SPF	Plywood	8d Nails	None	Cyclic CUREE	3
W-PAN	SPF	Plywood	3M VHB + 8d Nails	None	Cyclic CUREE	3
W-OAS	SPF	OSB	3M VHB	Sanded	Cyclic CUREE	3
W-OAP	SPF	OSB	3M VHB	Primed	Cyclic CUREE	3
W-ON	SPF	OSB	8d Nails	None	Cyclic CUREE	3
W-OAN	SPF	OSB	3M VHB + 8d Nails	None	Cyclic CUREE	3
					TOTAL	23

Notes:
1) Pressure applied for adhesive application was a minimum of 414 kPa (60 psi) for 60 seconds

6.2 Monotonic Test Results

Monotonic tests were performed in accordance with ASTM E564-00 (ASTM 2000b). Two specimens were tested, and the calculated strengths matched within 15%; thus, according to the ASTM procedure, the testing of an additional wall assembly was unnecessary. The analysis of the monotonic tests was minimal as they were performed solely to calculate failure displacements for the calibration of the cyclic protocol.

6.2.1 Load-Displacement Curves

Load versus displacement curves for both monotonic specimens are illustrated in Figure 6.1. Average failure displacement is also depicted on the curves.

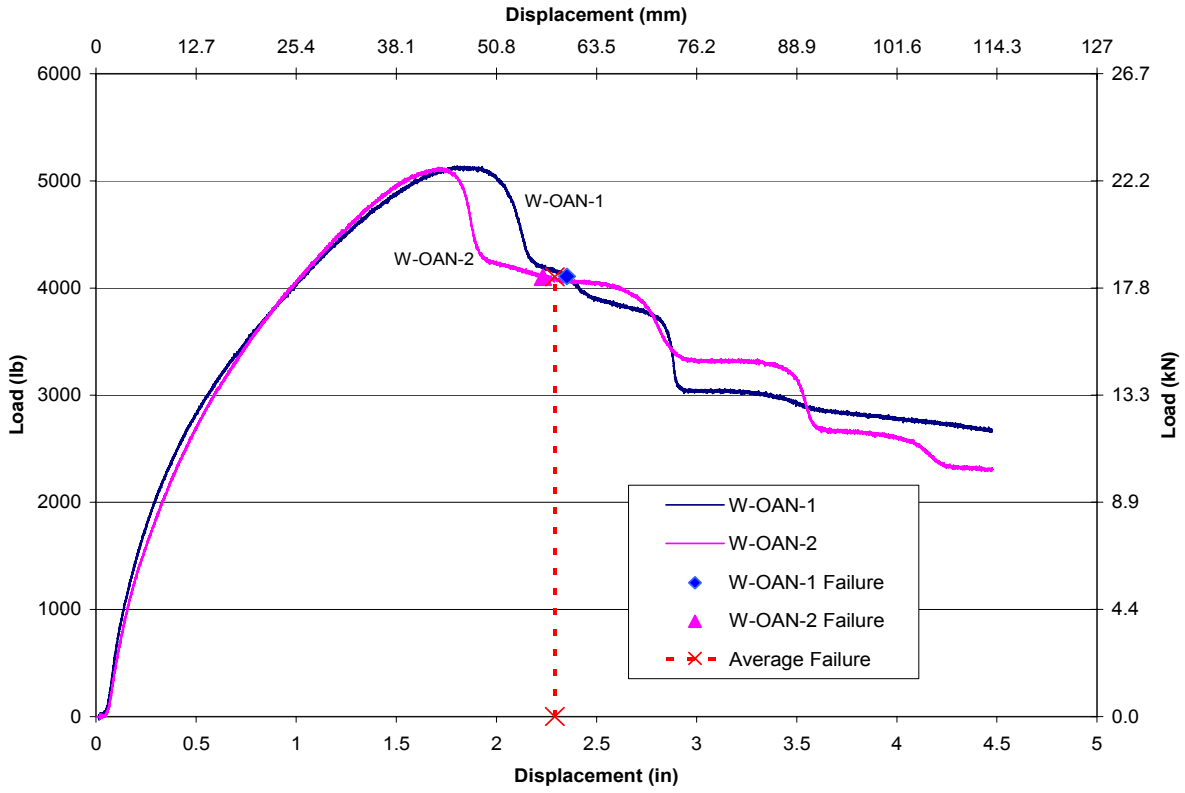

Figure 6.1: Monotonic Wall Test Load-Displacement Curves

Wall failures occurred in stages as illustrated by the load-displacement curves. Each successive drop in load capacity corresponds with the loss of adhesive bond along the edge of a sheathing panel as visually observed during the tests.

6.2.2 Target Cyclic Deflections (Δ)

As previously discussed in Section 3.7.4.1, ratios of displacements at peak load capacity between connection test configurations were used along with results of the monotonic wall test configuration to predict failure displacements for all shear wall specimens. Connection test displacement ratios are provided in Table 6.2.

Table 6.2: Connection Test Displacement Ratios

Type	Failure	S-OAN	Ratio
S-OAN	0.3629	0.36290	1.0000
S-OAS	0.4099	0.36290	1.1296
S-OAP	0.3932	0.36290	1.0835
S-PA	0.4269	0.36290	1.1764
S-PAN	0.3998	0.36290	1.1017

The W-OAN wall assembly was chosen because its corresponding connection specimen exhibited the smallest displacement capacity during connection tests therefore providing a conservative estimate of other wall configurations. Predicted monotonic and cyclic failure displacement values are listed in Table 6.3. These values were used to set the amplitude of the displacement controlled cyclic forcing function.

Table 6.3: Monotonic and Cyclic Failure Displacements

Full-Scale Wall Data						
		W-OAN-1		W-OAN-2		Average
$F_{failure}$	lbs	4108		4100		4104
	kN	18.27		18.23		18.25
$\Delta_{failure}$	in	2.352		2.232		2.292
	mm	59.73		56.70		58.21
Target Cyclic Displacement Predictions						
	Monotonic (Δ_{mon})		Cyclic (Δ=0.6Δ_{mon})		Rounded Cyclic[2]	
	(in)	(mm)	(in)	(mm)	(in)	(mm)
W-OAN	2.29	58.21	1.38	34.93	**1.4**	34.9
W-OAS	2.59	65.76	1.55	39.45	**1.6**	39.5
W-OAP	2.48	63.07	1.49	37.84	**1.5**	37.8
W-PA	2.70	68.48	1.62	41.09	**1.6**	41.1
W-PAN	2.52	64.13	1.51	38.48	**1.5**	38.5
W-ON[1]	6.00	152.40	3.60	91.44	**3.6**	91.4
W-PN[1]	6.00	152.40	3.60	91.44	**3.6**	91.4

Note 1: Nail-only displacements from previous research (Toothman 2003)
Note 2: Bold = Actual values used for testing

6.3 Cyclic Tests: Introduction

Twenty-one full-scale shear walls were cyclically tested to provide information about the seismic performance of wall assemblies constructed with acrylic foam PSA tape. In addition to seismic parameters, the strength recorded for each wall can be used to predict performance in hurricane-type conditions. Results from these tests are presented in this chapter as follows:

1. Overall numeric performance parameters for all specimens… (Section 6.4)
2. Wall assemblage strength comparison…..…….. (Section 6.5)
3. Wall assemblage toughness comparison……..… (Section 6.6)
    a. Displacement Capacity
    b. Hysteretic Energy
4. Earthquake performance parameters…… (Section 6.7)
    c. Cyclic Stiffness
    d. Equivalent Viscous Damping Ratios (EVDR)
    e. Ductility
    f. Response Modification Factor (R)
5. Overall Wall Response…….. (Section 6.8)

Due to the small number of specimens tested for each configuration, a full statistical analysis of the results was not performed. Despite the lack of repetition, the results were consistent throughout the study. Detailed information on performance characteristics of each specimen, including coefficients of variation, are presented in the Appendix which also contains the following information on each wall configuration:

1. Diagram of wall specimen construction
2. Average performance parameters and supporting figures for three-specimen set
3. Individual specimen construction and testing information including:
    a. Date of wall construction and testing
    b. Ambient and bond-line temperatures during testing
    c. Average moisture content of framing members
    d. Comments on test and data acquisition results
    e. Comments and pictures of the failure mode of each wall

f. Adhesive tape manufacturer lot numbers

4. Individual specimen performance parameters and supporting figures

Information that is provided in the Appendix provides a more in-depth look into the behavior and failure mechanisms associated with the adhesive tape bonding than can be provided in the main body of this report.

6.4 Cyclic Tests: Performance Parameter Results

Performance parameter information provided in this section represents an average of the results from each three-specimen set. This data was obtained by first analyzing the individual walls and then averaging the performance parameters as opposed to analyzing an average load-deflection curve. It is believed that the method used provides a better evaluation of each wall configuration as it is difficult to obtain a true "average" curve without sacrificing a segment of the full range of displacement or force data from each test.

Table 6.4 provides a summary of performance parameters for all wall configurations. These parameters are ultimate values and should be reduced if necessary by the appropriate allowable stress factor for use in design. Proportional limit values are provided in the table but are not further discussed, as their use was limited to determining the initial elastic stiffness and EEEP curves of the system. Additional commentary on all other performance parameters is provided in the following sections. The average Coefficients of Variation (COVs) for both peak loads and failure displacements are in the range of 8%, and COVs for other performance parameters are generally under 10%. Low COV values indicate consistent adhesive bonds were formed and lend credence to the accuracy of the results.

Table 6.5 provides the same performance parameter information on a per unit length basis. Again these values are ultimate parameters and should be used in conjunction with the applicable safety factors when used in design.

It is important to emphasize that the W-PAN and W-OAN subsets utilized one-half the number of nails as did the traditional nail-only wall configurations. A reduced nail set was used to explore the possibility of performance increases over traditional construction with the combined use of PSA tape and fewer nails.

Table 6.4: Full-Scale Shear Wall Performance Parameters

Key for Wall Subsets

W-ON 11 mm (7/16 in.) OSB Panels - 8d box nails only - 6x12 nailing schedule
W-OAN 11 mm (7/16 in.) OSB Panels - 8d box nails - 12x12 nailing schedule - 38 mm (1.5 in.) PSA Adhesive on Sheathing Perimeter
W-OAP 11 mm (7/16 in.) OSB Panels - No Nails - Primed Surfaces - 38 mm (1.5 in.) PSA Adhesive on Sheathing Perimeter
W-OAS 11 mm (7/16 in.) OSB Panels - No Nails - Sanded OSB - 38 mm (1.5 in.) PSA Adhesvie on Sheathing Perimeter

W-PN 9 mm (3/8 in.) Plywood Panels - 8d box nails only - 6x12 nailing schedule
W-PAN 9 mm (3/8 in.) Plywood Panels - 8d box nails - 12x12 nailing schedule - 38 mm (1.5 in.) PSA Adhesive on Sheathing Perimeter
W-PA 9 mm (3/8 in.) Plywood Panels - 38 mm (1.5 in.) PSA Adhesive on Sheathing Perimeter

Total Length Parameters (Averages)		**W-ON**		**W-OAN**		**W-OAP**		**W-OAS**		**W-PN**		**W-PAN**		**W-PA**	
EEEP Parameters	**units**	value	COV	value	COV	value	COV	value	COV	value	COV	value	COV	value	COV
Peak load, F_{peak}	Kips	4.881	4.891	8.292	8.056	6.299	1.247	4.389	5.556	4.633	7.220	7.779	10.905	5.113	12.705
	KN	21.710		36.883		28.017		19.523		20.607		34.600		22.745	
Drift at peak load, Δ_{peak}	in.	2.218	2.088	1.199	7.803	1.144	0.550	0.800	22.346	2.525	8.686	1.512	7.958	1.068	2.673
	mm	56.340		30.452		29.059		20.311		64.147		38.415		27.117	
Yield load, F_{yield}	Kips	4.336	5.921	7.199	6.354	5.373	2.671	3.857	5.525	4.141	6.111	6.783	11.118	4.373	12.058
	KN	19.284		32.021		23.899		17.155		18.419		30.169		19.452	
Drift at yield load, Δ_{yield}	in.	0.483	10.085	0.658	9.285	0.670	8.689	0.472	12.988	0.574	4.040	0.890	3.458	0.628	8.435
	mm	12.263		16.701		17.010		11.992		14.583		22.594		15.954	
Proportional limit, $0.4F_{peak}$	Kips	1.952	4.891	3.317	8.056	2.520	1.247	1.756	5.556	1.853	7.220	3.111	10.905	2.045	12.705
	KN	8.684		14.753		11.207		7.809		8.243		13.840		9.098	
Drift at prop. limit, $\Delta@0.4F_{peak}$	in.	0.217	8.917	0.302	8.764	0.314	7.151	0.216	14.226	0.257	4.571	0.408	3.614	0.294	9.051
	mm	5.516		7.681		7.964		5.476		6.522		10.368		7.457	
Failure load or $0.8F_{peak}$	Kips	4.289	12.105	6.634	8.056	5.039	1.247	3.511	5.556	3.805	5.364	6.223	10.905	4.091	12.705
	KN	19.079		29.507		22.414		15.618		16.923		27.680		18.196	
Drift at failure, $\Delta_{failure}$	in.	3.469	14.585	1.716	2.370	1.334	0.779	1.094	11.117	3.883	7.673	2.026	12.992	1.349	7.226
	mm	88.108		43.581		33.889		27.784		98.617		51.453		34.261	
Elastic stiffness, K_e @$0.4F_{peak}$	Kip/in.	9.099	5.092	11.051	10.572	8.099	6.935	8.473	6.870	7.279	4.764	7.728	13.891	6.979	4.862
	KN/mm	1.593		1.935		1.418		1.484		1.275		1.353		1.222	
Work until failure	Kip·ft.	7.151	18.654	4.863	10.789	2.748	2.904	2.210	27.535	8.168	7.802	5.266	19.980	2.249	9.793
	KN·m	9.695		6.593		3.725		2.996		11.074		7.139		3.049	
Ductility factor, μ		7.240	11.026	2.647	9.942	2.007	8.384	2.412	16.863	6.837	10.997	2.311	15.108	2.157	4.391

AVG Displacement Parameters	**W-ON**		**W-OAN**		**W-OAP**		**W-OAS**		**W-PN**		**W-PAN**		**W-PA**	
	in.	mm	in.	mm	in.	mm	in.	mm	in.	mm	in.	mm	in.	mm
Total Displacement	2.21	5.62	1.13	2.88	1.00	2.54	0.75	1.91	2.23	5.65	1.43	3.63	1.06	2.70
Shear Deformation	0.80	2.02	0.31	0.78	0.31	0.78	0.26	0.66	0.78	1.99	0.42	1.07	0.36	0.90
Rigid Body Rotation	0.31	0.79	0.26	0.67	0.26	0.66	0.12	0.30	0.33	0.84	0.35	0.89	0.19	0.47
Bending	1.11	2.81	0.57	1.44	0.43	1.10	0.38	0.96	1.11	2.83	0.66	1.67	0.52	1.33

Table 6.5: Full-Scale Shear Wall Performance Parameters Per Unit Length

Key for Wall Sub-sets	
W-ON	7/16" OSB Panels - 8d box nails only - 6x12 nailing schedule
W-OAN	7/16" OSB Panels - 8d box nails - 12x12 nailing schedule - 1.5" PSA Adhesive on Sheathing Perimeter
W-OAP	7/16" OSB Panels - No Nails - Primed Surfaces - 1.5" PSA Adhesive on Sheathing Perimeter
W-OAS	7/16" OSB Panels - No Nails - Sanded OSB - 1.5" PSA Adhesvie on Sheathing Perimeter
W-PN	3/8" Plywood Panels - 8d box nails only - 6x12 nailing schedule
W-PAN	3/8" Plywood Panels - 8d box nails - 12x12 nailing schedule - 1.5" PSA Adhesive on Sheathing Perimeter
W-PA	3/8" Plywood Panels - 1.5" PSA Adhesive on Sheathing Perimeter

Unit Length Parameters (Averages)		**Wall Subsets (Per Foot Length)**						
EEEP Parameters	**units**	W-ON	W-OAN	W-OAP	W-OAS	W-PN	W-PAN	W-PA
Peak unit load, v_{peak}	Kip/ft.	0.610	1.037	0.787	0.549	0.579	0.972	0.639
	KN/m	8.903	15.126	11.490	8.007	8.451	14.189	9.328
Drift at capacity, Δ_{peak}	in.	2.218	1.199	1.144	0.800	2.525	1.512	1.068
	mm	56.340	30.452	29.059	20.311	64.147	38.415	27.117
Yield unit load, v_{yield}	Kip/ft.	0.542	0.900	0.672	0.482	0.518	0.848	0.547
	KN/m	7.909	13.132	9.801	7.035	7.554	12.373	7.977
Drift at yield load, Δ_{yield}	in.	0.483	0.658	0.670	0.472	0.574	0.890	0.628
	mm	12.263	16.701	17.010	11.992	14.583	22.594	15.954
Proportional limit, $0.4v_{peak}$	Kip/ft.	0.244	0.415	0.315	0.219	0.232	0.389	0.256
	KN/m	3.561	6.050	4.596	3.203	3.380	5.676	3.731
Drift at prop. limit, $\Delta@0.4v_{peak}$	in.	0.217	0.302	0.314	0.216	0.257	0.408	0.294
	mm	5.516	7.681	7.964	5.476	6.522	10.368	7.457
Unit load at failure or $0.8v_{peak}$	Kip/ft.	0.536	0.829	0.630	0.439	0.476	0.778	0.511
	KN/m	7.824	12.101	9.192	6.405	6.940	11.352	7.462
Drift at failure, $\Delta_{failure}$	in.	3.469	1.716	1.334	1.094	3.883	2.026	1.349
	mm	88.108	43.581	33.889	27.784	98.617	51.453	34.261
Shear modulus, G $@0.4F_{peak}$	Kip/in.	9.099	11.051	8.099	8.473	7.279	7.728	6.979
	KN/mm	1.593	1.935	1.418	1.484	1.275	1.353	1.222
Work until failure per unit length	Kip·ft./ft.	0.894	0.608	0.343	0.276	1.021	0.658	0.281
	KN·m/m	3.976	2.704	1.528	1.229	4.541	2.928	1.250
EVDR @ Peak Cycle		0.216	0.171	0.191	0.175	0.203	0.157	0.168

6.5 Cyclic Tests: Shear Wall Strength

When designing a shear wall to resist monotonic loading such as that produced by high winds and hurricane conditions, the most important performance parameter is strength of the wall assemblage. Strength values in the form of peak, yield, and failure loads for each wall configuration are provided in Figure 6.2.

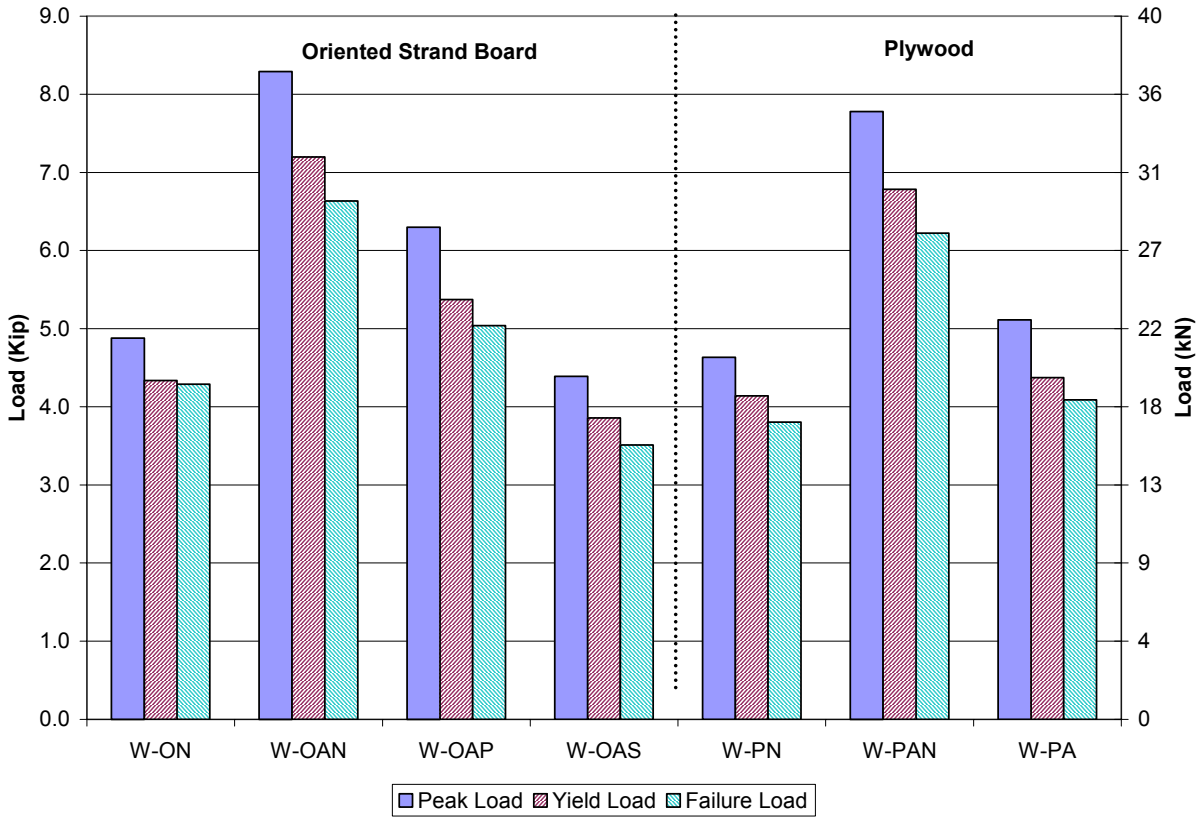

Figure 6.2: Average Load Capacities of Shear Wall Tests

6.5.1 General Strength Comparison

Figure 6.2 illustrates the effectiveness of the combination adhesive tape and nail systems. Though having only half of the nails as the traditional nail-only walls, the combination assemblages provided approximately 70% greater peak capacity (W-OAN vs. W-ON and W-PAN vs. W-PN). Capacity gains for both OSB and plywood walls were almost identical as the adhesive tape provided similar performance gains on both sheathing surfaces. Connection tests results indicated, however, that the substrate made a difference in the performance of the

adhesive bonds. It is believed that the difference in performance due to sheathing surface characteristics was within the variability of the wall tests and, therefore, did not manifest itself in the averaged results.

When comparing the performance of OSB versus plywood in wall systems utilizing mechanical fasteners, the thicker and denser OSB provided higher capacities by approximately 5-7%. This increase was observed in both nail-only and combination systems. In adhesive-only applications, the plywood wall configurations (W-PA) actually provided slightly better performance than the sanded OSB sheathing (W-OAS). This increase was attributed to the better bonding properties of plywood that were discussed in Chapter 5.

An adhesive-only OSB system without any surface treatments was not tested to save labor and material costs as its connection test performance was extremely poor. As with the connection tests, the surface priming of the sheathing panels allowed better adhesion and significantly increased the strength of the walls over surface sanding. Performance values were still, however, significantly lower than those of the combination systems.

Finally, comparison between adhesive-only systems and traditional construction shows similar performance values for both OSB and plywood-sheathed specimens. Though the primed OSB configuration provided some performance gain, it is not enough to justify the use of a PSA tape-based system over nailed-only shear walls.

6.5.2 Strength Design Tables

Table 6.6 is provided on the following page as a design aid for the use of acrylic foam PSA tapes in the construction of shear walls. It is important to note that these values depend upon the type of adhesive tape being used and should be modified based on the performance of a series of connection tests for products similar to 3M VHB 4941. This table provides the amount of increased shear that can be resisted per linear foot from the use of acrylic foam PSA tapes over traditional construction values.

Table 6.6 should be used in conjunction with IBC Table 2306.4.1 “Allowable Shear (pounds per foot) for Wood Structural Panel Shear Walls with Framing of Douglas-Fir-Larch, or Southern Pine for Wind or Seismic Loading” (ICC 2000). The values in the IBC table may be increased by the amount shown in Table 6.6 with the appropriate safety factor of three. These increases may be used on any wall-panel thickness, as the strength gains of the combination

system were purely additive when compared with the performance of a traditional shear wall. Also note that it is conservative to use these values along with a reduced nailing-schedule as provided in the IBC, as the strength modifiers were calculated based on a combination system using an extremely sparse nail-schedule of 305 mm (12 in.). It is suspected that even higher strength gains would result from the use of denser nail schedules due to high localized adhesive bonding pressures. There is, however, no data to substantiate this claim, and the strength gains shown in Table 6.6 should be used until further testing can be conducted.

Table 6.6: Strength Modifiers to IBC Table 2306.4.1 (ICC 2000)

Comparison to Nailed-Only Walls (OSB or Plywood) on a PER UNIT Basis								
Comparison Parameter	**units**	W-ON	W-OAN	W-OAP	W-OAS	W-PN	W-PAN	W-PA
ADDITIONAL Peak Unit Load, v_{peak}	lb / ft	0.0	426	177	-0.061	0.0	393	60
	KN / m	0.0	6.223	2.587	-0.897	0.0	5.738	0.877
ADDITIONAL Peak Unit Load Including ASD F.S.=3	lb / ft	0.0	**142**	59	-0.020	0.0	**131**	20
	KN / m	0.0	2.074	0.862	-0.299	0.0	1.913	0.292
Note: Bold values indicate design strength gains for combination adhesive walls over traditional construction								

From Table 6.6, an average increase of approximately 2 kN/m (135 lb/ft) is recommended for the design of combination tape and adhesive shear walls.

6.5.3 Shear Wall Strength Summary

In summary, the load capacity performance of each wall configuration tested provided the following information:

1. The combination of acrylic foam PSA adhesive tape in conjunction with a reduced schedule of mechanical fasteners can provide strength gains in excess of 70% of traditional construction values.
2. Adhesive-only systems provide similar strength performance to traditional shear walls and are, therefore, not recommended due to the lack of performance gains coupled with increased construction requirements.
3. The use of surface treatments, in particular priming, provides some strength gains for adhesive-based shear walls with OSB sheathing over walls without treatment.

6.6 Cyclic Tests: Shear Wall Toughness

The toughness of a shear wall specimen is a general term that describes both the overall displacement capacity of the system as well as the hysteretic energy in relation to the interstory drift of the wall. While a minimum strength is still important for seismic design, tougher shear walls can better withstand large base excitations in earthquake loading. Therefore, though the information on strength developed in the previous section is important, this section will examine both toughness components and will provide overall conclusions based on the general trends observed for each specimen configuration.

6.6.1 Displacement (Interstory Drift) Capacity

Average displacement capacities for each wall configuration are illustrated in Figure 6.3. Specimen naming follows the convention used throughout this report and places nailed-only (traditional) systems first, followed by combination and adhesive-only wall assemblages.

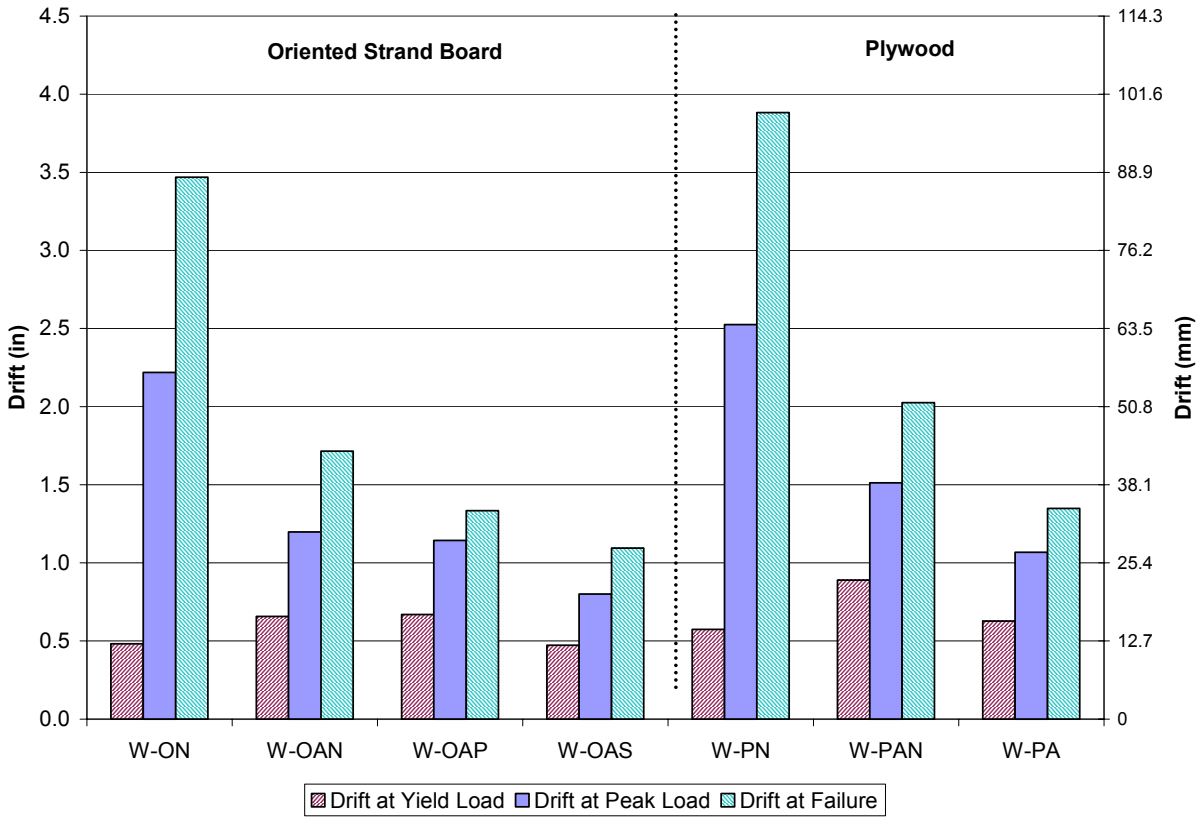

Figure 6.3: Interstory Drift Capacities

Displacement capacities of the walls constructed using only mechanical fasteners exceeded both combination wall systems and adhesive-only systems by a wide margin. The quantitative comparison data provided in Table 6.7 reveals that wall assemblages that utilized a combination system had approximately half of the displacement capacity of the nailed-only specimens. Adhesive-only systems provided even less displacement capacity. Increased performance of the traditional walls resulted from the ability of the mechanical fasteners to deform and develop plastic hinges at high displacements. Displacement capacity of the adhesive wall systems was limited by the ability of the adhesive to undergo local deformations between sheathing and framing members. As the wall system experienced increased overall displacements, the local differential between framing members and sheathing members increased. Results from connection tests indicated that this local deformation capacity was in the range of eight times the thickness of the adhesive tape.

Table 6.7: Displacement Capacity Comparison

	Oriented Strand Board				Plywood		
	Traditonal	Combination	Adhesive-Only		Traditional	Combination	Adh-Only
Δfailure	W-ON	W-OAN	W-OAP	W-OAS	W-PN	W-PAN	W-PA
in	3.47	1.72	1.33	1.09	3.88	2.03	1.35
mm	88.1	43.6	33.9	27.8	98.6	51.5	34.3
% Diff	-	49	38	32	-	52	35

If this data alone was examined, it would appear that the use of adhesive tape is not a viable alternative to traditional construction for seismic loadings. There are, however, several other factors involved that must first be discussed before making such a conclusion.

6.6.2 Hysteretic Energy

The second main component of the toughness of a shear wall is the hysteretic energy (also referred to as damping energy) of the system at certain displacement levels. Though calculating the work to failure is a good comparison indicator between walls tested with the same protocol, examining the hysteretic energy for a particular loading cycle's displacement is not dependent on the forcing function used to test the wall and is better suited for discussion.

It is important to note that there are currently limits in most of the major building codes as to the acceptable life-safety interstory drift that a building should be designed to sustain. In the International Building Code, these allowable story drifts range depending on the seismic use

group as summarized in Table 6.8 (ICC 2000). For the most common application of light-frame residential housing, the applicable drift limit for a 2.4 m (8 ft) wall element is 61 mm (2.4 in.). This limit corresponds to 2.5% of the height of the wall. The hysteretic energy of the wall assemblage is only critically important up to the code allowable displacements.

Table 6.8: Allowable Drift to Height Ratios
(Values extracted from IBC Table 1617.3 (ICC 2000))

Building Type	Seismic Use I		Seismic Use II		Seismic Use III	
	ratio	for 8ft (in)	ratio	for 8ft (in)	ratio	for 8ft (in)
Typical non-masonry construction	0.025	**2.400**	0.020	1.920	0.015	1.44
Masonry cantilever shear wall buildings	0.010	0.960	0.010	0.960	0.010	0.96
Other masonry shear wall buildings	0.007	0.672	0.007	0.672	0.007	0.672
Masonry wall frame buildings	0.013	1.248	0.013	1.248	0.010	0.96
All other buildings	0.020	1.920	0.015	1.440	0.010	0.96
Note: 1 in. = 25.4 mm						

Figure 6.4 illustrates the hysteretic energy versus interstory drift of the different wall configurations constructed with OSB sheathing. Note that data was still recorded for each wall for displacements beyond the failure criteria corresponding with $0.8F_{peak}$.

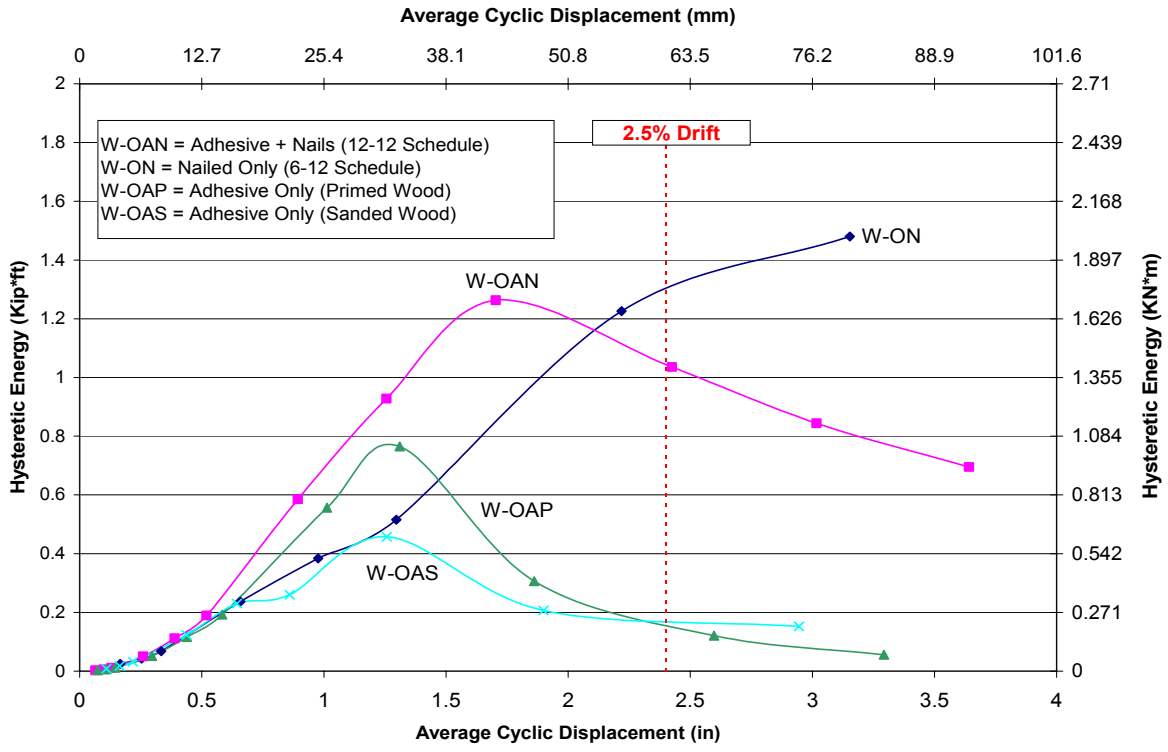

Figure 6.4: Hysteretic Energy vs. Displacement of OSB Wall Specimens

The hysteretic energy of the combination wall system was greater than that of the traditional nailed-only system through displacements corresponding to the allowable drift limit. This result indicated that though overall displacement capacities and therefore ductility values (which are discussed in a later section) are larger for nailed-only walls, the combination systems are actually better suited for seismic loadings. Adhesive-only systems performed poorly in comparison to the other wall configurations. The combination of low hysteretic energy values and displacements lead to the conclusion that adhesive-only wall systems are not well-suited for seismic applications. Further details on earthquake performance are provided in a later section.

Figure 6.5 illustrates the hysteretic energy versus interstory drift of the different wall configurations constructed with plywood sheathing. Similarly to the OSB walls, plywood-sheathed walls continued to hold load well past their defined failure displacements. This data was recorded and is included in the hysteretic energy plot.

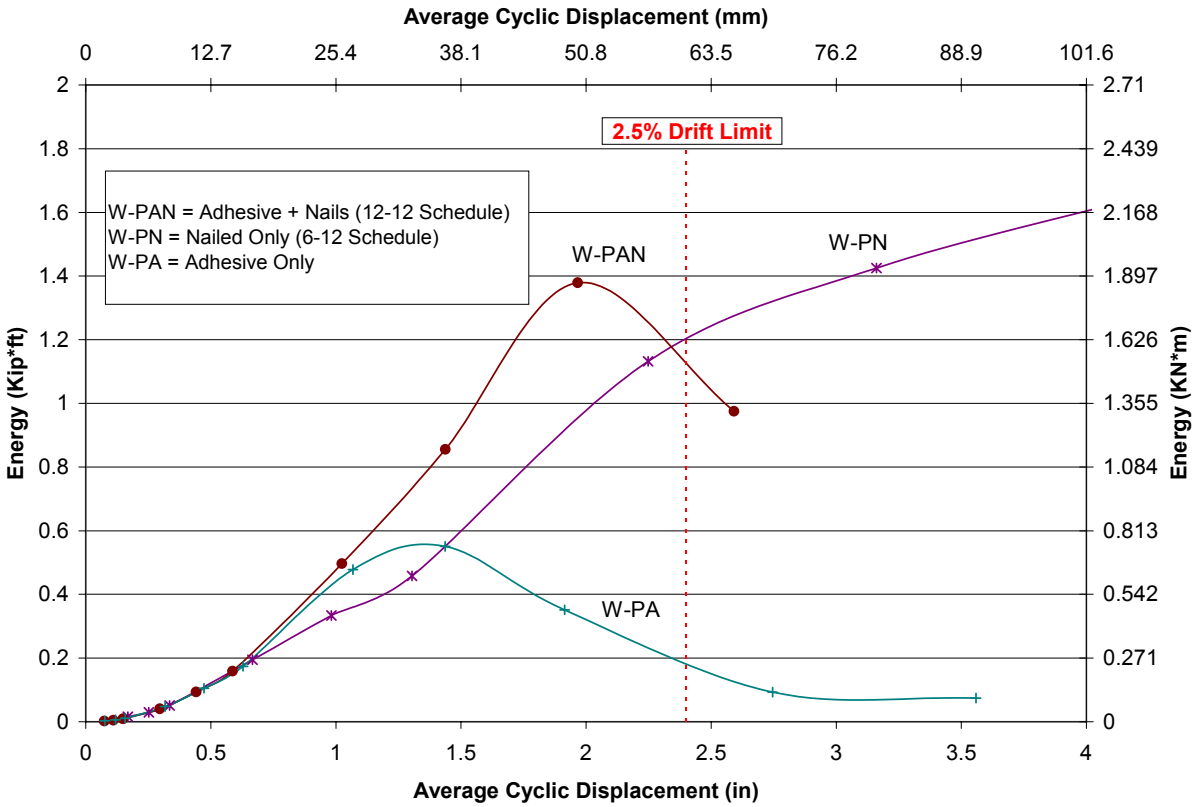

Figure 6.5: Hysteretic Energy vs. Displacement of Plywood Wall Specimens

The plywood wall specimens exhibited the same general trends as the OSB specimens. The combination system moderately outperformed the traditional wall system to approximately the drift limit, while the adhesive-only wall specimens exhibited poor performance overall. Again, this parameter indicates that the combination system would perform well under cyclic loading, though additional parameters must first be examined before a definitive conclusion can be drawn.

6.6.3 Shear Wall Toughness Summary

In summary, the toughness parameters of each wall configuration tested provided the following information:

1. The displacement capacities of adhesive-only systems and combinations systems are approximately 30% to 50% of traditional nail-only wall assemblages, respectively.
2. Combination wall systems exhibit higher damping energies than traditional wall construction up to the code-imposed drift limit.
3. Adhesive-only wall systems exhibit poor damping energy performance and are not well suited for seismic applications.
4. OSB and plywood systems of the same configuration provide approximately equal (within 10%) damping energy performance at any given displacement value.

6.7 Cyclic Tests: Earthquake Performance

The preceding discussion of shear wall strength and toughness does not provide enough information to fully describe the overall performance of each wall system under seismic loading. This section examines cyclic stiffness, equivalent viscous damping ratios, and ductility values to provide a more complete evaluation of seismic performance. In addition, a brief discussion on the derivation and use of the response modification factor "R" is provided.

6.7.1 Cyclic Stiffness

Cyclic stiffness is correlated with the initial elastic stiffness of the system prior to subsequent displacement excitations. The ratio of initial elastic stiffness values at $0.4F_{peak}$ between walls using PSA tape and traditional nailed-only walls is listed in Table 6.9. These ratios reveal that the combination wall systems were initially 6% to 20% stiffer than traditional walls. In addition, adhesive-only walls were found to be approximately 10% less stiff than traditional construction. Coefficients of variation for these stiffness values were approximately 5% as listed previously in Table 6.4.

Table 6.9: Elastic Stiffness Comparison of Adhesive to Traditional Shear Walls

Comparison Parameter	units	W-ON	W-OAN	W-OAP	W-OAS	W-PN	W-PAN	W-PA
RATIO of Elastic Stiffness at $0.4F_{peak}$	Unitless	1.000	1.215	0.890	0.931	1.000	1.062	0.903

As the wall is excited and damage occurs, the cyclic stiffness of a specimen as defined in Chapter 4 can be plotted versus the drift of the system to provide an indicator of the stiffness degradation of the wall over time. Plots of this nature are provided in Figures 6.6 and 6.7 for the wall configurations tested with OSB and plywood sheathing, respectively. This data provides a good indicator of the amount of damage that a wall assemblage will sustain during loading. The ability of a shear wall to maintain stiffness through large deformations is desirable, as systems with low stiffness values will sustain larger displacements at smaller loads and incur more damage to brittle finish materials.

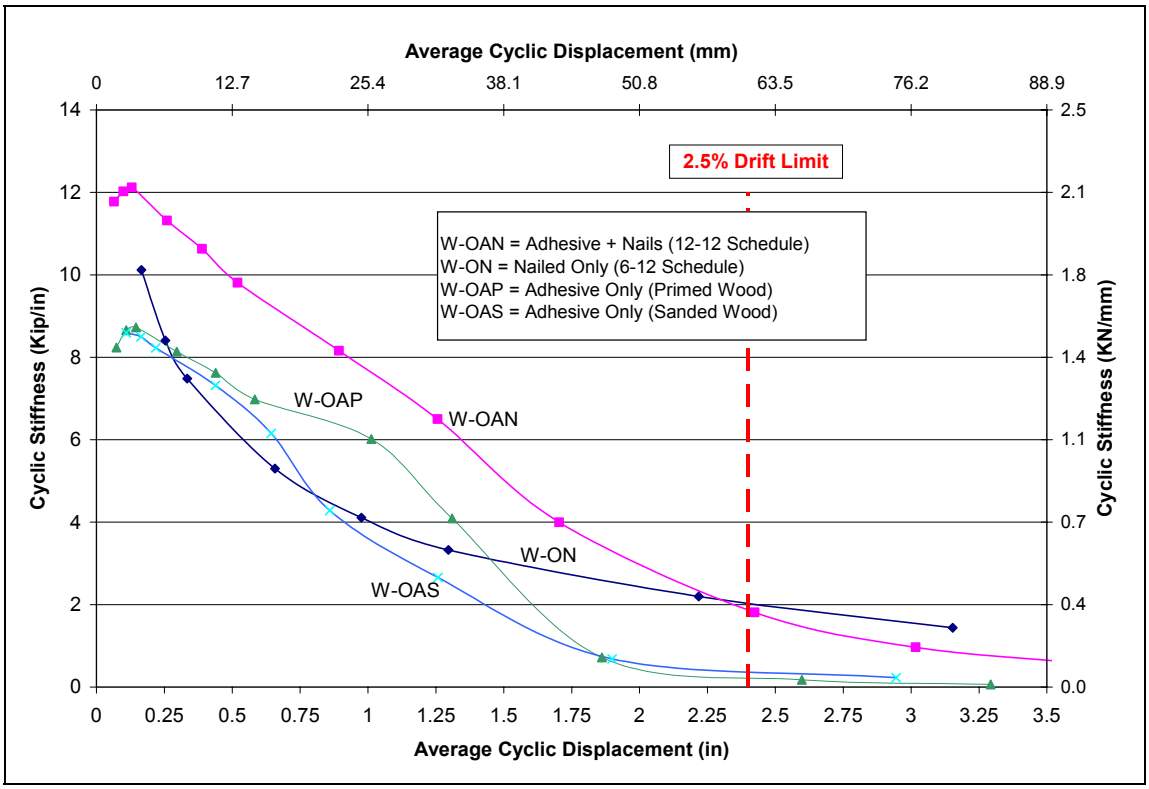

Figure 6.6: Cyclic Stiffness Degradation (OSB Walls)

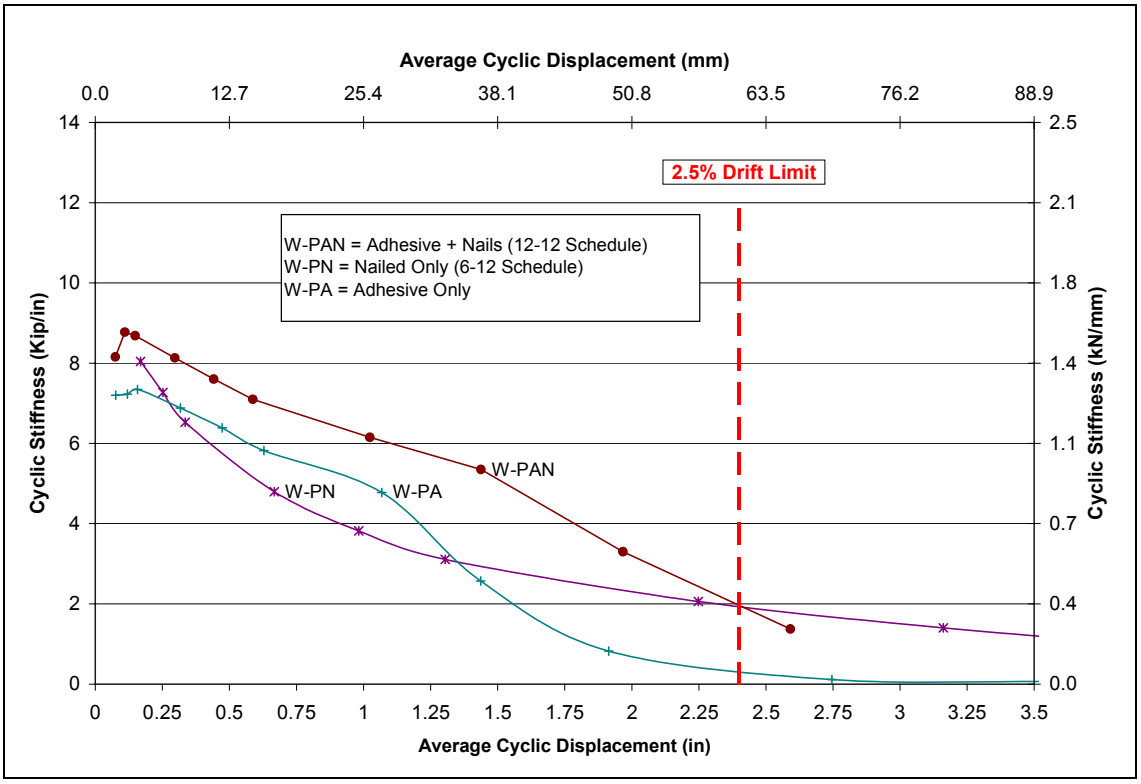

Figure 6.7: Cyclic Stiffness Degradation (Plywood Walls)

The data illustrated in Figures 6.6 and 6.7 indicates that combination shear walls utilizing both OSB and plywood sheathing maintained cyclic stiffness values averaging 60% higher than traditional wall systems through displacements up to the drift limit. The stiffness values converged to become approximately equal at this point.

The reason behind this trend is explained by the difference in failure mechanisms between the two types of wall construction. In traditional construction utilizing only mechanical fasteners, the stiffness degradation is a result of the crushing of the wood fibers surrounding the sheathing nail shank. As explained by Heine (1997), the crushing of wood fibers forms a cavity around the nail shank, thus leaving it unsupported during the initial deflection of subsequent loading cycles. These cavities are enlarged at increased wall displacements as more fibers are crushed. During the travel of the nail shank through these cavities, resistance is provided only by the bending resistance of the nail, as well as friction. As cavities grow larger, the rate at which resisted load increases is reduced and cyclic stiffness degrades.

In wall assemblies which utilize a combination of adhesive tape and mechanical fasteners, the mechanism of stiffness degradation was observed to be somewhat different. In these systems, the adhesive tape surrounded each nail and provided a constant bond along the perimeter of the sheathing panel. This bond limited the overall differential movement of the sheathing in relation to the main member. By limiting the differential movement, the adhesive tape absorbed a large amount of the energy in the system, and the wood cavities formed by the nail shanks were smaller than those in traditional construction. During this period of displacement, the stiffness degradation resulted from the stretching and fatigue of the adhesive tape as its maximum local displacement limit was approached. Additional stiffness degradation occurred due to the smaller impact of wood fiber crushing. As displacements increased, the ability of the adhesive tape to sustain loads was reduced, and more of the wall's load capacity was transferred to the mechanical fasteners, and stiffness degraded further in the traditional manner.

Cyclic stiffness degradation of the adhesive-only systems was even more pronounced due to the absence of redundancy that had been present in combination walls utilizing mechanical fasteners and tape. As the tape experienced larger movements and the adhesive's displacement limit was approached, there was a noticeable loss of stiffness, and the loading resistance of the wall assemblages quickly decreased.

6.7.2 Equivalent Viscous Damping

The equivalent viscous damping ratio (EVDR) as defined in Chapter 4 compares the hysteretic (damping) energy of the system with the strain (potential) energy of the system to provide a property that can be used to compare the damping characteristics of various wall assemblages. The EVDR is only an approximation for all displacements that occur for quasi-static cyclic tests beyond the elastic limit. This limit corresponded to displacements of approximately 19 mm (0.75 in.) for the majority of tests. As described by Heine (1997), the low loading rates used in this study should theoretically result in zero viscous damping due to the lack of inertial forces. Energy is, however, dissipated due to the compression of the wood grain, the friction within nailed sheathing to framing connections, and the deformation of the adhesive tape. Due to the highly non-linear behavior of timber structures, the EVDR is not appropriate to compare wood-framed construction with other materials (Foliente and Zacher 1994)

The EVDRs for OSB and plywood wall systems are plotted in Figures 6.8 and 6.9. Though the actual unit of these ratios is $(radian)^{-1}$, the values were multiplied by 100 to form an EVDR "percentage" for ease of discussion.

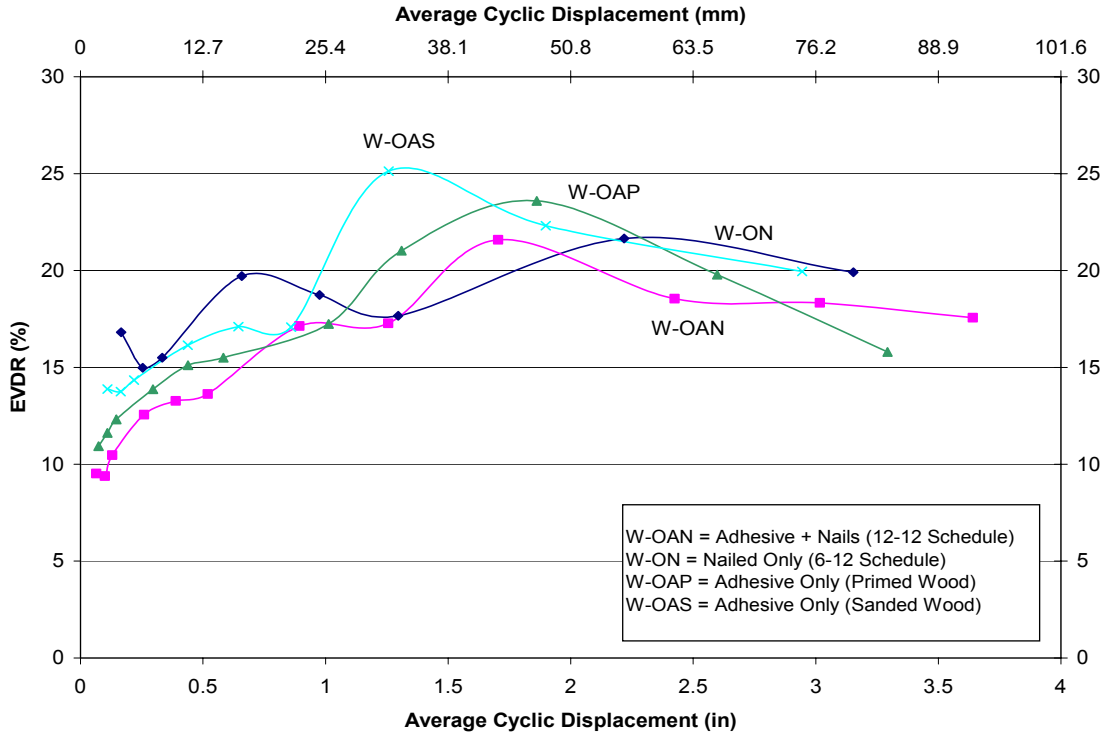

Figure 6.8: Equivalent Viscous Damping Ratios (OSB Walls)

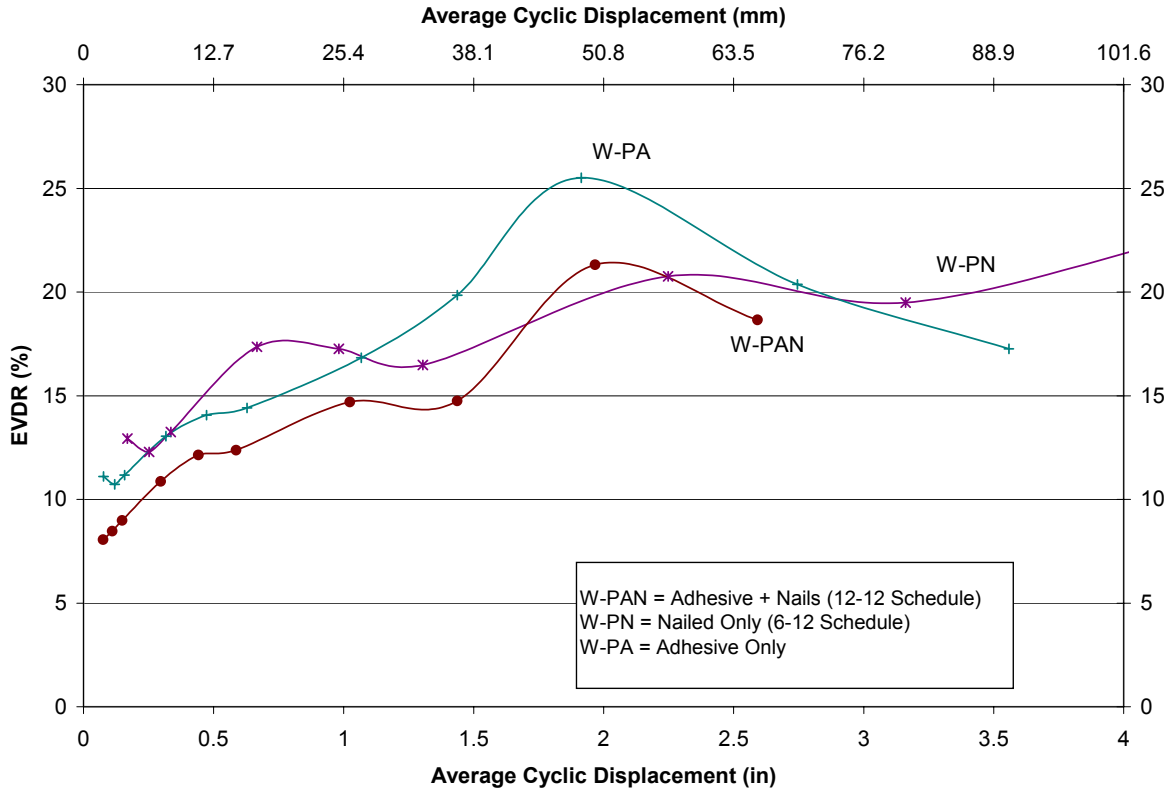

Figure 6.9: Equivalent Viscous Damping Ratios (Plywood Walls)

The data in Figures 6.8 and 6.9 shows no clear trends between EVDR ratios of different wall configurations. Damping ratios in the elastic region for which the EVDR is most accurate were approximately 10% to 15% (0.1 to 0.15 rad^{-1}). These ratios increased to 20% as stiffness degraded and hysteresis loops became elongated. Traditionally a default EVDR of 5% has been defined for light-framed timber structures (ICC 2000). This value is incorporated into the rather ambiguous system response factor (R) where the significance of this difference is often overshadowed by other assumptions. The R-factor is discussed in greater detail in Section 6.7.4.

6.7.3 Ductility

The ductility of a wall system is defined as the ultimate deformation capacity divided by the yield deformation. As described in Chapter 4, this value is extremely dependent on the nature of yielding and failure definitions used in its formulation. Ductility values for each wall system calculated using the definitions previously set forth in this study are listed in Table 6.10.

Table 6.10: Ductility Comparison

Wall Type	W-ON	W-OAN	W-OAP	W-OAS	W-PN	W-PAN	W-PA
Ductility μ	7.240	2.647	2.007	2.412	6.837	2.311	2.157
COV	11.026	9.942	8.384	16.863	10.997	15.108	4.391

The average ductility of nailed-only systems is approximately three times that of the combination systems, which is slightly larger than that of adhesive-only systems. These values do not mean that the wall assemblages utilizing adhesive tapes were brittle. Though they were definitely more brittle than nailed-only systems, each combination wall system continued to hold significant loads for cyclic displacements well beyond failure (the end of the EEEP line). An example of this ductile failure is represented by the hysteresis curve of wall W-OAN-3, illustrated in Figure 6.10.

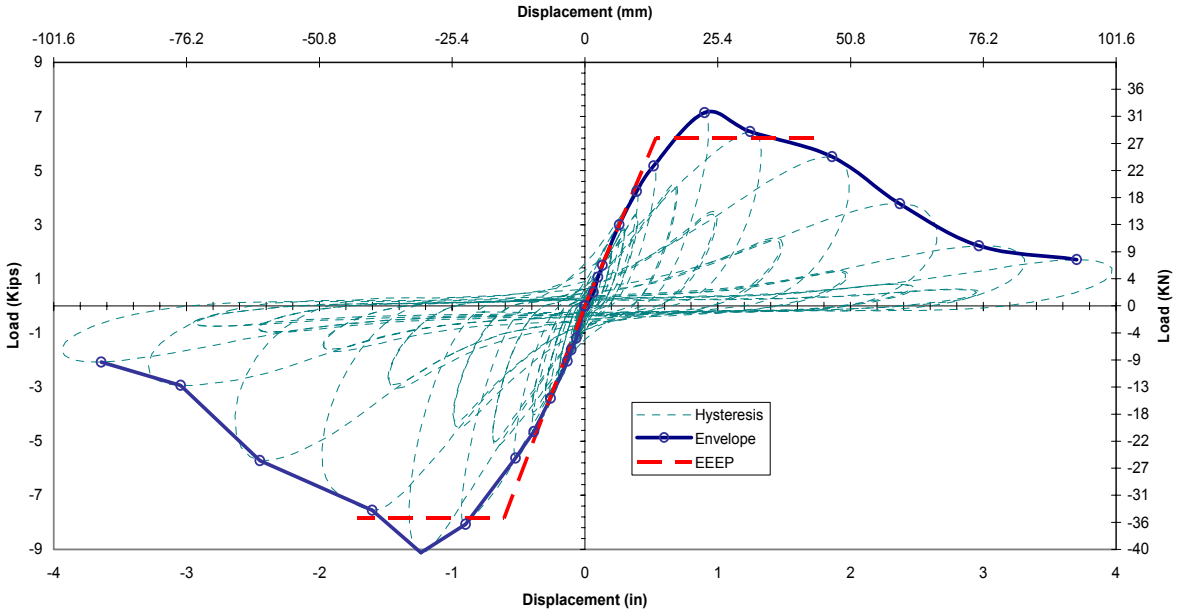

Figure 6.10: Example of Ductile Combination System Failure (W-OAN-3)

The ductile failure represented in Figure 6.10 is typical of combination wall specimens constructed with both OSB and plywood sheathing. Because loading fell below 80% F_{peak} rather quickly, the definition of failure was met, and the failure displacement was relatively low. Also, the yield displacement of combination systems was on average 65% higher than that of traditional shear walls. The combination of the large yield displacement and small failure displacements led to low ductility estimates. For the W-OAN series illustrated in Figure 6.10, if the failure criterion was lowered to $0.60F_{peak}$, the ductility value would increase by almost two-fold. This discussion is not meant to imply that the criteria and definitions used to define ductility in this study are flawed; rather, it is to show the significance that such definitions can have upon performance parameters between studies.

The ability of combination systems to sustain loads over displacements beyond failure was attributed to the redundancy of the failure mechanism as previously described. Adhesive-only walls, though displaying similar ductility ratios to combination systems, did not exhibit the same amount of reserve load capacity. It is believed that this discrepancy is due to the ability of the combination walls to transfer their load from the stronger but less ductile adhesive tape to the weaker but more ductile mechanical fastening system at higher displacements. This phenomenon was also observed in the connection test results (see Chapter 5).

6.7.4 The System Response Modification Factor "R"

The system response modification factor (R) has been one of the most controversial components in the development of seismic design provisions. This factor is utilized in current design codes to reduce the linear elastic design response spectra to the design forces at the strength level (Uang 1991). The International Building Code (ICC 2000), NEHRP (BSSC 1994), the Uniform Building Code (ICBO 1999), and the Structural Engineering Association of California Blue Book (SEAOC 1999) all include some form of the R-factor. Despite its widespread use, the development of the system response factor remains ambiguous and largely empirical.

6.7.4.1 Current use of the R-factor

An example of the confusion surrounding the R-factor is presented in the Appendix of the SEAOC Blue Book which states in part (SEAOC 1999):

> "While the present process of evaluating the factors [R] is largely empirical and judgmental, these factors have been provided such that the engineer can better understand the properties of inelastic response…These present provisions do not allow the calculation of the total system strength factor R_o and the maximum demand force factor Ω_o, In the future it is anticipated that this could be done…It is not currently possible to prescribe the appropriate modeling procedures for the building system [to analytically determine R]."

The code, in essence, directs the designer to use the R-factors listed in the provisions without providing a true explanation of their nature or a method for generating such values for alternative construction methods.

For the purpose of discussion, the International Building Code's simplified base shear force will be examined. Equation 16-49 in the 2000 edition of the IBC is as follows (ICC):

$$V = \frac{1.2S_{ds}}{R}W \tag{6.1}$$

where: S_{ds} = ground acceleration
R = response modification factor
W = total dead weight of system
V = base shear

The process of calculating base shears (V) involves the use of hazard maps to determine ground acceleration factors as well as soil conditions. An example of these calculations is presented at the end of this chapter in Section 6.11. More in-depth analysis involves the calculation of the fundamental period of the building being designed to further refine acceleration values for long and short-term excitations. It seems somewhat farcical that these meticulously determined ground accelerations are then divided by an R-factor that was initially agreed upon by committee in the 1950s (ATC 1995).

6.7.4.2 Research on Analytical Formulation of R

Several papers have been published in the last 15 years addressing the concern over the ability to derive an R-factor analytically. A comprehensive review of the history of the response

modification factor including a proposal for the creation of an analytical derivation process was published by the Applied Technology Council in the ATC 19 report (ATC 1995). This paper suggested that the response modification factor be broken into three components as shown in the following equation:

$$R = R_S R_\mu R_R \tag{6.2}$$

where: R = System Response Modification Factor

R_S = Over-strength Factor

R_μ = Period-Dependant Ductility Factor

R_R = Redundancy Factor

Additionally, the possible need for a fourth, viscous damping factor (R_ξ) was considered. These factors were discussed as elaborated upon below, but their actual calculation was not clearly defined.

The over-strength factor (R_S) was expressed as a ratio of the actual base shear of a structure, calculated through nonlinear static analysis of the building displaced to the limiting state of response, to the design base shear of the structure. In Report 158, the APA – Engineered Wood Association conducted a series of cyclic shear wall tests and took the ultimate strength divided by the yielding strength of the system as the over-strength factor (Rose 1998).

The ductility factor (R_μ) has been described with multiple conflicting equations by Newmark and Hall (1982), Krawinkler and Nassar (1992), and Miranda and Bertero (1994). APA Report 158 utilized the Newmark and Hall method, which is the most commonly accepted equation, and was derived as follows:

For frequencies between 2Hz and 8Hz: $R_\mu = (2\mu - 1)^{0.5}$ (6.3)

For frequencies less than 1 Hz : $R_\mu = \mu$ (6.4)

Where μ represents the ductility ratio.

In this context, the ductility ratio is not the maximum displacement ductility as defined in this thesis, but rather the difference in displacement at peak loading and yield loading.

The redundancy factor (R_R) is a measure of the ability of an entire structural system to provide multiple failure mechanisms. Though ATC-19 (1995) provides some guidance for redundancy factors, this value is usually taken as 1.0 to represent a structure that has been designed according to sound engineering principles to provide alternate load-paths upon component failure.

The fourth factor considered, but eventually not included in Equation 6.2, is the viscous damping factor R_ξ. Some previous researchers have discussed the need for this damping coefficient and found that its effects might already be generally included in the ductility reduction factor R_μ (Uang 1991). Wu and Hanson (1989) proposed damping factors relating to the viscous damping properties of the system as listed below in Table 6.11. Note that their research indicated that these factors should not be used to "reduce the force demands of the system unless the forces developed in the viscous elements are explicitly accounted for in the design process" (ATC 1995).

Table 6.11: Viscous Damping Factors

Viscous Damping (EVDR)	R_ξ
5	1.00
10	1.19
15	1.39
20	1.56

Current earthquake design methodologies use base EVDR values of 5%. While this might be true for many building structures, light-frame wood housing appears to have an EVDR of 10-15% in the elastic range and up to 20% in the inelastic range, as discussed in Section 6.7.2 of this thesis. The final draft of CUREE's *Recommendations for Earthquake Resistance in the Design and Construction of Woodframe Buildings* contains research that also determines the viscous damping ratio to be approximately 15% (Cobeen et al., 2002).

6.7.4.3 Conclusions and Recommendations for PSA Tape Walls

Though much thought and discussion on an analytical method for calculating response modification factors have been recently circulated, there are still no guidelines in place that are actually accepted and used in practice. The current IBC code provisions for R-factors are still

based on earlier codes as well as engineering judgment dispensed by a committee that is equally influenced by the industries representing various building materials (Dolan 2003).

As a basis for discussion on R-factors for walls utilizing PSA tapes, the method as presented by the Engineered Wood Association in Report 158 (Rose 1998) on the data generated in this project was carried out as displayed in Table 6.12.

Table 6.12: R-factor Calculations

Test Type	F_y (lb)	Δy (in)	F_{peak} (lb)	Δ_{peak} (in)	$R_S = F_{peak} / Fy$	Rμ short	Rμ long	Rtotal[1]
W-ON	4.336	0.483	4.881	2.218	1.13	4.594	2.86	4.20
W-OAN	7.199	0.658	8.292	1.199	1.15	1.823	1.63	1.99
W-OAP	5.373	0.670	6.299	1.144	1.17	1.708	1.55	1.91
W-OAS	3.857	0.472	4.389	0.800	1.14	1.694	1.55	1.84
W-PN	4.141	0.574	4.633	2.525	1.12	4.399	2.79	4.02
W-PAN	6.783	0.890	7.779	1.512	1.15	1.700	1.55	1.86
W-PA	4.373	0.628	5.113	1.068	1.17	1.700	1.55	1.90

Note 1: R total represents the average of the ductility factor for short and long periods multiplied by the over-strength factor.

It would appear that response modification factors of four should be used for nail-only walls, and two should be used for walls with adhesive tapes. This method of calculation is, however, fundamentally flawed. First, over-strength and ductility values depend highly on the definition of yielding being used. The APA used a Sequential Phased Displacement protocol initially developed for masonry research (Gatto and Uang 2002) and a bilinear curve approximation that appears to produce lower yield force estimates than the CUREE and EEEP approach used in this thesis. Obviously, lower yielding loads would increase ductility and over-strength ratios. Second, both testing methods completely ignore the effect of finish materials present in most houses which can be significant (Uang 1991). Third, the effect of damping properties is also essentially ignored. The APA distributed a commentary on many of these issues to supplement Report 158 (APA 1998a).

Furthermore, the data in Table 6.12 suggests that similar R-values should be used for combination walls and adhesive-only walls. This similarity should certainly not be the case. Combination walls have been proven to have much better hysteretic damping properties and hold significantly larger loads well past their defined failure displacements than adhesive-only walls. Neither of these conclusions are represented by this analytical approach.

In conclusion, though much work has been done on the development of the R-factor, its calculation for use in current building standards still falls to engineering judgment. The IBC 2000 currently lists an R-factor of 6.5 for building frame systems utilizing light-frame walls with wood structural shear panels (Table 1617.6). In comparing the combination systems to traditional nailed construction, many factors need to be taken into account. First, displacement capacities of the combination systems are only half that of traditional walls (which translates almost directly to the 2:1 ratio of R-factors produced by the analytical procedure summarized in Table 6.11). Combination systems, however, do not exhibit a brittle failure, and they do demonstrate redundancy in their mechanical fastening system which leads to additional post-failure load-capacity as shown in Figure 6.10. Additionally combination wall systems provide slightly increased damping performance and maintain higher cyclic stiffness values up to the code drift limitations. In concession to the lower ductility and displacement capacity demands, but with consideration of the other cyclic performance parameters discussed, it is recommended that combination acrylic foam adhesive and mechanical fastener wall systems be assigned a system response modification factor of **R=5.0-5.5**. This factor is in the range of specially reinforced masonry shear walls.

6.7.4.4 Ramifications of Proposed R-factor

Ramifications of the proposed reduction of the system response modification factor, R, from 6.5 to 5.5 for the use of acrylic foam tapes can be examined through its use in Equation 6.1 (IBC simplified base shear Equation 16-49). When using the combined system, neither the weight of the wall assemblage nor the site acceleration factor will change significantly. Therefore the only change will come from the R-factor. A reduction in R from 6.5 to 5.5 will result in a penalty of approximately 18% higher required base shear resistance (V). However, strength gained from using the adhesive tape is conservatively estimated as 2 kN/m (135 lb/ft). This strength gain was calculated using an extremely sparse nail schedule, and it is most likely conservative for denser nail schedules. Nevertheless, the gain in strength more than offsets the base shear penalty in all but the strongest wall configurations provided in the IBC (ICC 2000).

6.7.5 Earthquake Performance Summary

In summary, the earthquake performance of each wall assembly configuration tested provided the following information:

1. Combination wall systems provided initial elastic stiffness ratios that were 6% to 20% higher than traditional walls. Cyclic stiffnesses were maintained at values averaging approximately 60% higher than traditional wall systems up to code-imposed displacement limits. Higher stiffness values allow the combination wall system to deflect less at given loadings thus providing better protection for finish materials.
2. Adhesive-only systems provided initial elastic stiffness ratios that are 10% lower than those of traditional walls. Cyclic stiffness degradation occurred at lower displacements, and overall performance was poor when compared with other systems. Surface treatments applied to the OSB walls appeared to have little effect on this variable.
3. Equivalent Viscous Damping Ratios for all systems tested ranged from 10% to 15% initially, to over 20% during highly inelastic behavior. Current seismic codes use 5% damping, but these findings coincide with recent light-frame research conducted by the CUREE-Caltech Woodframe Project (Cobeen et al., 2002).
4. Ultimate ductility values for combination wall systems were calculated to be three times lower than those of traditional wall systems. Combination wall systems were shown to exhibit ductile failures with significant load-bearing capacity provided after their defined failure.
5. A system response modification factor of R=5-5.5 was proposed for combination wall systems. This factor was based on a review of the uses of R, proposed analytical procedures for its calculation, and sound engineering judgment.
6. Due to the poor cyclic stiffness and ductility performance of adhesive-only wall systems in conjunction with the low damping energies previously calculated, they are not recommended for seismic use.

6.8 Cyclic Tests: Overall Wall Response

This section provides information on the overall response of cyclically tested wall assemblages. A discussion on displacement components as well as typical failure modes and other general test observations are provided. The reader is directed to the Appendix for specific discussions as well as photographs and figures detailing the performance of each individual wall specimen.

6.8.1 Deformation Components

As defined in Chapter 4, the three main deformation components contributing to the overall deflection of the wall specimens are rigid body rotation (RBR), shear deformation (SD), and connection slip plus bending. A numeric listing of the deformation components was provided in Table 6.4. For ease of comparison, an additional component breakdown is presented graphically in Figure 6.11 and in percentage comparison form in Table 6.13. These components were calculated at deflections corresponding to the peak load resisted by the wall.

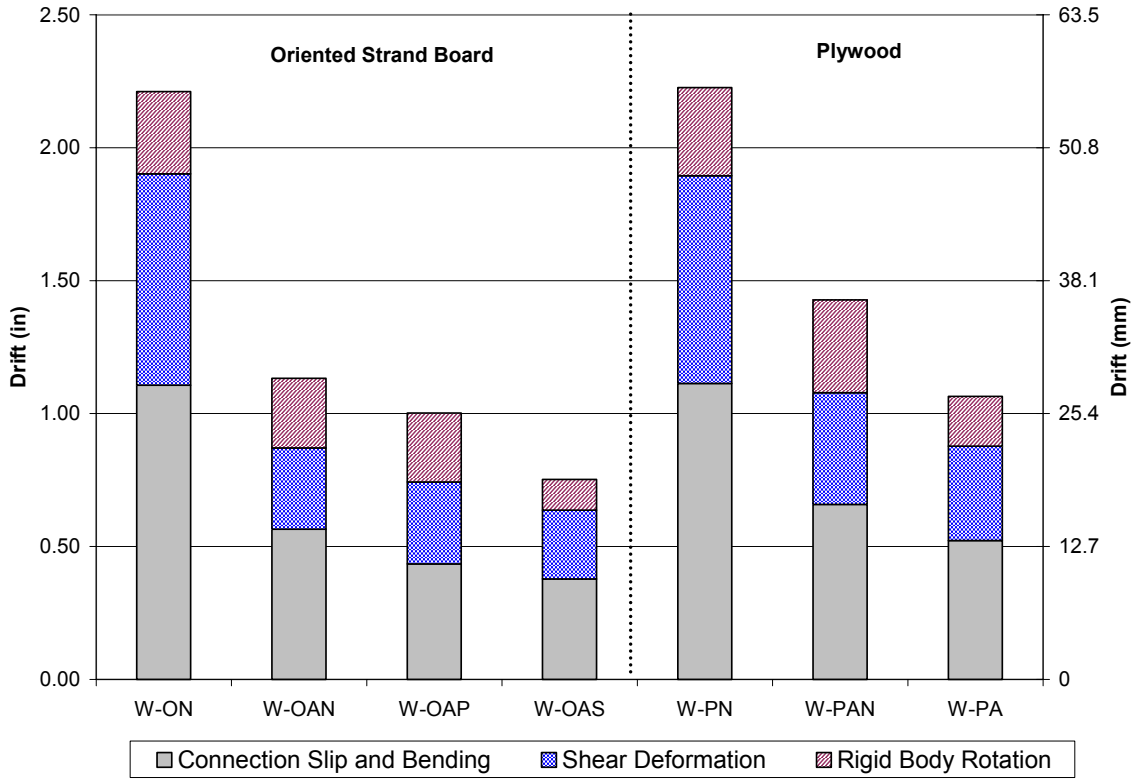

Figure 6.11: Summary of Deflection Components

Table 6.13: Displacement Component Percentage Comparison

Parameter (% Displacement @ Δpeak)	Wall Assembly Configurations						
	W-ON	W-OAN	W-OAP	W-OAS	W-PN	W-PAN	W-PA
Shear Deformation	36	27	31	34	35	29	33
Rigid Body Rotation	14	23	26	15	15	24	18
Connection Slip and Bending	50	50	43	50	50	46	49

Average Parameter Comparisons	OSB Avg	Ply Avg	Nail - Only Average	Combination Average	Adhesive Average
Shear Deformation	32	33	36	28	33
Rigid Body Rotation	20	19	14	24	20
Connection Slip and Bending	48	48	50	48	48

Connection slip and bending of the chords in the wall specimen was the controlling deformation component for all tests primarily due to the large displacements observed between sheathing and framing members and the use of hold-down devices on the end-studs. These hold-down devices serve to prevent the overturning (rigid body rotation) motion of the walls. It should be noted that many previous researches such as Gatto and Uang (2001) have found that chord bending produces negligible contributions to overall wall displacements and therefore the connection slip component is most likely controlling. As shown by Toothman (2003) and others, the appropriate use of hold-down devices can increase the strength of a wall assembly over similarly configured non-engineered specimens by up to three times. When hold-down devices are not used, the bending component of deflection approaches zero, and the rigid body rotation component controls, as shown by Bredel (2003) using the same testing protocol and apparatus as this study. At extremely large displacements (post-failure), there were many instances in which the interior studs pulled completely away from the sill plate, while the end-studs remained intact due to the hold-down devices. This situation is illustrated in Figure 6.12.

Figure 6.12: Effectiveness of Hold-Down Devices on End Studs

Data in Table 6.13 also appears to illustrate a trend towards a higher rigid body component and lower shear deformation component in combination wall assemblies when compared to traditional wall construction. This trend is likely caused by the higher cyclic stiffness provided by the continuous adhesive bond. High stiffness values forced the wall to deform less and rotate slightly more. Adhesive-only wall systems, which had cyclic stiffness values similar to the nailed-only case, also had deformation components similar to traditional walls.

6.8.2 Failure Modes

OSB and plywood-sheathed, nail-only wall assemblies failed in a similar manner. As displacements increased, the mechanical fasteners formed plastic hinges at the interface between sheathing and main members. The nails then pulled out of the sheathing along the sole plate and end studs of the wall as shown in Figure 6.13 (a). Increased displacements resulted in the unzipping of the center nailing line from the sheathing panels. Also, the interior studs pulled partially, and sometimes fully, away from the sole plate, while the hold-downs prevented pull-out of the end-studs as shown in Figure 6.13 (b).

(a)

(b)

Figure 6.13: Nail-Only Failures

(a) Sheathing Nail Pull-Out

(b) Interior Stud Pull-Out (No Pull-Out at Hold-Down)

Adhesive-only walls exhibited sharply different failure modes than the traditional wall specimens. During the initial cycles of each test, the adhesive was observed to "roll" back and forth between the main members and the sheathing panels. As deflections increased, the bond at the sole-plate began to weaken. Loss of load capacity was then observed to occur rather suddenly when the centerline bond failed, and the sheathing panels fell away from the framing as illustrated in Figure 6.14. This failure appeared to initiate due to the contact between sheathing panels along the center stud that began when the movements of the sheathing panels exceeded the small distance left between them at construction. There was little to no pull-out of studs at the top or bottom plates as the adhesive bond holding the sheathing panels failed before the displacement of the system became large enough to induce such movements.

Figure 6.14: Centerline Failure of Adhesive-Only Bond

There was a noticeable difference between adhesive-only OSB and plywood failures. This difference appeared to be due to the increased thickness and out-of-plane bending strength of the OSB panels. As the plywood wall assemblies neared failure, the sheathing panels buckled slightly out-of-plane between the perimeter bonds, and in some cases, loud cracking noises were heard due to the localized failure of the plywood at the point of maximum bending stress. OSB panels did not exhibit this behavior. However, similar results between the two configurations suggested that its effect on wall performance was minimal.

Though failure of the adhesive-only walls was more brittle than that of other wall configurations, strength values did approach that of the nailed-only systems, and good adhesive bonds were formed between the sheathing and the main members. A typical post-failure

bridging of the adhesive tape between the two surfaces is illustrated in Figure 6.15. Another important point is that in all of the tests, there was never a cohesive failure within the tape itself. All failures were of adhesive bonds and appeared to occur randomly between the adhesive tape and the sheathing or main framing members.

Figure 6.15: Post-Failure Bridging of Adhesive Tape Between Framing and Sheathing

Wall specimens constructed with both adhesive tape and mechanical fasteners predictably failed due to a combination of the factors observed for the adhesive-only and nailed-only specimens. Failure typically initiated along the specimen centerline due to weakening of the adhesive bond. The presence of mechanical fasteners served to maintain the pressure between sheathing and framing members and delayed the bond failure beyond the limits of adhesive-only walls. When the bond did begin to fail, the nails often pulled out of the cavities that had been formed in the framing members with little observed deformation as illustrated in Figure 6.16.

Figure 6.16: Typical Minimal Deformation of Nail in Combination System (Left) Vs. Nail-Only (Right)

The greater durability of the combination wall systems as opposed to the adhesive-only systems allowed them to maintain load capacity through larger deformations, and therefore pull-out of the interior and end studs was observed along the top plate. In many instances the top plate pulled completely away from the interior studs. Failures of this nature were observed visually as well as through the recorded data as illustrated in Figure 6.17. This Figure compares observed failure modes versus the recorded diagonal string potentiometer data. Specimens that maintained proper connections exhibited consistent diagonal displacement and uplift readings. Specimens that had large stud separations exhibited diagonal displacement readings that drifted upwards with each cycle before becoming wildly erratic with complete separation.

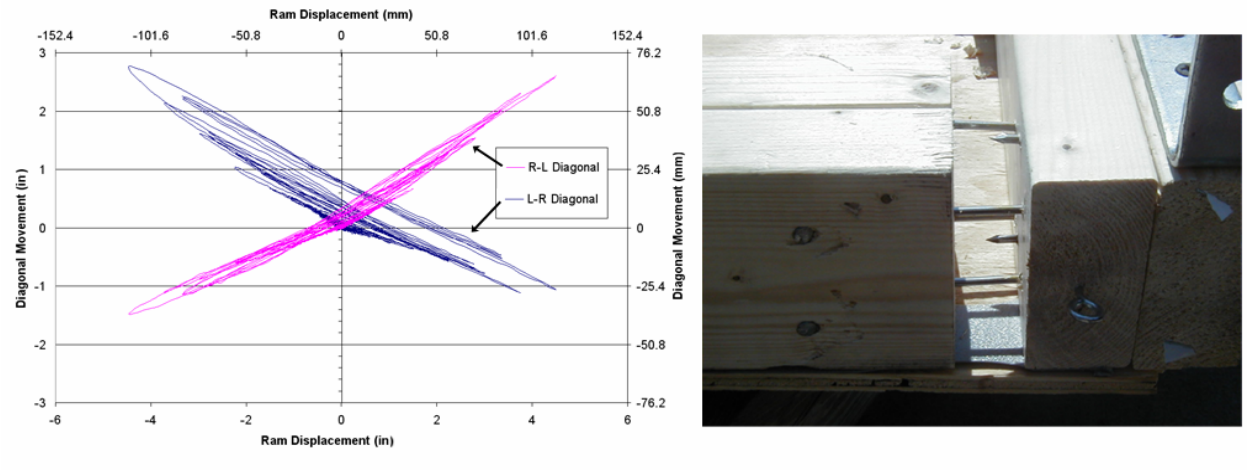

(a)

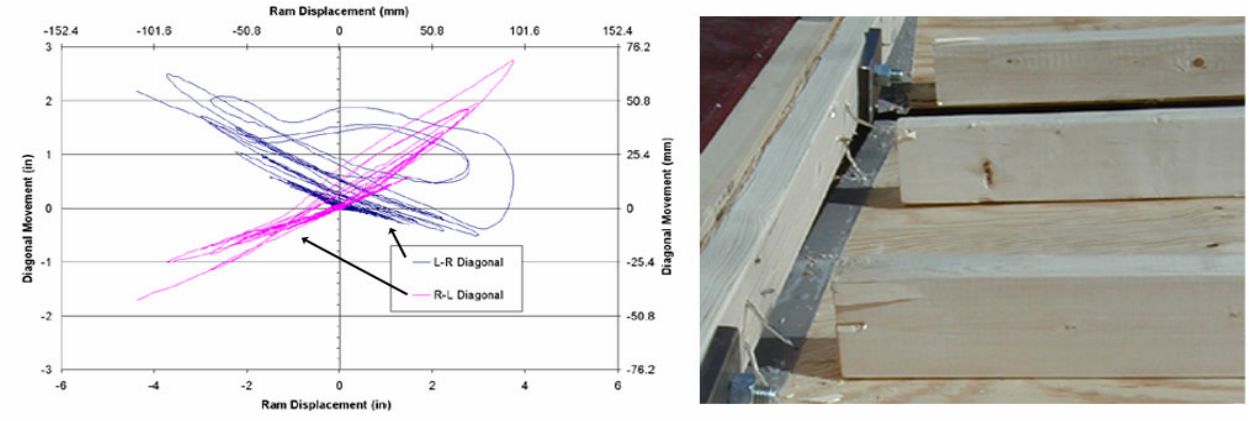

(b)

Figure 6.17: Observed and Recorded Diagonal Displacement Data

(a) Diagonal Displacement Graph Moves Upwards Slightly Due to Small Pull-Out

(b) Diagonal Displacement Graph Moves Erratically Due to Complete Pull-Out of Studs

6.8.3 Commentary on Moisture and Temperature Effects

It addition to the performance parameters discussed in the previous sections, several other variables were monitored throughout the tests. These variables included moisture content, ambient temperature, and temperature at the bond line. This section describes the effects of these variables as well as the consequences involving an error that occurred during testing of one of the wall configurations.

Average moisture contents of the main framing members during construction ranged between 10% and 15%. After being held in a conditioned environment for 2 weeks, average moisture contents were consistently 9%. Due to the small range of moisture contents tested, there was little opportunity for this variable to affect the performance of the wall specimens, and no noticeable effect was observed. This finding is consistent with the connection results presented in Chapter 5. Prior research on acrylic foam tapes bonded to aluminum coupons has proven their superior stability in wet conditions over epoxy bonding systems (Brockmann and Hüther 1996), but this finding should be confirmed for wood substrates with additional testing.

Walls were constructed and stored in an indoor laboratory under temperature-controlled conditions. However, they were mounted in an outdoor apparatus for testing. Ambient temperatures during wall testing ranged from 17˚C (62˚F) to 38˚C (100˚F) due to the position of the testing platform outside and the range of temperatures between early morning and afternoon. A thermocouple attached to the wall near the bond-line prior to the wall's removal from the laboratory showed increases in temperature of up to 7˚C (13˚F) during testing. This increase was believed to be due to the ambient temperatures being considerably higher than lab temperatures and not due to energy dissipation of the adhesive tape. No observable effect on the performance of the wall systems occurred due to the change in temperatures. It is possible that extremely low or high temperatures would cause the adhesive tape to react in a more brittle or ductile manner, respectively. Placement of the adhesive tape between sheathing and main framing members would, however, shield it from direct sunlight, and the effects of any cladding insulation placed on the outside of the walls would provide additional thermal protection. It is, therefore, doubtful that the temperatures would far exceed those present during wall testing. No data was recorded at extremely low temperatures, and therefore their effect remains unknown until further testing can be completed.

6.8.4 Commentary on CUREE Testing Protocol

Though not originally a planned variable, an error in testing lead to an interesting observation on the displacement values used to calibrate the CUREE testing protocol. The target cyclic displacement for wall configuration W-OAS was calculated by monotonic test ratios to be approximately 41 mm (1.6 in.). The displacement actually used during the first two tests was inadvertently entered as 69 mm (2.7 in.) which was the monotonic testing value prior to application of the 60% cyclic reduction factor. This error was caught and fixed for the third and final W-OAS specimen. The average backbone curves for the three tests are displayed in Figure 6.18.

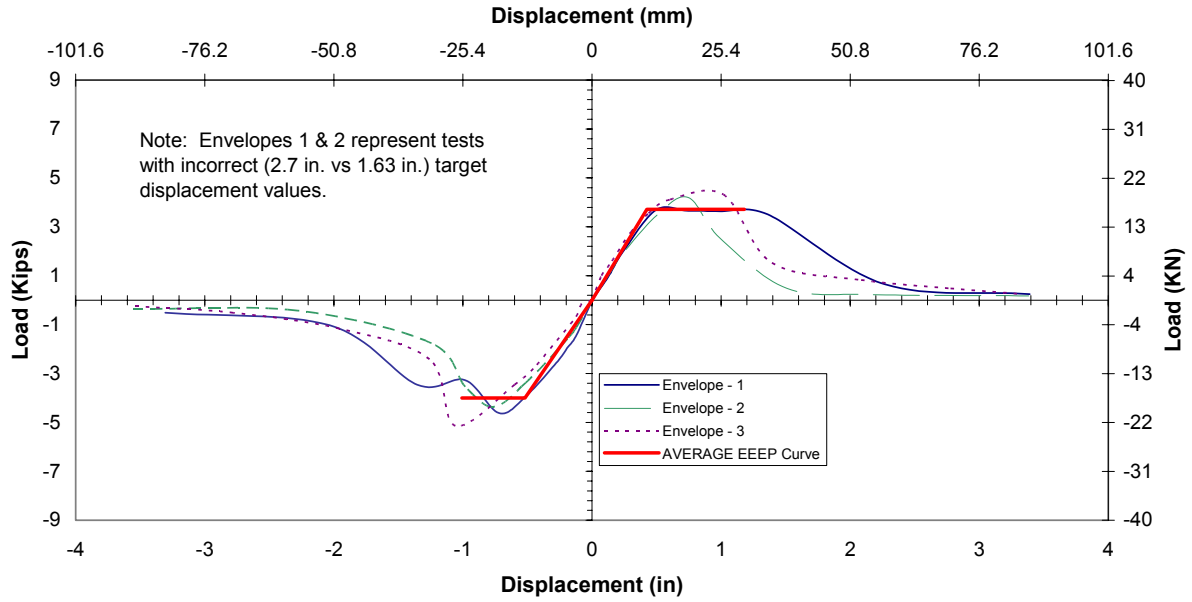

Figure 6.18: Average Backbone Curves of W-OAS Test Series

One might expect that the two test specimens subjected to increased deflections would fail sooner or at lower loads. This conjecture was not the case as can be observed in Figure 6.18. It appears that the difference in target displacements had no effect on the performance of the wall. It is believed that this lack of effect was due to the failure modes of the adhesive-only walls. As described in the previous section, adhesive-only walls typically failed when the adhesive bond reached its maximum deflection limit between sheathing and framing at the centerline. The CUREE protocol does not induce a large amount of fatigue on the system (Gatto and Uang 2002), and therefore each wall still failed at approximately the same displacement

value. In summary, the failure displacement was similar (within 10%) for each specimen; it was just attained more quickly for the walls with the incorrectly elevated displacement values.

Another note on the CUREE protocol is that, in general, the adhesive-only and nail-only walls did fail at values near the target peak displacements. None of the combination walls, however, failed until the primary cycle immediately following the target deflection, as displayed in Table 6.14. Examining the CUREE time-history listed in Table 3.10 reveals that a large jump in amplitude of 0.5Δ occurs following the target deflection 1.0Δ. It is notable that failure of all six combination adhesive and mechanical fastener walls occurred at this instance. CUREE Publication No. W-02 includes comments noting that this large step increase might result in smaller capacity and that "it is permissible to reduce the step size of the primary cycles with amplitude > 0.4Δ" (Krawinkler et al, 2001). The large increase in amplitude was initially specified to simulate the response of an actual earthquake as determined by research for the CUREE publication. The function of Δ as intended by the protocol is to serve as a benchmark for acceptability criteria. Increments of Δ beyond the target displacement provide additional information for the benefit of the researcher and should be modified according to the objective of the project. For shear wall specimens that have the possibility of failing in a brittle manner, such as the adhesive-only configurations in this study, it is recommended that post-Δ step-sizes of 30% be used for future CUREE-based testing. The reduced step-size will provide a smoother backbone curve and prevent failures from being prematurely forced by large displacement increases. Currently the CUREE protocol is being prepared for inclusion in the American Society for Testing and Materials standards as ASTM E 2126. Committee discussion regarding the new standard includes a provision for the post-Δ step-size increase to be presented as $(1+x\Delta)$ where x should be $\leq 50\%$. Further discussion of the ASTM E 2126 standard includes the recommendation of x=0.3 (30%) as a lower bound to be placed in the commentary (Salenikovich 2003). This research supports the inclusion of these provisions in the final standard that will be published by 2005.

Table 6.14: Comparison of Target and Actual Failure Displacements

Specimen	W-ON	W-OAN	W-OAP	W-OAS	W-PN	W-PAN	W-PA
1							
Target Δ	3.6	1.38	1.49	2.7	3.6	1.51	1.62
Actual $\Delta_{failure}$	3.063	1.722	1.324	1.219	4.165	1.654	1.425
Ratio Actual/Target	0.85	1.25	0.89	0.45	1.16	1.10	0.88
2							
Target Δ	3.6	1.38	1.49	2.7	3.6	1.51	1.62
Actual $\Delta_{failure}$	3.162	1.763	1.348	0.929	4.012	2.211	1.211
Ratio Actual/Target	0.88	1.28	0.90	0.34	1.11	1.46	0.75
3							
Target Δ	3.6	1.38	1.49	1.55	3.6	1.51	1.62
Actual $\Delta_{failure}$	4.182	1.663	1.331	1.134	3.874	2.204	1.411
Ratio Actual/Target	1.16	1.21	0.89	0.73	1.08	1.46	0.87
AVERAGE							
Ratio Actual/Target	0.96	1.24	0.90	0.51	1.12	1.34	0.83

6.8.5 Loading Rate Effects

Loading rates used to test viscoelastic materials such as the acrylic foam tape investigated in this study can have a significant effect on their performance. Higher frequency shaking and impact loading can produce noticeably higher load capacities and stiffnesses in specimens constructed with viscoelastic adhesives. This effect was directly observed in the differences between the monotonically and cyclically tested W-OAN shear wall series. The CUREE cyclic protocol produces peak loads in traditional shear walls similar to, or slightly greater than, monotonic testing (Gatto and Uang 2002). The average load capacity of the monotonic W-OAN walls was 22.9 kN (5130 lb), and the same cyclic wall configuration produced an average peak load of 36.9 kN (8292 lb). It is believed that the 60% strength gain of the CUREE test is the direct result of the increased strain rates induced in the cyclically loaded walls. Tests on a similar 3M VHB product adhered to an aluminum substrate have shown that an increase in strain rate of ten fold can enhance strength by 60-80%, as well as significantly raise stiffness values (Brown 1999). Strength gains predicted by monotonic shear wall tests for acrylic foam tape adhesives are to be viewed as conservative. One valid concern that warrants further study is that high frequency earthquakes could increase the strength and stiffness of wall specimens with acrylic foam adhesive to levels resulting in brittle failure.

6.9 Feasibility of Acrylic Foam PSA Tape Wall Manufacturing

In order for acrylic PSA foam tapes to be used in construction, a feasible and economically viable manufacturing process must be found. This section provides a brief overview of both of a possible manufacturing method and cost information and comparisons.

6.9.1 Manufacturing Methods

The proper construction of adhesive tape-based shear walls requires the use of a fairly high activation pressure to "wet-out" the tape and form a strong bond. This fact precludes the field construction of such wall assemblies due to the lack of equipment and the possibility for attaching the wall panels in an incorrect orientation. Unlike nails, the adhesive tape could not easily be removed if sheathing panels shifted during construction. The walls must, therefore, be constructed as pre-fabricated modular units. In the laboratory environment, pressure was applied using a constrained air-hose system. This procedure is too cumbersome and slow for manufacturing. The best possibility for manufacturing lays with the use of industrial truss roller systems such as that shown in Figure 6.19.

Figure 6.19: MiTek® RoofGlider Truss Roller System (Used With Permission MiTek® 2003)

Truss rollers consist of a large metal barrel that is driven over a flat layout bed containing wood members in a truss configuration. This barrel imbeds metal connectors that attach the wood pieces together to form a modular roof truss. This equipment is available from and is in use by numerous manufacturers and companies. Personal correspondence with one manufacturer

verified the possibility of their use for applying pressure to adhesive shear wall systems (MiTek 2003). MiTek's® RoofGlider system utilizes a 4.3 m (14 ft) roller with a clearance adjustable up to 152 mm (6 in.) and a table length of 16.5 m (54 ft), thus easily accommodating an entire shear wall length. The roller is 610 mm (24 in.) in diameter and weighs approximately 80 kN (18,000 lb). Conservatively assuming a 25.4 mm (1 in.) bearing length and a 2.4 m (8 ft) wall height, this system provides 1300 kPa (190 psi) of pressure. Other manufacturers supply equipment with similar specifications. One drawback the duration that pressure is applied. This study concluded that 15 seconds or longer was sufficient to "wet-out" the bond. Fifteen seconds was chosen because it was the lowest time tested. Truss rolling equipment moves much more quickly, at rates of around 30 m/min (100 ft/min). Further research would need to be performed to test the effect of such high pressurization speeds on adhesive bonding.

6.9.2 Economic Viability

In order for a product to succeed in the marketplace, it must be economically viable. A rough breakdown of raw material costs of a 2.4 m x 2.4 m (8 ft x 8 ft) shear wall is listed in Table 6.15. These costs can vary significantly, depending on the location and raw material price of timber products. Cost estimates were developed based on typical 2003 prices at retail lumber yards in the Virginia area. The addition of approximately 12.2 m (40 ft) of acrylic foam tape is more difficult to price accurately. Currently, a 33 m (36 yd) roll of 38 mm (1.5 in.) wide 3M VHB 4941 product has a suggested consumer price of $108.50 (3M Customer Response Center, 2003). Based upon this price, the raw material cost of adhesive tape for a single shear wall would be approximately $40.00 – almost doubling the price of the wall. Pricing would most likely be reduced if the bulk manufacturing of wall panels began. In the pre-manufacturing process, any additional labor costs for wall construction would be small.

Table 6.15: Rough Material Cost for 2.4 m x 2.4 m (8 ft x 8 ft) Shear Wall

Material	Quantity	Unit Price	Total Price
No. 2 8ft Stud	12	$2.20	$26.40
3/8 in Plywood Sheathing	2	$9.75	$19.50
Hardware	Varies		$5.00 (approx)
Total			$50.90

While the use of acrylic foam tapes in shear walls might seem improbable due to the increase in wall costs, other factors must be taken into consideration. The first factor is the length of shear walls required for a typical residential structure. In a typical home, there will likely be a need for only a few full-scale wall panels except in the most extreme environmental conditions. The wind design example presented in the following section calculates necessary lengths of about 6m (20 ft) for hurricane-force winds. The additional material cost of approximately $100 for an increase in strength of 30% or greater over 6 m (20 ft) of shear wall appears reasonable. The second factor is comparison to similar products. Currently, Simpson offers a pre-manufactured shear wall known as Simpson Strong Wall®. A type SW48x8 section of this product that is 1.2 m (4 ft) in length and 2.4 m (8 ft) in height can be ordered for around $280 (Richard Lumber Company 2003). This price was quoted from a distributor, includes labor costs, and might vary depending on location and dealer. The performance of this product is extremely high with published shear resistances of 16.6 kN/m (1136 lb/ft) (Simpson 2003). Using IBC allowable stress values and acrylic foam tape, a 15/32 sheet of structural-grade sheathing with 8d nails at 203 mm (8 in.) on center would have a shear resistance of (430 + 140) = 570 lb/ft. This value is almost exactly half that of the Simpson product, and therefore twice the length would need to be used. The price, however, of the double length of shear wall would likely be comparable to, or less than, that of the Simpson product.

6.9.3 Feasibility Summary

Much additional testing and research would have to be performed before a combination acrylic foam adhesive tape shear wall could be profitably manufactured and sold. The equipment necessary to pre-manufacture panels is already widely available in truss manufacturing plants. The economics depend greatly on the quantities and labor costs associating with pre-manufacturing and are difficult to predict. Rough estimates indicate that the PSA adhesive tape product could offer competitive economics with other similar products.

6.10 Wind Design Example

The following example illustrates the possible uses for acrylic foam PSA adhesive combination shear walls in high wind regions. This example is performed in U.S. Customary Units as current construction practice in the United States relies on such units. Equation references refer to the allowable stress design procedure as outlined in the International Building Code (ICC 2000). This example by no means incorporates all design checks associated with the development of a residential structural system. It is meant strictly as an aid to illustrate the possible benefits of PSA combination systems in shear wall applications. PSA-based wall systems would most likely be used as pre-manufactured units. The geometry involved in this example, as well as the use of the perforated shear wall method, are provided strictly as an exercise and might not reflect actual design conditions. Readers are directed to the *Diaphragms and Shear Walls* guide published by the APA (2001) for more complete examples of shear wall and component design. A smaller font is used to differentiate numeric calculations from regular text.

Given:

A single family, two-story residential house utilizing conventional light-frame construction with a relatively flat roof is to be built along the costal region of Charleston, South Carolina. Due to space limitations on-site, the width of the house is limited to 50 ft along the coastline and 37 ft transverse to the coast. Floor to floor heights are 8 ft, and interior partition walls are assumed to offer negligible shear resistance. Exterior shear walls are assumed to be symmetrical in layout. Southern Pine lumber will be used. An overall view of the proposed house, as well as the shear wall geometry, is presented in Figures 6.20 and 6.21.

Find:

1. *Calculate the required first-story shear to be resisted and select an appropriate wall configuration utilizing the perforated shear wall method.*
2. *Estimate the wind speed that can be resisted if a similar wall utilizing a combination of PSA adhesive tape with a reduced nail schedule is implemented.*
3. *Estimate the increase in wall openings that can be incorporated using a combination PSA adhesive tape and mechanical fastener system.*

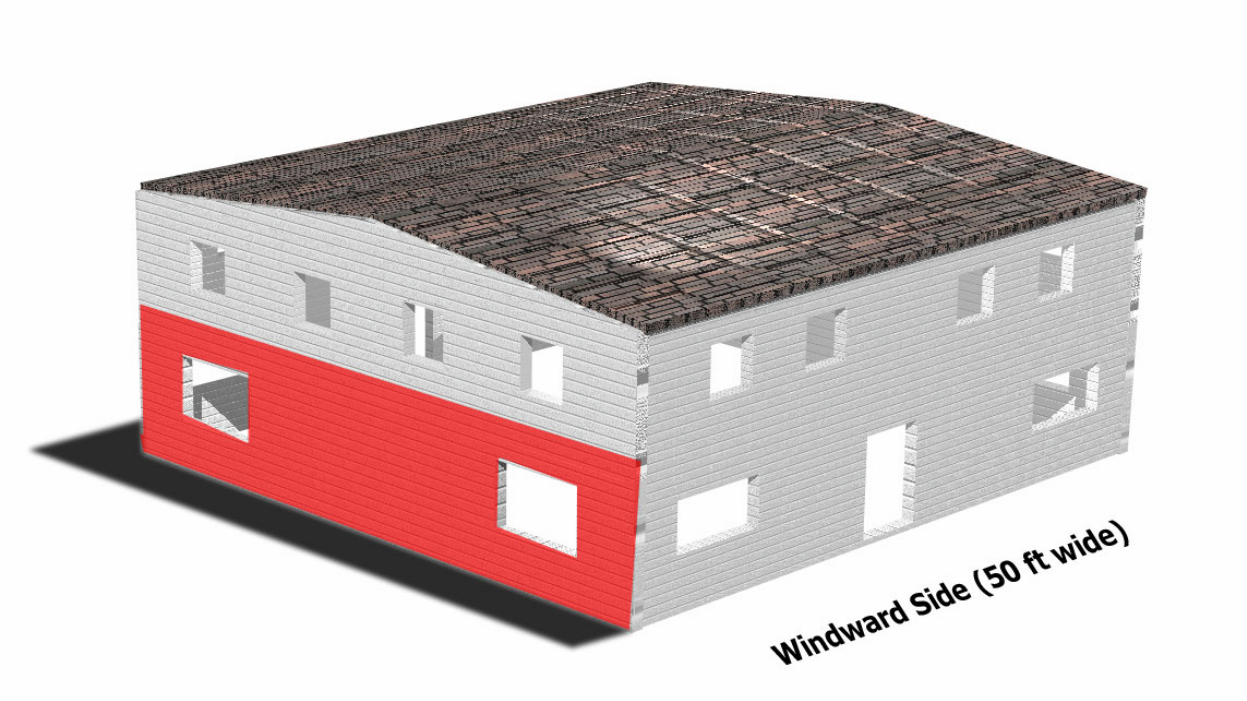

Figure 6.20: Basic House Configuration (Highlighted = Shear Wall to be Designed)

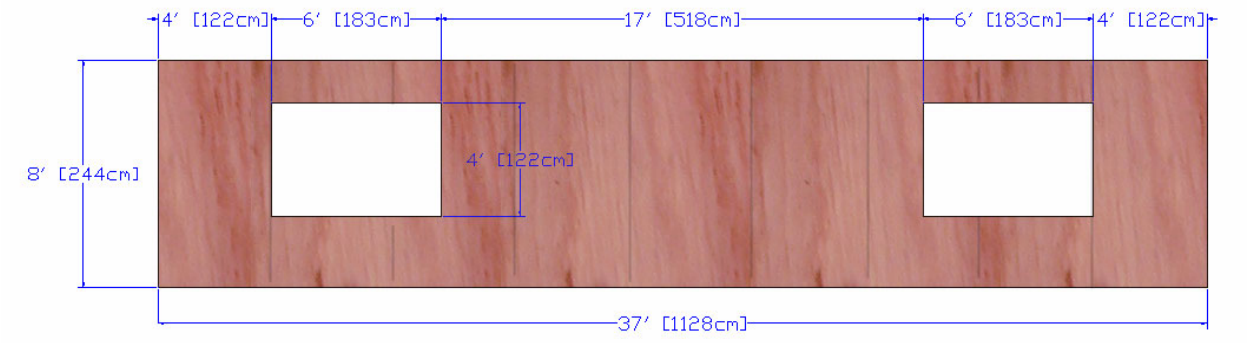

Figure 6.21: Proposed Shear Wall Geometry

1. Calculate the required first-story shear to be resisted and select an appropriate wall configuration utilizing the perforated shear wall method.

Solution: Part I: Calculate Wind Pressures (Method Based On ASCE-7, 1998)

1). Determine Location Wind Speed (Figure 1609 Basic Wind Speed)

$V := 130$ mph

2). Determine Exposure Catagory (Sec. 1609.4)

Category = C "Terrain including shorelines in hurricane prone regions"

3). Determine Importance Factor (Table 1604.5)

Cagetory = I "Typical Buildings and Structures"

$I_w := 1.0$ Wind Importance Factor

4). Determine Kz and Compute Velocity Pressure

$K_z := 0.86$ For 16ft tall structures

$q_h := 0.00256 \cdot 0.85 \cdot K_z \cdot I_w \cdot V^2$ $q_h = 31.63$ psf

5). Determine Pressures on Main Wind Force Resisting System (MWRS)

For relatively flat roofs the external pressure factor (Gcpf) =

$GCpf_{windward} := 0.4$ Zone 1 (Figure 1609.6)

$GCpf_{leeward} := -0.29$ Zone 4 (Figure 1609.6)

External Pressures =

$P_{ewindward} := q_h \cdot GCpf_{windward}$ $P_{ewindward} = 12.65$ psf

$P_{eleeward} := q_h \cdot GCpf_{leeward}$ $P_{eleeward} = -9.17$ psf

Note that + indicates towards the building so the windward and leeward pressures are actually acting together

$P_{total} := P_{ewindward} - P_{eleeward}$ $P_{total} = 21.82$ psf

6). Alternately use IBC Tables 1609.6.2.1 (1) with Adjustment Factor Table 1609.6.2.1 (4)

$P_{unadjusted} := 17.8$ psf (total windward + leeward for this geometry)

$C_{adj} := 1.226$ (adjustment for height and exposure category)

$P_{total2} := P_{unadjusted} \cdot C_{adj}$ $P_{total2} = 21.82$ psf (matches longer procedure)

Conclusion: Use 12.65psf for windward pressures and 9.2psf for leeward pressures.

Note: ASD General Load Combination (1605.3.1) used with 1.0W.

Solution: Part II: Calculate Required Shear Resistance from Design Loads

Wind pressure tributary areas and the resulting forces from these areas on the roof and second floor diaphragms are displayed in Figures 6.22 and 6.23.

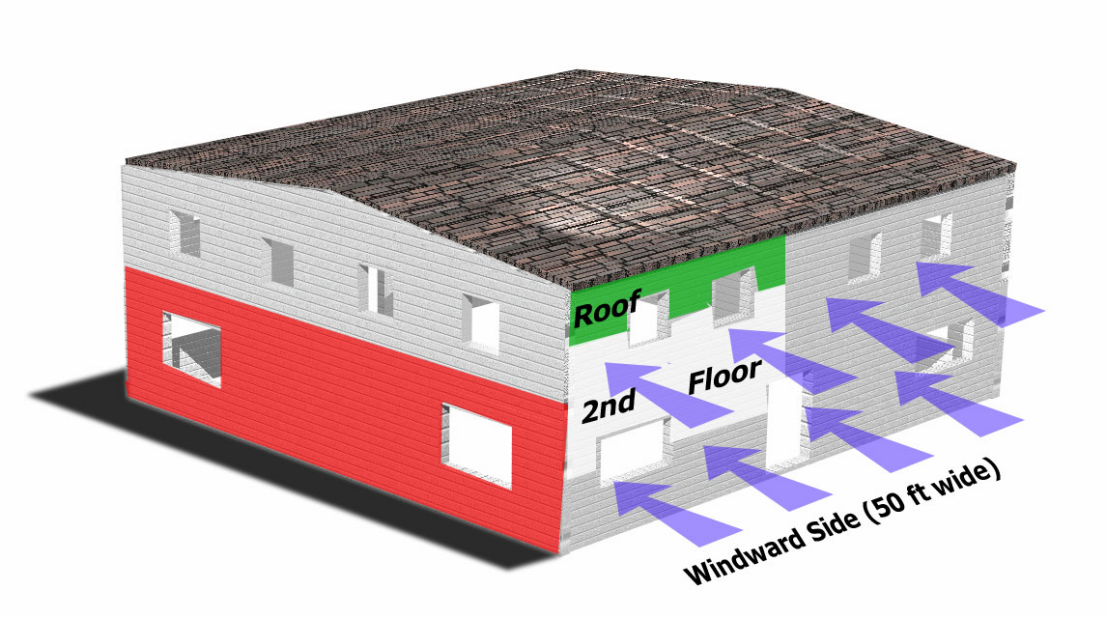

Figure 6.22: Wind Tributary Areas

Dark Highlight (Green) = ½ Wind Tributary Area for Roof Diaphragm

Light Highlight (White) = ½ Wind Tributary Area for 2nd Floor Diaphragm

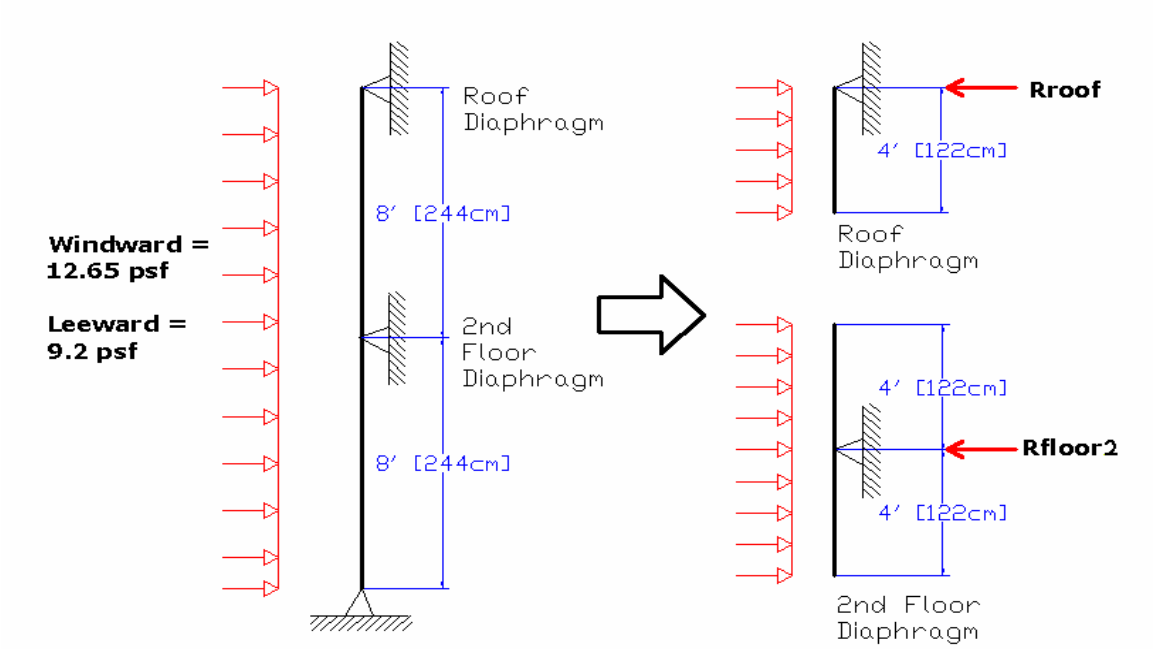

Figure 6.23: Reactions on Diaphragms

1) Assign linear load to diaphragms based on wind tributary areas

a) Calculate Roof Diaphragm Loading

$h := 8.0$ ft per wall height

$R_{roofL} := P_{eleeward} \cdot \frac{h}{2}$ $R_{roofL} = 36.69$ plf (Leeward)

$R_{roofW} := P_{ewindward} \cdot \frac{h}{2}$ $R_{roofW} = 50.60$ plf (Windward)

b) Calculate 2nd Floor Diaphragm Loading

$h := 8.0$ ft per wall height

$R_{2ndfloorL} := P_{eleeward} \cdot \frac{h + h}{2}$ $R_{2ndfloorL} = 73.37$ plf (Leeward)

$R_{2ndfloorW} := P_{ewindward} \cdot \frac{h + h}{2}$ $R_{2ndfloorW} = 101.20$ plf (Windward)

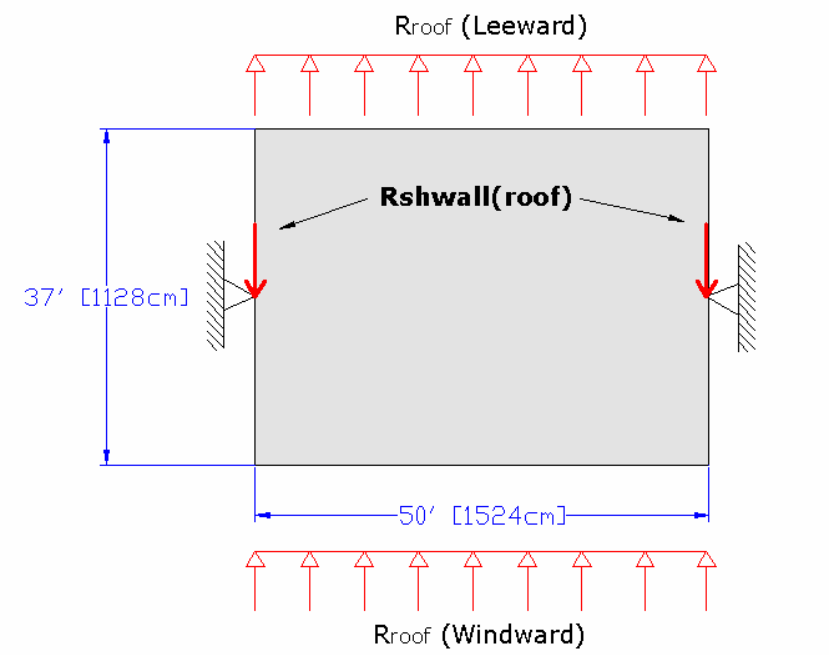

Figure 6.24: Roof Diaphragm Reactions

2) Calculate reactions on 2nd floor shear walls

$L := 50$ ft of diaphragm length

$R_{shearwallR} := (R_{roofL} + R_{roofW})\frac{L}{2}$ $R_{shearwallR} = 2182$ lbs must be resisted

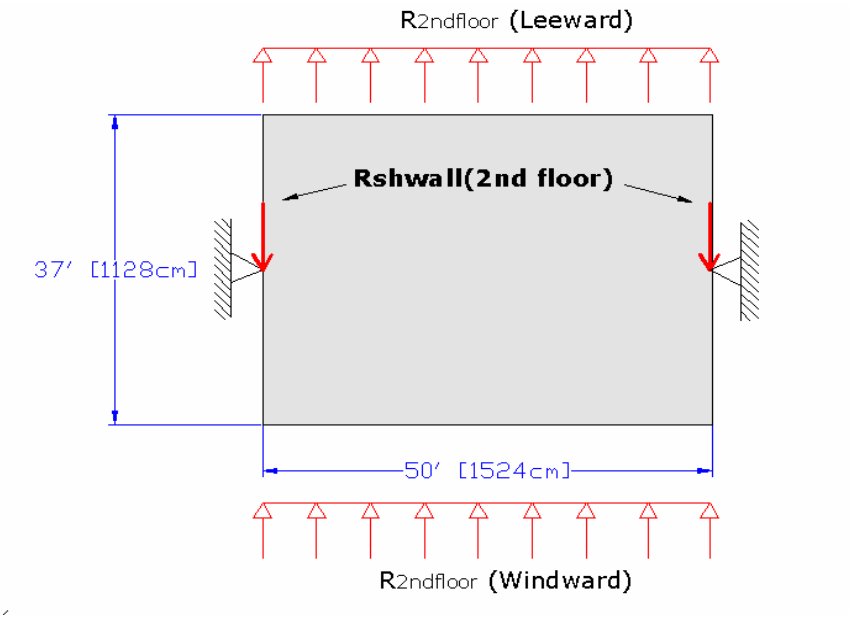

Figure 6.25: 2nd Floor Diaphragm Reactions

3) Calculate reactions on 1st floor shear walls

$$R_{shearwallFlr} := \left(R_{2ndfloorL} + R_{2ndfloorW}\right) \cdot \frac{L}{2} + R_{shearwallR}$$

$R_{shearwallFlr} = 6547$ lbs must be resisted by each 1st floor shear wall

Solution Part III: Design Shear Wall to Resist Required Load

1) Calculate load per foot needed using Perforated Shear Wall Method

a) Max Opening Height = 4 ft Use H/2 (Table 2305.3.7.2)

b) Calculate % Full Height Sheathing

$Lfullht = 25$ ft $\quad Loverall := 37$ ft

$$\%fh := \frac{Lfullht}{Loverall} \cdot 100 \qquad \%fh = 67.57\ \%$$

c) Calculate Shear Capacity Adjustement Factor (SCAF)

$SCAF := 0.86$ (Table 2305.3.7.2)

d) Calculate Required Shear

$$Vreq := \frac{R_{shearwallFlr}}{SCAF \cdot Lfullht} \qquad Vreq = 304.5 \text{ plf}$$

2) Select appropriate shear wall configuration

a) For Wind Loading - values in Allowable Shear Table 2306.4.1 may be increased by 40% (per 2306.4.1).

b) Try 3/8 in. APA Rated Sheathing with 8d Nails @ 6 in. perimeter, 12 in. interior

$Vprovided := 220 \cdot 1.4$ $Vprovided = 308.0$ plf

Answer to Question 1: 3/8 in. APA Rated plywood sheathing with 8d Nails @ 6 in. perimeter, 12 in. interior, provides sufficient shear capacity (308 plf) to resist design loading (306 plf).

2. Estimate the wind speed that can be resisted if a similar wall utilizing a combination of PSA adhesive tape with a reduced nail schedule is implemented.

Solution:

1) Calculate additional strength provided by combination PSA system

a) From Table 6.6 use additional strength value for plywood walls

$V_{psa} := 130$ plf

b) Total shear provided

$V_{new} := Vprovided + V_{psa}$ $V_{new} = 438.0$ plf

2) Back-calculate wind pressure that can now be resisted

a) Back-calculate maximum shear using perforated method

$Vreq := V_{new} \cdot Lfullht \, SCAF$ $Vreq = 9417$ lbs

b) Back-calculate pressure that corresponds to this shear load

$$Pressure := Vreq \cdot \left(\frac{2}{L}\right) \cdot \left(\frac{2}{3 \cdot h}\right) \qquad Pressure = 31.39 \text{ psf}$$

3) Calculate maximum wind speed from IBC Table 1609.6.2.1

a) Adjust for height and location of house

$C_{adj} = 1.23$ (Calculated Previously)

$$Ptables := \frac{Pressure}{C_{adj}} \qquad Ptables = 25.60 \text{ psf}$$

b) From table find maximum speed

V of 155 mph produces 25.4 psf < 25.6 psf strength

Answer to Question 2: The use of a PSA combination wall system with a 12-12 nailing schedule will allow the same house to withstand a 25mph increase in wind gusts, thus improving its strength to resist 155mph winds. This is a result of the 40% increase in load capacity provided by the adhesive tape.

3. Estimate the increase in wall openings that can be incorporated using a combination PSA adhesive tape and mechanical fastener system.

Solution:

See if an extra window can be placed into the shear wall and still be adequate to resist the wind-loads calculated in Part I as shown in Figure 6.26.

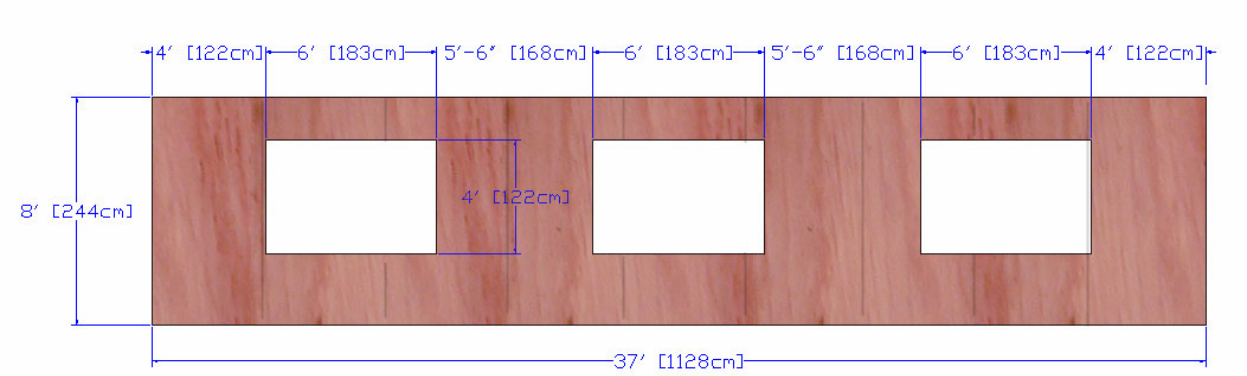

Figure 6.26: Shear Wall With Additional Window

From the solution to the first question, the total shear that must be resisted is 6547 lb. The only factors which change are the percent full height sheathing and the Shear Capacity Adjustment Factor (SCAF). The resistance of the combination system was calculated to be 438 plf as opposed to 308 plf for a similarly configured nail-only wall.

1) Calculate Load per foot needed using Perforated Shear Wall Method

a) Max Opening Height = 4 ft Use H/2 (Table 2305.3.7.2)

b) Calculate % Full Height Sheathing

$Lfullht = 19$ ft $Loverall := 37$ ft

$$\%fh := \frac{Lfullht}{Loverall} \cdot 100 \qquad \%fh = 51.35 \ \%$$

c) Calculate Shear Capacity Adjustement Factor (SCAF)

$SCAF := 0.80$ (Table 2305.3.7.2)

d) Calculate Required Shear

$$Vreq := \frac{R_{shearwallFlr}}{SCAF \cdot Lfullht} \qquad Vreq = 431 \text{ plf}$$

Answer to Question 3: A third window may be added to the shear wall and still resist the required loading using 3/8 in. APA rated plywood sheathing with 8d Nails @ 12 in. perimeter, 12 in. interior, and perimeter acrylic foam PSA tape. This system provides sufficient shear capacity (438 plf) to resist design loading (431 plf).

6.10.1 Wind Design Example Conclusions

This design example illustrates the procedure for the use of combination PSA acrylic tapes and mechanical fastener shear walls in hurricane-force winds. Calculations showed that the addition of the adhesive tape increased allowable wind loads from 130 mph to 155 mph due to a 40% strength increase.

Calculations also showed that the use of adhesive tape would allow the addition of a third window into the geometry of the shear wall using the same wall panel configuration as with traditional construction.

6.11 Seismic Design Example

The following example illustrates the possible uses for acrylic foam PSA adhesive combination systems in high seismic zones. The example is performed in U.S. Customary Units as current construction practice in the United States relies on such units. Equations refer to the allowable stress design procedure as outlined in the International Building Code (ICC 2000). This example by no means incorporates all design checks associated with the development of a residential structural system. It is meant to serve strictly as an aid to illustrate the possible benefits of PSA combination systems in shear wall applications. PSA adhesive-based wall systems would most likely be used as pre-manufactured units. The geometry involved may be impractical for real-world design conditions. Readers are directed to the *Diaphragms and Shear Walls* guide published by the APA (2001) for more complete examples of shear wall and component design. A smaller font is used to differentiate numeric calculations from regular text.

Given:

A single family, two-story residential house utilizing conventional light-frame construction with a relatively flat roof is to be built in the high seismic zone near Charleston, South Carolina. Due to space limitations on-site, the dimensions of the house shall be 50 ft by 37 ft. Floor to floor heights are 8 ft, and interior partition walls are assumed to offer negligible shear resistance. Exterior shear walls are assumed to be equal in layout. Douglas-Fir lumber will be used. An overall view of the proposed house, as well as the geometry of the shear walls, is presented in Figures 6.27 and 6.28. Design dead loads shall be 22 psf for the roof (assuming future attic storage area), 18 psf for the second floor, and 80 plf for wall elements.

Find:

1. *Calculate the required first-story shear to be resisted assuming the building is shaken parallel to the 37 ft shear wall section. Assume three, 6 ft wide windows reduce full-height shear wall segments to 19 ft in length. Select an appropriate wall configuration utilizing the traditional shear wall method.*
2. *Recalculate the required shear force resistance using the proposed R value of 5.5 for combination adhesive tape walls and recommend an appropriate wall configuration.*

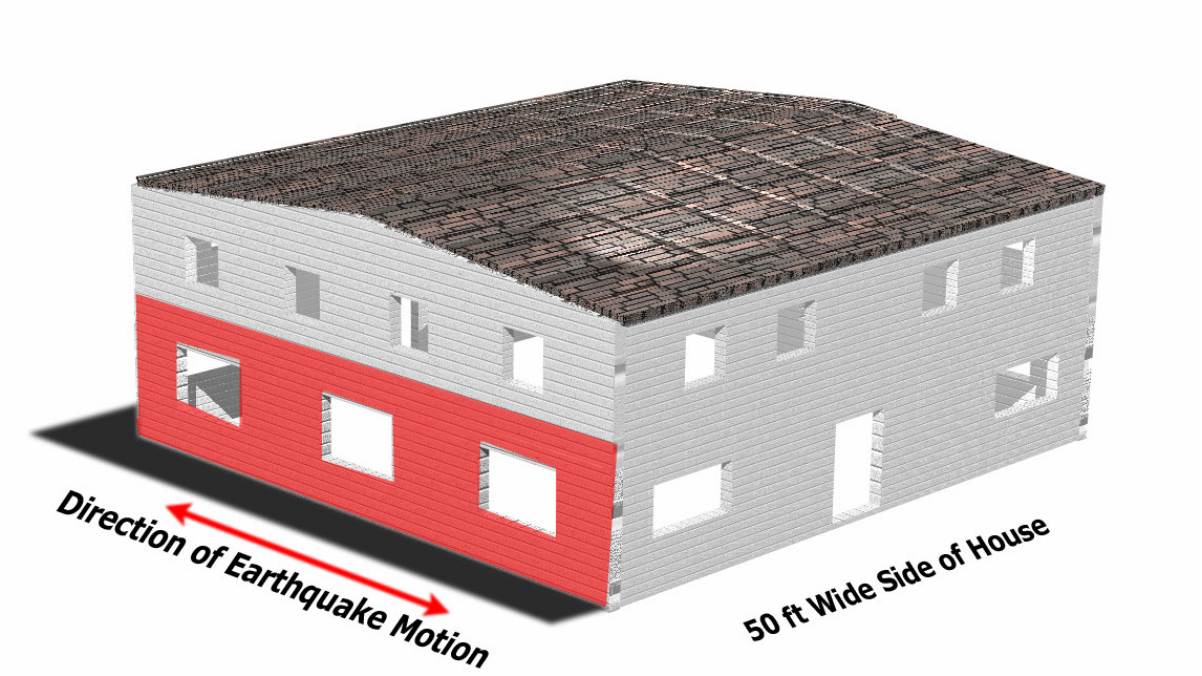

Figure 6.27: Basic House Configuration (Highlighted Wall = Shear Wall to be Designed)

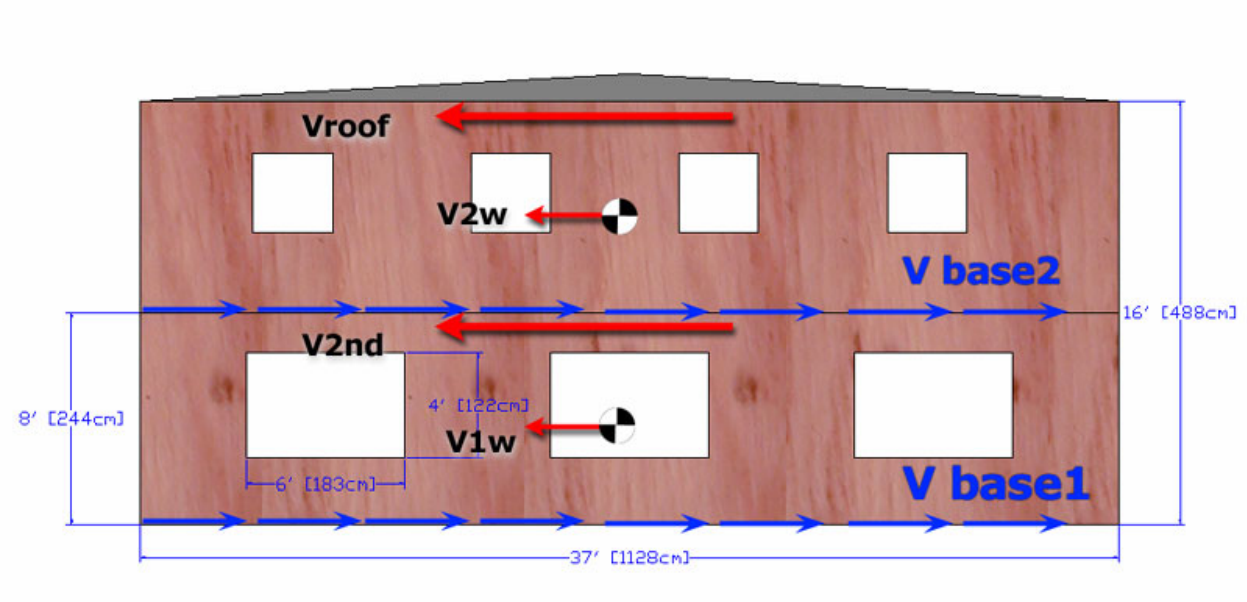

Figure 6.28: Force Distribution on Shear Wall

Vroof: Reaction from roof diaphragm due to earthquake forces

V2nd: Reaction from 2nd floor diaphragm due to earthquake forces

V1w and V2w: Inertial forces from wall weights

Vbase2: Shear which 2nd floor shear wall must resist

Vbase1: Design shear for first floor shear wall (this problem)

1. Calculate the required first-story shear to be resisted assuming the building is parallel to the 37 ft shear wall section. Assume three, 6 ft wide windows reduce full-height shear segments to 19 ft in length. Select an appropriate wall configuration utilizing the traditional shear wall method.

Solution:

1) Calculate seismic design category and accelerations

a) Seismic Importance Factor (Use Group) (Table 1604.5)

$I_E := 1.00$

b) Maximum short period acceleration (Figure 1615 (1))

$S_s := 1.45$ (Site specific gravity ratio)

c) Maximum period of 1 second acceleration (Figure 1615(2))

$S_1 := 0.40$ (Site specific gravity ratio)

d) Site Class

D class used as no soil report has been provided (Sec. 1615.1.1)

e) Site Coefficients

$F_a := 1.0$ dependent on S_s and Site Class (Table 1615.1.2 (1))

$F_v := 1.4$ dependent on S_s and Site Class (Table 1615.1.2 (2))

f) Maximum considered earthquake spectral response accelerations

$S_{MS} := F_a \cdot S_s$ $S_{MS} = 1.45$ g for short periods (0.2 sec)

$S_{M1} := F_v \cdot S_1$ $S_{M1} = 0.56$ g for 1 second periods

g) 5% damped design spectral response accelerations

$S_{DS} := \frac{2}{3} \cdot S_{MS}$ $S_{DS} = 0.97$ g for short periods (0.2 sec) Eq. 16-18

$S_{D1} := \frac{2}{3} \cdot S_{M1}$ $S_{D1} = 0.37$ g for 1 second periods Eq. 16-19

h) Seismic design category

Category D per Table 1616.3 (1 and 2), per 1616.3

Note: At present the use of adhesive shear walls is prohited by IBC Sec. 2305.3.9 for this seismic design category. It is proposed that this section be amended to allow the use of PSA acrylic tapes as previously discussed in Chapter 5 of this thesis.

2) Determine base shear coefficient

Note: As this structure meets seismic description 1 in Table 1616.6.3 the simplified analysis procedure of Section 1617.5 is allowable, and maximum base shear can be directly calculated using Eqn. 16-49. As an exercise this example will perform the slightly more detailed equivalent lateral force procedure in Section 1617.4. and trace inertial forces from the roof down.

a) Importance Factor

$I_E = 1.00$ as previously determined from (Table 1604.5)

b) Response Modification Factor

$R := 6.5$ For light frame walls with wood structural shear panels in a building frame system per Table 1617.6.

c) Seismic Response Coefficient

$$C_s := \frac{S_{DS}}{\left(\frac{R}{I_E}\right)} \quad C_s = 0.15$$ Eq. 16-35, Sec. 1617.4.1.1

d) Checking maximum coefficients

$h_n := 16$ ft

$C_t := 0.020$ Building period coefficient per Sec. 1617.4.2.1

$T_a := C_t \cdot h_n^{0.75}$ $T_a = 0.16$ Approximate Fundamental Period Eq. 16-39 (updated)

$$C_{smax} := \frac{S_{D1}}{\left(\frac{R}{I_E}\right) T_a} \quad C_{smax} = 0.36$$ per Eq. 16-36

$C_s = 0.15$ < $C_{smax} = 0.36$ O.K.

e) Checking minimum coefficients

$C_{smin} := 0.044 \cdot S_{DS} \cdot I_E$ $C_{smin} = 0.0425$ per Eq 16-37

$C_s = 0.15$ > $C_{smin} = 0.04$ O.K.

Use Cs = 0.149

3) Determine Roof Diaphragm Loads (Refer to Figures 6.27 and 6.28 for force diagrams)

a) Roof Diaphragm Weight (includes attic provisional weight)

$Roof_{DL} := 22$ psf

$W_{roof} := Roof_{DL} \cdot 37 \cdot 50$ $W_{roof} = 40700$ lbs

b) Calculating the Load on the Roof Diaphragm

$F_{px} := C_s \cdot (W_{roof})$ $F_{px} = 6053$ lbs (Equation 16-65)

$F_{pmax} := 0.3 \cdot S_{DS} \cdot I_E \cdot (W_{roof})$ $F_{pmax} = 11803$ lbs (Sec. 1620.3.3)

$F_{pmin} := 0.15 \cdot S_{DS} \cdot I_E \cdot (W_{roof})$ $F_{pmin} = 5902$ lbs (Sec. 1620.3.3)

Use Fpx

So uniform load on roof diaphragm =

$w_{roof} := \frac{F_{px}}{L} \cdot 0.7$ $w_{roof} = 84.74$ plf

0.7 Factor for ASD basic load combinations Section 1605.3.1 (ASD - LRFD conversion)

c) Calculating shear on second floor walls due to roof diaphragm

$V_{roof} := w_{roof} \cdot \frac{L}{2}$ $V_{roof} = 2118$ lbs

4. Determine 2nd Floor Diaphragm Loads

a) Roof Diaphragm Weight

$Regular_{DL} := 18$ psf

$W_{2ndflr} := Regular_{DL} \cdot 37 \cdot 50$ $W_{2ndflr} = 33300$ lbs

b) Calculating the Load on the Roof Diaphragm

$F_{px} := C_s \cdot (W_{2ndflr})$ $F_{px} = 4952$ lbs (Equation 16-65)

$F_{pmax} := 0.3 \cdot S_{DS} \cdot I_E \cdot (W_{2ndflr})$ $F_{pmax} = 9657$ lbs (Sec. 1620.3.3)

$F_{pmin} := 0.15 \cdot S_{DS} \cdot I_E \cdot (W_{2ndflr})$ $F_{pmin} = 4829$ lbs (Sec. 1620.3.3)

Use Fpx

So uniform load on 2ndfloor diaphragm =

$w_{2nd} := \frac{F_{px}}{L} \cdot 0.7$ $w_{2nd} = 69.33$ plf

0.7 Factor for ASD basic load combinations Section 1605.3.1 (ASD - LRFD conversion)

c) Calculating shear at interface between walls due to second floor diaphragm

$V_{2nd} := w_{2nd} \cdot \frac{L}{2}$ $V_{2nd} = 1733$ lbs

5. Inertial Forces due to wall self-weights

$Wall_{DL} := 80$ plf (based on 10 psf walls, 8 ft in height)

$V_{1w} := 0.7C_s \cdot Wall_{DL} \cdot 37 \quad V_{1w} = 308.1$ lbs

$V_{2w} := V_{1w}$ Conservatively ignoring openings

6. Calculate total shear load needed at 1st story (Traditional Shear Wall Design)

$$V_{base1} := \frac{V_{roof} + V_{2nd} + V_{1w} + V_{2w}}{19} \quad V_{base1} = 235 \text{ plf}$$

7. Select appropriate shear wall configuration (Table 2306.4.1)

Try 7/16 in. APA rated OSB sheathing panels with 8d nails
@ 6 in. perimeter, 12 in. interior

$V_{provided} := 240$ plf $> V_{base1} = 235$ plf O.K.

Answer to Question 1: A wall configuration utilizing a 7/16 in. APA rated OSB sheathing system with 8d nails @ 6 in. perimeter, 12 in. field provides sufficient shear capacity (240 plf) to resist design loading (235 plf).

2. Recalculate the required shear force resistance using the proposed R-value of 5.5 for combination adhesive tape walls and recommend an appropriate wall configuration.

Solution

To avoid unnecessary repetition, only the recalculated variables will be displayed. The same accelerations and steps to calculate weight and inertial contributions were used as shown in the previous portion of the problem.

1. Recalculate variables using an R of 5.5

$C_s = 0.18$

$V_{roof} = 2503.67$ lb

$V_{2nd} = 2048.45$ lb

$V_{1w} = 364.17$ lb

$V_{2w} = 364.17$ lb

2. Calculate new required base shear

$$V_{base1} := \frac{V_{roof} + V_{2nd} + V_{1w} + V_{2w}}{19} \quad V_{base1} = 278 \text{ plf}$$

3. Select appropriate shear wall configuration (Table 2306.4.1)

Try 3/8 in. APA rated plywood sheathing with 8d nails @12 in. perimeter & inter and PSA adhesive tape.

$V_{provided} := 220 + 130 \quad V_{provided} = 350.0$ plf

$V_{provided} = 350.0$ plf > $V_{base1} = 278$ plf

Answer to Question 2: A wall configuration utilizing a 3/8 in. APA rated plywood sheathing system with 8d nails @ 12 in. perimeter, 12 in. field provides sufficient shear capacity (350 plf) to resist design loading (278 plf).

6.11.1 Seismic Design Example Conclusions

This design example illustrates the procedure for use of combination PSA acrylic tapes and mechanical fastener shear walls in high seismic zones. Note that for simplicity, this design ignored the dead load contribution of approximately 10 psf associated with interior walls. Calculations showed that the use of an R-factor of 5.5 increased the required base shear load from 235 plf to 278 plf (an 18% jump). Further calculations revealed that a thinner 3/8 in. plywood combination adhesive tape system using a reduced nail schedule could provide 26% more resistance than required. Seismic performance was greatly increased over the thicker 7/16 in. nail-only OSB wall, which provided only 2% more resistance than required.

6.12 Summary

Performance results were presented and trends examined for nail-only, combination, and adhesive-only cyclic wall specimens. Strength, toughness, and seismic capabilities of each wall configuration were discussed in detail. Further information was presented on monotonic testing, displacement parameters, failure modes, moisture and temperature effects, and loading protocol effects. Finally, design examples were performed using recommended procedures for adhesive tape and mechanical fastener-based walls in both high wind and seismic regions. Based on the results that have been presented, the following conclusions can be drawn.

1. Use of acrylic foam adhesive tape, in conjunction with a nail schedule reduced in density by 50% in comparison to code recommendations, will result in a strength gain of at least 2.07 kN/m (142 lb/ft) for OSB sheathed specimens and 1.913 kN/m (131 lb/ft) for plywood sheathed specimens over current traditional construction allowable shear values.
2. Strength gain and nail schedule reduction for combination wall configurations is applicable to all wall thicknesses and is most likely conservative for nail schedules more dense than the 305 mm (12 in.) schedule tested.
3. Adhesive-only systems provide similar strength performance to traditional shear walls. Priming provides slightly greater capacity, but the increase does not further justify the use of adhesive-only walls.
4. Traditional construction methods resulted in OSB specimens that were approximately 5-7% stronger than plywood specimens due to material thickness and density properties.
5. Combination wall systems have a displacement capacity which is half that of traditional construction. Adhesive-only wall systems have displacement capacities as little as one-third that of traditional construction.
6. Combination wall systems exhibited higher hysteretic damping than traditional wall construction up to the code imposed drift limits. The damping performance of adhesive-only walls is poor.
7. Hysteretic damping of similarly configured OSB and plywood wall specimens was approximately equal throughout the range of displacements tested.

8. Combination wall systems have an initial elastic stiffness which is approximately 6% to 20% higher than traditional wall construction. Cyclic stiffness values of such walls degrade less and are consistently higher than nail-only construction through displacements corresponding to code drift limits. Higher stiffness values allow the combination wall system to deflect less at given loadings, thus providing better protection for finish materials.
9. Adhesive-only wall systems offer poor cyclic stiffness performance. This behavior, in combination with poor damping and nominal strength performance, resulted in the conclusion that adhesive-only wall systems are inadequate for seismic applications.
10. Equivalent Viscous Damping Ratios (EVDRs) of all walls ranged from 10% to over 20% at high deformations. These values well exceed the 5% values currently used in codes, and are consistent with current wood-frame research.
11. Nail-only walls achieved significantly higher ductility values of up to three times that of combination wall systems. The failure mode of combination systems was still shown, however, to be quite ductile.
12. A system response modification factor of 5-5.5 was proposed for combination wall systems. This factor was based on a review of the uses of R, proposed analytical procedures for its calculation, and sound engineering judgment.
13. Connection slip plus bending accounted for approximately half of the overall displacement for all walls tested due to the hold-down devices used to restrain rigid body rotation. Shear deformation and rigid body rotation were similar, with stiffer wall configurations, such as the combination system, having lower shear deformations and larger rotations.
14. Nail-only walls failed due to fastener fatigue and unzipping of the nail lines. Adhesive-only walls failed rather suddenly due to adhesive bond failure at the center-line. Combination systems failed in part due to both methods.
15. Moisture content of the wood framing and temperature during testing had no observable effect on the performance of any wall configuration. The effect of green lumber and extremely low temperatures should be studied with additional experimentation.

16. The CUREE protocol appears to provide good results for most wall systems. It is recommended that a step-size of 30% instead of 50% be used at displacements beyond Δ for systems with moderate to low ductility to provide a smoother testing curve and prevent premature forced failure.
17. A possible manufacturing process using truss-rolling equipment was explored and is believed to be viable pending additional time of pressure application research. Economic viability is also promising.

Chapter 7

Summary and Conclusions

7.1 Summary

The focus of this thesis was to quantify the performance of connections and full-scale shear walls constructed with acrylic foam pressure sensitive adhesive (PSA) tapes. The two main objectives associated with this study were to first investigate the bonding characteristics of adhesive tape to wood substrates and then to expand this investigation to cover adhesive-based shear walls subjected to high wind and seismic loadings. These objectives were achieved by conducting 287 monotonic connection tests and 23 reversed-cyclic wall tests.

The connection test portion of this study was broken into four parts. The first part was a preliminary study comparing the bonding capabilities of adhesive tape on several different substrates with different surface treatments. This testing also served to answer questions on the effect of moisture content and framing member type on connection performance. From this initial investigation, questions of optimum application pressure and duration of application pressure arose. These questions were answered by the next two parts of the study through additional connection testing. Results from these two side-studies were then used to construct and test the remaining specimens. Variables investigated within the main study were: the use of OSB versus plywood sheathing, the effect of priming and surface sanding on adhesion, and the comparison of connections involving mechanical fasteners with those that utilized only adhesive tape or a combination of the two. Connection test results were then analyzed for performance parameters such as loading and displacement capacity, ductility, and amount of work performed.

Results from the connection tests were used to decide which configurations warranted full-scale testing, as well as to calibrate the cyclic loading protocol. A limited number of full-scale walls were first tested monotonically to provide ultimate displacement data. The remaining walls were tested using the CUREE general displacement-based forcing function. Performance of traditional nail-only walls was then compared to the performance of both adhesive-only and combination specimens. Combination specimens were constructed with adhesive tape and a reduced nail schedule. Additionally, the effects of sheathing type and surface treatment were explored. Data gathered from these tests was analyzed and used to provide recommendations on

the wind and seismic capabilities of each wall configuration. These results were then incorporated into design examples to provide engineering guidance for the use of adhesive-based shear wall systems.

7.2 Conclusions

Results and conclusions of this study as determined from the analysis of all test data are presented in the following sections. The first section contains overall conclusions regarding the applicability of acrylic foam pressure sensitive adhesive tape for structural uses in housing construction. The following sections contain more specific results from which the overall conclusions were drawn.

7.2.1 Overall Conclusions and Recommendations

Based upon the performance of acrylic foam PSA tape in both connection and shear wall tests, the following observations were made:

1. An application pressure of 207 kPa (30 psi) or greater is required to form a sound bond between acrylic foam adhesive tape and a wood substrate. Peak performance values are obtained more consistently with pressures of 414 kPa (60 psi) or greater.

2. The duration of pressure application has no observable effect on the performance of the adhesive tape connections. The minimum time as limited by the range of this study is 15 seconds. It is hypothesized that higher pressures with lower application times will produce similar results.

3. Section 2305.3.9 of the International Building Code should be amended to allow the use of pressure sensitive adhesive tapes in shear wall construction if the following two conditions are met: 1) Such adhesives are used in conjunction with a minimum number of mechanical fasteners determined as one-half of the code recommended schedule. 2) The adhesive is proven by connection testing or more thorough methods to offer similar or greater performance when compared to those adhesives investigated by this study.

4. Use of acrylic foam PSA tapes, in combination with a reduced nail schedule, is a viable method for supplementing wall strengths above current design values for wind loading. Allowable shear values for wall assemblies constructed with a 50% reduction in nail schedule may be increased by 2.07 kN/m (142 lb/ft) for OSB sheathing and 1.913 kN/m (131 lb/ft) for plywood sheathing. These values have been divided by a safety factor of three for allowable stress design. Strength gains are most likely conservative for dense nail schedules, but shall not be increased unless further testing is performed.

5. A response modification factor of R=5.0-5.5 is recommended for light-frame shear wall assemblages constructed with acrylic foam PSA tapes. This value is a reduction of 1 unit from the current factor for light-frame timber shear walls. This reduction was made as a concession to the decreased displacement capacity of the adhesive system but with consideration to the ductile failure mode, excellent damping capabilities, and reduced cyclic stiffness degradation exhibited by the combination wall system.

6. Shear walls constructed with only acrylic foam adhesive provide similar cyclic strength capacities to traditional wall construction. Adhesive-only walls are not recommended for seismic applications due to their poor displacement capacity, high cyclic stiffness degradation, and small hysteretic damping values.

7. The CUREE loading protocol appears to produce good results for the majority of tests performed. It is recommended that the step-size of the protocol be reduced after Δ from 50% to 30% to produce a smoother loading curve and to prevent the premature failure of wall specimens associated with the current load-step.

The above conclusions represent the main results and recommendations based on both connection and wall test data as presented in Chapters 5 and 6 of this thesis. Some additional observations specific to each study are listed in the following two sections.

7.2.2 Connection Test Results and Observations

The following paragraphs represent general observations and conclusions that were drawn from the four-part connection test study. For further details and elaboration of results, the reader is directed to Chapter 5.

1. Neither the moisture content nor the framing lumber from which each connection test originated appeared to have an effect upon the overall performance of the connection. This study was limited to surface dry lumber and these findings do not pertain to green boards.

2. The displacement limit between wood members joined with acrylic foam tape is approximately eight times the thickness of the tape tested. This value far exceeds the value of three times the thickness of the tape that is listed in the manufacturer's literature.

3. ADCO AT-2 and 3M VHB 4941 adhesive tapes both exhibited similar performance. Each of these tapes provided approximately three times the displacement capacity of the Avery 2333 product.

4. OSB specimens bonded with adhesive tape benefit greatly from the use of priming and surface sanding. Both treatments serve to increase the surface energy and negate the roughness of the wood substrate. Priming the surface provides a 100% gain in load capacity and 62% gain in displacement capacity. Sanding provides a 60% increase in load capacity with a 6% gain in displacement capacity. These benefits carried over into the cyclic wall tests; however the resulting overall wall performance still provided only a marginal improvement over traditional shear wall construction.

5. Plywood specimens do not benefit greatly from the use of surface treatments because their surface energy is already high due to the finish sanding applied during manufacturing. Plywood panels also provide a smoother bonding surface than OSB sheathing panels.

6. OSB specimens provide better performance than plywood specimens when only mechanical fasteners are used due to the increased density of the material. Plywood specimens provide improved performance when adhesive is used due to the more favorable surface characteristics.

7. The elastic stiffness of nailed connections was considerably higher than that of the adhesive-based connections. Nailed connections were between two and three times as stiff in OSB as in plywood. This trend was not observed in the cyclic wall tests where the adhesive-based walls provided similar or higher stiffness values. This reversal is most likely due to the viscoelastic behavior of the adhesive under high loading rates.

8. All connection failures were interfacial adhesive bond failures between the sheathing or framing members and the PSA tape. At no time was the internal shear strength of the tape exceeded. Most failures initiated from the "rolling" effect of the adhesive tape between sheathing and main members.

9. Systems that used a combination of mechanical and adhesive fasteners exhibited areas of increased localized bonding surrounding the nailing location. This phenomenon was also observed in tests of full-scale walls and is believed to be due to the high pressure concentrations induced by the nailing process.

10. Displacement capacities provided by traditional construction adhesives such as wood glue and Liquid Nails® were determined to be only 20-25% of the displacement capacities of acrylic foam PSA tapes. Stiffness values of traditional construction adhesives were also found to be between 10 and 15 times greater than those of acrylic foam tapes. These low displacement capacities and high stiffness values lead to extremely brittle failures.

7.2.3 Wall Test Results and Observations

The following paragraphs represent general observations and conclusions that were drawn from the full-scale cyclic testing of shear wall specimens. For further details and elaboration of results, the reader is directed to Chapter 6.

1. Effects of surface treatments such as priming and sanding were hard to quantify due to the lack of an adhesive-only OSB set. Such a full-scale set was not tested due to the configuration's weak connection performance. As with connection tests, priming provided a noticeable performance gain in full-scale wall tests, but these gains were not significant when compared to traditional construction.

2. As predicted by the connection testing, OSB wall specimens constructed utilizing only mechanical fasteners had load capacities 5-7% greater than plywood specimens due to the increase in density and thickness of the sheathing material.

3. Displacement capacities of combination wall systems constructed with both adhesive tape and mechanical fasteners were approximately half of traditional nail-only wall construction. Adhesive-only wall assemblages exhibited displacement capacities as small as one-third those of traditional construction.

4. Combination wall systems exhibited better hysteretic damping performance than traditional wall construction up to the code-imposed drift limits. Adhesive-only walls provided poor damping performance. In all similar configurations, there were no observable differences in damping performance of OSB and plywood-sheathed systems.

5. Equivalent Viscous Damping Ratios (EVDRs) of all wall configurations were calculated to be between 10% and 15% in the elastic range. These values are two to three times as high as current code interpretations for light-frame timber structures. Even higher EVDRs of approximately 20% were calculated for larger displacements, but the EVDR method is not a good indicator of damping ratios in the inelastic range of deformation.

6. Higher cyclic stiffness values for combination wall systems allow less deflection at given loadings, thus providing better protection for finish materials. Cyclic stiffness values remained higher for combination wall systems as compared to traditional wall construction through displacements up to the code-imposed drift limits. Adhesive-only walls exhibited overall poor stiffness performance.

7. Ductility of nail-only walls was up to three times that of the combination wall systems. Ductility is, however, an extremely sensitive parameter depending heavily on the definitions of yielding and failure, and it is not believed to be a good indicator of wall performance.

8. Connection slip plus bending accounted for approximately half of the overall displacement of each wall configuration. The remainder of the displacement was split fairly evenly between rigid body rotation and shear deformation. Shear deformation values appeared to be inversely proportional to the cyclic stiffness of the wall system.

9. Moisture content of the main timber framing did not have an observable effect on wall performance. The temperature at which tests took place, between 17˚C (62˚F) to 38˚C (100˚F), also had no effect on wall performance.

10. Use of automated roof-truss rolling equipment is believed to be a workable method for the application of pressure in a pre-manufacturing environment. The economic viability of such a system appears to be plausible, but further study is necessary for better estimates.

7.3 Future Research

During this study, numerous connections and full-scale shear wall configurations were tested. Due to the time and expense involved with such specimens, there was a limit on the number of variables that could be properly explored. Only a single wall geometry, nail schedule, and adhesive tape were used to generate the majority of the cyclic test results. Furthermore, as with the initial development of any new product or method, results of this study have not only lead to answers, but also to further questions. In order for the use of acrylic foam PSA tapes to gain wide acceptance for manufacturing and use in the construction industry, these questions must be answered through additional research. Some of the topics and issues that need to be investigated are:

1. Additional types and thicknesses of acrylic foam tape need to be tested. The 3M company alone produces over 20 different types of double coated acrylic foam tapes. These tapes have different thicknesses and are formulated for different uses such as cold-weather bonding. Using a thicker tape than the VHB 4941 utilized in this study might provide better adhesion capabilities to the relatively rough wood surfaces. Companies might also consider the reformulation of adhesive tapes to allow smaller activation pressures. Additionally, the specific development of a wood primer capable of filling porous surfaces, while still providing strong chemical bonds to acrylic foam tapes, would be advantageous. Single-lap-shear tests on such products could be run relatively quickly and cheaply to verify their performance and the need for full-scale testing.

2. Full-scale tests should be conducted to determine the effect of denser nail schedules on adhesive tape performance. All tests conducted with adhesive tape and nails for this study used a relatively sparse 305 mm (12 in.) nail schedule. It is hypothesized that the additional strength provided by the use of adhesive tape might increase in proportion to the density of fasteners due to the effect of increased localized pressures around the nails. Furthermore, the testing of a wall with a fairly dense 102 mm (4 in.) wall schedule using adhesive tape without the application of pressure could determine whether the localized pressures due to pneumatic nailing are sufficient to “wet out” the adhesive tape. If

significant strength gains could be achieved without the need for pre-application of pressure, the resulting product might be useful for field construction purposes.

3. Computer modeling needs to be performed to determine if the data gained from connection tests can accurately predict full-scale cyclic testing. The use of the CASHEW (Cyclic Analysis of SHEar Walls) program recently developed by the CUREE wood frame project specifically for the prediction of quasi-static shear wall performance would be of particular interest (Folz and Filiatrault 2001). Connection and hysteretic information determined from this study could be used within this program to determine if full-scale wall data can be accurately produced. Successful analytical predictions would allow for the testing of an expanded variable set with little expense using only connection tests and an occasional full-scale test for verification.

4. Tests to determine load-rate effects of dynamic movements on adhesive-based shear walls need to be conducted. Testing in this study was limited to the quasi-static frequency of 0.5 Hz. Actual earthquakes can exhibit significantly higher frequencies. Performance of acrylic foam adhesive tape is highly dependent upon the rate of strain due to its viscoelastic nature (Heitman 1990), and seismic loading rates might result in higher load capacities and brittle behavior. Full-scale shake table testing could be conducted, and finite element programs such as DYNWALL which was developed, and since updated, by Dolan (1989) could be used to predict dynamic wall performance.

5. Further testing into the duration of pressure application needs to be performed to expand upon the limitations of this study. If the possible manufacturing method of truss rollers is to be used, application times less than 1 second need to be investigated as opposed to the 15 second minimum utilized in this study.

6. Long-term durability of adhesive-tape-based walls needs to be investigated. Though the durability of the adhesive tape has been proven with metal substrates (Heitman 1990), the ability of tape to resist fatigue cycles, creep, water damage, and possible UV exposure when adhered to wood substrates warrants further study.

7. Temperature effects on both wall construction and performance need to be characterized. Manufacturers' data provides thermal limits on adhesive application, but the use of adhesive tape in extremely cold or warm environments should be investigated.

8. Additional wall geometries including smaller widths of 0.61 m (2 ft) and 1.22 m (4 ft) and larger heights of 2.74 m (9 ft) and 3 m (10 ft) need to be tested if the pre-manufacturing of this product is to be viable for a large number of housing needs. The effect of high aspect ratios on the supplemental strength of the adhesive tape is of specific interest.

9. Out-of-plane tensile strength of adhesive tape specimens bonded to wood substrates should be evaluated for two reasons: First, the tensile strength of the tape could play a major role due to the internal pressures and external loads applied by hurricane-force winds. Secondly, the possible use of adhesive tapes to prevent uplift of roof sheathing panels during high winds would depend heavily on tensile data.

10. Use of adhesive tapes or other fastening devices on interior studs needs to be tested. This study only used adhesive tape around the perimeter of the wall panels for maximum shear resistance with minimum material. Small strips of tape were placed on the interior studs to prevent out-of-plane buckling of the sheathing panels. These strips were not, however, fully pressurized and were sometimes ineffective. It is hypothesized that the use of a few mechanical fasteners or a strip of fully pressurized adhesive tape on interior studs could increase the overall capacity of the wall assembly through the prevention of buckling.

This thesis provides a solid foundation of experimental results and analysis upon which future research into the use of acrylic foam PSA tapes in shear wall applications can be built. Continuing investigation on topics such as those presented in this section will, along with the first steps taken by this study, provide and continue to expand the engineering uses of acrylic foam PSA tapes for structural applications in housing construction.

Bibliography

[1] 3M. (1998). *VHB™ Double Coated Acrylic Foam Tapes and Adhesive Transfer Tape*. Technical Data, March 1998. 3M Bonding Systems Division, St. Paul, MN.

[2] 3M Consumer Response Center. (2003). Personal communication. 3M Company, 2 March 2003.

[3] ADCO. (2000). *AT-2 Gray Very High Bond Acrylic Tape.* Product Data Sheet, August 2000. ADCO Product, Inc., Michigan Center, MI.

[4] American Forest and Paper Association (AF&PA). (2001). *National Design Specification for Wood Construction, 2001 Edition*. ANSI/NF&PA NDS 2001. AF&PA, Washington, D.C.

[5] American Forest and Paper Association (AF&PA). (2002). *Regional Production and Market Outlook for Structural Panels and Engineered Wood Products*. Economics Report E68. AF&PA, Washington, D.C.

[6] American Society for Testing and Materials. (2000a). ASTM D 1761-88 (2000) "Standard Test Methods for Mechanical Fasteners in Wood." *ASTM Annual Book of Standards*, Vol. 4.10, ASTM, West Conshohocken, PA.

[7] American Society for Testing and Materials. (2000b). ASTM E 564-00 "Standard Specification of Static Load Test for Shear Resistance of Framed Walls for Buildings." *ASTM Annual Book of Standards*, Vol. 4.11, ASTM, West Conshohocken, PA.

[8] American Society for Testing and Materials. (2002a). ASTM E 72-02 "Standard Test Methods of Conducting Strength Tests of Panels for Building Construction." *ASTM Annual Book of Standards*, Vol. 4.11, ASTM, West Conshohocken, PA.

[9] American Society for Testing and Materials. (2002b). ASTM E 2126-02a "Standard Test Methods for Cyclic (Reversed) Load Test for Shear Resistance of Framed Walls for Buildings." *ASTM Annual Book of Standards*, Vol. 4.11, ASTM, West Conshohocken, PA.

[10] Anderson, G.T. (2001). *Experimental Investigation of Group Action Factor for Bolted Wood Connections.* Master's Thesis. Virginia Polytechnic Institute and State University, Blacksburg, VA.

[11] APA – The Engineered Wood Association. (1994). *APA Source List – Adhesives for APA Glued Floor Systems.* APA, Tacoma, WA.

[12] APA – The Engineered Wood Association. (1998a). *Commentary on Load and Resistance Factor Design (LRFD) and Seismic Response Modification Factor (R) for Shear Walls.* APA, Tacoma, WA.

[13] APA – The Engineered Wood Association. (1998b). *Structural Adhesives for Plywood-Lumber Assemblies.* Technical Note No. Y391C. APA, Tacoma, WA.

[14] APA – The Engineered Wood Association. (2001). *Diaphragms and Shear Walls.* APA Design/Construction Guide. APA, Tacoma, WA.

[15] APA – The Engineered Wood Association. (2002). *Design Capacities of APA Performance Rated Structural-Use Panels.* Supplemental Update to Technical Note No. 375B. APA, Tacoma, WA.

[16] ASCE-7. (1998). *Minimum Design Loads for Buildings and Other Structures.* American Society of Civil Engineers, Reston, Virginia.

[17] ATC. (1995). *Structural Response Modification Factors.* ATC-19 Report, Applied Technology Council, Redwood City, California.

[18] Aune, P. and M. Patton-Mallory. (1986). "Lateral Load-Bearing Capacity of Nailed Joints Based on the Yield Theory: Experimental Verification." *Research Paper FPL 470,* USDA, Forest Service, Forest Products Laboratory, Madison, Wisconsin, 1986.

[19] Avery Dennison. (2001). *Avery Dennison™ FM 2333.* Product Information Bulletin, March 2001. Avery Dennison Specialty Tape Division, Painesville, OH.

[20] Barbosa, A.P., E.B. Mano, and C.T. Andrade. (2000). "Tannin-based Resins Modified to Reduce Wood Adhesive Brittleness." *Forest Products Journal,* Vol. 50, No. 5, Forest Products Research Society, 89-92.

[21] Bredel, D. (2003). *The Performance Capabilities of Tall Light-Frame Shear Walls Sheathed with Long OSB Panels*. Master's Thesis. Virginia Polytechnic Institute and State University, Blacksburg, VA.

[22] Brockmann, W. and K.J. Grüner. (2002). "Bandwidth of Load- and Temperature-Dependant Creep-Behavior of Pressure Sensitive Adhesives." *Proceedings of the 25th Annual Meeting of the Adhesion Society, Inc. and The Second World Congress on Adhesion and Related Phenomena (WCARP-II),* Orlando, FL, 2002, 280-282.

[23] Brockmann W. and R. Hüther. (1996). "Adhesion Mechanics of Pressure Sensitive Adhesives." *International Journal of Adhesion and Adhesives,* Vol. 16, No. 2, 81-86.

[24] Brown, T. (1999). "The Strain-Rate Sensitivity of Adhesive Tape and its Significance for Design." *Proceedings of the Second Australasian Congress on Applied Mechanics,* ACAM 1999, Canberra, Australia, Feb 1999.

[25] BSSC. (1994). *NEHRP Recommended Provisions for the Development of Seismic Regulations for New Buildings.* Building Seismic Safety Council, Washington, D.C.

[26] CEN. (1995). *Timber Structures – Test Methods – Cyclic Testing of Joints Made with Mechanical Fasteners.* Comité Europeen de Normalisation, IN TC 124.117, European Committee for Standardization, Brussels, Belgium.

[27] Cobeen, K., J. Russel, and J.D. Dolan. (2002). "Earthquake Hazard Mitigation of Woodframe Construction (Final Draft)." *CUREE-Caltech Woodframe Project*, Consortium of Universities for Research in Earthquake Engineering, Richmond, CA.

[28] Cornell, R.W. (1953). *Journal of Applied Mechanical Trans.* ASME, Vol. 17, 335-364.

[29] Countryman, D.R., and J.D. Rose. (1970). "Field-glued Plywood Floors." *Forest Products Journal,* Vol. 20, No. 10, Forest Products Research Society, 17-26.

[30] Davis, G. (1997). "The Performance of Adhesive Systems for Structural Timbers." *Int. J. Adhesion and Adhesives,* Vol. 17, No. 3, 247-255.

[31] Dean, J.A., W.G. Stewart, and A.J. Carr. (1986). "The Seismic Behavior of Plywood Sheathed Shearwalls." *Bulletin of the New Zealand National Society for Earthquake Engineering,* Vol. 19, No. 1, 48-63.

[32] Diekmann, E.F. (1995). "Diaphragms and Shearwalls," *Wood Engineering and Construction Handbook.* K.F. Faherty and T.G. Williamson (Eds.), McGraw-Hill, New York, NY.

[33] Dinehart, D.W. (1998). *The Dynamic Behavior of Wood Framed Shear Walls with Passive Energy Dissipation Devices.* PhD Dissertation. University of Delaware, Newark, DE.

[34] Dinehart, D.W. and H.W. Shenton III. (1998). "Comparison of Static and Dynamic Response of Timber Shear Walls." *Journal of Structural Engineering,* ASCE, Vol. 124, No. 6, 686-695.

[35] Dinehart, D.W. and H.W. Shenton III. (2000). "Model for Dynamic Analysis of Wood Frame Shear Walls." *Journal of Engineering Mechanics,* ASCE, Vol. 126, No. 9, 899-907.

[36] Dolan, J.D. (1989). *The Dynamic Response of Timber Shear Walls.* Thesis submitted in partial fulfillment of the requirements for the degree of Doctor of Philosophy, University of British Columbia, Vancouver, Canada.

[37] Dolan, J.D. (2003). Professor of Civil and Environmental Engineering at Washington State University. Personal communication. Pullman, WA. 2 March 2003.

[38] Dolan, J.D. and M.W. White. (1992). "Design Considerations for Using Adhesives in Shear Walls." *Journal of Structural Engineering,* ASCE, Vol. 118, No. 12, 3473-3479.

[39] Durham, J.P. (1998). "Seismic Response of Wood Shearwalls with Oversized Oriented Strand Board Panels." Master's Thesis. University of British Columbia, Vancouver.

[40] Easley, J.T., M. Foomani, and R.H. Dodds. (1982). "Formulas for Wood Shear Walls." *Journal of Structural Division,* ASCE, Vol. 108, No. 11, 2460-2478.

[41] Erdogan, F. and M. Ratwani. (1971). *Journal of Composite Materials,* Vol. 5, 378-393.

[42] Falk, R.H. (1986). *Experimental and Theoretical Study of the Behavior of Wood Diaphragms.* Thesis submitted in partial fulfillment of Ph.D. degree, Washington State University, Pullman, Washington.

[43] Falk, R.H. and R.Y. Itani. (1988). "Finite Element Modeling of Wood Diaphragms." *Journal of Structural Engineering,* ASCE, Vol. 115, No. 3, 543-559.

[44] FEMA 273. (1997). NEHRP *Guidelines for the Seismic Rehabilitation of Buildings,* Federal Emergency Management Agency, Washington, D.C.

[45] Ficcadenti S., M. Steiner, G. Pardoen, and R. Kazanjy. (1998). "Cyclic Load Testing of Wood-Framed, Plywood Sheathed Shear Walls Using ASTM E564 and Three Loading Sequences." *Proceedings, 6th U.S. National Conference on Earthquake Engineering,* EERI.

[46] Filiatrault, A. (Ed). (2001). "Woodframe Project Testing and Analysis Literature Reviews." *CUREE-Caltech Woodframe Project Report No. W-03,* Consortium of Universities for Research in Earthquake Engineering, Richmond, CA.

[47] Filiatrault, A and R.O. Foschi. (1991). "Static and Dynamic Tests of Timber Shear Walls Fastened with Nails and Wood Adhesive," *Canadian Journal of Civil Engineering,* Vol. 18, No. 5, National Research Council Canada, Ottawa, 749-755.

[48] Foliente, G.C. (1995). "Hysteresis Modeling of Wood Joints and Structural Systems." *Journal of Structural Engineering,* ASCE, Vol. 121, No. 6, 1013-1022.

[49] Foliente, G.C. and E.G. Zacher. (1994). "Performance Tests of Timber Structural Systems Under Seismic Loads." *Analysis, Design and Testing of Timber Structures Under Seismic Load Proceedings of a Research Needs Workshop*, University of California, Forest Products Laboratory, Richmond, CA, 21-86.

[50] Folz, B. and A. Filiatrault. (2001a). "CASHEW - Version 1.1: A Computer Program For The Cyclic Analysis of Wood Shear Walls." *CUREE-Caltech Project Report No. W-08*, Consortium of Universities for Research in Earthquake Engineering, Richmond, CA.

[51] Folz, B. and A. Filiatrault. (2001b). "Cyclic Analysis of Wood Shear Walls." *Journal of Structural Engineering,* ASCE, Vol. 127, No. 4, 433-441.

[52] Folz, B. and A. Filiatrault. (2002). "A Computer Program for Seismic Analysis of Woodframe Structures (SAWS)." *CUREE-Caltech Project Report No. W-21*, Consortium of Universities for Research in Earthquake Engineering, Richmond, CA.

[53] Forest Industries and Paper Products, updated December 21, (1998), accessed January 12, 2003. "Oriented Strand Board." *Industry Canada,* Ottowa, ON. Internet address: http://strategis.ic.gc.ca/SSG/fb01135e.html

[54] Foschi, R.O. (1974). "Load-Slip Characteristics of Nails." *Wood Science,* Vol. 7, No. 1, 69-76.

[55] Foschi, R.O. (1977). "Analysis of Wood Diaphragms and Trusses." *Canadian Journal of Civil Engineering,* Vol. 4, No. 3, 345-362.

[56] Gatto, K. and C.M. Uang. (2002). "Cyclic Response of Woodframe Shearwalls: Loading Protocol and Rate of Loading Effects." *CUREE-Caltech Project Report No. W-13*, Consortium of Universities for Research in Earthquake Engineering, Richmond, CA.

[57] Geiss, P.L. and W. Brockmann. (1997). "Creep Resistance of Pressure Sensitive Mounting Tapes." *Journal of Adhesion,* Vol. 63, 253-263.

[58] Goland, M. and E. Reissner. (1944). *Journal of Applied Mechanical Trans.,* ASME, Vol. 11, A17-A27.

[59] Griffiths, D.R. (1984). "Determining the Racking Resistance of Timber Framed Walls." *Proceedings of the Pacific Timber Engineered Conference, Auckland, New Zealand, Vol. 1, Timber Construction,* Institute of Professional Engineers, Wellington, New Zealand, 504-512.

[60] Gupta, A.K. and G.P. Kuo. (1985). "Behavior of Wood-Frame Shear Walls." *Journal of Structural Engineering,* ASCE, Vol. 111, No. 8, 1722-1733.

[61] Gupta, A.K. and G.P. Kuo. (1987). "Wood-Frame Shear Walls with Uplifting." *Journal of Structural Engineering,* ASCE, Vol. 113, No. 2, 241-259.

[62] Gutkowski, R.M. and A.L. Castillo. (1988). "Single- and Double-Sheathed Wood Shear Wall Study." *Journal of Structural Engineering,* ASCE, Vol. 114, No. 6, 1268-1284.

[63] Harding, N. and A.H.R. Fowkes. (1984). "Bolted Timber Joints." *Proceedings of Pacific Timber Engineering Conference, Auckland, New Zealand*, May, 1984, Vol. III Wood Science, 872-883.

[64] Hart, Kennth M. (1999). "Held Together With Tape." *Mechanical Engineering Design,* November 3, 30-32.

[65] He, M., F. Lam and H.G.L. Prion. (1998). "Influence of Cyclic Test Protocols on Performance of Wood-Based Shear Walls." *Canadian Journal of Civil Engineering,* Ottawa, Vol. 25, No. 3, 539-550.

[66] He, M., H. Magnusson, F. Lam, and H.G.L. Prion. (1999). "Cyclic Performance of Perforated Wood Shear Walls with Oversize OSB Panels." *Journal of Structural Engineering,* ASCE, Vol. 125, No. 1, 10-18.

[67] Heine, C.P. (1997). *Effect of Overturning Restraint on the Performance of Fully Sheathed and Perforated Timber Framed Shear Walls*. Master's Thesis. Virginia Polytechnic Institute and State University, Blacksburg, VA.

[68] Heine, C.P. (2001). *Simulated Response of Degrading Hysteretic Joints with Slack Behavior*. Ph.D. Disseration. Virginia Polytechnic Institute and State University, Blacksburg, VA.

[69] Heine, C.P. and J.D. Dolan. (2001). "A New Model to Predict the Load-Slip Relationship of Bolted Connections in Timber." *Wood and Fiber Science,* Vol. 33, No. 4, 534-549.

[70] Heitman, B. T. (1990). *Structural Engineering Properties of Acrylic Foam Tape.* Master's Thesis. Michigan Technological University, Houghton, MI.

[71] Hoyle, R.J. (1976). "Designing Wood Structures Bonded with Elastomeric Adhesives." *Forest Products Journal,* Vol. 26, No. 3, Forest Products Research Society, 28-34.

[72] Hoyle, R.J. (1981). "Evaluating Elastomeric Adhesives Used to Construct Wood Buildings." *Adhesives Age*, Vol. 24, No. 7, 43-48.

[73] Hoyle, R.J. and J.K. Hsu. (1978). "Shear Strength and Shear Modulus of an Elastomeric Adhesive Subject to Repeated Stress." *Wood Science*, Vol. 11, No. 2, 65-68.

[74] International Code Council (ICC). (2000). *International Building Code*. ICC, Washington D.C.

[75] International Conference of Building Officials (ICBO). (1999). *Uniform Building Code*, Whittier, California.

[76] ISO. (1998). *Timber Structures – Joints Made with Mechanical Fasteners – Quasi-Static Reversed-Cyclic Test Method.* ISO/TC 165 WD 16670. Secretariat, Standards Council of Canada.

[77] Itani, R.Y. and C.K. Cheung. (1984). "Nonlinear Analysis of Sheathed Wood Diaphragms." *Journal of the Structural Division,* ASCE, Vol. 110, No. 2, 2137-2147.

[78] Johansen, K.W. (1949). "Theory of Timber Connections." *International Association for Bridge and Structural Engineering,* Vol. 9, 249-262.

[79] Källsner, B. (1984). *Panels as Wind-Bracing Elements in Timber-Framed Walls.* Wood Technology Report No. 56, Swedish Institute for Wood Technology Research, Stockholm, Sweden.

[80] Kamiya, F. (1988). "Nonlinear Earthquake Response Analysis of Sheathed Walls by a Computer-Actuator On-Line System." *Proceedings, International Conference on Timber Engineering,* Vol. 1, 838-847.

[81] Karacabeyli, E. (1996). "Quasi-Static Reversed-Cyclic Testing of Nailed Joints." *International Council for Building Research Studies and Documentation,* Working Commission W18 – Timber Structures, Meeting Twenty-Nine, Karlsruhe, Germany, Paper 29-7-7

[82] Karacabeyli, E. and A. Ceccotti. (1998). "Nailed Wood-Frame Shear Walls for Seismic Loads: Test Results and Design Considerations." *Structural Engineering World Wide,* San Francisco, CA, Paper T207-6.

[83] Kivell, B.T., P.J. Moss, and A.J. Carr. (1981). "Hysteretic Modeling of Moment-Resisting Nailed Timber Joints." *Bulletin of the New Zealand National Society for Earthquake Engineering,* Vol. 14, No. 4, 233-243.

[84] Krawinkler, H. and A.A. Nassar. (1992). "Seismic design based on ductility and cumulative damage demands and capacities." *Nonlinear Seismic Analysis and Design of Reinforced Concrete Buildings, Fajfar*, Krawinkler, Ed., Elsevier Applied Science, New York.

[85] Krawinkler, H., F. Parisi, L. Ibarra, A. Ayoub, and R. Medina. (2001). "Development of a Testing Protocol for Wood Frame Structures." *CUREE-Caltech Woodframe Project Report No. W-02*, Consortium of Universities for Research in Earthquake Engineering, Richmond, CA.

[86] Lam, F., H.G. Prion and M. He. (1997). "Lateral Resistance of Wood Shear Walls with Large Sheathing Panels." *Journal of Structural Engineering,* ASCE, Vol. 123, No. 12, 1666-1673.

[87] Loferski, J.R. (2002). Professor of Wood Science at Virginia Polytechnic Institute. Personal interview. Blacksburg, VA. 7 October 2002.

[88] Loferski, J.R. and A. Polensek. (1982). "Predicting Inelastic Stiffness Moduli of Sheathing to Study Nail Joins." *Wood Science,* Vol. 15, No. 1, 39-43.

[89] Macco Adhesives Division. (2001). *Liquid Nails Adhesive*. Product Data Sheet No. 9940, Cleveland, OH.

[90] Malhotra, S.K. and B. Thomas. (1982). "Behavior of Nailed Timber Joints with Interface Characteristics." *Wood Science,* Vol. 5, No. 2, 161-171.

[91] McGee, W.D. and R.J. Hoyle. (1974). "Design Method for Elastomeric Adhesive Bonded Wood Joist-Deck System." *Wood and Fiber,* Vol. 6, No. 2, 144-155.

[92] Medearis, K. and D.H. Young. (1964). "Energy Absorption of Structures Under Cyclic Loading." *Journal of Structural Division ASCE 90 (ST1),* 61-91.

[93] Miranda, E. and V.V. Bertero. (1994). "Evaluation of Strength Reduction Factors for Earthquake-Resistance Design." *Earthquake Spectra,* EERI, Vol. 10, No. 2, 357-379.

[94] MiTek® Consumer Services, updated (2003), accessed March 2, 2003. **"**MiTek® RoofGlider Trakless Roof Truss Roller System." Chesterfield, MI. Internet Address: http://www.mitek.ca/products/roofglider.htm/

[95] Newmark, N.M. and W.J. Hall. (1982). *Earthquake Spectra and Design.* EERI Monograph Series, EERI, Oakland.

[96] North American Steel Framing Alliance (NASFA), updated (2003), accessed January 22, 2003. "Market Trends." *NASFA,* Washington, D.C. Internet address: http://www.steelframingalliance.com/facts/mrkttrends.html

[97] Patton Mallory, M. (1989). "Yield Theory of Bolted Connections Compared with Current U.S. Design Criteria," *Proceedings of the Pacific Timber Engineering Conference, Wellington, New Zealand,* Institute of Professional Engineers, 322-329.

[98] Pellicane, P.J. (1988). "Strength and Ultimate Slip Characteristics of Wood Joints with Elastomeric Construction Adhesives." *Forest Products Journal,* Vol. 38, No. 6, Forest Products Research Society, 55-59.

[99] Pellicane, P.J. (1992a). "Superposition Theory Applied to Nail/Glue Joints in Wood: Part I – Strength Behavior." *Journal of Testing and Evaluations,* Vol. 20, No. 5, 363-368.

[100] Pellicane, P.J. (1992b). "Superposition Theory Applied to Nail/Glue Joints in Wood: Part II – Load-Slip Behavior." *Journal of Testing and Evaluations,* Vol. 20, No. 6, 449-453.

[101] Pellicane, P.J. and G.C. Robinson. (1997). "Effect of Construction Adhesive and Joist Variability on the Deflection of Light-Frame Wood Floors." *Journal of Testing and Evaluation,* Vol. 25, No. 2, 163-173.

[102] Pellicane, P.J., G.C. Robinson, and D. Reichler. (1999). "Elastomeric Adhesives in Wood Connections: Short-Term Behavior." *Journal of Materials in Civil Engineering,* Vol. 11, No. 3, 266-272.

[103] Peterson, J. (1983). "Bibliography on Lumber and Wood Panel Diaphragms." *Journal of Structural Engineering,* ASCE, Vol. 109, No. 12, 2838-2852.

[104] Pinder, C. (1981). "Double-Stick Tapes for Heavyweight Fastening." *Assembly Engineering,* Vol. 24, No. 5, 22-25.

[105] Porter, M.L. (1987). "Sequential Phased Displacement (SPD) Procedure for TCCMAR Testing." *Proceedings, 3rd Meeting of the Joint Technical Coordinating Committee on Masonry Research*, US-Japan Coordinated Research Program.

[106] Ramskill, T.E. (2002). *Effect of Cracking on Lab Bolt Performance.* PhD Dissertation. Virginia Polytechnic Institute and State University, Blacksburg, VA.

[107] Richard Lumber Company. (2003). Sales Representative of Richard Lumber Company. Personal communication. Pleasonton, CA. 2 March 2003.

[108] Rose, J.D. (1995). *Performance of Wood Structural Panel Shear Walls Under Cyclic (Reversed) Loading.* Technical Forum Presentation, Portland, Oregon, June 28, 1995.

[109] Rose, J.D. (1998). *Preliminary Testing of Wood Structural Panel Shear Walls Under Cyclic (Reversed) Loading.* APA Research Report 158. APA – The Engineered Wood Association, Tacoma, WA.

[110] SAC/BD. (1997). "Protocol for Fabrication, Inspection, Testing, and Documentation of Beam-Column Connection Tests and Other Experimental Specimens." *SAC Steel Project Background Document.* Report No. SAC/BD-97/02, SAC Joint Venture, Sacramento, CA.

[111] Salenikovich, A.J. (2000). *The Racking Performance of Light-Frame Shear Walls.* PhD Dissertation. Virginia Polytechnic Institute and State University, Blacksburg, VA

[112] Salenikovich, A.J. (2003). Postdoctoral Associate at Mississippi State University. Personal communication. Mississippi State, MS. 14 March 2003.

[113] SaRibeiro, R.A. and M.G. SaRibeiro. (1991). "Load-Slip Behavior of Nailed Joints: An Improved Model." *1991 International Timber Engineering Conference,* London, 3.03-3.19.

[114] SEAOC. (1999). *Recommended Lateral Force Requirements and Commentary "Blue Book."* Seventh Edition. Seismology Committee – Structural Engineers Association of California, Sacramento, CA.

[115] Simpson. (2003). *Simpson Strong-Wall® Shearwall*. Technical Data, 2003. Simpson Strong-Tie Co., Inc., Dublin, Ca.

[116] Simpson Plywood, accessed January 13, (2003). "How Plywood is Made." *Simpson Plywood,* Shelton, Washington. Internet address: http://www.simpson-plywood.com/vintro.htm

[117] Skaggs, T.D. and J.D. Rose. (1996). "Cyclic Load Testing of Wood Structural Panel Shear Walls." *Proceedings of the International Wood Engineering Conference; New Orleans, Louisiana.* IWC, 2-195 -200.

[118] Smardzewski J. (1999). "Technological Heterogeneity of Adhesive Bonds in Wood Joints." *Wood Science and Technology,* Vol. 36, No. 3, Springer-Verlag, 213-227.

[119] Smart, J.V. (2002). *Capacity Resistance and Performance of Single-Shear Bolted and Nailed Connections: An Experimental Investigation.* Master's Thesis. Virginia Polytechnic and State University, Blacksburg, VA.

[120] Smith, J. (1987). "New Vistas in Very High Bond Adhesive Tapes." *Assembly Engineering,* Vol. 30, No. 12, 16-18.

[121] Steiner, T. (2002). "3M Primer 94." Email to Don Ohanehi. 12 July 2002.

[122] Stewart, W.G. (1987). *The Seismic Design of Plywood Sheathed Shearwalls.* Thesis submitted in partial fulfillment of Ph.D. degree, University of Canterbury, New Zealand.

[123] Tarabia, A.M. and R.Y. Itani. (1997). "Static and Dynamic Modeling of Light-Frame Wood Buildings." *Computers and Structures,* Vol. 63, No. 2, 319-334.

[124] Thurston, S.J. and P.F. Flack. (1980). "Cyclic Load Performance of Timber Sheathed Bracing Walls." *Central Laboratories Report 5-80/10,* Ministry of Works and Development, Wellington, New Zealand.

[125] Tissell, J.R. (1990). *Structural Panel Shear Walls – APA Research Report 154.* APA – The Engineered Wood Association, Tacoma, WA.

[126] Toothman, A.J. (2003). *Monotonic and Cyclic Performance of Light-Frame Shear Walls with Various Sheathing Materials.* Master's Thesis. Virginia Polytechnic and State University, Blacksburg, VA.

[127] Toumi, R.L. and W.J. McCutcheon. (1978). "Racking Strength of Light-Frame Nailed Walls." *Journal of Structural Division*, ASCE, Vol. 104, No. ST7, 1131-1140.

[128] Uang, C.M. (1991). "Establishing R (or R_w) and C_d factors for Building Seismic Codes." *Journal of Engineering Structures,* Vol. 20, No.4-6.

[129] Uniform Building Code (UBC). (1991). International Conference of Building Officials, Whittier, Calif.

[130] van de Lindt, J.W. and M.A. Walz. (2003). "Development and Application of Wood Shear Wall Reliability Model." *Journal of Structural Engineering,* ASCE, Vol. 129, No. 3, 405-413.

[131] Vick, C.B. (1971). "Elastomeric Adhesives for Field Gluing Plywood Floors." *Forest Products Journal,* Vol. 21, No. 8, Forest Products Research Society, 34-42.

[132] Volkersen, O. (1938). "Die Nietkraftverteilung in zugbeanspruchten Nietverbindungen mit konstanten Laschenquerschnitten." *Luftfahrtforschung,* Vol. 15, 41-47.

[133] White, M.W., and J.D. Dolan. (1995). "Nonlinear Shear-Wall Analysis." *Journal of Structural Engineering,* ASCE, Vol. 121, No. 11, 1629-1635.

[134] Wood Promotion Network, updated (2003), accessed March 8, 2003. "Why Wood is Good." *Wood Promotion Network,* Chicago, IL. Internet address: http://www.beconstructive.com

[135] Wu, J. and R.D. Hanson. (1989) "Study of Inelastic Spectra with High Damping." *ASCE Journal of Structural Engineering,* Vol. 115, No. 6, 1412-1431.

[136] Zink, A.G., R.W. Davidson, and R.B. Hanna. (1996). "Finite Element Modeling of Double Lap Wood Joints." *Journal of Adhesion,* Vol. 56, 217-228